COASTAL WATER QUALITY

by

David William Mardon

Submitted in fulfilment of the requirements for the degree of
Master of Science in Engineering
In the
Civil Engineering Programme
University of Natal
2003

Durban

ABSTRACT

This research focuses on the pathogenic pollution of coastal recreational waters. Pollution of this resource can have serious social and economic implications. The health of the public could be compromised and there may be associated adverse impacts on the tourism industry.

A section of coastline along the Durban Bight and including some of the nation's premier bathing beaches, was used for a case study. The water quality condition of the beaches was evaluated against both local and international marine recreational water quality standards. Most of Durban's bathing beaches were found to have good water quality. However beaches situated close to stormwater drains regularly experience poor water quality conditions. The relationships between beach water quality, the pollution sources and environmental factors such as rainfall were quantified. A weak correlation was found between rainfall and beach pathogenic pollution levels. No correlation was found between successive fortnightly beach samples indicating that the time scales of coastal dispersion processes are significantly shorter than the beach monitoring period. The research also indicates a need to update the SA marine water quality standards. The exclusive use of Escherichia coli (E.coli) as the indicator of faecal pollution is inconsistent with international trends towards the use of Enterococcus, which is a more robust pathogen indicator for marine environments.

The main aim of the research was to develop a model to predict the water quality conditions of beaches. The Coastal Water Quality Model (CWQM) is intended to serve two functions: firstly to provide daily estimates of pathogenic pollution levels for beach management (e.g. closure under poor water quality conditions), and secondly to provide decision-makers with a tool for predicting the effects of changes on future water quality conditions. The CWQM was formulated as a stochastic state-space lumped advection diffusion model. A Kalman Filter was used for state estimation. Parameter estimation using the Extended Kalman filter was investigated but found to be unsatisfactory due to large input uncertainties and sparse measurements. An alternative statistical fitting procedure was therefore used for parameter estimation. The model was shown to produce accurate predictions of pathogenic pollution for the case study site. To further demonstrate it's utility, it was used to evaluate options for improving the poor water quality at Battery Beach. The results show that a constructed wetland could be effective in this case.

PREFACE

I, David William Mardon hereby declare that the whole of this dissertation is my own work and has not been submitted in part, or in whole to any other University. Where use has been made of the work of others, it has been duly acknowledged in the text. This research work was caried out in the Centre for Research in Environmental, coastal and Hydraulic Engineering, School of Civil Engineering, surveying and Construction, University of Natal, Durban, under the supervision of Professor D. D. Stretch.

1 DECEMBER 2003
Date

Signature

As the candidates supervisor I have approved this dissertation for submission

Professor D. D. Stretch

1 DECEMBER 2003
Date

ACKNOWLEDGEMENTS

I would like to express my gratitude to the following:

- My parents for their constant support and understanding.
- Professor Stretch, for his continued support and motivation.
- eThekwini Municipality Water and Sanitation, and particularly Siobhan Jackson, for providing the water quality data for this study.
- The South African Weather Service for providing weather data for this study.

The research was made possible by a grant from the Innovation Fund, administered by the Department of Arts, Culture, Science & Technology, and forms part of the SA-ISIS project (www.sa-isis.co.za)

TABLE OF CONTENTS

LIST OF FIGURES

LIST OF TABLES

LIST OF PLATES

LIST OF SYMBOLS

A	Area
A	Advection diffusion coefficient matrix
B	Input coefficient matrix
C_{AC}	Wind to current advection coefficient
C_k	Cell concentration
$C_{outside}$	Concentration of the waters seaward of the cell boundary
D	Observation transformation matrix
F	EKF linearization matrix
$FACTOR$	Projection factor
H	Input transition matrix
I	Identity matrix
I_k	Input concentration
I_0	energy absorbed by the seawater surface
k	Decay rate
K	Kalman gain
k_w	extinction coefficient
L	Wind fetch distance
L	EKF partial derivative matrix
L_{cell}	Cell length
M	EKF partial derivative matrix
n	Manning's roughness
P	Process noise covariance matrix
Q	Input noise covariance matrix
Q_P	Point input flow rate
Q_{AC}	Surface advection current flow rate
R	Reynolds number
R	Measurement noise covariance matrix
S	Discrete step input transition matrix
S_{AC}	Advection current speed
S_{Wind}	Wind speed
t	Time
T_{90}	T90 timescale
T_{ADV}	Advection timescale
T_{CM}	Cross-shore mixing timescale
T_d	Decay timescale
T_D	Disappearance timescale
u_k	Input concentration vector
u_{*a}	Wind friction velocity

U_y	Wind velocities at height y
V_a	Wind-induced surface drift velocity
V_{AC}	Surface advection current velocity
V_{cell}	Cell volume
x_k	State vector
y_k	Observation vector
z	Depth
z_k	Augmented state vector
α	Light attenuation coefficient per unit depth
θ	Parameter vector
ϕ	Discrete step state transition matrix
Φ	State transition matrix
$\omega(t)$	Input noise process
$\varepsilon(t)$	Measurement noise process
ξ	Parameter noise process
η_t	Augmented input noise process
σ	Standard deviation
σ'	Shape parameter (lognormal distribution)
μ	mean
μ'	Scale parameter (lognormal distribution)

LIST OF ABBREVIATIONS

ADCP	Acoustic doppler current profiler
ARF	Area reduction factor
BEACH	Beaches Environmental Assessment, Closure, and Health
CBD	Central business district
CDF	Cumulative density function
CFU	Colony forming units
CV	Coefficient of variation
CWQM	Coastal Water Quality Model
DWAF	Department of Water Affairs and Forestry
EEC	European Economic Community
E.coli	Escherichia coli
EKF	Extended Kalman filter
EMWSS	eThekwini Municipality Water and Sanitation Services
EPA	Environmental Protection Agency
EU	European Union
FEE	Foundation for Environmental Education
FF	First flush
GM	Geometric mean
GME	Geometric mean exceedance
HRT	Hydraulic residence time
KF	Kalman filter
RBAC	Rainfall-based alert curve
RBM	Regional Bypass Model
RC	Runoff coefficient
RWQO	Receiving Water Quality Objectives
SA-ISIS	South African Integrated Spatial Information System
SMTM	Simple Mixing and Transport Model
SS	Suspended solids
SSL	Single sample limit
SWD	Stormwater drain
SWEM	System-Wide Eutrophication Model
SWMM	Storm Water Management Model
TWQR	Target Water Quality Range
WQ	Water quality

CHAPTER 1:
INTRODUCTION

1.1 Introduction

The ultimate goal of water quality management in South Africa is to keep the water resources suitable for their designated uses. The coastal waters are used for a variety of purposes, from mariculture to recreation and even for the disposal of waste. Many of South Africa's beaches are used for marine recreational activities. Poor beach water quality can have serious social and financial implications by having negative impacts on public health and the tourism industry. This research focuses on the pathogenic pollution of coastal marine recreational waters.

1.2 Motivation for the Study

The primary motivation behind the research was to develop a coastal water quality model (CWQM) for inclusion into SA-ISIS. The South African Integrated Spatial Information System (SA-ISIS) is a web-based, decision-support system. The vision behind SA-ISIS was to create a system combining up-to-date information, models, and analytical tools; which government decision makers, planners, developers and investors may use to make appropriate informed development decisions.

To achieve the objectives set for the model, the CWQM was formulated to have two applications:

- **Real-time:** The CWQM could make real-time daily predictions of the pathogenic pollution along the coastline using current environmental information and previous observations of the true pathogenic pollution. These predications may be used by beach management to determine if beach closures are necessary; or presented on the Internet for beach users to make informed decisions.
- **Off-line:** The CWQM would use a number of years of environmental information to produce statistical information about the pathogenic pollution levels along the coastline. The results of the CWQM may be compared against water quality guidelines. Using this mode decision makers may run **"what-if"** and **"now-what"** scenarios, to determine the effect that new or existing developments may have on the water quality of the nearshore region.

The coastline selected for development of the Coastal Water Quality Model (CWQM) was the eight-kilometre stretch of Durban's Bight, from the Port of Durban entrance in the south to the Umgeni River in the north. This included Durban's "Golden Mile", which is a 6km stretch of beachfront stretching from Addington Beach in the south to Blue Lagoon Beach (Umgeni South Beach) in the north. The Golden Mile is a key tourist attraction for Durban and the bathing beaches support the hotels built along it. Adverse and even perceived poor water quality conditions experienced by tourists could have serious financial implications to the hotels and tourism industry of Durban.

Since conception of this research at least two newspaper articles have appeared in the *Natal Mercury* Newspaper featuring articles relating to poor water quality at Battery Beach (Carnie, 2003) and public concerns over the urban stormwater outlets on the Durban beachfront (Carnie, 2002). Combined with this are new tourism developments, such as the Suncoast Casino Complex and probable utilisation of historically problematic beaches (e.g. Battery Beach). There is a need to analyse the causes of pathogenic pollution of the bathing beaches, to evaluate methods to reduce the occurrence of poor water quality conditions, and to inform the public when such conditions may exist.

1.3 Objectives of the Study

The primary objective of the study was to develop a simple coastal water quality model that could be used to predict pathogenic water quality conditions along the coastline of South Africa. The following criteria were set for the model:

1. The CWQM should be simple and not require high level modelling expertise to use.
2. The CWQM should use readily available information concerning the nearshore region and pollution sources
3. The CWQM should be able to reproduce past & present conditions and to predict any effects that future changes to the nearshore region or pollution sources may have on the water quality along the coastline.

In order for the model to be correctly formulated and applied to the nearshore environment a full understanding of the following is necessary:

1. Water quality guidelines of South Africa, and other countries with respect to pathogenic pollution of recreational marine waters.
2. Historical water quality conditions of the coastline.
3. Environmental conditions of the region, such as rainfall, wind and solar radiation.
4. The inter-relationships between the pollution at adjacent beaches, rainfall, stormwater drains and rivers

Once the CWQM was formulated, the aims were to:

1. Investigate the parameter fitting efficiency of the Extended Kalman Filtering algorithm for the CWQM.
2. Determine the optimal model parameters to fit the CWQM to Durban's "Golden-mile" stretch of beaches.

Investigate the differences in applying the CWQM in either its off-line or real-time application.

CHAPTER 2:
LITERATURE REVIEW

2.1 Water Quality

Water quality is a broad term used to describe the chemical, physical and biological qualities of water, usually with reference to the intended use of the water. Water quality characteristics are influenced by substances, which either dissolve or are suspended in water.

The classification of "good or bad" water quality is not simply determined by the scientific analysis of the water. Water that is suitable for industrial use is not necessarily suitable for drinking or bathing. Therefore, good water quality is determined on the basis of its intended use.

The focus of this research is on the pollution of coastal water by waterborne pathogens.

2.1.1 Waterborne Pathogens

Waterborne pathogens are disease-causing organisms, microorganisms, viruses or protozoans that can be transmitted to people when they consume or come in contact with untreated or inadequately treated water. (The effects of urbanization on water quality: Waterborne pathogens, 2003)

Microorganisms can be found in both aquatic and terrestrial environments, and most perform important functions within their respective environments. Ecosystems rely on microorganism decomposers, which convert organic matter to nutrients that can be used by plants and animals higher in the food chain. Humans and animals have microorganisms resident in their digestive tracts and rely on them for digestion. These microorganisms are then excreted in large numbers in faecal matter. A small percentage of these microorganisms have been linked to disease and death. Pathogens can infect the body through skin contact or ingestion of contaminated water.

Pathogens that find themselves in the open environment are easily transported by water. The pathogens that are of most interest to aquatic related illnesses can be grouped into 3 subcategories – bacteria, protozoa, and viruses.

Bacteria are microscopic, unicellular organisms that reproduce by binary fission. Not all bacteria are pathogenic, but pathogenic bacteria that can be found in surface water are often classified as coming from warm-blooded animals (Hoadley, 1976).

Protozoans are also unicellular organisms that reproduce by binary fission. Pathogenic protozoans exist in the environment as cysts, protecting themselves from harsh environmental conditions such as temperature and salinity. Once the cysts are ingested they hatch, grow and multiply infecting the host with the associated disease (Hoadley, 1976).

Viruses are sub-microscopic infectious agents that require a host to live. The virus has a nucleic acid core that is protected by a protein or lipoprotein shell that can determine what surface to attach itself to. Once inside the host the virus reproduces, manifesting the associated diseases. Viruses are excreted in the faeces of infected individuals. Enteric viruses post major threats to human health (Hoadley, 1976).

2.1.1 Water Quality Indicators

There are various techniques by which water quality can be tested, from scientific analysis of water samples to biological analysis and enumeration of such things as fish, invertebrates, molluscs, etc. Since the presence, absence or relative abundance of certain groups give clues to the water's health over the long term. In all these methods indicators are used to identify the quality of the water.

Water has many different uses; each use has a different definition of what "acceptable" water quality is. Therefore the intended use of the water source will determine what indicators determine "acceptable" water quality.

The identification and enumeration of pathogens such as viruses in water is a difficult and very costly procedure. So instead of looking for the actual viruses, laboratory methods are used to identify the presence and density of indicator organisms.

When the water source is to be used for recreational activities there are 4 main groups of indicators used for scientific analysis of water samples.

- **Physico-Chemical Properties** such as: Temperature, Salinity, pH, Floating Matter, Suspended Solids, Clarity, Turbidity and Colour.
- **Inorganic constituents** such as: Hydrogen Sulphide.
- **Organic constituents** such as: Algal Toxins.
- **Microbiological indicators** such as: Total Coliforms, Faecal Coliforms, E.coli, Enteroccus, and Human Pathogens

2.1.2 Microbiological indicators

The coliform bacteria group is found in the intestines of warm-blooded animals. The presence of these bacteria is an indication that pathogens from untreated or partially treated sewage or contaminated runoff may be found in the relevant aquatic system.

2.1.2.1 Total Coliforms

The total coliform group is a general group encompassing all coliform bacteria. The group is easier to test for but does not make the distinction between coliforms coming from faecal matter of warm-blooded animal or those naturally present in the environment.

2.1.1.1 Faecal Coliforms

Faecal coliforms bacteria are a sub-group of total coliforms bacteria. They are more closely related to faecal matter and do not readily replicate in the water environment. (DWAF, 1995) The presence of faecal pollution by warm-blooded animals indicates the possible presence of pathogens responsible for infections diseases.

A set volume of the sampled water is cultured on an m-FC agar at 44.5°C. Faecal coliform bacteria will produce blue colonies within 20 – 24 hours of incubation. The colonies are then counted and results are given as colony counts per 100ml or colony forming units (CFU) per 100ml. (DWAF, 1996)

2.1.2.2 Escherichia coli (E. coli)

Escherichia coli (E. coli) is a member of the faecal coliform bacteria group. E.coli is used as an indicator because it is highly specific to faecal contamination from humans and warm-blooded animals and because these bacteria cannot normally replicate in any natural water environment. (DWAF, 1995) The presence of faecal pollution by warm-blooded animals indicates the possible presence of pathogens responsible for infectious diseases.

As with faecal coliform bacteria, E. coli will produce blue colonies on an m-FC agar within 20 – 24 hours of incubation at 44.5°C however only E.coli bacteria will test indole-positive at 44.5°C. (DWAF, 1996) E. coli are enumerated as colony counts per 100 ml or CFU per 100ml.

A few examples of bacterial pathogens whose presence are indicated by E. coli are: Salmonella spp., Shigella spp., Vibrio cholerae and pathogenic E.coli. These bacteria can cause diseases such as gastroenteritis, dysentery, cholera and typhoid fever. (DWAF, 1996)

2.1.2.3 Enterococci: Faecal Streptococci

Enterococci (faecal streptococci) bacteria are used to indicate the presence of faecal pollution by warm-blooded animals, which could contain pathogens responsible for infectious diseases. They are the preferred indicators of faecal pollution in marine environment, as they survive longer than that of coliform bacteria in water and sediments. (DWAF, 1995)

The bacteria produce typical reddish colonies on m-enterococcus agar after 48 hours incubation at 35°C. (DWAF, 1996) These colonies are counted and the results are given as the number of colony counts per 100ml or CFU per 100ml.

A few examples of bacterial pathogens for which streptococci is an indicator of are: Salmonella spp., Shigella spp., Vibrio cholerae and pathogenic E. coli. These bacteria can cause diseases such as gastroenteritis, dysentery, cholera and typhoid fever. (DWAF, 1996)

2.2 Water Quality Guidelines

2.2.1 South African Water Quality Guidelines

The *South African Water Quality Guidelines* are a set of guidelines, produced by the *Department of Water Affairs and Forestry* (DWAF, 1996), which specify the quality of water needed for different uses. These guidelines cover both fresh and marine waters and the whole spectrum of water uses, including agriculture, mariculture, recreation, and industrial.

The guidelines are used for the management of water quality in South Africa. The ultimate goal in water quality management is to keep the water resources suitable for their intended uses. To maintain water as a sustainable resource the *Receiving Water Quality Objectives* (RWQO) is used. This approach consists of a RWQO for non-hazardous substances and a pollution minimisation and prevention approach for hazardous substances.

The RWQO implies that water quality objectives, set for a particular marine environment subject to potential impact from a development, must be based on the water quality requirement of all designated uses in that region. Both point and diffuse loads are taken into account, while recognising that the marine environment has a certain capacity to assimilate waste without detrimental effect.

The aquatic environment has many uses from agriculture to industrial, however the main interest of this research is the recreational use of marine waters. This research focuses on the pathogenic pollution of marine waters used for recreation.

2.2.2 Target Water Quality Range

Each water quality indicator or constituent has a specified "No effects range". This is a range at which the levels of a particular constituent would have no known or anticipated adverse effect on the fitness of the water for its designated use or on the heath of the aquatic ecosystem.

The aim of DWAF is to maintain South Africa's water resources so that they remain within this "No effects range". The guidelines therefore refer to the "No effects range" as the Target Water Quality Range (TWQR).

2.2.3 Characterisation of Recreational Water Use

Water quality guidelines for recreational use consider three main sub-uses: Full-contact, Intermediate-contact and Non-contact recreation. (DWAF, 1995)

2.2.3.1 Full-contact Recreation

Full-contact recreation is determined by the fact that the full body is likely to come into contact with and ingest water during the activity. Activities include swimming, diving, water skiing, surfing, paddle skiing and wind surfing. The people that participate in these activities span a wide range of ages, from infants to the elderly. The health status of users may also vary: people that are not completely healthy are still inclined to swim while people taking part in more strenuous activities such as surfing are more likely to be fit and healthy.

These activities occur all along the South African coastline, particularly at coastal cities and holiday towns. Warmer water temperatures increase the density of full-contact water activities that occur.

2.2.3.2 Intermediate-contact recreation

Intermediate-contact recreation is where the users may come in contact with the water. Such activities include boating, wading and angling. The age groups that participate span from children to the elderly and the health status of these individuals may also vary.

These activities occur all along the South African Coastline, particularly at coastal cities and holiday towns

2.2.3.3 Non-contact Recreation

Non-contact recreation involves recreation with no direct contact with the water and includes sightseeing, walking, horse riding, etc. These activities are predominantly concerned with the aesthetic appreciation of the water.

The economic value of the region is often closely related to the aesthetic quality of the recreational waters.

2.2.4 Guidelines for Coastal Marine Waters: Microbiological Indicators

The water quality guideline for coastal marine recreational waters is still under development and does not include TWQR for all microbiological indicators. The only microbiological indicators in a marine environment that have a specified TWQR are those of the Faecal Coliform bacteria. As yet there are no guideline values specified for Enterococcus or Human Pathogens in marine recreational waters of the South African coastal zone.

2.2.4.1 Faecal Coliform Bacteria (incl. E. coli)

The SA WQ guidelines for Full-contact and intermediate-contact recreation stipulate that the following criteria should not be exceeded. (DWAF, 1995)

80 percent of the samples may not exceed 100 counts per 100ml 95 percent of the samples may not exceed 2000 counts per 100ml

The guidelines are lacking in that they don't stipulate a sampling frequency or durations for consideration. However, these guidelines are very similar to those set by the EU Bathing Water Directive (76/160/EEC) and therefore the sampling frequency and other requirement are assumed to be similar. The EU Bathing Water Directive is discussed in Section 2.2.7.

2.2.5 Guidelines for Inland Waters: Microbiological Indicators

The water quality guidelines for inland recreational waters (DWAF, 1996) are applicable to all inland waters that are used for recreational purposes, namely rivers, streams, canals, dams, ponds and other impoundments. The guideline gives target water quality ranges for a wider range of microbiological indicators than the guidelines set for coastal marine recreational waters. The Guideline also gives ranges of indicator or constituent levels where certain effects to the aquatic system and water users can be expected.

Application of the Target Water Quality Range (TWQR)

The TWQR is an indicator level range that should not be exceeded by the geometric mean or median of fortnightly samples over a maximum of a three-month period. This three-month period should preferably be selected to coincide with seasons. This criterion assumes an average intake of water during full contact recreation of 100 ml per recreational event.

2.2.5.1 Faecal Coliform Bacteria

Full-contact recreation

Faecal coliform range (CFU/100ml)	**Effects**
Target Water Quality Range 0 – 130	Risk of gastrointestinal effects expected. The presence of faecal coliforms indicate a possible risk to health, but the absence of indicators does not guarantee no risk
130 – 600	Risk of gastrointestinal illness indicated at faecal coliforms levels that occasionally fall in this range. Risk increases if the geometric mean or median levels are consistently in this range
600 – 2000	Noticeable gastrointestinal health effects expected in the swimmer and bather population. Some health risk, if single samples fall in this range, particularly if such events occur frequently. Four out of five samples should contain < 600 faecal coliforms/100 ml, or 95 % of faecal coliform analyses should be < 2 000 / 100 ml
> 2000	As the faecal coliform count increases above this limit, the risk of contracting gastrointestinal illness increases. The volume of water ingested in order to cause adverse effects decreases as the faecal coliform density increases

Table 2-1: SA Standards for faecal coliform bacteria levels for full-contact recreation (DWAF, 1996)

Intermediate-contact recreation

Faecal coliform range (CFU/100ml)	**Effects**
Target Water Quality Range 0 – 1000	Health effects are indicated for intermediate contact with recreational water. If water contact is extensive, such as may occur for novice water skiing or novice windsurfing and if full-body immersion is likely to occur, the more stringent criteria proposed for full-contact recreation may be more appropriate
1000 – 4000	It may be expected that limited contact with water of this quality is associated with a risk of gastrointestinal illness. The upper limit of this range corresponds to the limit recommended by the Australian guidelines for at least four out of five samples collected over 30 days
> 4000	Intermediate recreational contact with water can be expected to carry an increasing risk of gastrointestinal illness as faecal coliform levels increase

Table 2-2: SA Standards for faecal coliform bacteria levels of intermediate-contact recreation (DWAF, 1996)

Non-contact recreation

The guideline states that provided there is no contact with the water, the public health risk due to disease transmission, as indicated by faecal coliforms, is of no concern.

2.2.5.2 Escherichia coli Bacteria (E. coli)

Full-contact recreation

Faecal coliform range (CFU/100ml)	**Effects**
Target Water Quality Range 0 – 130	A low risk of gastrointestinal illness is indicated for contact recreational water use. This is not expected to exceed a risk of typically < 8 illnesses/1 000 swimmers
130 – 200	A slight risk of gastrointestinal effects among swimmers and bathers may be expected. Negligible effects are expected if these levels occur in isolated instances only
200 – 400	Some risk of gastrointestinal effects exists if geometric mean or median E. coli levels are in this range, particularly if this occurs frequently. The risk is minimal if only isolated samples fall in this range. Re-sampling should be conducted if individual results > 400 /100 ml are recorded
> 400	Risks of health effects associated with contact recreational water use increase as E. coli levels increase. The volume of water that needs to be ingested in order to cause ill effects decreases as the E. coli density increases. Gastrointestinal illness can be expected to increase approximately in accordance with the following relationship, based on US EPA epidemiological studies: $y = -150.5 + 423.5(\log x)$ where y = illness rate/100 000 persons x = number of E. coli /100 ml

Table 2-3: SA Standards for E. coli levels for full-contact recreation (DWAF, 1996)

Intermediate-contact recreation

When the guideline was created there was insufficient information for the development of criteria for E. coli in water used for intermediate contact recreation.

Non-contact recreation

The Guideline states that provided there is no contact with the water and that the restriction is clearly signposted then the public health risk due to the transmission of diseases (as indicated by E. coli) are not of concern. It goes further to suggest that health effects should not result from rare accidental water contact, nor should bacterial populations indicated by E. coli cause adverse effect to the other aquatic organisms.

2.2.5.3 Enterococci: Faecal Streptococci

Full-contact recreation

Faecal Streptococci Range (CFU/100ml)	Effects
Target Water Quality Range 0 - 30	Low risk of gastrointestinal illness indicated. Not expected to exceed a risk of typically < 8 cases in 1000 swimmers.
30 - 60	Slight risk of gastrointestinal effects expected. Negligible effects expected if isolated instances only.
60 - 100	Some risk of gastrointestinal effects, particularly if this occurs frequently. Risk is minimal if only isolated samples fall in this range. Re-sampling should be conducted if individual results > 100 /100 ml are recorded
> 100	Risks of health effects increase as faecal streptococci levels increase. The volume of water which needs to be ingested in order to cause ill effects decreases as the faecal streptococci density increases

Table 2-4: SA Standards for faecal Enterococci levels for full-contact recreation (DWAF, 1996)

Intermediate-contact recreation

Faecal Streptococci Range (CFU/100ml)	Effects
Target Water Quality Range 0 - 230	Health effects indicated. If water contact is extensive, such as may occur for novice water-skiing or novice windsurfing and if full-body immersion is likely to occur, refer to the more stringent criteria proposed for full-contact recreation
230 – 700	Limited contact associated with a risk of gastrointestinal illness
> 700	Expected increasing risk of gastrointestinal illness as faecal streptococci levels increase

Table 2-5: SA Standards for faecal Enterococci levels for intermediate-contact recreation (DWAF, 1996)

Non-contact recreation

The Guideline states that provided no contact with water occurs and the non-contact recreation restriction is clearly signposted, public health risks due to possible disease transmission, as indicated by faecal streptococci levels, are not of concern and that health effects should not result from rare accidental water contact.

2.2.6 US EPA Standards

The U.S. Environmental Protection Agency (EPA) administers the water quality standards program for the United States. It is responsible for providing water quality criteria recommendations, approving state-adopted standards for interstate waters, evaluating adherence to the standards, and overseeing enforcement of standards compliance.

The relevant guideline information necessary for the development of standards is contained in two EPA documents; *Water Quality Standards Handbook*, second edition (1983) and *Ambient Water Quality Criteria for Bacteria* (US EPA, 1986). Prior to these guidelines, recommendations came from two documents; *Water Quality Criteria* (NTAC, 1968) and *Quality Criteria for Water* (US EPA, 1976).

Pre 1983 Guideline Criteria

Both documents that were used prior to 1983 utilised faecal coliforms as the criteria for water quality with respect to pathogenic pollution. The recommendations for recreational waters were that maximum densities not exceed geometric means of 200 counts per 100 ml, calculated form a minimum of five samples equally spaced over a period of not more than 30 days.

Post 1986 Guideline Criteria

The Faecal bacteria concentration was selected as a primary indicator of possible pathogens or parasites. Of the faecal bacteria, Enterococci and Escherichia coli were considered to have a higher degree of association with the outbreaks of certain diseases than the general faecal coliform group (US EPA, 1986). In *Ambient Water Quality Criteria for Bacteria* it was stated that:

> "The similarities in the relationships of E.coli and enterococci to swimming associated gastroenteritis in freshwater indicate that these two indicators are equally efficient for monitoring water quality in freshwater, whereas in marine water environments only enterococci provided a good correlation." (US EPA, 1986)

The etiological agent for acute gastroenteritis was found to be most likely viral (Cabelli, 1981) and the ultimate source of this agent was found to be human faecal waste. Although E.coli was considered the most faecal specific of the coliform indicators (Dufore, 1976), in the marine environment enterococci is a preferred indicator of the virus due to its superior survival in the marine waters (Fattal et al, 1983; Prüss, 1998).

EPA Criteria for Bathing (Full Body Contact)
Recreational Waters

Freshwater

Based on a statistically sufficient number of samples (generally not less than 5 samples equally spaced over a 30-day period), the geometric mean of the indicated bacterial densities should not exceed one or the other of the following:[1]

E.coli	126 per 100 ml; or
Enterococci	33 per 100 ml.

No sample should exceed a one sided confidence limit (C.L.) calculated using the following as guidance:

Designated bathing beach	75% C.L.
Moderate use for bathing	82% C.L.
Light use for bathing	90% C.L.
Infrequent use for bathing	95% C.L.

based on a site-specific log standard deviation, or if site data are insufficient to establish a log standard deviation, then using 0.4 as the log standard deviation for both indicators.

Marine Water

Based on a statistically sufficient number of samples (generally not less than 5 samples equally spaced over a 30-day period), the geometric mean of the enterococci densities should not exceed 35 per 100 ml.

No sample should exceed a one sided confidence limit using the following as guidance:

Designated bathing beach	75% C.L.
Moderate use for bathing	82% C.L.
Light use for bathing	90% C.L.
Infrequent use for bathing	95% C.L.

based on a site-specific log standard deviation, or if site data are insufficient to establish a log standard deviation, then using 0.7 as the log standard deviation.

[1]Only one indicator should be used. The regulatory agency should select the appropriate indicator for its conditions.

Table 2-6: US EPA criteria for full-contact recreation (US EPA, 1986)

2.2.7 The Blue Flag Campaign Guidelines

To indicate safe recreational water environments The Foundation for Environmental Education (FEE) as part of the Blue-Flag Campaign makes use of appropriate guidelines to assess water quality. Prior to 2003, the *EU Bathing Water Directive* (EEC, 1976), written in 1976, was used. Subsequently a new bathing water quality directive (COM, 2002) has been accepted that follows World Health Organisation guidelines for safe recreational water environments (WHO, 2001).

2.2.7.1 1976 EU Bathing Water Directive Guidelines

The guidelines as defined by the 1976 EU Bathing Water Directive are summarised as follows:

Parameter	Guideline Value	Accepted % test results higher than Guide value	Imperative values	Accepted % test results higher than Guide value
Total Coliforms	500 / 100ml	20 %	10000 / 100ml	5 %
Faecal Coliforms	100 / 100ml	20 %	2000 / 100ml	5 %
Faecal Streptococci	100 / 100ml	10 %	-	-

Table 2-7: 1976 EU microbiological bathing water quality criteria (EEC, 1976)

The 1976 EU Bathing Water Directive sets a required sampling regime.

- A minimum sampling frequency of one fortnight, being not less than 18 days.
- Sampling must be taken within 5 – 17 days prior to the start of the bathing season
- There must be at least 5 equally spaced samples taken over a bathing season, no matter how short the season may be.

2.2.7.2 2002 EU Bathing Water Directive Guidelines

The 2002 guidelines propose legally binding '*Good Quality*' and '*Excellent Quality*' 95-percentile values for Enterococcus and E.coli concentrations in bathing waters.

Microbiological Parameters	Excellent Quality (Guide)	Good Quality (Obligatory)
Enterococcus (CFU/100ml)	100	200
Escherichia coli (CFU/100ml)	250	500

Table 2-8: 2002 EU microbiological bathing water quality criteria (COM, 2002)

The 95-percentile value (V_{P95}) as defined in COM (2002) is calculated as follows:

1. Take the $\log_{10}$ value of all bacterial enumerations in the data sequence to be evaluated
2. Calculate the arithmetic mean of the $\log_{10}$ values (μ)
3. Calculate the standard deviation of the $\log_{10}$ values (σ)
4. The upper 95 percentile point (V_{P95}) of the data probability density function is derived as follows: $V_{P95} = 10^{(\mu + 1.65 * \sigma)}$

To analyse the quality of the bathing water, the previous three-year period of sampled data is required. Calculating the V_{P95} values for both E.coli and Enterococcus and comparing against the guideline values from Table 2-8 the water quality of bathing beaches are classified as follows:

1. If **EITHER** E.coli or Enterococcus are higher than the obligatory (Good Quality) value then the bathing water is classified as "***Poor Quality***"
2. If **BOTH** E.coli or Enterococcus are equal to or better (less) than the obligatory (Good Quality) value then the bathing water is classified as "***Good Quality***"
3. If **BOTH** E.coli or Enterococcus are equal to or better (less) than the guide (Excellent Quality) value then the bathing water is classified as "***Excellent Quality***"

2.2.7.3 South African Blue Flag Guidelines

The official position of FEE is that, for non-European countries, Blue Flag status will be awarded if the beach meets the host countries guidelines with respect to pathogenic pollution. Subsequently, South African beaches are evaluated using SA Marine WQ guidelines discussed in Section 2.2.4. The guidelines are similar to the 1976 EU Bathing Water Directive guidelines.

2.2.8 Conclusions and Recommendations

There is a worldwide trend towards using faecal streptococci or enterococci as the preferred indicator of pathogenic pollution in coastal marine waters. This is due to longer survival times of enterococci in marine environment as apposed to E. coli (Fattel et al, 1983; Prüss, 1998).

SA guidelines for marine recreation have similar criteria to the 1976 EU guidelines, in using E.coli as the indicator of pathogenic pollution in marine waters and in the water quality target ranges set. Subsequent to the start of this research, FEE have updated their water quality guidelines to those suggested by the World Health Organisation, this in turn indicates a need for South Africa to do the same. An interesting conclusion drawn from the WHO guidelines is that **Both** E.coli and Enterococcus should be used in classifying a beaches bathing water quality.

SA Water Quality Guidelines for inland Recreational waters compare favourably with those suggested by the US EPA.

2.3 Beach Water Quality Monitoring Organisations

2.3.1 eThekweni Metro

The water quality of Durban's beaches and other water resources incorporated in the eThekweni Metropolitan Area are managed by the eThekwini Municipality Water and Sanitation Services (EMWSS).

In order to maintain sustainable water resources, samples are taken from the main bathing beaches along Durban's coastline on a fortnightly basis. The local pollution sources are also monitored through the monthly sampling of urban stormwater drains and the Umgeni River.

Physical, chemical and biological analysis is performed on the water samples to determine the water quality. EMWSS are responsible for identifying possible contamination of water resources and for rectifying the problems. They are also responsible for informing the water users if for any reason they may be adversely affected by the use of the resource.

2.3.1.1 EMWSS Sampling Procedures

The sampling of the coastal waters and pollution sources are preformed by qualified EMWSS personal at the follow frequency:

1. Beaches - Fortnightly
2. Stormwater drains - Monthly
3. Rivers and channels - Monthly

Two samples are taken at each sampling position:

1. A sterilised glass bottle is used for biological analysis.
2. A plastic bottle is used for chemical analysis.

The beaches are sampled by the EMWSS as follows:

1. Samples are taken in approximately knee-deep water.
2. The containers are first rinsed out with a small volume of the water.
3. Special care is taken with the biological sample not to hold the glass bottle near the opening or to touch the inside of the screw-on cap.
4. The samples are then taken and labelled accordingly.
5. For biological reasons the glass bottle is stored in a closed cooler-box

Stormwater drains, rivers and channels are sampled using the sampling procedure described for the beach samples, except for the sampling position. Where possible the samples are taken directly from the water sources. In cases such as stormwater drains it may be impossible to get close enough to take a sample, thus a sampling bucket is used from which the samples are taken.

2.3.1.2 EMWSS Testing Procedures

Pathogenic pollution is determined by testing for E.coli and Enterococcus using standard methods (Clesceri et al, 1992) that enumerate the presence of indicator microorganisms with the counts reported in CFU per 100ml of water (EMWSS, 2002a; EMWSS 2002b)

The enumeration techniques make it impossible to accurately distinguish colony counts greater than approximately 40 colonies, due to the degree of crowding that occurs. Therefore, the method specifies that smaller samples of the 'polluted' water be used for culturing. The enumeration of the colony counts is done using the culture plate that comes closest to the criterion of 3-30 colonies per membrane.

The E.coli testing procedure suggests the following sample culture volumes based on experience gained with the samples from various sources:

1. Potable water - 100 ml
2. River water - 0.20 and 0.01 ml
3. Stormwater outfalls 1.0 and 0.2 ml
4. Beaches - 5 and 1 ml
5. Bathing pools - 100 ml

The Enterococcus method suggests that the analyst estimates the volume expected to yield a suitable membrane colony count (20 – 50) and select two additional volumes representing approximately one tenth and ten times this volume respectively. Analysis of the Enterococcus results provided by the EMWSS guidelines suggests that the volumes selected for culturing are usually those suggested by the E.coli testing procedure.

The colony counts are scaled by 'rounded up' and presented as colony forming units per 100 ml (CFU/100ml). An example of the rounding up procedure is:

$$CFU / 100ml = \frac{Count * 100}{Sample \quad size \quad (ml)}$$

2.3.1.3 Testing Procedures Errors and Uncertainties

The methods used to enumerate the indicator colony counts mean that the results have inherent errors and uncertainties associated with them. Siobhan Jackson of EMWSS reported that some literature does mention that a 1-log variance between samples is acceptable. However, duplicate tests performed at the EMWSS laboratory both inter-technician and intra-technician have found measurement errors of less than 10 percent, on average.

There are errors associated with the 'rounding up' of colony counts to CFU/100ml. The colony counts cultured at any given sample volume is limited to integer accuracy. When the count is rounded up to counts per 100ml there is a round-off error associated with the result. For example, if thirteen colonies were counted the errors would be:

- 13 counts @ 5ml cultured = 260 ± 10 CFU/100ml
- 13 counts @ 1ml cultured = 1300 ± 50 CFU/100ml

Problems arise when the counts within the water sample are higher than expected. The plates become uncountable and the actual pollution of the water body cannot be determined accurately. In this situation the results are given as greater than 39.9 colonies per specific volume cultured. For example:

- 5ml cultured = >799 CFU/100ml
- 1ml cultured = >3999 CFU/100ml

2.3.2 The Blue-Flag AWARD

The Blue Flag Campaign is owned and run by the independent non-profit organisation Foundation for Environmental Education (FEE). The Blue-Flag is an "eco-label" award that is a symbol of high environmental standards as well as good sanitary and safety facilities at a beach or marina. The Campaign includes environmental education and information for the public, decision makers and tourism operators.

The Blue-Flag award is based on a set of criteria involving beach management, safety, information and beach water quality (FEE, 2003). The Blue-Flag criteria and representative beaches may be viewed at http://www.blueflag.org

2.3.3 BEACH Watch

The US EPA initiated the Beaches Environmental Assessment, Closure, and Health (BEACH) Program in response to the growing concern about public health risks posed by polluted bathing beaches. The national program was initiated to protect public health at beaches, and to counteract the increasing frequency of beach closures due to public health concerns.

The BEACH program focuses on five target areas to meet the programs goals of improving public health and environmental protection programs for beach users and providing the public with information about the quality of beach water:

- Strengthening beach standards and testing
- Providing faster laboratory test methods
- Predicting pollution, with the use of models and other methods
- Investing in health and methods research
- Informing the public, with the use of online information etc.

More information of the BEACH Watch Program may be found at:
http://www.epa.gov/waterscience/beaches/index.html

2.4 Sources of Pollution

Pathogenic pollution in coastal waters can originate from a variety of sources. These include rainfall and groundwater runoff from the land or direct physical contamination of the coastal waters.

Organism	Concentration number /ml
Total coliform	10^5 - 10^6
Faecal coliform	$10^4 - 10^5$
Faecal streptococci	$10^3 - 10^4$
Salmonella	$10^0 - 10^2$
Enteric viruses	$10^1 - 10^2$

Table 2-9: Types and numbers of microorganisms found in untreated domestic waste (Metcalf and Eddy 1991)

Table 2-9 shows the concentration numbers of microorganisms one might expect to find in untreated domestic waste. Average figures are however misleading as sewage strength may vary according to the time of day and the amount of rainfall and/or infiltration. If the faecal coliform numbers are compared against the SA WQ Guideline the required dilution in each case may be calculated as indicated in Table 2-10.

Faecal coliforms

Guideline values: 100 CFU per 100ml in 80% of samples
2000 CFU per 100ml in 95% of samples

Concentration per ml = $10^4 - 10^5$
Concentration per 100ml = $10^6 - 10^7$

$10^4 - 10^5$ times dilution required for 100 CFU per 100ml
500 – 5000 times dilution required for 2000 CFU per 100ml

Table 2-10: Dilution required for untreated waste to satisfy SA Coastal WQ guidelines

Table 2-10 shows that the dilution may be less than 10^4 to 10^5 for only 20% of samples and less than 500 to 5000 and for only 5% of samples. With normal loading of aquatic systems the percentage of untreated waste to the receiving body is small enough to satisfy these criteria. However, when unnaturally large volumes of untreated waste enter the receiving water body or insufficient mixing occurs, then the dilution targets required might not be achieved resulting in high pathogenic pollution counts.

2.4.1 Urban Runoff and Stormwater Drains

> "Urban run-off is typically highly polluted with pathogenic and organic substances that are a public health threat" (Zoppou, 2000).

When rain falls on a watershed such as an urban area, it could either fall on an impervious or pervious area. On pervious areas some of the precipitation will infiltrate while the rest will form surface runoff, which will eventually be collected into stormwater drains and be discharged into a receiving water body, e.g. the sea. On impervious surfaces almost all the precipitation is converted into runoff, resulting in an increase in runoff volume and flow rates.

Pollution that may be found on the surfaces in the catchment are dislodged by the rain and transported by the runoff into the eventual receiving water body. The type of activity on the catchment dictates the volume of runoff and the types and quantities of pollutants within the runoff. The potential pollution levels will depend on the intensity and duration of the precipitation and the time since the last precipitation event (Zoppou, 2000).

The source of urban runoff pollution is not restricted to pollution found on the catchment surface. The failure of urban infrastructure can result in sewer infiltration, leachate from landfills, and direct connection of sewers to stormwater drains, which can have serious pollution implications for the receiving water bodies. Sewer infiltration through burst pipes is usually associated with high rainfall events. The diversity of the source and types of pollutants encountered in an urban catchment makes the prediction of stormwater pollution extremely complex.

2.4.1.1 The First flush Phenomena

The "First flush" (FF) is the runoff that occurs at the beginning of a rain event. It is generally thought to be more pronounced on impervious surfaces. The first flush carries with it concentrations of pollutants that have accumulated during the period of dry weather between rain events. Thereafter further runoff carries less and less pollution as the duration of the storm continues.

The first flush is an important consideration in the design of stormwater treatment plants. Since most of the pollution is carried within the first flush, only the volume of the first flush needs to be treated and the subsequent runoff may be ignored. Traditionally the "first half-inch rule" is used, namely that for impervious cover 90 percent of the total pollution load is contained within the runoff of the first half-inch of rainfall (ECSD, 1990). Further research has however shown this to be a poor assumption.

ECSD (1990) found that for a development with a 90 percent impervious cover the first half-inch of runoff of a larger storm may only remove on average about 40 percent of the total pollution load.

Schueler (1994) reported that the half-inch rule worked effectively for most stormwater pollutants for sites with less than 50 percent impervious cover. However it was found that above 50 percent impervious cover the pollutant load captured dropped off sharply. For sites with 70 percent impervious cover only 78 percent of the annual pollutant load was captured, while for 90 percent cover it dropped to 64%.

Figure 2-1 and Figure 2-2 are regenerated figures from ECSD (1990) which show the total annual percentage of Faecal coliform bacteria and Streptococci at increasing runoff levels from varying levels of surface cover imperviousness.

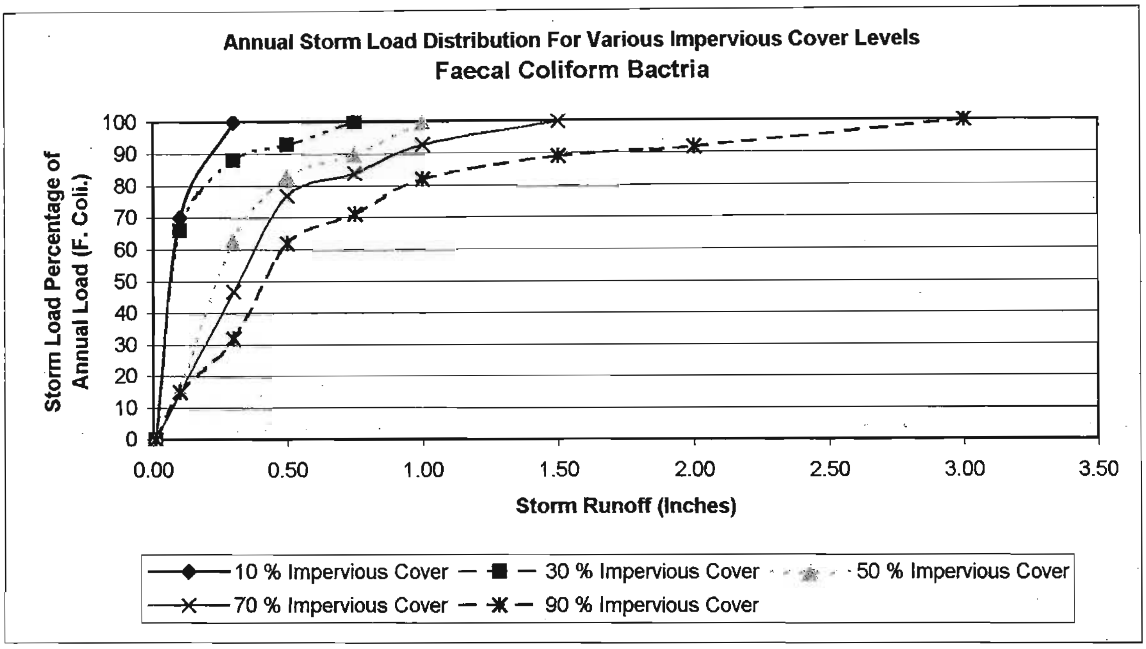

Figure 2-1: Annual storm load distribution for various impervious cover levels - Faecal Coliform Bacteria (ECSD, 1990)

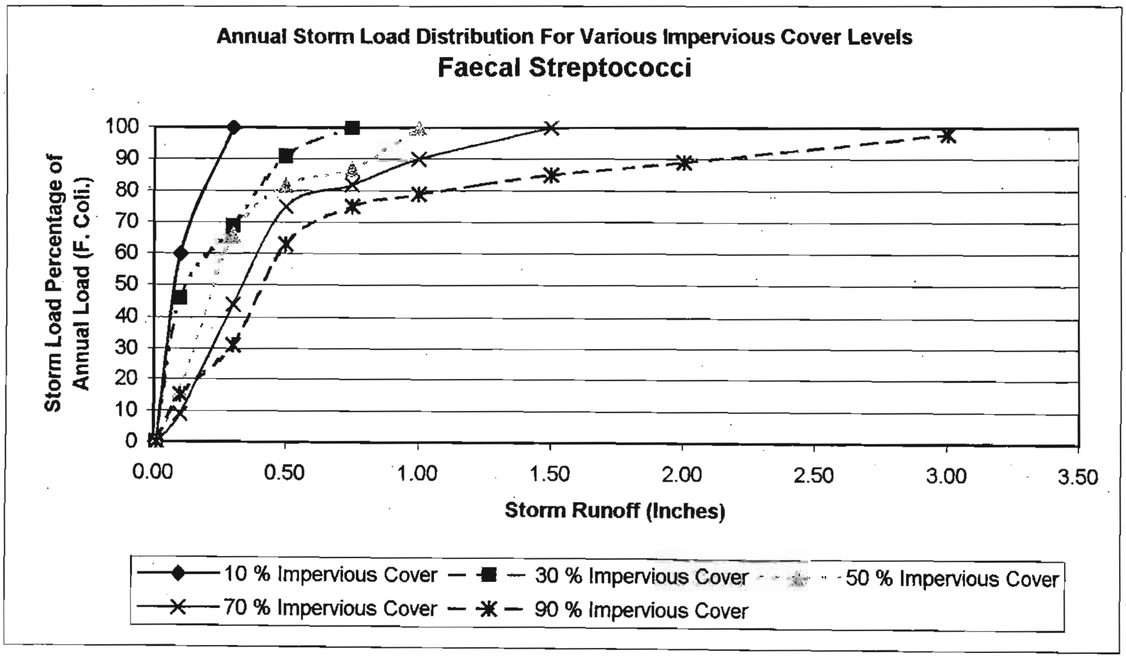

Figure 2-2: Annual storm load distribution for various impervious cover levels - Faecal Streptococci (ECSD, 1990)

2.4.1.2 Modelling Urban Storm Water Runoff

An internationally accepted model for modelling of urban stormwater is the US EPA Storm Water Management Model (SWMM). SWMM is a dynamic rainfall-runoff simulation model, primarily but not exclusively for urban areas, applicable to single-event or long-term (continuous) simulation. It is one of the most successful models produced by EPA for the water environment. It may be used for analysis of quantity and quality problems related to stormwater runoff, combined sewers, sanitary sewers, and other drainage systems in urban areas, with many applications in non-urban areas as well. It may also be used for planning, design and area-wide control and impact assessment. (Storm Water Management Model, 2003)

The SWMM model was considered as a model to produce the stormwater input for predicting the pathogenic pollution of coastal waters. Detailed information about the drains was needed as well as loading rates and factors. The less information available, the poorer the stormwater estimates. It was therefore decided that the model would be overly complex and require information unavailable under present conditions. It was decided that alternative, more simplistic, methods should be developed.

2.4.2 Rivers

Rivers can be major sources of pollution to the nearshore region. The pollution potential that a river poses depends on a variety of factors such as the size of the river, developments along the river, type of developments, etc. Rivers can introduce large volumes of freshwater into the nearshore region. Therefore, even if the river is moderately polluted the shear volume of water can have serious water quality implications for marine receiving waters.

With the development of urban and industrial areas, rivers have traditionally acted as conduits of pollution through legal and illegal practices. Through natural processes anything that is added to a river higher up in a catchment will eventually find its way to the coast and could lead to the pollution of the nearshore region. For example, Water purification schemes deal with the treatment of urban wastewater. The schemes process the raw wastewater and then need to dispose of the treated water. Rivers are normally used to dispose of the treated water. The quality of the discharged water is usually closely monitored under strict guidelines. Under normal conditions, although the treated water is still polluted to a certain degree, the effect on the river is not detrimental. Problems can however arise when excessive rains and floods increase the volumes of untreated wastewaters beyond the capacity of the schemes. When this happens, untreated wastewater sometimes bypasses the treatment works and enters the river untreated.

In SA untreated wastewater is also a problem with informal settlements and townships adjacent to rivers and streams. In these areas no wastewater treatment is provided and raw sewage can enter the rivers and streams directly.

Industrial wastewaters are also (both legally and illegally) discharged into local water sources such as rivers and streams. These can include toxic waste that can have serious public health concerns.

The pollution level present in rivers is complex and often unpredictable, requiring complex models.

2.5 Physical Dynamics of Pollution Mixing and Dispersion

The nearshore region of the coastline is a complex dynamic natural system. The physical processes such as currents and mixing may vary from one position to another due to factors such as: nearshore bathymetry, shape of the coastline, and man-made structures such as piers, groynes, etc.

The outflows from rivers and stormwater drains tend to be less saline and hence lighter than the ambient coastal waters, a plume typically forms as the buoyant water spreads away from the mouth of the river outfall. Surface freshwater plumes can be particularly sensitive to the wind stress because they are thin (AGU, 1995). An idea of the mixing and advection processes that occur within the nearshore region is illustrated in Plate 2-1 and Plate 2-2, which show the freshwater plumes from the Mtamuna and Tongati River during the 1987 KwaZulu Natal floods.

Plate 2-1: Mtamuna River during 1987 floods (CSIR, 1989)

The advection processes within the Mtamuna River mouth region was to the North (right) as indicated by the muddy brown freshwater plume. However, the advection processes prevalent at the Tongati River were to the South (left).

Plate 2-2: Tongati River during 1987 floods (CSIR, 1989)

An important concept to note is how the freshwater plume stays within the nearshore zone propagating along it rather than mixing further out to sea. The mixing between the nearshore and deeper waters is inhibited due to stratification caused by differences in salinities and temperature (AGU, 1995). Freshwater plumes can also be dramatically affected by the orientation of wind stresses (Chao, 1998). Masse and Murthy (1990) showed that downwelling-favourable winds concentrate the plume in a narrow current adjacent to the coast, while upwelling-favourable winds tend to restrict the coastal current forcing the plume to spread offshore and thin at the mouth region. The consequence of this is that mixing with ambient ocean water is enhanced during upwelling favourable winds, while during downwelling favourable winds mixing is inhibited (AGU, 1995). The mixing timescales between the nearshore zone and deeper water are much longer than those of the advection processes. Although these photographs were taken during flood conditions, the behaviour of the nearshore zone with respect to the freshwater plume will be the same under normal conditions.

Freshwater enters the nearshore zone from rivers as well as stormwater drains and contains varying levels of pollution. The pollution would be advected along coastline similar to fresh water plume, depending on the magnitudes and direction of the advection and mixing processes.

2.5.1 Wind Driven Surface Currents

Wind propagating across a water body surface due to the shear stress induced at the air-water interface generates waves and causes a drift current.

At low wind velocities, where the wind is influenced by surface friction and by the form drag of the capillary waves, the wind drives the surface current directly or through the micro-breaking and viscous dissipation of the capillary waves, in which the energy is lost in turbulence and eventually dissipated and the corresponding wave momentum enhances the surface current (Tsanis, 1987). At higher wind speeds the breaking of gravity waves adds considerably to the energy dissipation and contributes to the mixing of the surface waters (Tsanis, 1987).

Mardon (2000) investigated the cross-currents at the Port of Durban entrance, using data from an acoustic doppler current profiler (ADCP). It was found that the near-shore currents can be divided into two basic depth regimes: The surface current in the top 2 to 3 meters and a sub-surface current below 4 meters depth. It was shown that the surface current is strongly dependant on local wind conditions.

Wu (1974) showed that a ratio between the wind-induced surface drift velocity, V_a, and the wind friction velocity, u_{*a}, may be found which varied between 0.4 and 0.7. The following empirical expression was obtained:

$$\frac{V_n}{u_{*a}} \approx 0.53 \qquad (2\text{-}1)$$

Zhan and Hisashi (1992) indicated that the surface drift current may be intensified by the existence of opposing swell when swell steepness increase. However the surface drift current was not intensified where swell propagated in the direction of the wind. The average values calculated over the range of the experiment were as follows:

Pure wind waves: $$\frac{V_n}{u_{*a}} \approx 0.53 \qquad (2\text{-}2)$$

Swell propagating opposed to wind direction: $$\frac{V_n}{u_{*a}} \approx 0.65 \qquad (2\text{-}3)$$

Swell propagating in the direction of the wind: $$\frac{V_n}{u_{*a}} \approx 0.46 \qquad (2\text{-}4)$$

Wu (1974) presented a graph, reproduced in Figure 2-3, which shows the variation of wind-induced, and wave-induced currents at increasing fetch lengths. The 3 different lines in Figure 2-3 represent different wind velocities (U_y) of 5, 10 and 20 m/s measured at an elevation above the water surface. The elevation height, y, was proposed by Wu (1971) to be

$$y = \begin{cases} 7.34 * R^{\frac{2}{3}} * 10^{-7} m & R < 5*10^{10} \\ 10m & R > 5*10^{10} \end{cases} \qquad (2\text{-}5)$$

where

$$R = \frac{U_y L}{v_a}$$

The variable R is the fetch Reynolds number; U_y is the wind velocity at the proposed height and L is the wind fetch distance.

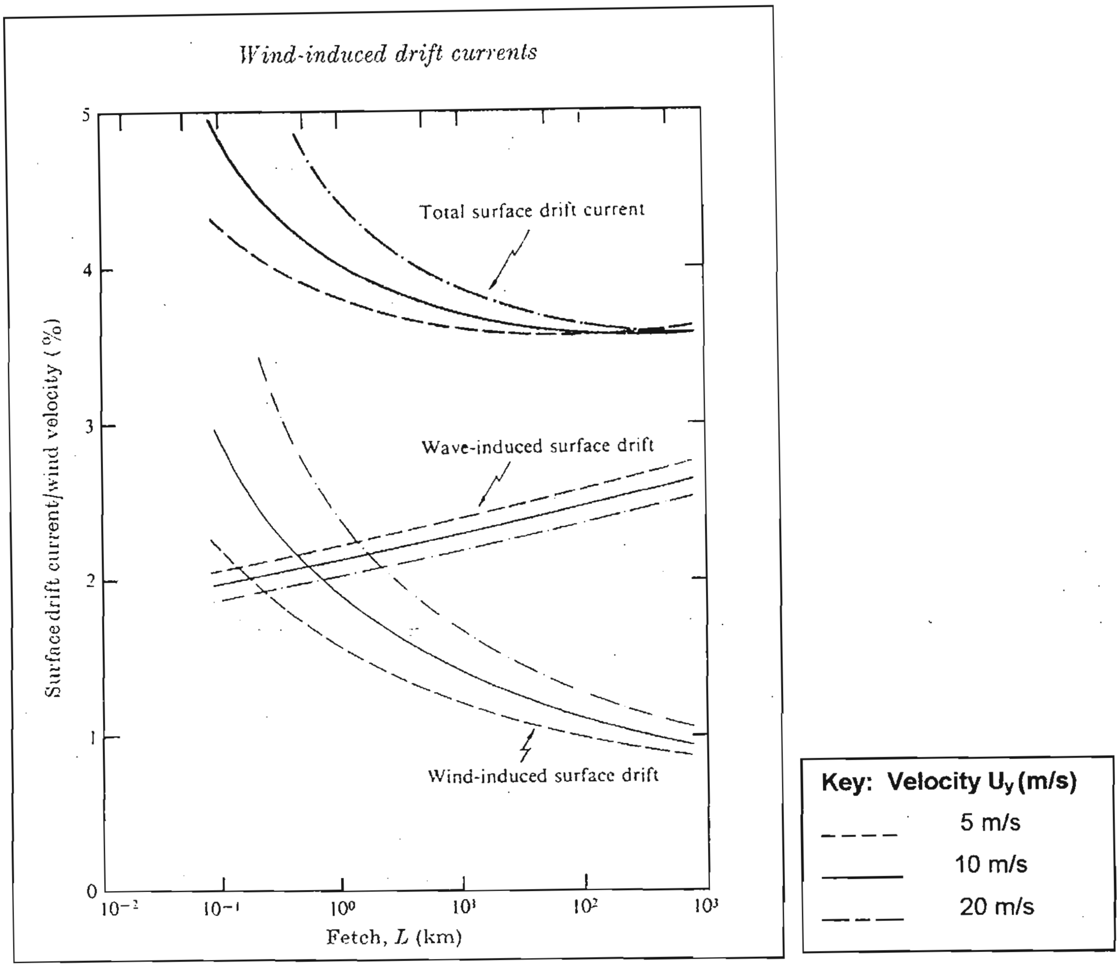

Figure 2-3: Variation of wind-induced and wave-induced surface drift currents with fetch (Wu, 1974)

Considering Figure 2-3 it is evident that with exception of very short fetch lengths, the total surface current is predominantly wave-driven. The ratio between the surface drift and the wind velocity decreases gradually as the fetch increases and approaches a constant value of about 3.5% at very long fetches (Wu, 1974).

The longer and harder the wind is propagated across the water surface, the deeper the wind generated surface current will penetrate the water column. Mardon (2000) showed the following trends when correlating the currents with the winds within the surface current regime:

1. The strongest correlation between the averaged surface current and the wind was found when considering winds of 8 m/s or more, and when using a 40-minute lag between the current and wind.
2. The deeper the current, the higher the wind speed required for correlation and the longer the lag time between the wind and current.

2.5.2 Longshore Currents

Longshore currents are generated by the interaction between breaking waves and the coastline. When waves propagate obliquely to a beach there is a mean flux of long-shore momentum and the gradients act as a driving force for the mean longshore current.

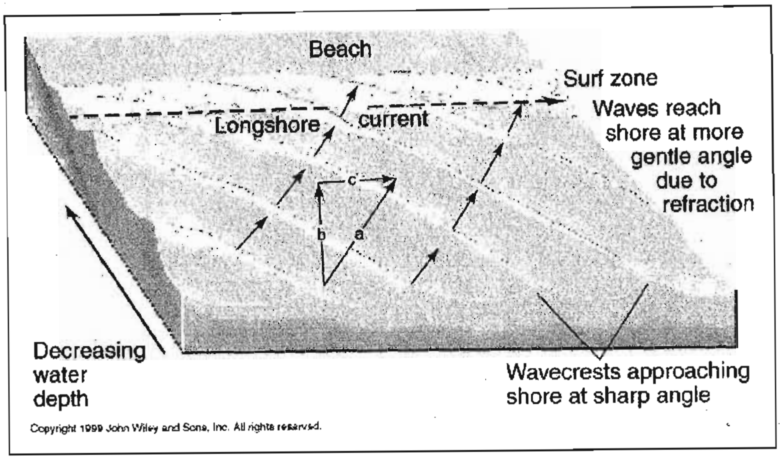

Figure 2-4: Wave forcing of longshore current (Skinner et al, 1999)

The longshore current is the main factor responsible for the littoral drift of sand along the coastline, which depending on incident wave directions, frequencies and heights is able to move large volumes of sand. For example the sand-pumping scheme at Durban requires the annual pumping of 600000m^3 of sand to replenish the beaches since the natural littoral drift is cut off by the construction of a breakwater at the Port of Durban entrance (Laubscher, 1990).

2.5.3 Rip Currents

Rip Currents are strong surface currents flowing seaward from the shore in the upper layer of the water column. A rip current is usually visible as a band of agitated water that is the return movement piled up on the shore by incoming waves and wind. When the side current meets an obstacle like a sandbar, channel, hole, rock jetty or pier the flow of water is diverted away from the beach forming a rip current. Therefore shore protection structures will normally have rip currents associated alongside them.

> "A rip current consists of three parts: the feeder currents flowing parallel to the shore line inside the breaker zone; the neck, where the feeder currents converge and flow through the breakers in a narrow band or "rip" (neck); and the head, where the current widens and slackens outside the breaker line." (CEM, 2002)

Typical nearshore circulation including rip currents is shown schematically in Figure 2-5.

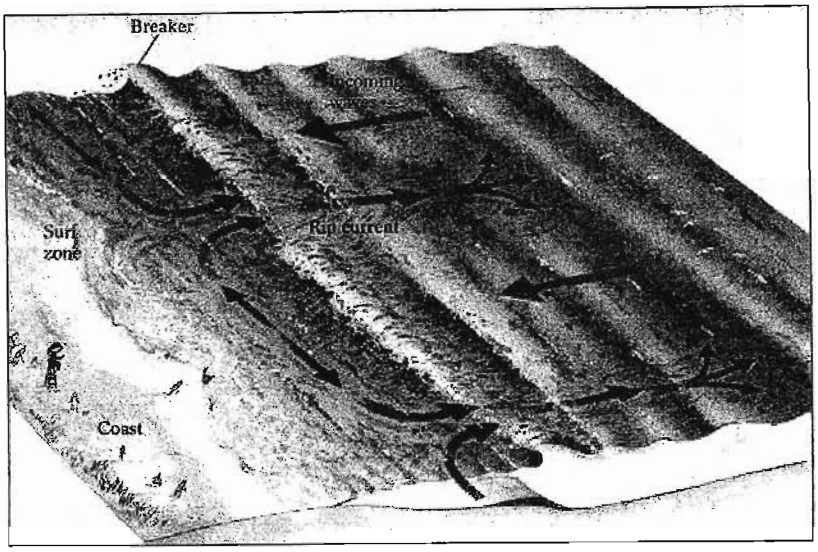

Figure 2-5: Illustration of Rip Currents (Anderson, 2002)

2.5.4 Conclusions

It has been shown that the nearshore currents within the region of interest are a complex combination of interactions between environmental forces such as winds and waves and the physical nature of nearshore region.

The wind has a measurable effect on the water body in the generation of surface currents. The longer and harder the wind is sustained in a constant direction the more a current is generated, even at short fetch lengths.

Wave direction, height and frequency all have an effect on the generation of longshore currents whose direction may be inferred from the angle between the waves and the coastline. Shore protection structures designed to retard beach erosion have an effect on the currents that propagate along the coastline, which may need to be taken into account in any modelling process.

Rip currents can increase the mixing of the nearshore region by removing the surf zone surface water and transporting it offshore.

2.6 Microbiological Processes

The main reason for modelling coliforms is to provide a method of predicting the level of potential pathogenic pollution. Coliform levels are generally estimated as a function of their initial loading and disappearance rate. The disappearance rate is usually a function of time and distance travelled from the source and other environmental factors such as light intensity, water temperature, salinity etc (US EPA, 1985).

2.6.1 Factors Affecting Disappearance Rates

Once coliforms are introduced into the water environment, the environmental conditions of that environment determine to what extent the coliform numbers may change due to regrowth or mortality. The factors that determine the change of the coliform levels can be classified into three categories: physical, physicochemical and biochemical-biological. Other factors that may cause faecal coliforms and streptococci number to appear to increase may be the disaggregating of clumps of organisms (US EPA 1985).

2.6.1.1 Physical Factors

The physical factors that may result in changes in coliform populations in natural waters include: Photo-oxidation, Adsorption, Flocculation, Coagulation, Sedimentation and Temperature.

Light, with its role in photo-oxidation, has always been considered one of the most statistically significant factors in coliform population changes. Chamberlin and Mitchell (1978) found that statistically significant relationships could be found between light intensity and coliform disappearance rates. However they also observed that it was difficult to show statistically significant relationships between coliform disappearance rates and many other factors usually hypothesized to affect the coliform disappearance rates.

Work by Sieracki (1980), Kapuscinski and Mitchell (1983) and Lantrip (1983) has shown that while enteric bacterial pathogens and viruses are also light dependent, viruses are generally less sensitive than coliforms and may not be accurately modelled by coliform decay rates (US EPA, 1985).

Adsorption, coagulation, flocculation and sedimentation may affect the coliform disappearance rates (US EPA, 1985). However there is a lack of quantitative data available to support this. Adsorption is the attachments of coliform bacteria to suspended particles while coagulation is the coalescence of bacteria into clumps and flocculation is the formation of soft, loose aggregates incorporating much water. Sedimentation is the settling of bacterial particles and aggregate from the water medium.

Temperature is an important factor, because it is able to influence almost all other mechanisms (US EPA, 1985). Lantrip (1983) proposed that temperature might be the single most important modifier of decay rates.

2.6.1.2 Physicochemical Factors

The Physicochemical factors that may result in changes in the coliform population in natural waters include: Osmotic effects, pH, Chemical toxicity and Redox potential.

US EPA (1985) states that survival rates of E. coli in natural seawater and artificial salt solutions are inversely proportional to the salinity levels. It was documented that in general, E. coli had been found to survive longer in lower pH salt solutions (pH < 8) than under alkaline conditions.

2.6.1.3 Biochemical and biological Factors

The Biochemical and biological factors that may result in changes in coliform population within natural waters include: Nutrient levels, Presence of organic substances, Predators, Bacteriophages, Algae and Presence of faecal matter.

2.6.2 Modelling Biological Processes

2.6.2.1 Simple First-Order Kinetics Approach

A long-established method for modelling the coliform evolution is to use a simple first-order kinetics approach (Chamberlin and Mitchell, 1978).

$$\frac{dC}{dt} = -kC \tag{2-6}$$

$$C_t = C_0 e^{-kt} \tag{2-7}$$

where

C	= Coliform concentration, in CFU of counts /100ml
C_0	= Initial coliform concentration, in CFU of counts /100ml
C_t	= Coliform concentration at time t, in CFU of counts /100ml
k	= Disappearance rate, in hr^{-1}
t	= Exposure time, hours

US EPA (1985) presents a listing of coliform bacteria disappearance rates from various studies measured in situ in freshwater which summarised the work of Mitchell and Chamberlin (1978). The summarized table gives a median rate for the in situ studies of 0.04 hr^{-1}(25 hrs) with 60 percent of the values less than 0.05 hr^{-1}(20 hrs) and 90 percent less than 0.22 hr^{-1}(4.5 hrs).

2.6.2.2 Modified First-Order Kinetics Approach

Frost and Streeter (1924) in their work on the Ohio River found that the log decay of coliforms was non-linear with time. The simple first order decay expression given by equation (2-6) is only an approximation of the actual decay process and may overestimate or underestimate dC/dt as a function of time.

> "One approach to solving the problem of a time-variable decay rate is to decompose the death curve into two components, each having their own decay rate (Velz, 1970)" (US EPA, 1985).

The decay of the coliform is therefore modelled as a combination of two decay processes, namely:

$$C_t = C_0 e^{-kt} + C'_0 e^{-k't} \tag{2-8}$$

where

C_t	= Coliform concentration at time t, in counts /100ml
C_0, C'_0	= Concentrations of the two hypothetical organisms, in counts /100ml
k, k'	= Decay rates for the two organisms, day
t	= Exposure time, days

US EPA (1985) gives values for the parameters (for E. coli) in equation (2-8) taken from Phelps (1944) that are reproduced in Table 2-11

Parameter	Warm Weather	Cold Weather
C_0 (Percent)	99.51	97
k (1/day)	1.075	1.165
Half-life (day)	0.64	0.59
C'_0 (Percent)	0.49	3
k' (1/day)	0.1338	0.0599
Half-life (day)	5.16	11.5

Table 2-11: Values for the combination decay process in Ohio River (Phelps, 1944)

From Table 2-11 the T-value, in hours, which is equal to k^{-1}, is roughly equal to 25.7 hours for warm weather and 27.2 hours in cold weather.

In an effort to attempt to produce more accurate predictions of coliform counts, Lombardo (1972) formulated the dynamics of the coliform population, including streptococci, with separate first-order expressions. US EPA (1985) showed a summary of the decay rates reported by Lombardo (1972), which is reproduced in Table 2-12.

Indicator	Num	Median		Minimum		Maximum	
		k (1/hr)	T (hr)	k (1/hr)	T (hr)	k (1/hr)	T (hr)
Total Coliforms	16	0.038	26.3	0.01	100.0	0.105	9.5
Faecal Coliforms	13	0.048	20.8	0.008	125.0	0.13	7.7
Faecal Streptococci	5	0.007	142.9	0.002	500.0	0.063	15.9

Table 2-12: Summary of decay rates reported by Lombardo (1972) (US EPA, 1985)

2.6.2.3 Light-dependent Disappearance Rate Coefficient

The incident light levels have a strong influence on coliform decay rates as mentioned before. It would therefore be prudent to estimate the incident light levels at various levels in the water column in order to accurately estimate the decay rates. Chamberlin and Mitchell (1978) suggested a light depth-dependent disappearance rate coefficient as (US EPA, 1985)

$$k' = k_l I_0 e^{-\alpha z} \tag{2-9}$$

where

k' = Light dependent coliform disappearance rate, hr^{-1}

k_l = Proportionality constant for the specific organism, cm^2/cal

I_0 = Incident light energy at the surface, cal/cm^2-hr

α = Light attenuation coefficient per unit depth

z = Depth in units consistent with α

If the water column is assumed vertically mixed, a depth-averaged decay rate may be calculated using the depth-averaged light intensity as (US EPA, 1985):

$$\overline{I} = I_0 \left(\frac{1 - e^{-\alpha H}}{\alpha H} \right) \tag{2-10}$$

where

$\overline{k}$ = Depth-averaged light-dependent disappearance rate, hr^{-1}, such that $\overline{k} = k_l \overline{I}$

$\overline{I}$ = Depth-averaged light intensity, $cal/cm^2/hr$

H = Depth of the water column with units consistent with α

Laboratorial and field research studies have been undertaken to understand and clarify the proportionality constants of individual organisms. Table 2-13 summarises the findings reported in US EPA (1985).

Organism	Study	k_l (cm^2/cal)	Data Source
Faecal Coliform	Estimated from a field and lab studies	0.042	Mancini (1978)
	22 Chamber study		Lantrip (1982)
	Mean	0.005	
	Minimum	0.000	
	Maximum	0.011	
Escherichia coli	4 Field studies		Gameson and Gould (1975)
	Mean	0.362	
	Minimum	0.321	
	Maximum	0.385	
	4 Lab studies		Gameson and Gould (1975)
	Mean	0.354	
Faecal Streptococci	3 Lab. Studies		Gameson and Gould (1975)
	Minimum	0.048	
	Maximum	0.123	
	12 Field studies		Foxworthy and Kneeling (1969)
	Mean	0.091	
	Minimum	0.004	
	Maximum	0.184	
	23 Chamber studies		Lantrip (1982)
	Mean	0.008	
	Minimum	0.001	
	Maximum	0.028	

Table 2-13: Selected organism k_l estimates from studies (US EPA, 1985)

2.6.3 T_{90} Decay Rate Investigation

The T_{90} timescale is the time required for faecal coliform counts to decrease by one decimal logarithm. Faecal coliform behaviour is a function of several parameters such as salinity, turbidity, sunlight radiation etc. The value of the T_{90} decay rate varies over a large scale, from 1 hour or less to several days (Guillaud et al, 1997).

The T_{90} timescales may be utilised in the simple first-order kinetic equation by relating it to the decay rate k.

$$k = \frac{\ln 10}{T_{90}} \qquad (2\text{-}11)$$

Guilaud et al. (1997) conducted field tests on the French coast with the aim of producing an "abacus" for engineers that would allow T_{90} values to be approximated with respect to local conditions. It was found that the T_{90} value (hrs) was related to the light intensity ($\mu Em^{-2}h^{-1}$) that was received by bacteria chambers at varying water depths which was calculated using Lamberts Law, which determines how much of incoming light energy is reflected. Whence

$$T90 = a * \left\{ I_0 \left[\frac{\left(1 - e^{-k_w h}\right)}{k_w h} \right] \right\}^b \qquad (2\text{-}12)$$

Where h = depth (m), k_w = extinction coefficient (m^{-1}) and I_0 = energy absorbed by the seawater surface ($\mu Em^{-2}h^{-1}$) and values for the parameters were estimated as a = 53683 and b = -0.666.

The extinction coefficient was related to the suspended solids (SS) in mg/l present in the water by:

$$k_w = 0.189 * SS^{0.799} \tag{2-13}$$

Using the light intensity experienced along the South African coastline, the range of T_{90} and subsequent k-decay rates may be calculated for yearly, seasonal and monthly time periods and used for modelling. (See Section 3.6.3)

2.6.4 Conclusions

The first-order kinetic approach to the coliform decay is a widely accepted approach to estimating pathogenic pollution levels. This approach is therefore appropriate for application in the present context.

The incident light levels experienced by the coastline should be used in order to obtain reasonable estimates for the respective indicator decay coefficients and feasible ranges for these coefficients.

2.7 Predictive Water Quality Modelling Techniques

Decision makers experience difficulties when attempting to advise bathers of the risk during periods of poor water quality. Consequently the users of recreational beaches may often be exposed to potentially high waterborne pathogens levels. The primary cause may be low frequency of monitoring beach water quality levels. Poor water quality is only identified at the time of sampling so that detrimental levels during the unmeasured period may remain undetected. Another factor is the 24 to 48 hours delay in testing water samples. This means that the response time for decision makers to advise bathers of possible risks or to close beaches is at best 24 to 48 hours after the samples are taken.

Models are therefore needed to give an indication of possible water quality conditions.

2.7.1 Predictive methods Utilised in the BEACH Program

As part of the BEACH program, the US EPA reviewed a number of predictive methods that were currently being used or could be used (US EPA 1, 1999). It was found that the models that were being employed fell into two approach categories. Although there were two different approaches they both shared the same objective; to reduce the risk of illness due to exposure of users to water high in pathogen concentration.

The first approach was using simplistic models based on simple relationships between observed rainfall and pathogen concentration levels. An example is using regression analysis to relate rainfall to pathogen concentration. The models developed using this method are usually highly site-specific in their application, as they are derived from locally observed relationships between water quality and rainfall data.

The second approach involved deterministic type models. These models involve the complex modelling of the dominant mixing and transport processes in order to predict the possible water quality conditions based on a selected set of environmental and physical data.

It is important to note that it was found that in most cases the predictive tools were not used exclusively but were usually combined with water quality monitoring. It was found that the two processes were dependant on one another. It was also noted that once the modelling approach was proven to provide reliable water quality predictions the frequency of the water quality sampling could be reduced.

The US EPA report reviewed four types of Water quality models that were currently being used. These were:

1. Rainfall-based Alert Curves.
2. Point Source-Dominated Steady-State Predictive Tools.
3. Point Source-Dominated Dynamic Predictive Tools.
4. Hydrodynamic Mixing Zone Models.

2.7.1.1 Rainfall-based Alert Curves.

Rainfall-based alert curves (RBAC) are simplistic, "type-1" models. The objective of rainfall-based alert curve models is to establish a statistical relationship between rainfall events and pathogen concentrations. The relationships then serve as a management tool for developing the operational guidelines or predicted pathogen concentrations requiring beach advisories or closures.

The key rainfall characteristics that are required for the development of the RBAC are:

1. Amount of rainfall, in inches
2. Storm duration, in hours
3. Inter-event periods (dry days)
4. The lag time between rainfall events and receiving beach response, in hours
5. The season(s) of high usage of the beach resources

Kuntz (1998) showed that when non-point source pollution was being considered the antecedent rainfall conditions could be a very significant factor in explaining the relationship between rainfall and pathogen concentrations. It was found that higher pathogen concentrations were encountered during periods of low rainfall than during periods of normal rainfall.

Regression models can be developed for several pathogen species; however faecal coliform, E. coli and Enterococcus bacteria are the most common indicator species used in RBAC models (US EPA 1, 1999). The following are a few examples of beach closure guidelines based RBACs derived for the respective regions (US EPA 1, 1999).

City of Milwaukee
Guidelines for beach closure
• 48-hour closure after 0.3 to 0.69 inches of rainfall
• 72-hour closure after 0.7 to 1.49 inches of rainfall
• 96-hour closure after 1.49 inches of rainfall or more
• 96-hour closure in cases where a 48-hour or 72-hour advisory was already in effect

Table 2-14: City of Milwaukee beach closure guidelines (US EPA 1, 1999)

City of Stamford
Guidelines for beach closure under:
Normal rainfall conditions
• 24-hour closure after a rainfall event of 1 inch or more
Low rainfall / drought conditions
• 24-hour advisory following rainfall event ≥ 0.5 inches
• 24-hour closure after a rainfall event of 1 inch or more

Table 2-15: City of Stamford beach closure guidelines (US EPA 1, 1999)

The disadvantages of RBAC are that they are site specific and their development requires large monitoring data sets of both rainfall and water quality. If the catchment characteristics of either the pathogen loading or runoff were to change, the previously derived RBAC would not be applicable. The RBAC models also do not explicitly include the advection and diffusion processes thus they do not account for the spatial distribution of pathogens.

2.7.1.2 Point Source-Dominated Steady-State Predictive Tools.

The Simple Mixing and Transport Model (SMTM) was developed for the Virginia Bureau of Shellfish Sanitation (Hamerick et al. 1989). The model was designed to assist in the estimating of marina buffer zones to reduce the potential contamination of shellfish beds in the region. The buffer zones are based on the concentration of total faecal coliform in the water column. It was noted that although the SMTM was developed for estimating marina buffer zones, it may be applicable to the impacts of point source discharges on other recreational activities such as bathing (US EPA 1, 1999).

The SMTM is a steady state / tidally averaged simulation model based on a mixing and transport formulation. The decay of pathogens is modelled using the first-order decay function. The model algorithm predicts the horizontal distribution of pathogen concentrations and assumes a uniform distribution of pathogen concentrations in the vertical direction. The SMTM consists of three modelling options: wide river module, narrow channel module and the semi-enclosed bays or basins module.

An example of the calculation of buffer zones is given in US EPA (1999a). Of interest is the proposed decay coefficient, k_d, = 10^{-5} s^{-1} to describe the first-order decay of the pathogen concentration, with a corresponding decay timescale of approximately 28 hours (equation 2- 1).

The SMTM model was not deemed applicable to the current project because the region of interest was an open coastline. The model was formulated for enclosed or semi-enclosed water bodies, therefore not deemed applicable to an open coastline.

2.7.1.3 Point Source-Dominated Dynamic Predictive Tools.

An Example of a Point Source-Dominated Dynamic Predictive model is the Regional Bypass Model (RBM) developed to determine the impact of bacterial discharges on shellfish and beaches due to untreated wastewater in New York Harbour.

The objective of the model was to allow a rapid evaluation of water quality condition and determine impact areas where either increased monitoring frequency or temporary closure of recreational activities or shellfish harvesting was required. The model uses a known discharge and simulates the effect on the water quality at specific sensitive areas. The RBM is based on the System-Wide Eutrophication Model (SWEM) developed by the New York City Department of Environmental Protection (US EPA, 1999a). A first-order kinetic model is used to model the indicator or pollution concentration. The bacteria selected were the total coliform group, however other bacteria such as faecal coliform bacteria or enterococcus might be approximated using proportionality ratios (US EPA, 1999a).

The model output is given as maximum bacteria concentrations for 12-hour intervals beginning at the start of the discharge.

This type of model was not deemed applicable for the current project, because it relies heavily on knowing the exact pollution discharge into the region. In the current context the inputs remain effectively unknown during the modelling process (see Section 3.4).

2.7.1.4 Hydrodynamic Mixing Zone Models

Hydrodynamic Mixing Zone models provide a simulation of the mixing and transport processes. The models discussed in the US EPA Review are CORMIX3, PLUMES, and the JPEFDC model (US EPA 1, 1999).

The models are complex models and a major disadvantage of their implementation is that they require extensive input information about the discharge characteristics and receiving water body.

2.7.2 Potential Models to be utilised in the BEACH Program

The US EPA review (US EPA 1, 1999) identified possible models that may be utilised by the beach program. The models fell into two categories.

1. Watershed-Scale Loading Models: HSPF, SWMM & STORM
2. Receiving Water Models: Stream / River: CE-QUAL-RIV1, QUAL-2E & HSPF
   Lake / Estuary: CE-QUAL-ICM, CE-QAUL-W2, WASP, TPM & EFDC

These models all require extensive input data and require special effort for validation and calibration (US EPA 1, 1999).

2.7.3 Conclusions

The choice of the correct model to make predictions of water quality conditions will depend on the quality of the input data. Running a sophisticated model with poor input data will generally give poor results.

The RBAC type models although useful for beach closure management would not be appropriate in the present context due to the site-specific nature of their derivation and the lack of information on the spatial distribution of pathogens.

The SMTM approach is useful, however, the model is suited to a river or enclosed basin type region and not designed for use modelling an open coastline.

The RBM is not applicable as it is intended to provide information in a *what-if* manner. In the present context there is a need for a *what-now* type real-time prediction model. These models also require specific knowledge of the pollution entering the system, which at present is not available.

More complex models may be calibrated for specific runoff regions but to provide real-time predictions for an entire coastline with minimal data available, these models are overly complex.

CHAPTER 3:

ANALYSIS OF THE STUDY SITE COASTAL ENVIRONMENT

3.1 Introduction of the Sampling Beaches

The EMWSS samples the beaches along the length of eThekweni Metro's Coastline, from Sipingo Beach in the south to Umhlanga Rocks Main Beach in the North. The beaches that were of interest were those along the "Golden Mile" section of Durban's coastline, from Vetches Pier Beach in the south to Umgeni South Beach in the north.

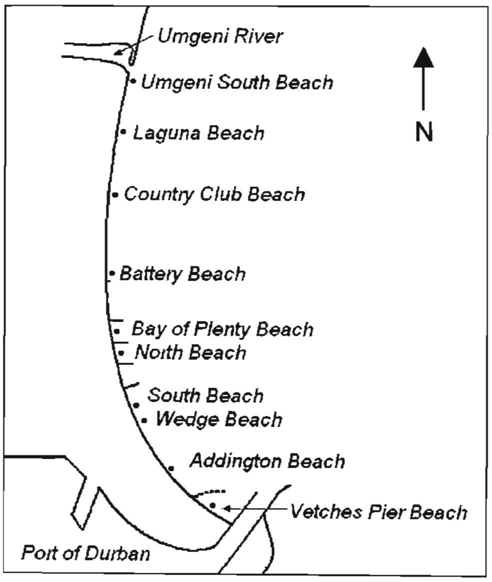

Figure 3-1: Approximate positions of the sampling beaches

Vetches Pier Beach

Vetches Beach is the first beach after the North Pier at the Port of Durban entrance. The name comes from the Vetches Pier, which is an old quay that is exposed at low tide.

Plate 3-1: Vetches Pier Beach looking northwards

This beach is not a designated bathing beach, however the southern end of the beach is where water sports enthusiasts launch small yachts, windsurfers and jetskis. Vetches Pier is also a favourite site for underwater activities such as snorkelling and scuba diving.

Addington Beach

Addington Beach is approximately 1 km north from the Port of Durban Entrance and is the most southerly designated bathing beach along the "Golden Mile".

Plate 3-2: Addington Beach looking southwards

This beach supports all forms of recreation and is often used as a venue for regional and national lifesaving contests.

South Beach

Durban's South Beach is the only beach in Durban to be awarded Blue Flag status by FEE. This beach is directly in front of some of the most prestigious hotels along the "mile". South beach is shown in the background of Plate 3-3 (in front of the blue and white building).

Plate 3-3: Wedge and South Beach looking southwards

Wedge Beach

Wedge Beach is shown in the foreground of Plate 3-3 (to the left of the jetty remains). The beach does not have a designated bathing area (manned by lifeguards) however is used for other full contact recreational activities (such as surfing, bodyboarding, etc.).

North Beach

North Beach is the stretch of beach running from the Bay of Plenty Pier in the North to the North Beach Pier (New Pier) in the South.

Plate 3-4: North Beach looking southwards

This is one of Durban's more famous beaches and currently hosts an international Pro-surfing event and the world's only night surfing event in July (winter). The beach is used as a bathing, bodyboarding and sunbathing beach year-round.

Bay of Plenty Beach

Bay of Plenty Beach is situated between Bay of Plenty Pier in the south and Somtseu stormwater drain in the north.

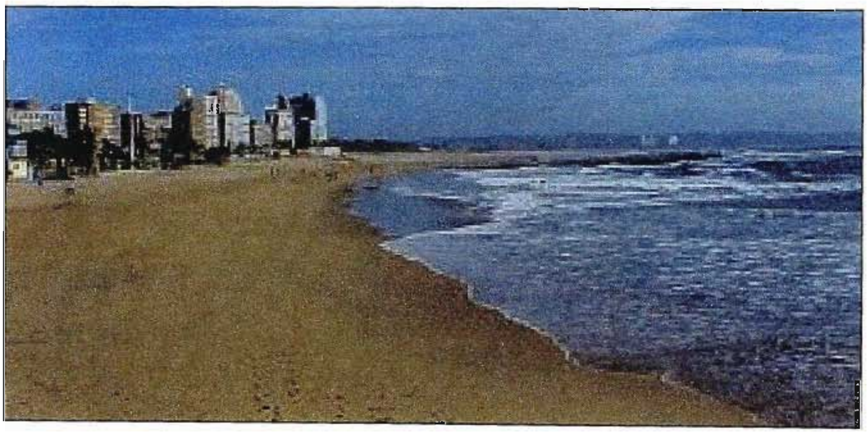

Plate 3-5: Bay of Plenty Beach looking northwards

Bay of Plenty Beach is a designated bathing beach and is used year round for swimming, sunbathing and surfing.

Battery Beach

Battery Beach runs from the Argyle Road stormwater drain in the south, to Oasis Beach in the north. It is a designated bathing beach and supports the Pirates Surf Lifesaving Club.

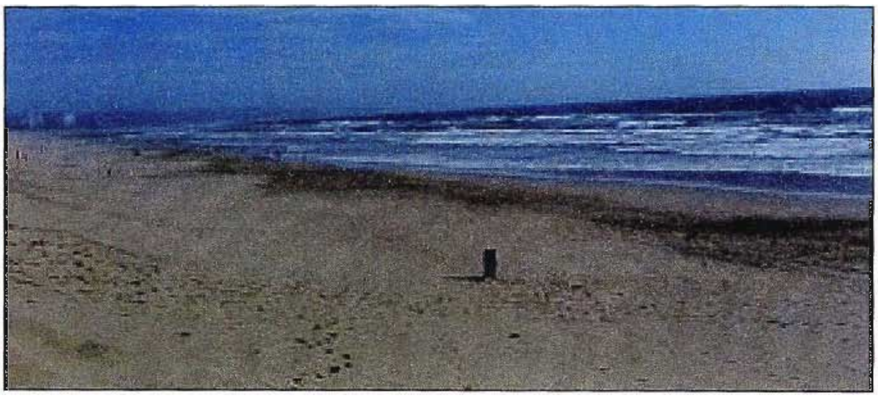

Plate 3-6: Battery Beach looking northwards

Country Club Beach

Country Club beach runs from the Walter Gilbert stormwater drain outfall in the south, northwards. It is also referred to as Sunkist Beach and supports the Sunkist Surf Lifesaving Club.

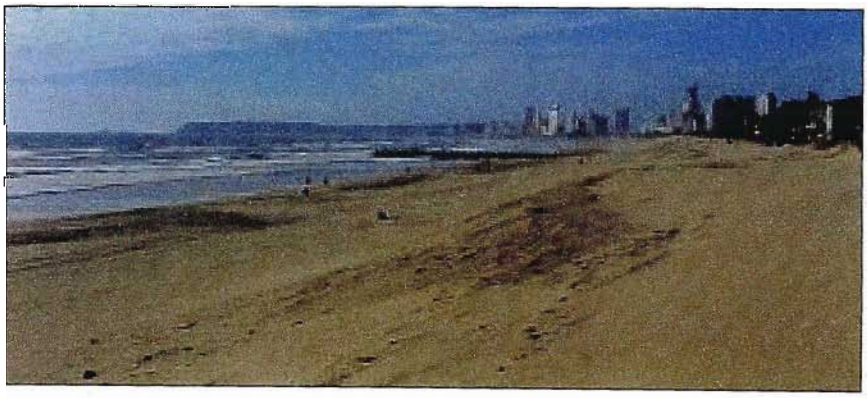

Plate 3-7: Country Club Beach looking southwards

The beach is a designated bathing beach but also supports kite activities, jetskiing and other water and beach activities.

Laguna Beach

Laguna beach is situated approximately 1km south of the Umgeni River Mouth. Laguna Beach has paddling pools and slides so that recreational activities and bathing are not restricted to the sea.

Plate 3-8: Laguna Beach looking southwards

The coastline running from the Walter Gilbert stormwater drain on the southern side of Country Club Beach to the Umgeni River mouth is uninterrupted by piers or stormwater drains. This combined with the wide flat beach area makes this stretch of coastline a magnet for kite related activities.

Umgeni South Beach

Umgeni South Beach is situated just south of the Umgeni River mouth and is the last beach sampling point considered in this study.

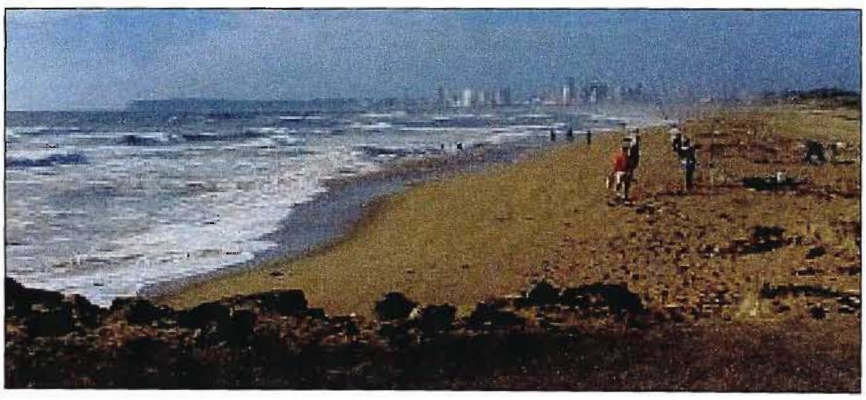

Plate 3-9: Umgeni South Beach looking southwards

This beach is not a designated bathing or recreational beach due to its close proximity to the Umgeni River mouth and often poor water quality. Accidental contact with the water is expected as this beach is used extensively for angling and other such activities.

3.2 Water Quality Analysis of the Sampling Beaches

Beach water quality sampling is undertaken by EMWSS on a fortnightly basis. The two microorganisms E.coli and Enterococcus were used to determine the pathogenic pollution levels of the beaches under consideration. The sampled periods for the two indicators analysed in this study are as follows:

1. E.coli data for the period January 1995 to August 2002 was analysed.
2. Testing for Enterococcus only started in March 1999, so Enterococcus data for the period March 1999 to August 2002 was analysed.
3. Wedge Beach is an exception as it has only been sampled from June 2000. Therefore, for this beach, for both E.coli and Enterococcus, the period June 2000 to August 2002 was analysed.

The results of the beach analysis were compared against water quality standards existing in South Africa with respect to coastal waters. The beaches were also compared against South African Inland Water Quality standards, as well as US EPA and EU set criteria for recreational bathing waters. The standards are discussed in Section 2.2, and specific application notes are noted below:

Definition of Specific Analysis Periods

Annual statistics are based on the full data set while seasonal values are calculated by grouping the data according to season: Summer (December to February), Autumn (March to May), Winter (June to August), and Spring (September to November).

SA and EU WQ Standards for Marine Recreation

The South African and European Union standards only consider E. coli as the indicator of pathogenic pollution. The guidelines are set with respect to certain exceedance criteria.

1. No more than 20% of the samples should exceeded 100 counts per 100ml
2. No more than 5% of the samples should exceeded 2000 counts per 100ml

SA WQ Standards for Recreation (Inland Waters)

The South African Inland guidelines set a target water quality range, which the geometric mean of the samples should not exceed. The limits are set for the two indicator organisms are:

1. The geometric mean of E. coli must be lower than 130 counts per 100ml
2. The geometric mean of Enterococcus must be lower than 30 counts per 100ml

Although these guidelines are set for inland (fresh) waters they are applied to the marine environment because they set a guideline with respect to Enterococcus.

US EPA Standards for Bathing Waters

The US EPA standards are set using two criteria:

1. Using the geometric mean of the samples.
2. A single sample maximum concentration with respect to the degree of use of the specific bathing beach.

A problem arose in the application of the EPA standards. The guidelines require that the geometric mean be calculated using at least 5 equally spaced samples over a 30-day period. The sampling of Durban beaches is done on a fortnightly basis; at most only 3 samples may be expected over a 30-day period. Consequently, only sections of the guideline criteria, with respect to the geometric mean, can be applied. The geometric mean could be calculated using either: 5 equally spaced data points or a 30-day period of data points. While it is understood that pathogenic pollution may survive longer than the indicator organisms, to force closure of a beach due to a single high count sampled more than 30 days previously seems extremely conservative. Therefore the geometric mean is calculated using an approximate 30-day sampling window comprising a minimum of three samples.

Geometric mean analysis of the beach-sampled data was done both seasonally and annually. The results are compared against the EPA guidelines to see whether there are seasonal or annual trends to the failure of water quality conditions of specific beaches.

For marine bathing waters, Enterococcus is the preferred indicator. Unfortunately, regular testing for Enterococci in bathing waters was only begun in 1999 resulting in only a few years of available data. Freshwater E. coli limits have therefore been included in the analysis of the beaches. By comparison with other guideline criteria and results, a judgement can be made on whether this is appropriate.

1. For marine waters the Enterococcus limit is set at 35 counts/100ml.
2. For fresh waters the E. coli limit is set at 126 counts/100ml.

To calculate the single sample concentration limits (SSL), log-standard deviations ($\sigma_{\log}$) of 0.7 and 0.4 have been used for Enterococcus and E.coli (fresh water) respectively. The calculation of these limits is as follows:

$$SSL = 10^{\left[Log(\mu_{Limit}) + factor * \sigma_{\log}\right]} \qquad (3\text{-}1)$$

The appropriate factors for the one-sided confidence level are:

Beach Use	C.L.	Factor	Log-Standard Deviation		Single sample count limit (cfu/100ml)	
			E.coli	Enterococcus	E.coli	Enterococcus
Designated bathing beach	75%	0.675	0.4	0.7	235	105
Moderated use for bathing	82%	0.935	0.4	0.7	298	158
Light use for bathing	90%	1.280	0.4	0.7	410	275
Infrequent use for bathing	95%	1.650	0.4	0.7	576	500

Table 3-1: Single sample limit values depending on beach bathing use

Statistical parameters

Statistical parameters used to analyse the beach sampling sets were:

The geometric mean: $$GM = \sqrt[n]{\prod_{i=1}^{n} x_i} \qquad (3\text{-}2)$$

or

$$\ln(GM) = \frac{1}{n}\sum_{i=1}^{n} \ln x_i \qquad (3\text{-}3)$$

The arithmetic mean or average: $$\bar{x} = \frac{1}{n}\sum_{i=1}^{n} x_i \qquad (3\text{-}4)$$

The standard deviation: $$\sigma = \sqrt{\frac{1}{n-1}\sum_{i=1}^{n}\left(x_i - \bar{x}\right)^2} \qquad (3\text{-}5)$$

The 95 percent confidence Interval: $$\bar{x} \pm 1.650\frac{\sigma}{\sqrt{n}} \qquad (3\text{-}6)$$

3.2.1 General Statistics Analysis Results

The average pathogenic pollution concentration of the beach sampling positions should give understanding of the dynamics of the nearshore coastal system. The summary of the average E.coli and Enterococcus concentrations are presented in Table 3-2 and Table 3-3. The values in brackets display a relative ranking position, with respect to the beaches and the seasons. For example (4-2) means that: the beach has the 4th largest average with respect to other beaches for that season; and the season has the 2nd largest average with respect to the other seasons for that beach.

	Annual	Summer	Autumn	Winter	Spring
Vetches Pier Beach	58 (9--)	47 (7-2)	47 (6-2)	85 (8-1)	39 (8-4)
Addington Beach	287 (4--)	47 (7-2)	39 (8-4)	547 (3-1)	41 (7-3)
South Beach	42 (10--)	44 (9-2)	38 (9-3)	51 (9-1)	34 (9-4)
Wedge Beach	77 (7--)	18 (10-4)	27 (10-3)	130 (7-1)	55 (6-2)
North Beach	67 (8--)	117 (6-1)	45 (7-3)	49 (10-2)	31 (10-4)
Bay of Plenty Beach	157 (6--)	174 (5-2)	112 (5-4)	178 (6-1)	165 (4-3)
Battery Beach	1682 (2--)	1206 (2-2)	2973 (1-1)	294 (4-3)	222 (2-4)
Country Club	253 (5--)	318 (4-1)	272 (3-2)	267 (5-3)	94 (5-4)
Laguna Beach	584 (3--)	443 (3-2)	212 (4-3)	1027 (2-1)	182 (3-4)
Umgeni South Beach	2385 (1--)	2730 (1-2)	2277 (2-3)	2828 (1-1)	1511 (1-4)

Table 3-2: Average E. coli concentration of sampling beaches (CFU/100ml)

For both E.coli and Enterococcus, the last four beaches have the worst average pathogenic pollution concentration. Therefore, it appears that the closer the beach is to the Umgeni River, which is just north of Umgeni South beach, the worse the average pathogenic pollution at the beaches becomes. The most polluted beach on average appears to be the Umgeni South beach, which was expected due to its close proximity to the river. The second most polluted sampling site and most polluted designated bathing beach is Battery beach, which is most likely linked to the Argyle Road stormwater drain, just south of the sampling position.

The Durban coastline falls within a summer rainfall region. It was assumed that since the source of most pathogenic pollution was from stormwater and river runoff, the poorest water quality should occur during the summer rainfall period. However, Table 3-2 reveals that, except for Country Club, Battery and North Beach, the largest average E.coli concentrations actually occur during the winter months. The summer months have on average the second largest E.coli averages. Battery beach, which should be closely linked to rainfall due to its proximity to the Argyle stormwater drain, has the largest average E.coli concentration during the autumn months. The winter average is almost twice that of the summer seasons average.

	Annual	Summer	Autumn	Winter	Spring
Vetches Pier Beach	29 (9--)	32 (8-2)	27 (6-3)	34 (8-1)	22 (10-4)
Addington Beach	47 (6--)	30 (9-2)	23 (9-4)	101 (5-1)	27 (7-3)
South Beach	28 (10--)	35 (7-1)	26 (8-3)	27 (9-2)	23 (8-4)
Wedge Beach	34 (7--)	22 (10-3)	13 (10-4)	60 (7-1)	37 (6-2)
North Beach	32 (8--)	59 (6-1)	27 (6-2)	26 (10-3)	23 (8-4)
Bay of Plenty Beach	63 (5--)	86 (5-1)	52 (5-3)	69 (6-2)	48 (5-4)
Battery Beach	379 (2--)	386 (2-2)	757 (2-1)	190 (3-3)	145 (2-4)
Country Club	125 (4--)	180 (4-1)	136 (3-2)	122 (4-3)	66 (4-4)
Laguna Beach	205 (3--)	320 (3-1)	118 (4-3)	286 (2-2)	105 (3-4)
Umgeni South Beach	989 (1--)	1635 (1-1)	995 (1-3)	1029 (1-2)	463 (1-4)

Table 3-3: Average Enterococcus concentrations of sampling beaches (CFU/100ml)

The Enterococcus indicator shown in Table 3-3 suggests a closer link to the rainfall. The beaches that are directly affected by the river and stormwater inputs (Bay of Plenty to Umgeni South) have the largest average Enterococcus concentrations during the summer rainy season.

The exception to this is Battery Beach whose maximum occurs in the autumn season. For the first five beaches (Vetches to North Beach) the difference between the largest and second largest is less apparent. However, there seems to be a pattern where the further away from the river the beach is situated, the greater the likelihood that the winter season has poorer water quality than the summer period.

3.2.2 SA Marine Recreational Water Quality Standards

The exceedance percentages of the SA WQ guideline concentration levels are given in Table 3-4 (100 CFU/100ml) and Table 3-5 (2000 CFU/100ml).

Designated Bathing	Annual	Summer	Autumn	Winter	Spring
Vetches Pier	7%	8%	6%	9%	5%
Addington	6%	11%	2%	6%	7%
South	6%	8%	4%	8%	2%
Wedge	8%	0%	0%	13%	15%
North	8%	18%	4%	8%	2%
Bay	13%	15%	15%	17%	2%
Battery	34%	28%	41%	40%	27%
Country Club	20%	26%	22%	17%	16%
Laguna	28%	47%	24%	22%	18%
Umgeni South	48%	72%	48%	38%	40%

Table 3-4: Exceedance of the SA WQ criteria 1 (100 CFU/100ml)

Designated Bathing	Annual	Summer	Autumn	Winter	Spring
Vetches Pier	0%	0%	0%	0%	0%
Addington	1%	0%	0%	2%	0%
South	0%	0%	0%	0%	0%
Wedge	0%	0%	0%	0%	0%
North	0%	0%	0%	0%	0%
Bay	0%	0%	0%	0%	0%
Battery	3%	5%	8%	0%	0%
Country Club	0%	0%	0%	0%	0%
Laguna	1%	0%	0%	2%	0%
Umgeni South	12%	21%	16%	11%	2%

Table 3-5: Exceedance of the SA WQ criteria 2 (2000 CFU/100ml)

The summer and autumn seasons usually have the greatest proportion of unacceptable water quality. It can be seen that all beaches from Vetches to Bay of Plenty satisfy both of the SA WQ guideline exceedance levels. The remaining beaches (Battery to Umgeni South) exceed the first guideline value annually and for most seasons, since more than 20% of the samples are greater than 100 CFU/100ml. Umgeni South exceeds the second guideline limit annually and for most seasons, spring being the exception. Battery Beach annually has less than 5% of samples greater than 2000 CFU/100ml, however during spring and autumn the limit is exceeded.

Battery Beach is the most problematic bathing beach since it fails both SA WQ criteria during the summer and autumn. North beach did not fail any of the exceedance criteria annually, however during summer 18% of samples were greater than 100 CFU/100ml. This should be of concern as bathing beaches are used intensively during the summer holiday period. Bay of

Beach is another beach were the percentage of samples greater than 100 CFU/100ml are only marginally less than the SA WQ limit.

3.2.3 US EPA Geometric Mean Analysis Results

The results of the beach WQ analysis with respect to the US EPA GM guideline limits for freshwater E.coli and marine Enterococcus are shown in Table 3-6.

Indicator	Escherichia coli		Enterococcus
Start Date	Jan-1995	Mar-1999	Mar-1999
End Date	Aug-2002	Aug-2002	Aug-2002
Vetches Pier Beach	0.0%	0.0%	6.4%
Addington Beach	0.0%	0.0%	4.9%
South Beach	0.0%	0.0%	6.1%
Wedge Beach	0.0%	0.0%	9.6%
North Beach	0.0%	0.0%	3.6%
Bay of Plenty Beach	3.8%	4.7%	5.9%
Battery Beach	29.0%	44.2%	33.7%
Country Club	9.5%	11.0%	19.5%
Laguna Beach	17.9%	25.3%	20.5%
Umgeni South Beach	50.9%	63.4%	63.4%

Table 3-6: Percentage exceedance of geometric mean E.coli (SA Inland) and Enterococcus (US EPA Marine) standards.

Battery beach is again seen to be the most polluted bathing beach, with the US EPA GM limits exceeded for approximately one third of the time.

The most interesting result concerns the difference between an assessment based on E.coli and Enterococci for the beaches from Vetches Pier to North. E.coli analysis indicates that the GM limit is never exceeded at those locations, whilst Enterococcus analysis indicates that the GM limit is exceeded for between 3% and 10% of samples. This suggests that Enterococcus is the more sensitive indicator of pollution for this marine environment, especially for beaches that have generally low E.coli indicator concentrations.

It is further interesting to note that in comparing the E.coli GM exceedance for periods 1995-2002 and 1999-2002, it is evident that the pollution of the beaches has increased in recent years.

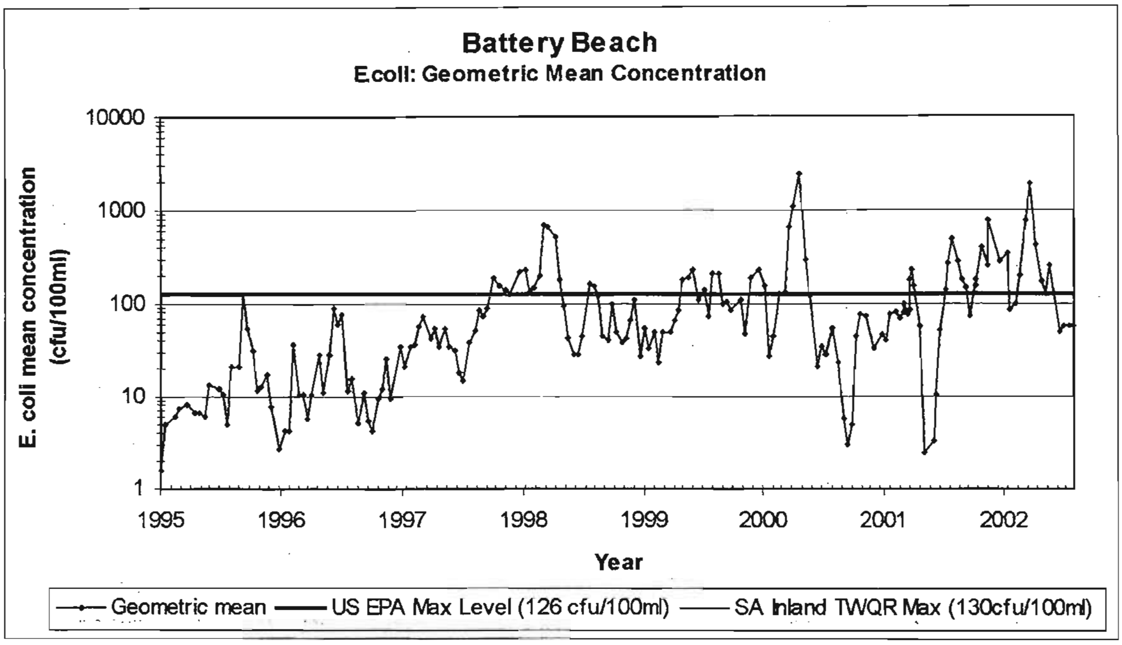

Figure 3-2: Geometric mean E.coli concentrations at Battery Beach (1995 to 2002)

The individual calculated geometric mean E.coli concentrations for battery beach from 1995 to 2002 are shown in Figure 3-2. It is evident that since 1995 the water quality has been getting progressively worse and that from mid-1997 the geometric mean for Battery Beach began to regularly exceed the US EPA and SA Inland limits.

3.2.4 US EPA Single Sample Limits

The application of SSL requires the specification of the "use" of the beaches. Therefore, beaches from Addington to Battery beach they are specified as "Designated bathing". Vetches, Country Club and Laguna Beach are specified as "Moderate use for bathing". Umgeni South beach, although not a bathing beach, is specified as "Infrequent use for bathing" to quantify the risk to users of beaches in the vicinity of the Umgeni River mouth.

Exceedance percentages for the Enterococcus SSL (accounting for the "use category" of the beaches) are shown in Table 3-7.

Designated Bathing	**Annual**	**Summer**	**Autumn**	**Winter**	**Spring**
Addington	4%	7%	0%	5%	6%
South	7%	7%	10%	5%	6%
Wedge	4%	0%	0%	10%	8%
North	6%	27%	0%	0%	0%
Bay	4%	14%	5%	0%	0%
Battery	23%	27%	32%	20%	11%
Moderate Use	**Annual**	**Summer**	**Autumn**	**Winter**	**Spring**
Vetches Pier	7%	7%	9%	0%	13%
Country Club	13%	20%	14%	5%	13%
Laguna	11%	29%	5%	11%	6%
Infrequent Use	**Annual**	**Summer**	**Autumn**	**Winter**	**Spring**
Umgeni South	25%	53%	29%	16%	6%

Table 3-7: Exceedance of the US EPA SSL for Enterococcus

Generally the summer season experiences the highest exceedance of the SSL (Enterococcus); the exceptions are Battery Beach (Autumn), South Beach (Autumn), and Vetches Pier Beach (Spring). Battery beach has the highest SSL exceedance of all the beaches (27% in summer and 32% in autumn). North beach may be problematic since although the SSL is exceeded annually in 6% of samples, all exceedances occur during the summer season (27%).

3.2.5 2002 EU Bathing Water Directive Guidelines

The 2002 EU bathing water directive states that a 3-year record of sampled indicator concentrations should be utilized for determining the quality of beach bathing waters. The period from November 1999 to August 2002 was analysed.

The 95th - percentile values for E.coli and Enterococcus, calculated in accordance with the 2002 EU Directive, are shown in Table 3-8 and Table 3-9 respectively.

Beach	Annual	Summer	Autumn	Winter	Spring
Vetches	161	151	122	219	168
Addington	187	301	62	536	107
South	119	142	94	185	47
Wedge	158	61	69	385	181
North	157	233	149	192	73
Bay of Plenty	249	432	311	200	102
Battery	2353	5555	5241	799	1224
Country Club	536	1196	614	465	353
Laguna	1083	1846	675	872	1404
Umgeni South	5383	9190	8111	2979	1517

Table 3-8: 95th-percentile analysis results for E.coli

The 95% E.coli values calculated for the beaches from Battery to Umgeni South beach exceed the "obligatory" limit of 500 CFU/100ml. The exception is Country Club Beach whose winter and spring 95% values fall below the "obligatory" level. Addington beach exceeds the 95% value during winter. The "guide" level (250 CFU/100ml) is exceeded at Bay of Plenty (Summer), Wedge (Winter) and Country Club (Winter And Spring) Beach.

Beach	Annual	Summer	Autumn	Winter	Spring
Vetches	219	271	113	85	548
Addington	148	188	79	144	219
South	141	130	158	129	136
Wedge	100	93	77	127	114
North	97	218	62	56	51
Bay of Plenty	108	217	104	68	88
Battery	649	891	1143	236	1175
Country Club	292	818	223	346	155
Laguna	438	1913	315	400	112
Umgeni South	1634	3852	1151	1114	793

Table 3-9: 95th-percentile analysis results for Enterococcus

Annually and seasonally the beaches from Battery to Umgeni South beach exceed the "obligatory" Enterococcus level (200 CFU/100ml), with the exception of during spring where the 95% values for Country Club and Laguna only exceed the "guide" level (100 CFU/100ml). The "obligatory" level is exceeded at Vetches Beach (annual, spring & summer), Addington Beach (spring), North beach (summer) and Bay of Plenty (summer). It is interesting to note that the 95% "obligatory" and "guide" Enterococcus values were exceeded at more beaches than was the case for the analysis using E.coli.

An overall assessment of Durban's bathing waters for the period August 1999 to August 2002, according to EU guidelines, is shown in Table 3-10.

Beach	Annual	Summer	Autumn	Winter	Spring
Vetches	Poor	Poor	Good	Excellent	Poor
Addington	Good	Good	Excellent	Poor	Poor
South	Good	Good	Good	Good	Good
Wedge	Good	Excellent	Excellent	Good	Good
North	Excellent	Poor	Excellent	Excellent	Excellent
Bay of Plenty	Good	Poor	Good	Excellent	Excellent
Battery	Poor	Poor	Poor	Poor	Poor
Country Club	Poor	Poor	Poor	Poor	Good
Laguna	Poor	Poor	Poor	Poor	Poor
Umgeni South	Poor	Poor	Poor	Poor	Poor

Table 3-10: EU Water Quality Assessment of Durban Waters (1999 – 2002)

Annually, North beach is the only beach to achieve an overall "Excellent" rating, while the beaches from Addington to Bay of Plenty Beach were found to have acceptable pathogenic pollution levels. Seasonally however the EU assessment varies substantially, with Addington beach failing during the winter and spring and North and Bay of Plenty beach failing during summer.

Using the 2002 EU guidelines, Battery Beach is yet again shown to be the most polluted bathing beach along Durban's coastline. The "poor" rating of the waters at battery beach suggest that this beach should not be used as a designated bathing beach. It is also of concern that particularly during summer, which is usually a more active bathing period, a large number of the designated bathing beaches have "poor" water quality assessments.

Note that the Enterococcus limits were usually the critical factor in defining the beach water quality of the designated bathing beaches.

3.2.6 Conclusions

A ranking of Durban's beaches that summarizes the results of our analysis is given in Table 3-11.

WQ Assessment	First Place	Second Place	Third Place
SA WQ	South	Addington	Vetches
US EPA GM	North	Addington	Bay of Plenty
US EPA SSL	Wedge	Addington	Bay of Plenty
2002 EU	North	Wedge	South
Overall	***North***	***Addington***	***Bay of Plenty***

Table 3-11: Durban's top water quality beaches (using annual assessments)

North Beach has the overall best water quality in terms of pathogenic pollution, with Addington Beach and Bay of Plenty Beach ranking second and third respectively. It is interesting that South Beach, which has been awarded "Blue-Flag" status, only ranks highest when E.coli is used as the sole indicator of pollution. However, when Enterococcus is used, South Beach does not rank as highly.

Overall the beaches that are most used by the public and that are closely linked to tourism have acceptable water quality. A disturbing exception is Battery that has been found to be the most polluted of all the designated bathing beaches and fails all water quality guideline limits on both an annual and a seasonal basis. A reduction in the unacceptably high levels of pathogenic pollution (as indicated by E.coli and Enterococcus concentration levels) is required, failing which this beach should be closed to bathing. Also worrying is the fact that during summer North Beach and Bay of Plenty Beach are close to failing the first SA WQ criteria, have significant percentages of samples exceeding the US EPA SSL and are found to have a "poor" EU WQ assessment.

Laguna and Country Club beaches, although not as bad as Battery, also often exceed water quality standards. Efforts should therefore be made to reduce the pollution levels at these beaches. However, since the main source of this pollution seems to be the Umgeni River, which has a large catchment area, significant improvement may be difficult to achieve in the short term.

Applying the US EPA and EU guidelines the results show that Enterococcus limits usually provide the more rigorous constraint i.e. beaches often exceed Enterococcus guideline values whilst being below E.coli limits. As previously noted, epidemiological studies have shown that Enterococcus is a more reliable indicator of pathogenic pollution in marine waters (Fattal et al, 1983; Prüss, 1998). The SA Water Quality guidelines should therefore be updated to incorporate Enterococcus as the main indicator organism for marine environments.

3.3 Introduction to the Urban Stormwater Drains

Major sources of pathogenic pollution to Durban's coastal marine zone are urban stormwater drains. There are six such urban stormwater drains (SWD) along the section of coastline under investigation and all are monitored by the EMWSS. The relative positions of the stormwater drains to the relevant EMWSS sampling beaches are indicated in Figure 3-3.

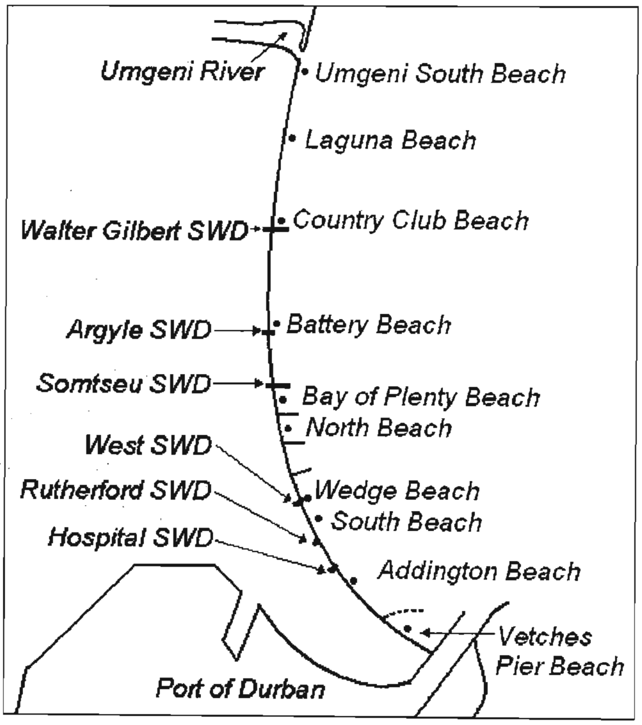

Figure 3-3: Illustration of the position of the SWD under investigation

The urban stormwater drains are (from south to north):

- **Hospital SWD** – which outfalls 200 m – 400 m north of the Addington Beach sampling position. See Plate 3-10.
- **Rutherford Road SWD** – which outfalls south of the South Beach sampling position.
- **West Street SWD** – which outfalls between the Wedge and North Beach sampling positions. See Plate 3-11.
- **Somtseu Road SWD** – which outfalls north of the Bay of Plenty sampling position, between Bay of Plenty and Snake Park beach. See Plate 3-12.
- **Argyle Road SWD** – which outfalls south of the Battery Beach sampling position, between Snake Park and Battery Beach. See Plate 3-13.
- **Walter Gilbert Road SWD** – which outfalls south of the Country Club Beach sampling position. See Plate 3-14.

The types and levels of pollution to be found within any urban stormwater drain may depend on a variety of environmental, physical and social factors for each urban catchment. The catchment size for each SWD is given in Table 3-11.

	Hospital	Rutherford	West	Somtseu	Argyle	Walter Gilbert
Catchment Area (m^3)	355000	144375	350000	744375	1618125	2203750

Table 3-12: Catchment sizes of the six urban stormwater drains

Based on the size of the stormwater drain catchment areas the drains may be grouped into two sets. As shown in Table 3-12 the first set of stormwater drains (Hospital, Rutherford and West) had small catchment areas, while the remaining set of three (Somtseu, Argyle and Walter Gilbert) had larger catchment areas.

3.3.1 The urban stormwater drains

Plate 3-10: Hospital stormwater drain

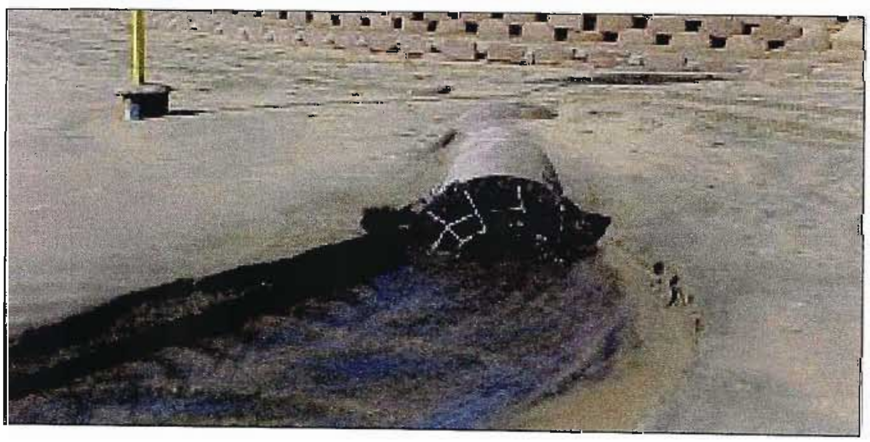

Plate 3-11: West Street stormwater drain

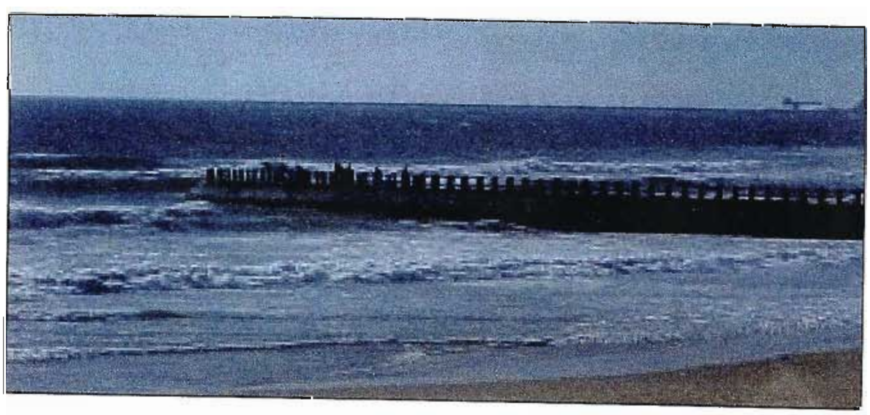

Plate 3-12: Somtseu Road stormwater drain

Plate 3-13: Argyle Road stormwater drain

Plate 3-14: Walter Gilbert Road stormwater drain

3.4 Water Quality Analysis of the Stormwater Drains

The six stormwater drains are sampled by EMWSS on average once a month. Unfortunately of the two indicators selected to determine the water quality of the beaches, Escherichia coli was the only microorganism indictor regularly enumerated from the sampled stormwater drains.

The SWD data analysed was for a similar period to that analysed for the beach WQ: January 1995 to August 2002. As previously mentioned, the stormwater drains are sampled approximately every 4 weeks, however over the period certain SW drains have on occasion been sampled more frequently.

3.4.1 General Statistical Analysis

A general statistical analysis was done to gain some understanding of the pathogenic pollution levels contained within the stormwater discharge, indicated by E. coli. The stormwater data was analysed annually and seasonally for the following statistical properties: Average (arithmetic mean) concentration, Geometric mean concentration, Standard deviation, Coefficient of variation, Skewness and Kurtosis.

3.4.1.1 General Analysis Results

The characteristics and processes surrounding the specific pathogenic pollution content of urban stormwater runoff make it difficult to predict the exact pathogenic pollution concentration at any given time. The pollution level of the SWD discharge may change over short timescales during rainfall events, peak during the first-flush, be low during large volume flows or fairly constant between rainfall events. (Taylor et al, 1993)

In Table 3-12 the average E.coli concentration of the various stormwater drains, for different seasons as well as the combined seasons, is presented. The numbers in brackets represent the specific ranking of the stormwater drain for that period (highest being no.1):

SWD	Annual	Summer	Autumn	Winter	Spring
Hospital	124004 (1)	19743 (4)	107245 (2)	227442 (1)	120215 (2)
Rutherford	43481 (3)	46631 (2)	31722 (3)	47055 (2)	57710 (4)
West	8661 (6)	10071 (6)	8002 (6)	10597 (4)	5708 (6)
Somtseu	14352 (5)	27484 (3)	9630 (5)	9601 (5)	12574 (5)
Argyle	83846 (2)	114017 (1)	53855 (1)	35053 (3)	143391 (1)
Walter Gilbert	16160 (4)	19023 (5)	12260 (4)	4065 (6)	31388 (3)

Table 3-12: Average E. coli concentrations of stormwater drains

Annually, Hospital SWD has the highest average E.coli concentration and Argyle SWD the second highest. Seasonally, Argyle SWD has the highest average E.coli concentration except for winter, when Hospital SWD is higher. There does not appear to be a correlation between the size of the catchment areas (Table 3-11) and the pathogenic pollution loading (indicated by the average concentration).

The SWD geometric mean E.coli concentrations are presented in Table 3-14. The drains all have significantly smaller geometric mean values than arithmetic mean values (Table 3-13). This suggests that the E.coli concentrations of the drains are not Gaussian distributed.

SWD	Annual	Summer	Autumn	Winter	Spring
Hospital	801 (5)	235 (6)	322 (5)	3365 (2)	1548 (4)
Rutherford	1032 (4)	3567 (4)	2651 (3)	70 (6)	1023 (5)
West	178 (6)	318 (5)	118 (6)	172 (5)	199 (6)
Somtseu	2031 (3)	8993 (2)	1472 (4)	702 (4)	2216 (3)
Argyle	6581 (1)	9621 (1)	6303 (1)	4180 (1)	7921 (1)
Walter Gilbert	3305 (2)	6992 (3)	4093 (2)	1023 (3)	3780 (2)

Table 3-14: Geometric mean E. coli concentrations of stormwater drains

The Argyle stormwater drain always has the highest geometric mean concentration, annually as well as seasonally. Argyle has a relatively large catchment are (Table 3-12), therefore the drain can be expected to be the heaviest polluter in this locality. There appears to be a correlation between the catchment area and the pollution loading of the stormwater drains (indicated by the geometric mean). The larger the catchment area, the greater the pathogenic pollution loading of the drain. Exceptions to this appear to be for Hospital (Winter) and Rutherford (Autumn) but these may be explained by a combination of the following:

1. The sample sizes were relatively small (±3 per season for ±8 years ≈ ±24 samples) therefore excessively large values single values may skew results.
2. The drains' runoffs are primarily due to direct rainfall runoff (refer to section 3.6.1).
3. Autumn and winter months have a greater proportion of dry-days (refer to Sections 2.7.1.1 and 3.6.1).
4. The winter months have the highest rainfall-per-rainy-day for the catchment region (refer to Section 3.6.1).

Therefore when analysing an urban region a rough estimate of the polluting potential of stormwater drains may be made using their physical characteristics. The order from most to least, or exceptions to the rule, will depend on the specific pollution loading potentials of their catchments.

The standard deviations of the SWD E.coli concentrations are presented in Table 3-15.

SWD	Annual	Summer	Autumn	Winter	Spring
Hospital	441737	59427	477628	555425	441887
Rutherford	113105	100547	85276	168254	96325
West	27253	24062	23661	37977	16999
Somtseu	37631	62940	27812	18276	26010
Argyle	241009	377190	105436	79564	289123
Walter Gilbert	43152	20007	20866	4352	84928

Table 3-15: Standard Deviation of E. coli concentrations for stormwater drains

The standard deviations all appear very large in comparison to the average E.coli concentrations. The Hospital drain has the largest standard deviation annually and for three out of the four seasons, with Argyle having the second highest values and the highest for summer.

An explanation for the high standard deviation values for specific stormwater drains that have small catchments may also explain the calculated high mean values. Smaller catchments, such as the Hospital SWD, have minimal baseflow and rainfall-runoff volumes. Therefore, pollution from the catchment would have limited mixing available thus increasing the coliform counts.

The magnitudes of the coefficient of variation for the stormwater drains are presented in Table 3-16. On average the standard deviations are approximately 300 percent larger than the average values. The magnitude of the values in Table 3-16 indicates that the distributions of the E.coli concentration may either be Gaussian distributed with large standard deviations or not Gaussian distributed at all.

SWD	Annual	Summer	Autumn	Winter	Spring
Hospital	3.56	3.01	4.45	2.44	3.68
Rutherford	2.60	2.16	2.69	3.58	1.67
West	3.15	2.39	2.96	3.58	2.98
Somtseu	2.62	2.29	2.89	1.90	2.07
Argyle	3.56	3.01	4.45	2.44	3.68
Walter Gilbert	2.67	1.05	1.70	1.07	2.71

Table 3-16: Coefficient of variation of stormwater drains

An indication of the distributed nature of the SWD E.coli concentrations is given by kurtosis and skewness. Table 3-17 is a summary of the kurtosis of the E.coli concentrations for different drains and periods. All stormwater drains appear to have high positive kurtosis values indicating that the distributions are all highly peaked. A Gaussian distributed random variable would have a kurtosis value of three.

SWD	Annual	Summer	Autumn	Winter	Spring
Hospital	19.50	20.68	29.23	8.06	24.06
Rutherford	23.92	8.61	15.93	23.58	2.14
West	40.13	8.35	27.91	36.10	29.96
Somtseu	29.11	20.72	38.82	5.89	5.99
Argyle	13.08	29.20	5.74	11.79	2.85
Walter Gilbert	59.33	2.33	11.89	3.26	17.87

Table 3-17: Kurtosis of E. coli concentrations for stormwater drains

The skewness of the SWD E.coli concentrations is summarised in Table 3-18. All the skewness values are positive and most are significantly larger than zero. This indicates that it is unlikely that the stormwater drain E.coli concentrations are Gaussian distribution. As Guassian distributions typically having a skewness of approximately zero. The positive nature of the skewness values indicates a distribution with an asymmetrical tail extending towards larger values.

SWD	Annual	Summer	Autumn	Winter	Spring
Hospital	4.43	4.39	5.30	2.99	4.84
Rutherford	4.38	3.03	4.02	4.76	1.77
West	5.73	2.99	4.98	5.80	5.32
Somtseu	4.72	4.32	6.03	2.49	2.60
Argyle	3.57	5.14	2.58	3.32	2.05
Walter Gilbert	7.14	1.47	3.24	1.60	4.12

Table 3-17: Skewness of E. coli concentrations for stormwater drains

3.4.2 Probability Distributions of Stormwater Concentrations

The pathogenic pollution level contained within the urban stormwater runoff is an important element in the modelling of pathogenic pollution on the surrounding beaches. The significant positive skewness and kurtosis values found for the stormwater drain data indicated that the distributions of the stormwater data were not Gaussian distributed. The hypothesis was made that the distribution of sampled stormwater concentrations may be described by a lognormal distribution.

It was also noted that some stormwater drains had a large percentage of zero concentration readings. The reason for this may have been either that the stormwater drains had no pathogenic pollution indicated by E.coli or zero readings or that the true concentrations were lost due to the insensitivity of the laboratorial analysis at low pollution counts (Section 2.3.1.3). Subsequently only the non-zero readings were considered for testing the lognormal distribution hypothesis.

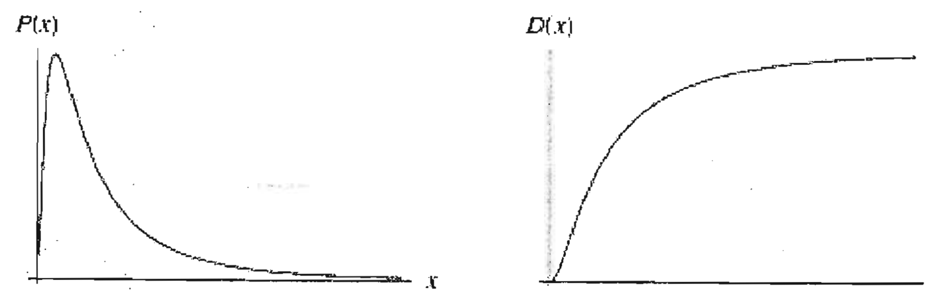

Figure 3-4: Lognormal probability and cumulative distribution functions

The probability density function for the lognormal distribution (Figure 3-4) is given by:

$$f(x|\mu',\sigma')=\frac{1}{x\sigma'\sqrt{2\pi}}e^{-\frac{(\ln(X)-\mu')^2}{2}} \qquad (3\text{-}7)$$

where

μ' is the scale parameter (calculated as the mean of the logarithms of x)

σ' is the shape parameter (calculated as the standard deviation of the logarithms of x)

The mean of the lognormal distribution may calculated as follows:

$$\mu=e^{\mu'+\frac{1}{2}\sigma'} \qquad (3\text{-}8)$$

The standard deviation of the lognormal distribution may be calculated as follows:

$$\sigma = \sqrt{\left(e^{2\mu' + \sigma'^2}\right)\left(e^{\sigma'^2} - 1\right)} \tag{3-9}$$

The hypothesis that the stormwater concentrations followed a lognormal distribution was tested using the Lilliefors test (Conover, 1980) and the Jarque-Bera test (Judge, et al. 1988).

1. The lilliefors test evaluates the hypothesis that the data has a normal distribution with unspecified mean and variance. This test compares the empirical distribution of the data with a normal distribution having the same mean and variance as the data, using a 95 percent confidence level.
2. The Jarque-Bera test evaluates the hypothesis that the data has a normal distribution with unspecified mean and variance. The Jarque-Bera test determines whether the sample skewness and kurtosis are unusually different than their expected values, as measured by a chi-square statistic, using a 95 percent confidence level.

The logarithms of the stormwater concentrations were tested against a Gaussian distribution using the above tests. If the distribution of the logarithms were accepted as Gaussian then the hypothesis that the stormwater concentrations followed a lognormal distribution was accepted.

3.4.2.1 Statistical Analysis Results

Table 3-18 shows the percentage of zero E.coli readings for each of the stormwater drains.

SWD	Annual	Summer	Autumn	Winter	Spring
Hospital	27%	33%	33%	18%	23%
Rutherford	23%	12%	10%	52%	26%
West	34%	26%	39%	36%	31%
Somtseu	7%	0%	9%	15%	4%
Argyle	1%	0%	3%	2%	0%
Walter Gilbert	5%	4%	0%	13%	4%

Table 3-18: Percentage zero E. coli readings within sampled SWD discharge

The first important observation is that there is a significant grouping in the data with the percentages in the case of the first three (Hospital, Rutherford and West) stormwater drains being much higher than the remaining three (Somtseu, Argyle and Walter Gilbert) stormwater drains. The first three drains had an average zero-percentage of 25 to 35 percent, while the second group had an average zero-percentage of below 10 percent. The reason for this may be explained by a number of factors:

1. **The size of the drains catchments -** The size of the drain catchments of the first group of drains are substantially smaller than the second group.
2. **Catchment characteristics** - The source of the discharge volume for the first group may be more exclusively due to direct rainfall runoff than the second group, whose discharge volumes may be supplemented by baseflows whose source is not exclusively direct rainfall runoff.

The source of the "zero" counts seems related to the EMWSS testing procedures discussed in section 2.3.1.3. The "zero" counts are most likely counts not registered on plates cultured the 1ml samples, making them readings of approximately 100 CFU/100ml and less.

The link between rainfall and pollution concentrations within the runoff may appear stronger when considering the first set of drains than the second. However, Table 3-18 also shows that the winter months appear to have a greater percentage of zero-readings for most drains. This may be related to the rainfall characteristics of the region where the winter months receive less rain than the summer months (3.6.1). The substantiation of the above conclusions is analysed in section 3.9.1.

The results of the Lilliefors and Jarque-Bera tests are shown in Table 3-19 and Table 3-20. The tabled results indicate whether the hypothesis that the non-zero E.coli sampled SWD concentrations followed a lognormal distribution was accepted (√) or rejected (FAIL). Detailed results of the fitted lognormal distributions may be found in Appendix C.

SWD	Annual	Summer	Autumn	Winter	Spring
Hospital	FAIL	√	√	√	√
Rutherford	√	√	√	√	√
West	√	√	√	√	√
Somtseu	FAIL	√	√	√	√
Argyle	√	√	√	√	√
Walter Gilbert	√	√	√	√	√

Table 3-19: Lilliefors test for lognormal distribution results (95% confidence level)

SWD	Annual	Summer	Autumn	Winter	Spring
Hospital	√	√	√	√	√
Rutherford	√	√	√	√	√
West	√	√	√	√	√
Somtseu	√	√	√	√	√
Argyle	√	√	√	√	√
Walter Gilbert	√	√	√	√	√

Table 3-20: Jarque-Bera test for lognormal distribution results (95% confidence level)

In general the hypothesis that the non-zero E.coli concentrations may be described by a lognormal distribution was accepted at the 95% confidence level. Both the Lilliefors and Jarque-Bera tests show that seasonal distributions for all drains may be described by seasonal lognormal distributions of E.coli concentrations.

An Example of the true cumulative distribution function (CDF) for the sampled E.coli concentration and fitted lognormal CDF is shown for the Argyle stormwater drain (annual) in Figure 3-5. This may be compared to the failed fitted annually lognormal distribution shown in Figure 3-6.

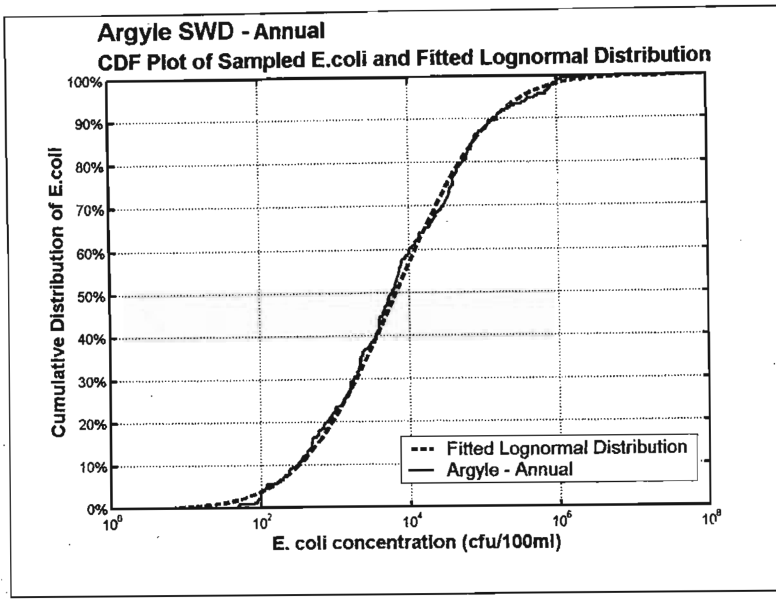

Figure 3-5: Argyle SWD E.coli distribution and fitted lognormal distribution

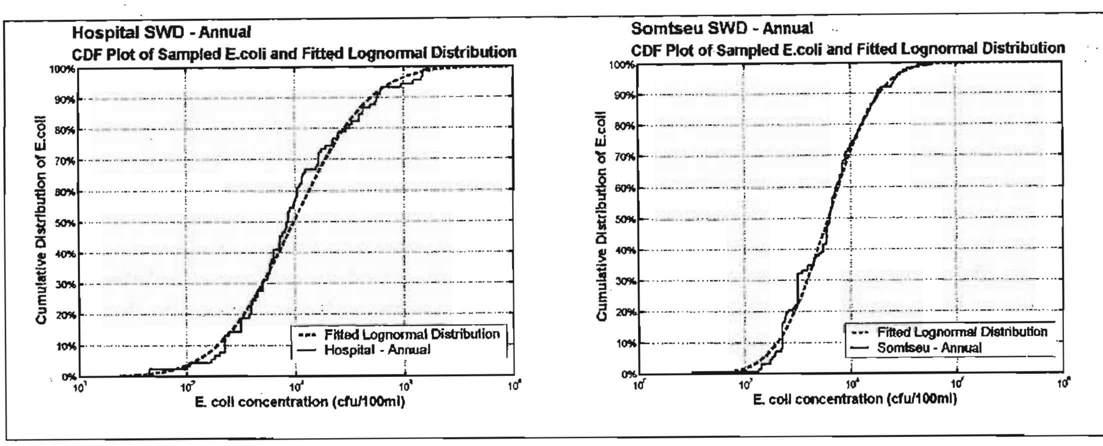

Figure 3-6: The failed lognormal E.coli distributions, Hospital and Somtseu SWD

Using visual analysis of the shape of the failed cumulative distribution graphs, qualitative assumptions can be made on the possible failure of the hypothesis.

1. The Hospital drain's fitted lognormal distribution may have failed due to a significant number of very high sampled concentrations. Therefore the "shape" of the lognormal distribution may have been violated.
2. The Somtseu drain's fitted lognormal distribution may have failed due to the errors in the lower concentration values as is evident in Figure 3-6. The discontinuities may be due to the enumeration and 'rounding up' techniques involved in the sample testing when dealing with lower than average or expected concentrations.

3.5 The Umgeni River

The Umgeni River rises in the Natal Midlands and flows through Midmar, Albert Falls and Nagle Dams before joining up with the Msindusi River and feeding into the Inanda Dam, which is approximately 18km from the Umgeni River Mouth, Plate 3-15. The Umgeni River catchment area is 4387km^2 however the catchment area below the Inanda Dam is approximately 340 km^2. The dams are used for water supply and have a combined capacity of 745.9 x 10^6 m^3, which represents 135 percent of the mean annual runoff of the catchment (Kienzle et al, 1997).

The Umgeni River catchment supports a broad spectrum of activities that contribute towards approximately 20% of the gross national product of the Republic of South Africa, but it also means that the Umgeni is subjected to almost every conceivable type of pollution. A major source of pollution in the Umgeni River system originates from the discharge of raw and treated sewage. A large percentage of the population, settled within the Umgeni catchment, live in settlements ranging from formal to informal in nature. The sanitation of informal settlement is normally nonexistent, while in some formal settlements the facilities were never designed to deal with the amount of raw sewage now present. Sanitation within informal settlements consists of pit latrines that are usually inadequately designed and constructed. During periods of rainfall or when the water table rises, the pit latrines and sewage from failed facilities contaminate the river. (Water Pollution in the Umgeni River, 2003).

Plate 3-15: 150° Combined strip photograph of the Umgeni River

The water quality of the Umgeni River (UR) is sampled by EMWSS at the positions shown in Figure 3-7. The data position 13, alongside the Ellis Brown Viaduct, was selected for analysis since it was closest to the river mouth, Plate 3-15, and provided the longest continuous record.

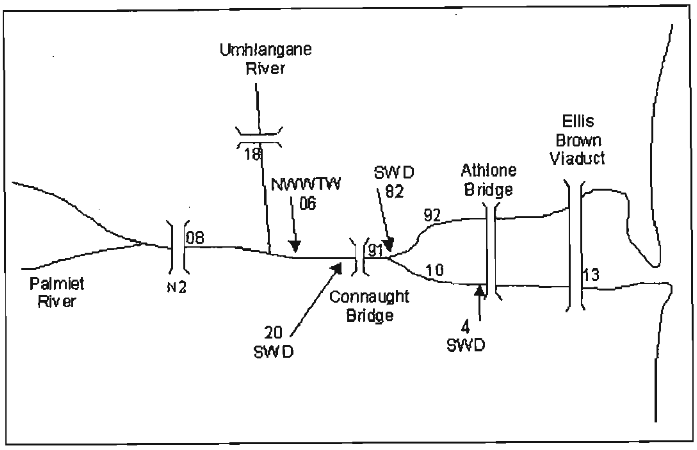

Figure 3-7: EMWSS Sampling positions along the Umgeni River (not to scale)

3.5.1 General Information and Water Quality

Basic statistics of the Umgeni River E.coli concentrations are presented in Table 3-21. On average during winter the highest pathogenic pollution levels are experienced, with summer having the lowest average concentration and spring the lowest geometric mean concentrations. This is most likely due to these months experiencing more rainfall and higher flows; as a result the pollution is more diluted.

	Geometric Mean (CFU/100ml)	Average (CFU/100ml)	Standard Deviation
Annual	2535	11497	33889
Summer	2431	7847	14645
Autumn	3262	14875	41008
Winter	3261	12983	37634
Spring	1645	10288	36444

Table 3-21: Umgeni River seasonal E.coli statistics at position 13

The average monthly flow rate of the Umgeni River, measured at Inanda Dam spillway is shown in Figure 3-8. The highest average flow rates, of approximately 25 m^3/s, occur during February and March. Comparing the monthly averages for several years, it is evident that there are large variations.

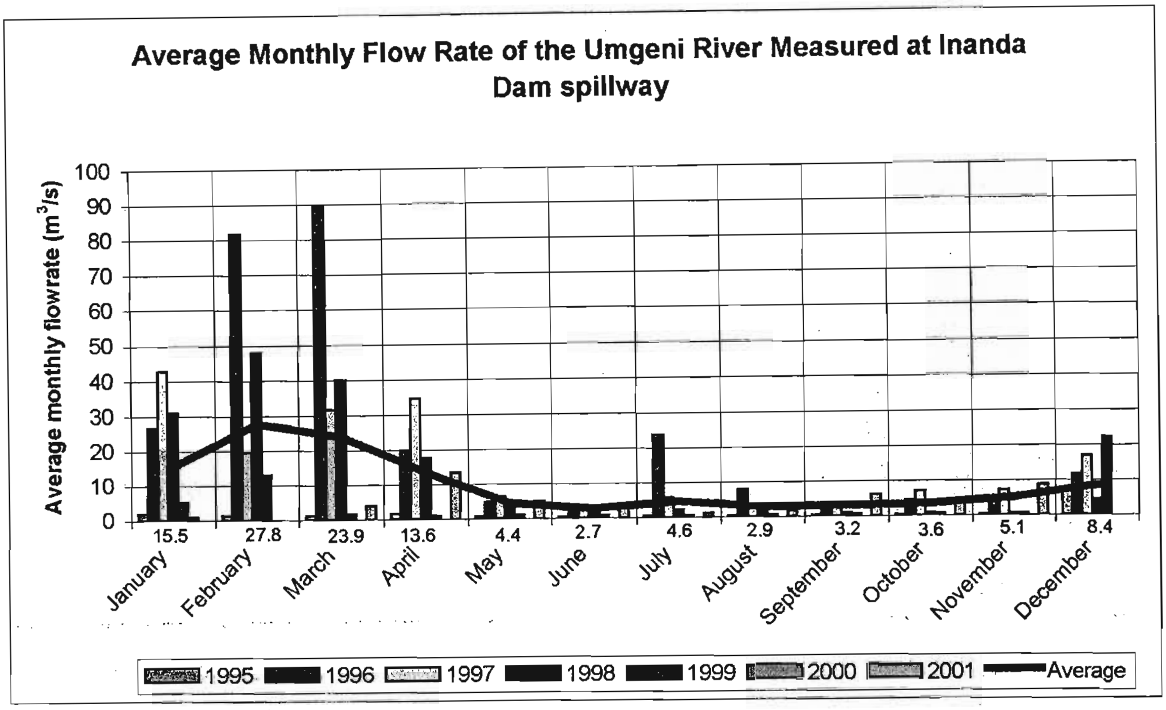

Figure 3-8: Monthly averaged flow rates measured at Inanda Dam spillway

Using the SA WQ Guidelines, the exceedance for the Umgeni River (measured at position 13) as an inland recreational water resource, is shown in Table 3-22.

Period	Exceedance of SA Inland WQ Guidelines	
	Full contact	Intermediate Contact
Annual	98%	70%
Summer	97%	71%
Autumn	100%	73%
Winter	100%	74%
Spring	95%	63%

Table 3-22: Exceedance of SA Inland WQ Guidelines for Umgeni River (position 13)

The results indicate that the pathogenic pollution levels of Umgeni River are high and the river should not be used for full or intermediate contact recreational activities. The high pathogenic pollution content of the river combined with the high flow rates combine to form a dominant polluter of the nearshore coastal zone.

3.5.2 Statistical Distributions of Umgeni River E.coli Concentration

The distribution of the pathogenic content of the river outflow was analysed. As with the stormwater drains the hypothesis was made that the river E.coli concentrations were lognormally distributed. The Jarque-Bera and Lilliefors Tests were used to test the hypothesis and the results are presented in Table 3-23.

	Annual	Summer	Autumn	Winter	Spring
Jarque-Bera Test	FAIL	√	√	√	FAIL
Lilliefors Test	FAIL	√	FAIL	√	√

Table 3-23: Results of lognormal distribution tests for UR Pos. 13 (95% confidence level)

The tests both fail for annual data, but the seasonal data all pass at least one of the tests. The annual cumulative distribution plot and fitted lognormal distribution are shown in Figure 3-9.

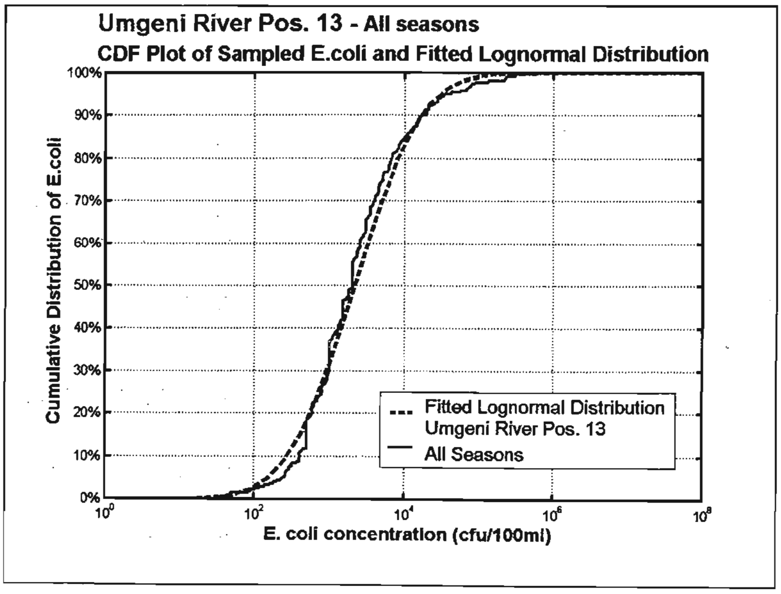

Figure 3-9: UR pos. 13 - Actual and Fitted lognormal E.coli Distribution

Although the tests fail at the 95 percent confidence level, it can be seen that the lognormal distribution gives a reasonable (visual) fit to the data. These lognormal distributions are later used for modelling the increasing in pathogenic pollution in the nearshore environment due to the Umgeni River.

3.6 Area Environmental Characteristics

In order for the dynamics of the water quality for a region to be understood and modelled, the environmental characteristics of the region need to be understood.

3.6.1 Rainfall Characteristics

Rainfall is an important factor in determining the water quality of the nearshore region. The depth of rainfall that falls onto the urban or river catchment will determine the volume of runoff added to the nearshore region. To determine the rainfall onto these catchments, three rain gauge site were available: Durban's Louis Botha Airport, Durban Botanical Gardens and a rain gauge on top of the Civil Engineering building at the University of Natal. Rain gauge readings for a number of years were available from the South African Weather Service for the Airport and Botanical Gardens sites.

The runoff from the urban catchments in the Durban CBD and surrounds was of particular interest. The Durban Botanical Gardens rain gauge is the closest to the CBD, and was therefore selected.

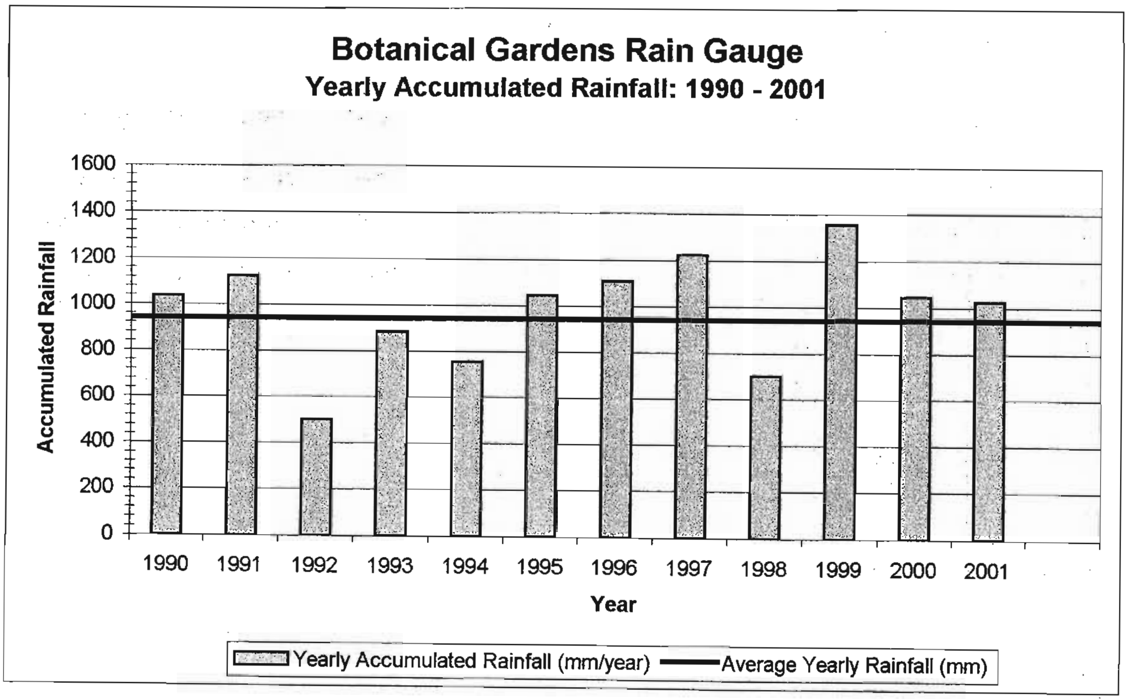

Figure 3-10: Yearly Accumulated Rainfall at Botanical Gardens Rain Gauge (1990 - 2002)

The average rainfall for the Durban CBD area, using recorded data from 1990 to 2002, was 950 mm/year as can be seen in Figure 3-10.

Durban is within a subtropical region and has a summer rainfall climate. Figure 3-11 shows the seasonal distribution of Durban's rainfall.

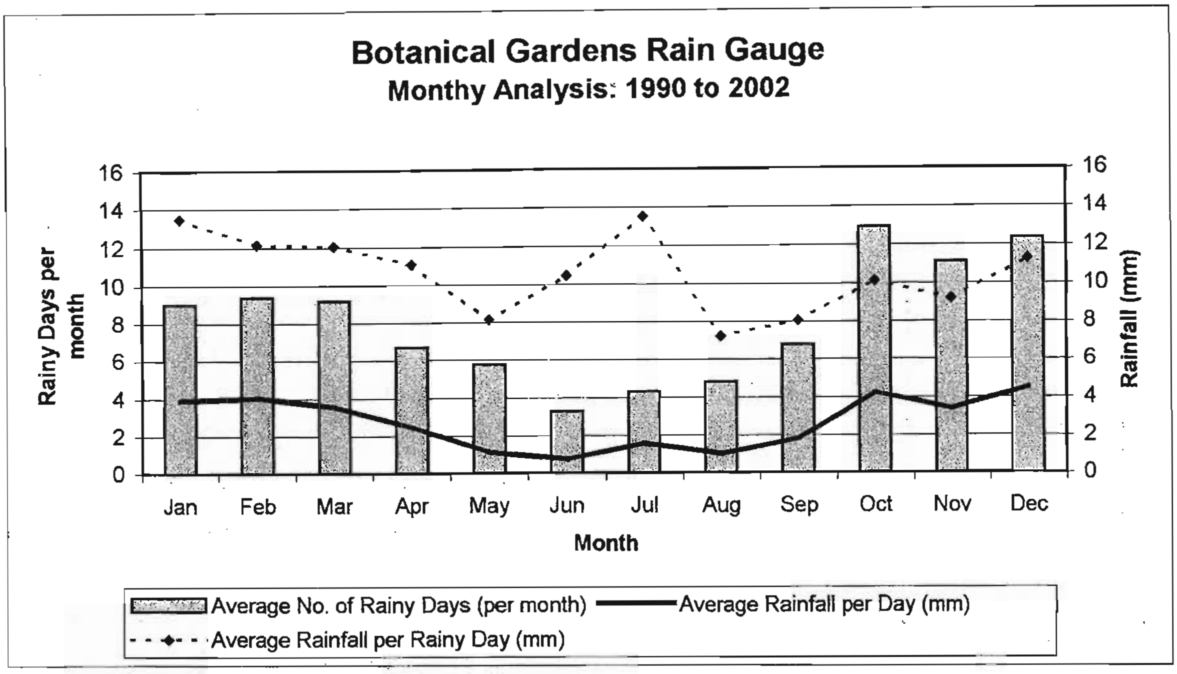

Figure 3-11: Monthly Analysis of Botanical Gardens Rain Gauge (1990 - 2002)

It was noted that the average rainfall per day remains fairly constant (approximately 4 mm/day) for six months of the year from October to March (mid-spring to early-autumn). However the October to December period has, on average, more rainy days per month than the January to March period. The disparity is balanced out by the fact that the January to March period has a greater depth of rainfall per rainy event than the preceding three-month period.

The lower number of rainy days per month and higher average rainfall per rainy day means that the poorest water quality conditions of the nearshore region would be expected to occur during the summer and early autumn period. This is a combination of the first-flush and number of preceding dry days phenomenon discussed in chapter 2.

Of particular interest in Figure 3-11 is that the maximum average rainfall per rainy day is not found within the six-month period from October to March, but during the July month. The low number of rainy days during this period means that pollution may be allowed to accumulate substantially and then combined with a large rainfall event could lead to problematic water quality conditions within the nearshore coastal region during the winter period. That is, average water quality conditions may be satisfactory, but could sporadically deteriorate during rare rainfall events.

3.6.2 Local Wind Characteristics

The Durban coastal region has relatively stable wind conditions with two dominant wind directions. The hourly average wind rose in Figure 3-12 shows that the wind usually either blows from the NNE to ENE direction or from the S to SW direction.

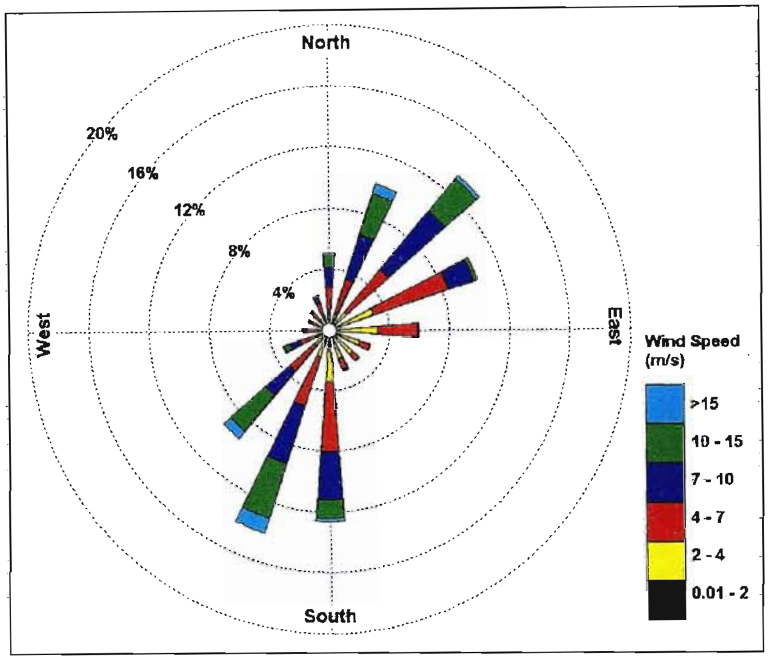

Figure 3-12: Hourly averaged wind rose measured at Durban Harbour (1995 – 2002)

A significant portion (41%) of hourly averaged wind speeds for may be classified as moderate to fresh breezes of stronger according to the Beaufort Wind Scale (see Appendix D). The mean hourly average wind speed is a moderate breeze of 6.67 m/s.

The wind rose for daily averaged wind conditions is shown in Figure 3-13.

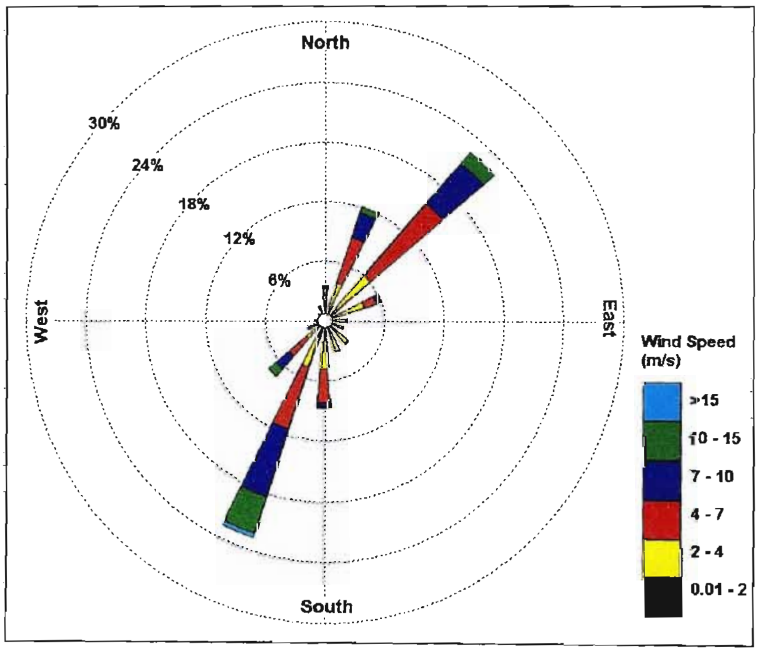

Figure 3-13: Daily averaged wind rose measured at Durban Harbour (1995 – 2002)

It can be seen that 48 percent of the daily averaged wind speeds are classified as moderate to fresh breezes (4 – 10 m/s) and just over 7 percent of the daily winds are classified as strong breezes (10 – 15 m/s). The mean daily average wind speed is 5.1 m/s.

Examination of seasonal daily averaged wind roses indicated the following characteristics:

1. During the summer months (December – February) the dominant wind direction is from the SSW direction. The mean daily average wind speed is 6.9 m/s.
2. During the autumn months (March – May) the dominant wind directions were from the SSW and NE directions. The mean daily average wind speed is 6.2 m/s.
3. During the winter months (June – July) the dominant wind directions were from the NE and S directions, but with a larger percentage of winds coming from the directions between the NE and S direction. The mean daily average wind speed was 6 m/s.
4. During the spring months (September – November) the winds came mostly from the SSW direction with a fairly strong secondary percentage of the winds coming from the NNE and NE direction. Spring had the highest mean daily average wind speed of 8 m/s

After comparing the wind roses generated for the Durban coastal region with the KwaZulu Natal (KZN) coastline (Figure 3-14) it is noted that the orientation of the coastline corresponds to the dominant wind directions identified by the wind roses.

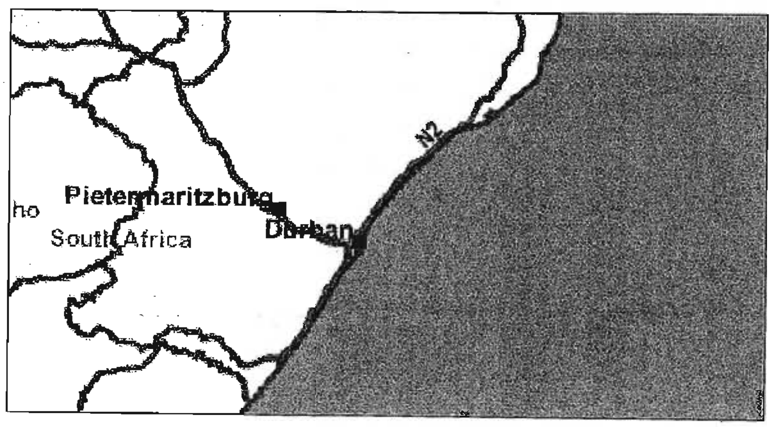

Figure 3-14: KZN Coastline

The strong conformity of the wind to the angle of the coastline means that the wind will have a strong influence in the movement of water up and down the coast through wind-induced waves and currents.

3.6.3 Incident Solar Radiation Characteristics

The incident solar radiation characteristics experienced by Durban are important for a number of physical, biological and social reasons. The main interest, within the scope of this research, was the relationship between the decay of microorganisms and pathogens and solar radiation levels, as discusses in sections 2.6.1.1, 2.6.2.3 and 2.6.3.

Recorded solar radiation for the Durban region for the period from 1999 to 2002 was analysed. The data was obtained from the South African Weather Service for the Louis Botha Durban International Airport. The results of the analysis are presented in Figure 3-15.

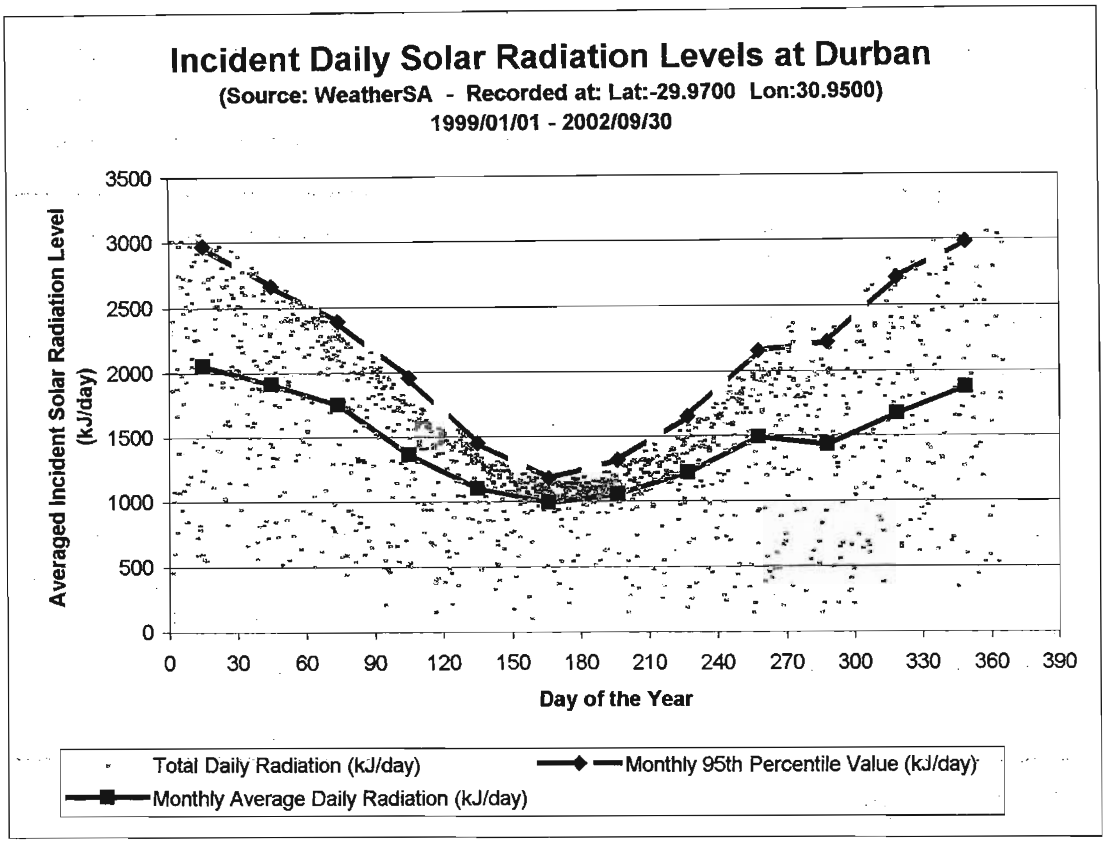

Figure 3-15: Incident solar radiation levels experienced at Durban Airport (1999 – 2002)

Examination of the solar radiation analysis indicated the following:

1. The peak solar radiation levels occur during the middle of January (mid summer), which was to be expected.
2. The average solar radiation levels decrease faster than they subsequently increase, thus the time taken for the levels to decrease to the "minimum" average levels in mid-June is shorter than the time taken for the levels to "peak" again in mid-January.
3. The cyclical nature shown in Figure 3-15 lends itself to the fitting of a cyclical function for describing the yearly variation of solar radiation levels.

3.6.3.1 Using the Incident Solar Radiation to Estimate an E. coli Decay Function

Recalling Section 2.6.3, the research by Guilaud et al. (1997) showed that the T90 decay timescale of E. coli may be related to light intensity using equations (2- 12) and (2- 13).

$$T90 = a * \left\{ I_0 \left[\frac{\left(1 - e^{-k_w h}\right)}{k_w h} \right] \right\}^b ; \qquad k_w = 0.189 * SS^{0.799}$$

Where h = depth (m), k_w = extinction coefficient (m^{-1}) and I_0 = energy absorbed by the seawater surface (μEm^{-2}h^{-1}) and values for the parameters were estimated as a = 53683 and b = -0.666.

Recall also that the T_d timescale for bacterial decay may be derived from the T90 timescale by the formula:

$$T_d = \frac{T90}{\ln(10)} \tag{3-10}$$

The equations (2- 13), (2- 14) and may be combined.

$$T_d = \frac{53683}{\ln(10)} * \left\{ I_0 \left[\frac{\left(1 - e^{-0.189 \cdot SS^{0.799} \cdot h}\right)}{0.189 \cdot SS^{0.799} \cdot h} \right] \right\}^{-0.666} \tag{3-11}$$

The light intensity absorbed by the surface of the sea depends on the initial incident solar radiation and the percentage of the radiation that is "lost" due to reflection and backscattering. The percentage of the initial energy absorbed depends on the sea albedo (α_a), state of the sky, length of day etc (Guillaud, et al, 1997).

"The albedo is the fraction of light that is reflected by a body or surface. "

(Schombert, 2002)

Whitehead et al. (2000) indicated that diffuse radiation reflected by the sea amounts to 6 to 11 percent. Assuming that the sky is cloudless the initial energy absorbed by the sea can be given by:

$$I_0 = I \cdot (1 - \alpha_a) \tag{3-12}$$

Where I is the light intensity at the surface of the water and α_a is the albedo value. The Equation (3-11) is now modified to include the effect of the albedo.

$$T_d = \frac{53683}{\ln(10)} \cdot (I)^{-0.666} \cdot (1 - \alpha_a)^{-0.666} \cdot \left[\frac{\left(1 - e^{-0.189 \cdot SS^{0.799} \cdot h}\right)}{0.189 \cdot SS^{0.799} \cdot h} \right]^{-0.666} \tag{3-13}$$

Equation (3-13) requires the light intensity to be in units of μEm^{-2}h^{-1}and the following conversion was used:

Solar Radiation -> light intensity conversion			
kJ/day ->	Jh^{-1}	=	x 1000
Jh^{-1} ->	$\mu Em^{-2}h^{-1}$	=	x 4.6
Daylight: Conversion from W/m² -> µE / (m² s) : value * 4,6			
(Taken from: http://www.pz-oekosys.uni-kiel.de/~schorsch/klima/klimadbeng.htm)			

The following equation is proposed as a means of describing the possible variation of the E.coli decay timescale T_d as a function of the day of the year. Where *D* is the day of the year and D_{Offset} is day of the maximum average decay time.

$$T_d(D) = Td_{mean} + Td_{amp} \cdot \cos\left(2\pi \cdot \frac{(D-1)+D_{offset}}{364}\right) \tag{3-14}$$

Equation (3-14) was solved for varying depths and suspended solids concentrations by minimising the sum of the square of the errors between the monthly-predicted decay timescales derived from the solar radiation (3-13) and the fitted T_d function (3-14). Figure 3-16 shows the solution for a depth of 2 meters and total suspended solids of 10 mg/l.

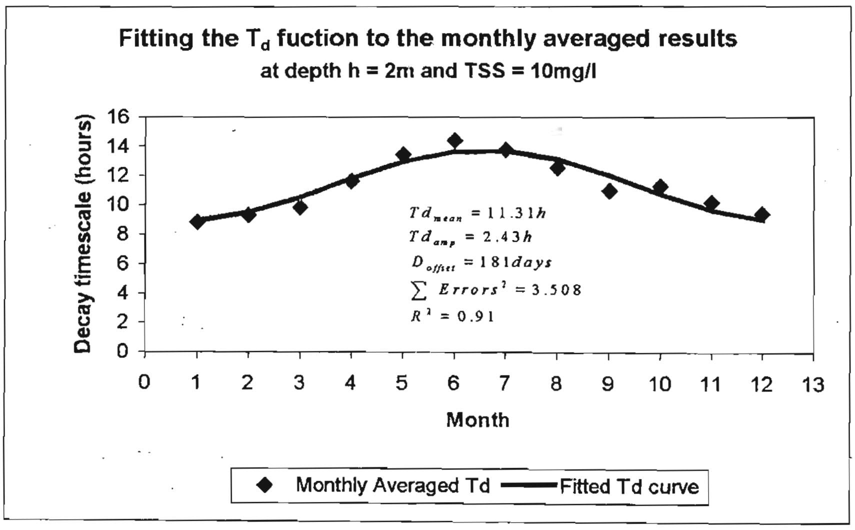

Figure 3-16: Fitting of the Td function to the averaged monthly E. coli decay

Equation (3-14) was found to be a good fit to the data with an R^2 value of 0.91. Contour graphs for T_d as a function of the parameters Td_{mean} and Td_{amp}, were calculated and are presented as Figure 3-17 and Figure 3-4.

Equation (3-14) was also fitted to the 95% max E.coli decay (see Figure 3-15) with an R^2 value of 0.91. The relevant contour graphs may be found in Appendix D.

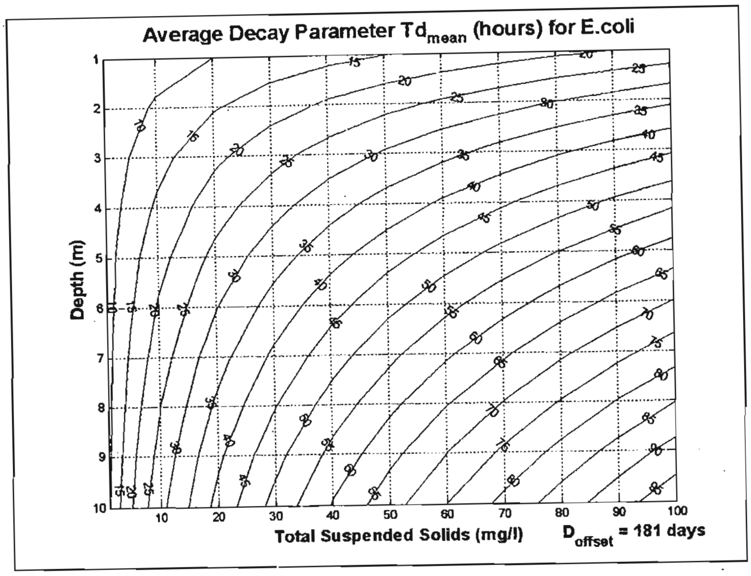

Figure 3-17: Contour plot of the Td_{mean} parameter for average E.coli decay based on Durban's solar radiation characteristics

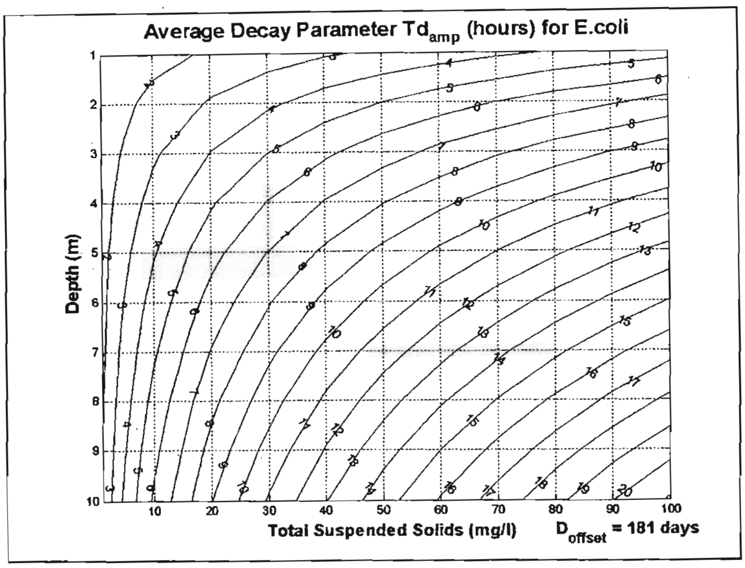

Figure 3-18: Contour plot of the Td_{amp} parameter for average E.coli decay based on Durban's solar radiation characteristics

The maximum and minimum E. coli decay timescale may be calculated for a specific depth in seawater by using the suspended solids concentration of the water column and applying an appropriate albedo factor.

$$T_d = (1-\alpha_a)^{-0.666} \cdot \left(Td_{mean} + Td_{amp} \cdot \cos\left(2\pi \cdot \frac{(D-1)+D_{offset}}{364} \right) \right) \quad (3\text{-}15)$$

The total suspended solid concentration is not recorded by the EMWSS. However the turbidity of the beaches, measured in Nephelometric Turbidity Units (NTU), is recorded. The average annual and seasonal turbidity was calculated for the beaches over the period of the beach water quality analysis and is shown in Table 3-24.

Beaches	All	Summer	Autumn	Winter	Spring
Vetches Pier	6.43	4.67	8.42	4.92	7.70
Addington	4.36	4.66	3.59	3.20	7.09
South	3.50	4.45	2.66	2.50	5.23
Wedge	3.08	4.35	1.94	2.40	4.14
North	2.71	3.74	2.28	1.92	3.54
Bay of Plenty	2.63	3.71	2.48	1.91	2.79
Battery	3.01	3.86	2.93	2.13	3.58
Country Club	2.89	4.71	2.12	2.24	3.15
Laguna	5.08	11.31	3.28	2.62	4.79
Umgeni South	12.94	23.62	14.80	5.63	8.47

Table 3-24: Average Turbidity of sampling beaches (NTU)

Packman et al. (1999) showed that for the urbanising streams the relationship between turbidity and TSS may be described as follows:

$$\ln\left(TSS\right) = 1.32 \cdot \ln(NTU) + 0.15 \tag{3-16}$$

Namsoo et al (1998) showed a linear regression relationship between total suspended solids concentration and turbidity as follows:

$$TSS = 1.584 \cdot NTU \tag{3-17}$$

Considering the turbidity characteristics of the sampling beaches presented in Table 3-24, an average turbidity value of 4.7 NTU was calculated. The relative total suspended solids predicted by equations (3-16) and (3-17) are shown in Table 3-25.

Method	Description	Turbidity (NTU)	TSS (mg/l)
1	TSS = exp(1.32*ln(NTU)+0.15)	4.7	8.96
2	TSS = 1.584*NTU	4.7	7.44

Table 3-25: Applying methods of finding TSS value from Turbidity

If total suspended solids concentration of 8 mg/l at a depth of 2 meters was considered, then using Figure 3-17 and Figure 3-18 a Td_{mean} of 10.4 hours and Td_{amp} of 2.2 hours may be approximated. Using an albedo of 10%, Equation (3-15) may be solved for the average E. coli decay function for Durban.

$$T_d = 11.2 + 2.3 \cdot \cos\left(2\pi \cdot \frac{(D-1) + D_{offset}}{364}\right) \tag{3-18}$$

However, Figure 3-17 and Figure 3-18 were derived using the values of the *a* and *b* parameters (2-12) suggested by Guilaud et al. (1997) for the French coast. Using the above formulation to determine the E. coli decay would require these parameter values to be set for the Durban coastal environment.

3.7 Testing relationships using the Correlation Coefficient

The correlation coefficient is a statistic metric for the association between two random variables. An association between variables means that the value of one variable can be predicted, to some extent, by the value of the other. If an assumption made is that both variables are jointly Gaussian distributed then the correlation may be interpreted as a measure of statistical independence. The range of the correlation coefficient is from 1 to –1; with 1 being perfect correlation, 0 being no correlation and –1 being perfect inverse correlation. The correlation of two variables, X and Y, is calculated using (3-19) (Helsel & Hirsh, 2002)

$$\rho_{X,Y} = \frac{Cov(X,Y)}{\sigma_X * \sigma_Y} \tag{3-19}$$

Statistical significance tests can be used to indicate the likelihood that the correlation result is due to chance. For jointly Gaussian variables, the significance of each correlation is determined using two statistical hypotheses:

1. $H_0 : \rho = 0$
2. $H_1 : \rho \neq 0$

A new random variable is defined by:

$$T = r \cdot \left[\frac{(n-2)}{(1-r^2)} \right]^{\frac{1}{2}} \tag{3-20}$$

where:

r	=	Sampled correlation coefficient
n	=	The sample size

The T value is then compared against percentile values t_α for the student's t-distribution, calculated using the approximate degrees of freedom (sample size –2) and confidence level α (α=0.05 for 95%) (Helsel & Hirsh, 2002). If the T value is larger than the calculated t_p then the correlation is considered significantly large. In other words, the H_0 hypothesis is rejected and H_1 is accepted.

There are several common pitfalls associated with the use of the correlation coefficient:

1. Correlation is symmetrical; therefore it does not providing evidence of which way causation flows.
2. If other variables also influence the dependent variable, then any correlation they share with the independent variable can be falsely attributed to the independent variable.
3. If there is a non-linear relationship between the two variables being correlated, the correlation can understate the relationship.
4. The correlation between two variables is attenuated as their measurement error increases.

3.8 Beach Data Correlations

3.8.1 Beach Sites vs. Beach Sites

The relationship between the pollution levels of the different sampling beaches was analysed using correlation analysis. Significant correlations between two beaches would mean that the polluter of a certain beach might be related to the polluter of another beach. The relationship may be due to the pollution generating mechanisms being the similar (such as rainfall catchment runoff) or that they have the same source of pollution. Due to the high measurement errors, significant correlations were not expected for all beaches.

Superior correlations were found using a form of thresholding, whereby only concentrations above certain limits were considered. For correlations between two beaches, thresholding on only one of the data sets was applied. This thresholding was considered to be appropriate since the focus was on determining if high pathogen levels at one beach may be related to high levels at another. The geometric mean values of the indicator concentrations were used as the thresholding levels, due to the non-Gaussian character of beach indicator concentrations.

The Cross-correlation relationships between the sampling beaches using E.coli and Enterococcus are shown in Table 3-26 and Table 3-27, respectfully. Only statistically significant values are shown (as determined by the t-test). The correlations indicate that the coastline may be roughly divided into two groups: The southern and northern beaches. The Southern beaches include Vetches to Wedge and the Northern group includes Battery to Umgeni South. North Beach and Bay of Plenty beach are within a transition zone and therefore may fall into either category.

	Vetches	**Addington**	**South**	**Wedge**	**North**	**Bay of Plenty**	**Battery**	**Country Club**	**Laguna**	**Umgeni South**
Beach Min Concentration	10	10	12	11	11	13	56	34	38	121
Vetches	1.00	0.77	0.61	---	0.52	0.30	---	0.40	---	---
Addington	0.65	1.00	0.65	0.65	0.52	---	---	0.33	0.26	---
South	0.55	0.73	1.00	0.78	0.48	---	0.27	0.35	---	---
Wedge	---	0.64	0.78	1.00	---	---	---	0.49	0.42	---
North	0.42	0.46	0.45	---	1.00	0.41	---	0.34	0.32	---
Bay of Plenty	0.32	---	0.26	---	0.60	1.00	0.45	0.62	0.38	---
Battery	---	---	0.28	---	---	0.37	1.00	0.39	0.23	0.25
Country Club	0.30	0.36	0.35	0.69	0.45	0.50	0.37	1.00	0.26	0.28
Laguna	---	0.35	0.34	0.48	0.44	0.60	0.34	0.49	1.00	0.56
Umgeni South	---	0.25	0.22	---	0.25	---	0.26	0.46	0.59	1.00

Table 3-26: Cross-Correlations of beach sampling sites E.coli concentrations

	Vetches	Addington	South	Wedge	North	Bay of Plenty	Battery	Country Club	Laguna	Umgeni South
Beach Min Concentration	8	7	8	11	8	8	25	16	16	82
Vetches	1.00	0.83	---	---	---	---	---	---	---	---
Addington	0.83	1.00	---	---	---	---	---	---	---	0.76
South	---	---	1.00	---	---	0.54	0.75	---	---	---
Wedge	---	---	---	1.00	---	---	---	0.67	0.69	---
North	---	---	---	---	1.00	0.58	---	0.45	---	---
Bay of Plenty	---	---	0.54	---	0.58	1.00	---	0.55	---	---
Battery	---	---	0.63	---	---	0.43	1.00	---	---	---
Country Club	---	---	---	0.67	0.45	0.55	---	1.00	0.65	---
Laguna	---	---	---	0.69	---	---	---	0.65	1.00	0.80
Umgeni South	---	---	---	0.52	---	---	0.42	0.40	0.79	1.00

Table 3-28: Cross-Correlations of beach sampling sites Enterococcus concentrations

The Southern beaches have generally higher cross-correlations with respect to E.coli; for example, the Enterococcus cross-correlation between Vetches and Addington Beach is 0.83. The lack of significant stormwater drains for this section suggests that the strong relationship may be due to a single pollution source such as the nearby Somtseu SWD, or possibly polluted water exiting from the Port of Durban through the entrance channel.

The Northern beaches also show statistically significant cross-correlations, but are generally lower than those of the Southern beaches. The pollution of this section of coastline is most likely due to several large stormwater drains as well as the Umgeni River. The pollution levels may be attributed to a combination of rainfall runoff from the SWD catchments, persistent baseflow from the SWD and flow inputs from the Umgeni River. Each of these pollution sources would have different indicator concentrations and flow volumes. The resultant cross-correlation may therefore have been reduced by the presence of several individual pollution sources and are thus lower than those for the southern beaches.

The natural processes of the nearshore region would also affect the cross-correlations of beach indicator concentrations. Pollution can move from one beach to another through advection, thus there might only be a relationship between adjacent beaches if the advection current moved the pollution to that adjacent beach. The distances between the beach sampling sites would also influence the cross-correlation coefficient. The northern beaches are generally more spread out than their southern counterparts.

3.8.2 Auto-Correlation of Beach Sites

The relationship between successive fortnightly beach samples was tested using the auto-correlation function. The auto-correlation function is simply the correlation of one variable offset by a time lag.

$$\rho_{X,Y} = \frac{Cov(X(t), X(t+\Delta t))}{\sigma_X{}^2}$$

No significant correlation was found between successive fortnightly beach samples indicating that the timescales of mixing and decay processes are significantly shorter than the beach monitoring period.

3.8.3 Beach Sites vs. Accumulated Rainfall

The relationship between the beach water quality and rainfall is a key element in applying the method of Rainfall-based Alert Curves (RBAC) that are used for coastal water quality management (see section 2.7.1.1).

The discharges from the six stormwater drains and the Umgeni River were the main source of pathogenic pollution loading in the Durban Bight. The stormwater drain flows are primarily due to runoff from rainfall on the urban catchments. A strong relationship between rainfall and measured pathogenic indicator levels at the sampling beaches was expected. Stronger relationships should exist at beaches closest to stormwater drains or rivers. The correlations between the pathogenic pollution levels indicated by E.coli and Enterococcus and the accumulated rainfall, are shown in Table 3-28 and Table 3-29 respectfully. Only Statistically significant values are shown.

Days Accumulated	1	2	3	4	5	6	7
Vetches	---	---	---	---	---	---	0.13
Addington	---	---	---	0.17	0.14	0.17	0.22
South	---	---	0.17	0.17	0.13	0.17	0.21
Wedge	---	---	---	---	---	---	---
North	---	---	0.13	0.14	---	0.20	0.26
Bay of Plenty	---	---	---	---	---	0.13	0.16
Battery	0.26	0.20	0.26	0.20	0.14	0.14	---
Country Club	---	---	0.17	0.15	---	0.20	0.23
Laguna	---	---	---	---	---	---	0.13
Umgeni South	---	---	0.17	0.15	---	0.13	0.14

Table 3-28: E.coli verses Accumulated Daily Rainfall

Days Accumulated	1	2	3	4	5	6	7
Vetches	---	---	---	---	---	---	---
Addington	---	---	---	---	---	---	---
South	---	---	---	---	---	---	0.26
Wedge	---	---	---	---	---	---	---
North	---	---	0.28	0.29	0.26	0.30	0.29
Bay of Plenty	---	---	---	---	---	---	---
Battery	0.32	0.29	0.23	---	---	---	---
Country Club	---	---	---	---	---	---	---
Laguna	---	---	0.25	---	0.24	0.27	0.29
Umgeni South	---	---	---	---	0.29	0.35	0.37

Table 3-29: Enterococcus verses Accumulated Daily Rainfall

The cross-correlations are generally small and insignificant (as determined by the t-test). Amongst the highest values were those at Battery Beach for the one and two day accumulated rainfall. Weakly significant correlations were only found for the other beaches using rainfall accumulations of three or more days. Scatter plots for battery beach concentrations verses one and three day-accumulated rainfall are shown in Figure 3-19.

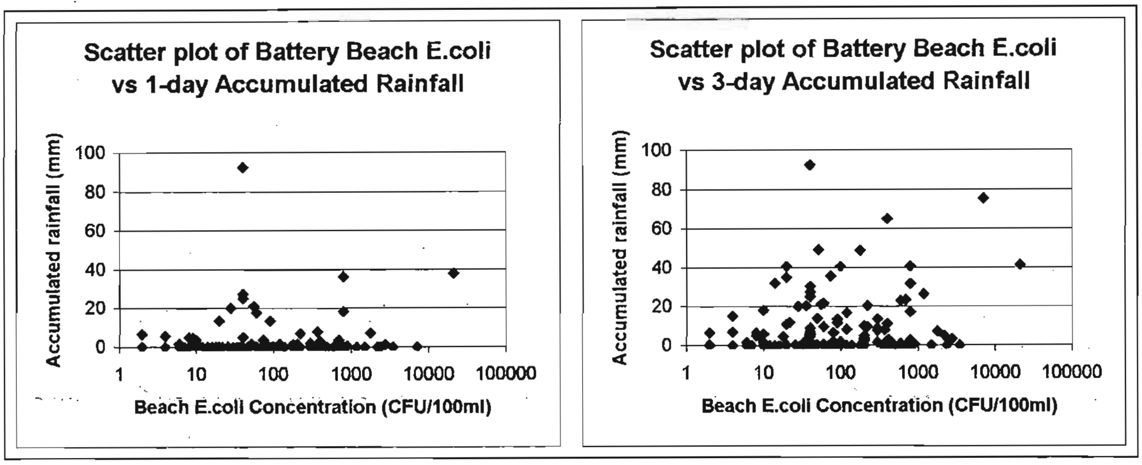

Figure 3-19: Scatter plots of Battery Beach E.coli concentrations verses 1 and 3 day accumulated rainfall totals

The scatter plots suggest reasons for the low correlations. It was noted that for all beaches a large percentage of the high indicator concentrations corresponded to zero accumulated rainfall totals. However, when rainfall was accumulated for three or more days there were more sampling days that had non-zero accumulated rainfall depths. Only then was a relationship between rainfall and beach water quality indicated. The disappearance timescale of the indicators is generally shorter than three days, therefore the correlations indicate only a weak-underlying relationship between rainfall and beach water quality. To investigate the relationship between rainfall and beach pathogen concentration in more detail, higher temporal resolution of sampling during and just after rainfall events is required.

3.8.4 Conclusions

The cross-correlation analysis indicates that pathogenic pollution levels at adjacent beaches are related. The auto-correlation coefficient indicates that there are relationships that exist between rainfall and the pathogenic pollution levels of beaches. These results suggest that the coastline may be modelled as a system of interconnected beaches.

However, calculation of high correlations may not be possible due to the underlying distribution of the pathogenic pollution of the beaches. It has been shown that the pollution inputs (SWD and Rivers) may be described by lognormal distributions. The distribution of the rainfall accumulations are likely not to be normally distributed either. Due to the non-Gaussian characteristics of the data sets the correlation cannot be interpreted in terms of statistical dependence. For example a cross-correlation of zero does not imply independence unless the random variables are jointly Gaussian distributed.

3.9 Stormwater Drain Data Correlations

3.9.1 Stormwater drains vs. Rainfall

The magnitude of the pathogenic pollution contained within urban stormwater runoff is due to a combination of rainfall runoff volume and pollution characteristics of the urban catchment environment. The relationship that may exist between stormwater pathogenic indicator content and the rainfall on the catchment, indicated by the cross-correlation coefficient is shown in Table 3-31 and Table 3-32.

Days Accumulated	1	2	3	4	5	6	7
Hospital	---	---	---	---	---	---	---
Rutherford	---	---	---	0.19	0.19	---	0.23
West	---	---	---	---	---	---	---
Somtseu	---	---	---	---	---	---	---
Argyle	---	---	---	---	---	---	---
Walter	---	---	---	---	---	---	---

Table 3-31: Cross-Correlation of Stormwater E.coli verses Non-zero accumulated rainfall

Days Accumulated	1	2	3	4	5	6	7
Hospital	---	0.20	0.18	---	---	---	---
Rutherford	---	---	---	0.35	0.37	0.27	0.31
West	---	---	---	---	---	---	---
Somtseu	0.23	0.27	0.24	---	---	---	---
Argyle	-0.19	-0.19	-0.19	---	---	---	---
Walter	---	---	---	---	---	---	---

Table 3-32: Cross-Correlation of Stormwater Enterococcus verses Non-zero accumulated rainfall

No significant correlations exist for E.coli for the first three days, with only Rutherford showing any correlation at all. One day significant correlations for Enterococcus exist only for Somtseu and Argyle, with hospital only being weakly correlated after two days.

Of interest was that Argyle was actually negatively correlated indicating that for Argyle, the more rainfall the less the average pathogenic pollution contained within the drain effluent. This may be caused by Argyle having a constant pathogenic pollution input into the drain whose flow rate is not dependent on rainfall. However, when it does rain the pollution from this source may be more diluted.

3.9.2 Stormwater drains vs. Inter-event period

The relationship between stormwater pollution concentrations and the inter-event period is used for the determination of the Rainfall-based Alert Curves (see section 2.7.1.1). The inter-event period is the duration in time between successive rainfall events. Usually it is expected that pollution would build up during the dry period and be washed off the catchment during the wet periods. A large proportion of the pollution is assumed to be captured in the "First flush", with further runoff having less and less pollution concentration the longer the rain event continues

(Taylor et al, 1993). Therefore, to determine significant relationships between the inter-event dry period and runoff pollution concentration, intensive sampling needs to be done during the 'First flush' period and for numerous rainfall events.

As previously mentioned the stormwater sampling is done on a monthly basis. The likelihood that sampling was done on a wet day and during the first flush period is extremely small. This may make it impossible to find any significant or credible relationship.

3.9.3 Stormwater Drains vs. Beach Sites

The relationship between urban runoff and beach water quality is crucial to the understanding of the nearshore coastal system. This relationship should be identifiable by determining the correlations between the pollution levels in the urban stormwater drains and surrounding waters. Unfortunately, due to the sampling procedures employed by the EMWSS, it was impossible to determine any significant correlations. One of the reasons was that beach sites and stormwater drains are not sampled simultaneously, but on different days, with the drains usually measured on days preceeding beach sampling.

In order to gain some understanding of the interaction between the stormwater drains and nearshore region an undergraduate research project (Brahmin, 2001) was done. A discussion of the analysis of the information collected is discussed in Section 1.1.

3.10 Case Study: Urban Runoff Water Quality (Brahmin, 2001)

The objective of the research performed by Brahmin (2001) was to determine the relationship between rainfall, stormwater flow, stormwater pollution and the resultant pollution of effected beaches. The Argyle Road stormwater drain and Battery Beach coastline were selected as a case study region. The Argyle SWD / Battery beach situation was chosen for various reasons:

1. Battery Beach was found to be the most polluted bathing beach along the golden mile.
2. The Argyle Road Stormwater drain was found to be highly polluted and most likely the main polluter of Battery Beach.
3. The open culvert running along the southern side of Argyle Road between Stanger Street and Brickhill Road was ideal for both water quality sampling and measurement of stormwater flow rates.

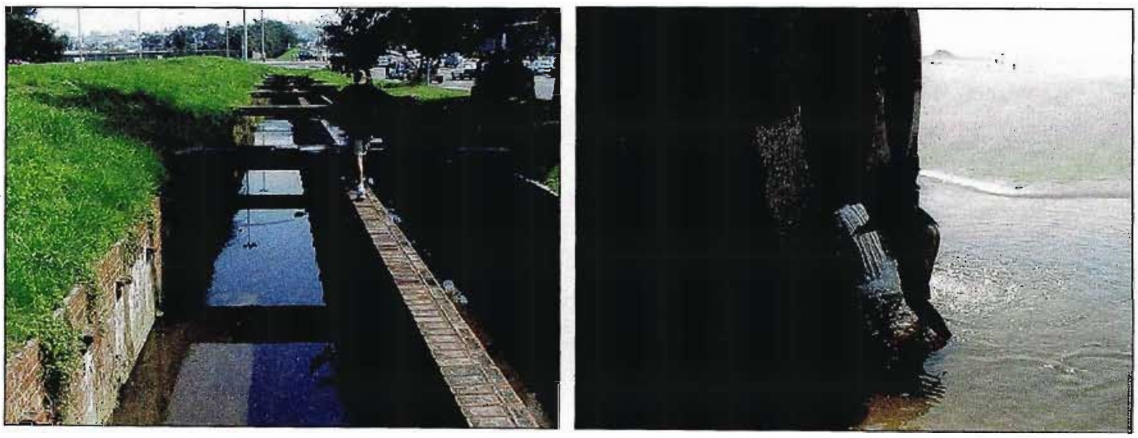

Plate 3-16: Argyle SWD open culverts and beach outfall (at low tide)

3.10.1 Measurement Procedures

<u>Water Quality</u>

Water quality samples were taken from the Argyle SWD daily from two sampling positions: One from the open culverts; and a second from the beach outfall on battery beach (as shown in Plate 3-16).

Water quality samples were taken at five positions along Battery beach daily. The five sampling positions, comprising one in front and two on either side of the Argyle SWD are shown in Plate 3-17.

The sampling methods used were the same as those as used by the EMWSS and analysis of the samples was performed by EMWSS.

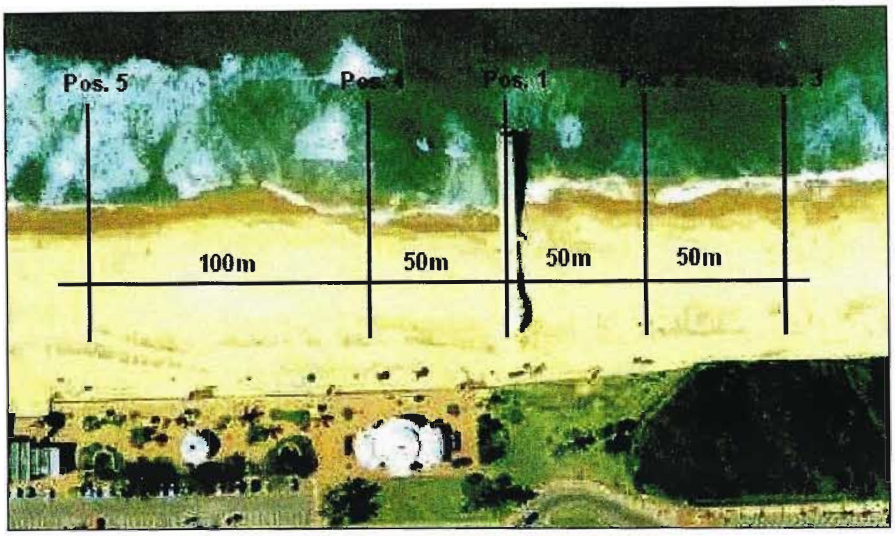

Plate 3-17: Sampling positions along Battery Beach

Stormwater flow rates were measured daily at the culverts at approximately midday. The velocity of the flow was determined using a specially designed float, by recording the time taken for the float to cover a fixed distance of 11 metres. The cross-sectional flow depth was recorded by taking two depth measurements.

3.10.2 Basic Analysis

<u>**Stormwater flow**</u>

The flow rates for each sampling time were calculated using two different methods:

The first flow rate, Q, was calculated using an average flow velocity, calculated from four float times, and the average of the two depth measurements. The width of the culvert is 2.6m, thus the flow rate was calculated as:

$$Q = (Width) * (Avg \quad Depth) * (Avg \quad Velocity)$$

The second flow rate was calculated by Manning's Equation (3-21) with the assumption of uniform flow. Using "As Built" longitudinal drawings of the Argyle SWD (Wesson, 2001) the slope, S, at the sampling position was 0.00116. Typical Manning's roughness, n, for open channel surfaces of concrete is given as 0.012 (Chow, 1988). Thus, the flow rate may be calculates as:

$$Q = \frac{1}{n} \cdot A \cdot R^{\frac{2}{3}} \cdot S^{\frac{1}{2}} \qquad (3\text{-}21)$$

Minimising the sum of the squares of the differences between the two calculated flow rates a site-specific n-value was calculated as 0.0178. Flow rates could then be calculated for the stormwater drain if the depth at the open culverts was known.

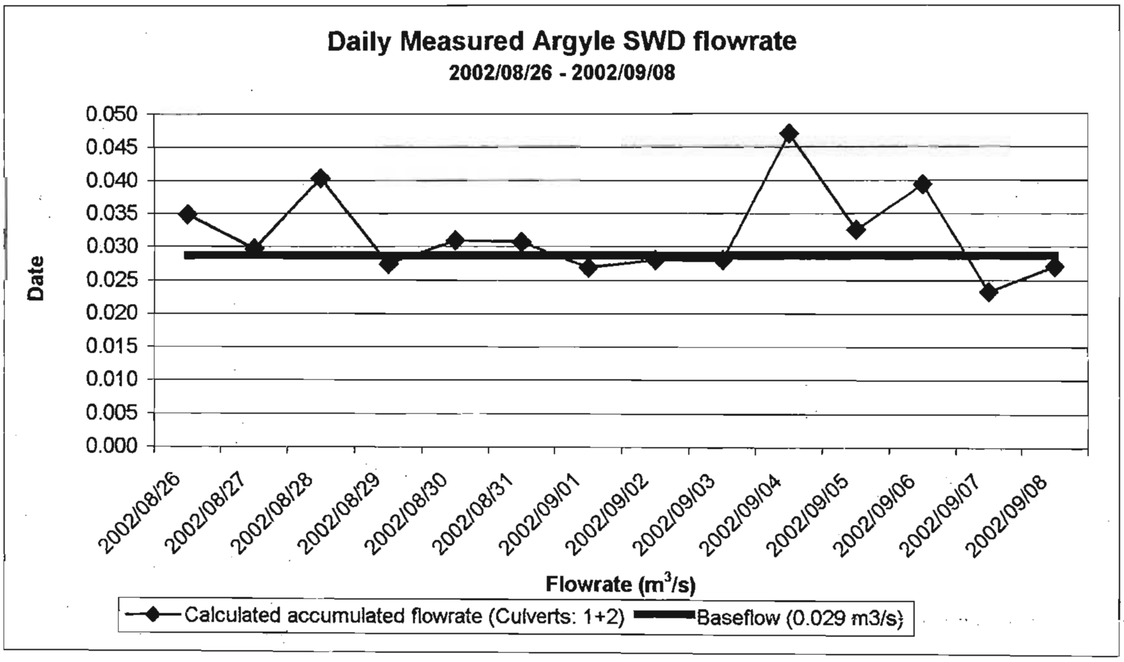

Figure 3-20: Daily measured Argyle SWD flow rate

The calculated flow rates over the period of sampling are shown in Figure 3-20. An estimated baseflow of 0.029 m^3/s was calculated for Argyle stormwater drain over the sampling period.

3.10.3 Beach Loading Analysis

The ability to accurately model the pathogenic pollution of Battery beach was analysed using a simple beach loading and simple decay model.

Method

The site dependence of the measured beach concentrations was removed by considering the total number of E.coli coliforms in the nearshore zone:

1. Each sampling position was considered as the centroid of a well-mixed cell dependant on the spacing between adjacent positions.
2. A Volume per length of coastline of 100 m^3/m was used to calculate the volume of each cell.
3. The total nearshore E.coli load (CFU) in the nearshore zone was calculated as a summation of the total counts within each of the cells.

The average 24-hr stormwater flow rate was calculated as a combination of the calculated rainfall runoff and the estimated baseflow, of 0.029 m^3/s. The rainfall runoff was calculated using the following parameters:

1. Area reduction factor (ARF) = 0.96
2. Runoff coefficient (RC) = 0.5
3. Catchment Area = 1618125 m^2

The E.coli counts measured in the stormwater drains were multiplied by the average 24-hr stormwater flow resulting in a daily stormwater drain E.coli loading (CFU) of the nearshore Battery Beach coastline.

A simple first-order decay model (see Section 2.6.2.1) is used to describe the disappearance of E.coli from the nearshore region (as derived later in Section 4.2)

$$C_t = C_{t-1} \cdot e^{-\frac{24}{T_D}} + I \cdot e^{-\frac{24}{T_D}}$$

where:

C_t is the calculated total indicator count at time t, in CFU

C_{t-1} is the previous calculated total indicator count, in CFU

I is the stormwater total input counts over the time interval (t-1,t), in CFU

T_D is the disappearance rate of the indicator, in hours

The optimum disappearance rate, T_D, was calculated by minimising the sum of the squared errors between the measured E.coli nearshore load and the predicted total E.coli load.

Results

The optimum disappearance rate, T_D, was calculated as 9.48 hours. The result of the beach loading analysis is presented in Figure 3-21.

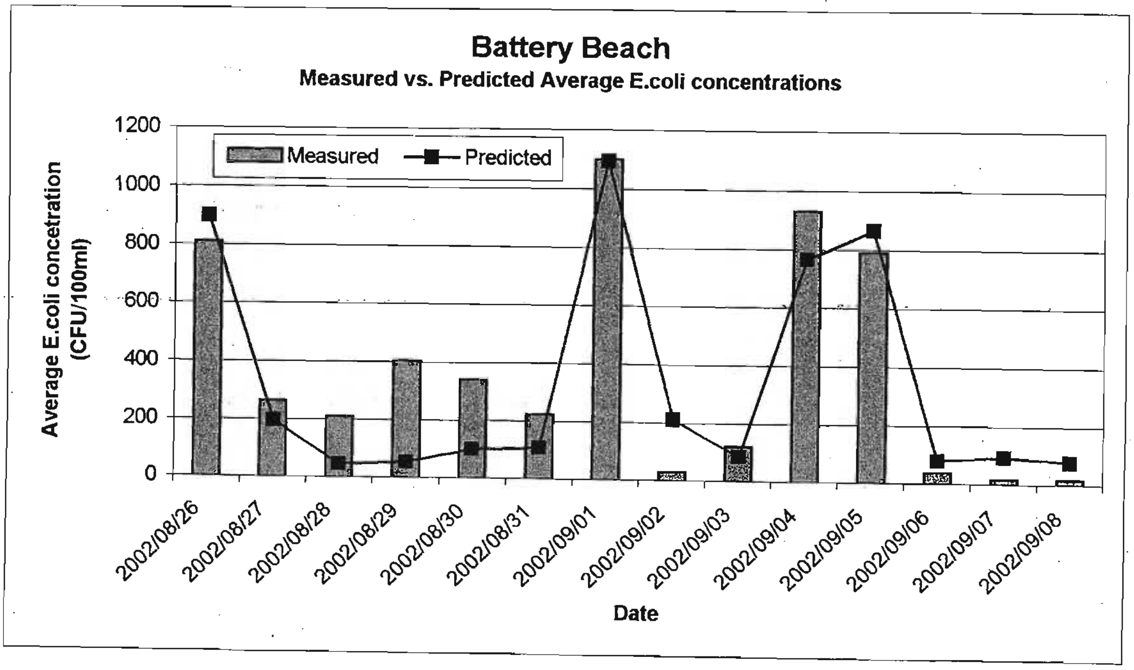

Figure 3-21: Measured vs. Predicted E.coli concentrations at Battery Beach (2002/08/26 – 2002/09/06)

It was noted in Figure 3-21, by considering the total loading of the nearshore zone and a simple first-order decay model the average peaks and probable hazardous water quality conditions may be identified. During periods of no rainfall, predictions may be inaccurate, however during these periods beach water quality may not be a problem.

3.10.4 Case Study Conclusions

Using estimated rainfall runoff and an averaged baseflow fairly accurate predictions may be made on the average pathogenic indicator concentration within the nearshore zone. However, daily sampling and testing of stormwater indicator concentrations are needed to make realistic predictions.

Simple models may be adequate at predicting general or average concentrations along a coastline. However, small area effects involving higher and possibly dangerous levels may not be identified.

Possible magnitudes for model parameters were found:

1. Site specific E.coli disappearance timescale, T_D, of approximately 9.5 hours
2. Rainfall runoff coefficient of 0.5

3.11 Conclusions

There are many conclusions that may be drawn from this chapter due to the wide spectrum of topics covered. However, a few of the important results were found.

Battery Beach, due to its use as a designated bathing beach, has a pathogenic water quality problem that needs to be addressed. Although the other beaches had better water quality conditions, the continued use of E.coli as the primary WQ indicator in the marine environment as apposed to Enterococcus needs attention. This was demonstrated by South Beach where if E.coli was used as the indicator, the water quality appeared never to fail the guidelines, while if Enterococcus guidelines were applied water quality standards were exceeded.

The environmental factors of the coastal zone, ie. wind, rainfall and radiation, have been reviewed and analysed.

Inter-relationships between beaches, rainfall, and stormwater drains have been investigated and shown to exist. The cross-correlations and auto-correlations found were generally small. However, due to the non-Gaussian distributed nature of most of the data sets the significance of the correlations could not be accurately interpreted. The lack of sufficient sampled data around particular events (e.g. SWD and Beach sampling during rainfall events) meant that known relationships between rainfall and the pathogenic content of the SWD and beaches could not be determined.

It was demonstrated that if SWD concentrations were known the pollution levels within the effected nearshore zone could be predicted and possible model parameters were developed.

CHAPTER 4:
COASTAL WATER QUALITY MODEL FORMUALTION

4.1 Introduction

The coastal water quality model (CWQM) is a tool for the analysis of the water quality of the coastal nearshore zone. The modelling tool can provide the user with two main analysis techniques. It can be used to make predictions of the current bathing water quality conditions at beaches, especially during times when measurements of water quality are not available. A more advanced function of the CWQM is in its application as "what-if" analysis and evaluation tool, where the effects of changes in the coastal environment (eg. developments) can be evaluated.

The coastal nearshore region is subject to complex coastal dynamics involving a range of physical and microbiological processes. These complex processes have been simplified and a CWQM has been formulated as a *state-space discrete, lumped advection-diffusion type model.* The model uses indicator microorganism concentrations as the indictor of pollution and water quality conditions.

4.1 Introduction of the CWQM Formulation

In order to formulate a model to describe the complex processes in nearshore coastal region the processes needed to be isolated and simplified. To describe the coastal processes the nearshore coastline was divided into a series of **cells** acted on by a range of processes as shown in Figure 4-1.

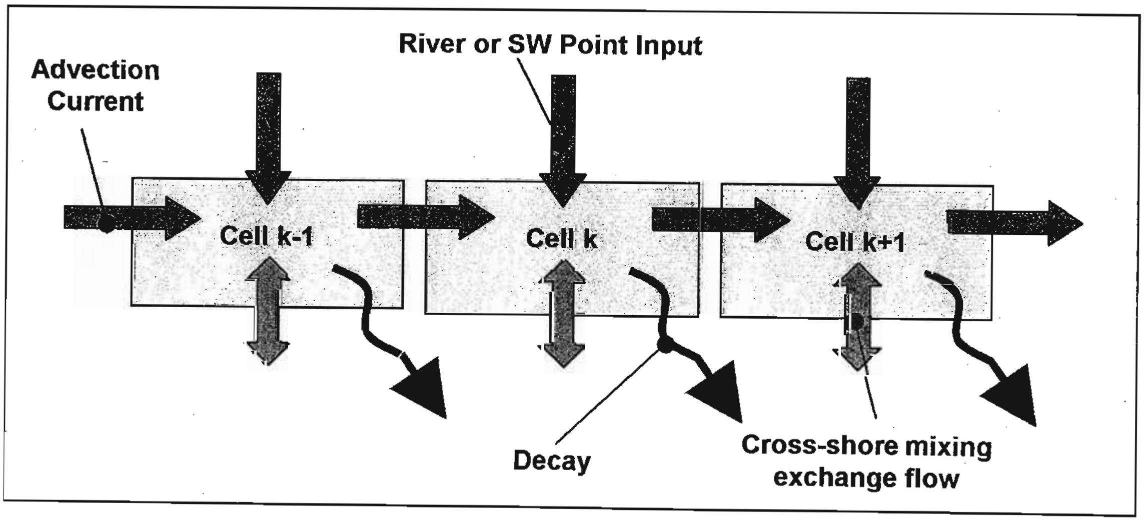

Figure 4-1: The simplification of the nearshore coastal processes

The cells are considered to be homogeneous units, meaning that the indicator concentration within each cell is assumed uniform. The nearshore coastal cells are assigned a set of physical characteristics that describe each cell; a length, volume and orientation.

1. The cell *lengths* are the length of the coastline that each individual cell covers.
2. The cell *volumes* are specified as: Length x Average depth x Average width. The cells are conceived as describing the well-mixed nearshore zone.
3. The cell *orientations* are specified using the bearing of the individual cells (in degrees North).

Coastal processes such as the decay, advection and diffusion of pollution affect each cell. Each Individual cell can have pollution inputs, i.e. an increase in indicator concentration, by point inputs. All the processes affecting each cell are modelled as linear processes that are parametized by their characteristic timescales (see section 2).

A "*state-space*" description of the model can be derived to describe the evolution of the cell 'states' as a function of time and their positions with respect to each other.

The pollution concentrations or "*states*" of the cells are calculated at "*discrete*" time intervals, Δt, and the assumption is made that the processes affecting the cells remain stable over these time intervals.

The *"lumped advection-diffusion"* description of the model refers to the method used to combine the effects that the processes have on the states of the cells (As discussed in Section 2). Since all the processes are modelled as linear processes, they may be superimposed, and their combined effect on the states determined. There are then basically two combined processes that affect the states of the cells:

1. The advection of pollution from one cell to another
2. The disappearance of that pollution in each cell through mixing and decay processes

4.3 Mathematical Description of System Processes

The coastal processes modelled in the CWQM are indicated in Figure 4-1. In this section their mathematical description is presented and the system equations for the model are specified. For simplicity, each of the represented processes will be considered separately. Since all the processes are linear they may be superimposed to evaluate their combined effects.

4.2.1 Decay of Pathogenic Pollution

The decay model of the indicator microorganism and associated pathogenic pollution is described by a first order kinetics approach, Equation (2-6) (See Section 2.6.2.1).

$$\frac{\partial C_k}{\partial t} = -kC_k \quad \text{or} \quad \frac{\partial C_k}{\partial t} = -\frac{C_k}{T_d} \tag{4-1}$$

Where

C_k	=	Indictor concentration, in CFU/100ml
k	=	Indictor decay rate, in hr^{-1}
T_d	=	Indictor decay timescale, in hrs

The indictor decay rate is related to the 'T_{90}' value, which is the time necessary to decrease the indicator concentration by one decimal logarithm. (See Section 2.6.3) . Using the T_{90} value the decay rate, k, can be calculated from: $k = Ln(10)/T_{90}$. A decay timescale $T_d = 1/k$. Whence:

$$T_d = \frac{T_{90}}{Ln(10)} \tag{4-2}$$

The decay of pathogenic pollution is known to depend on a number of physical, chemical and environmental parameters. (See Section 2.6.1). The T_d parameter may therefore be expected to vary over a range of timescales from hourly, to daily, to seasonally; depending on such factors as solar radiation, turbidity of the water, etc.

4.2.2 Pollution Point Inputs

The CWQM assumes pollution is introduced to the cells by point inputs. Typical point inputs are stormwater drains, canals and rivers. The discharge from these point inputs comes from two sources, direct runoff from the catchment and a persistent base flow. The pollution that enters the cells is suspended in fresh water thus the increased pollution occupies a surface plume in the upper water column until significant mixing takes place.

Considering the species conservation equation, the change in pollution of the cells due to the point input is modelled by:

$$\therefore \frac{\partial}{\partial t}\left(V_{cell}\cdot C_k\right)=Q_p\cdot I_k(t)$$

$$\therefore \frac{\partial}{\partial t}C_k=\frac{Q_p}{V_{cell}}\cdot I_k(t) \qquad (4\text{-}3)$$

$$\therefore \frac{\partial C_k}{\partial t}=\frac{1}{T_P}\cdot I_k(t)$$

where:

T_P is the time needed for the point input flow to replace the volume of the cell, hrs

$$T_P=\frac{V_{cell}}{Q_P} \qquad (4\text{-}4)$$

V_{cell}	=	Cell volume, in m^3
Q_P	=	Point input flow rate, in m^3/hr
C_k	=	Cell concentration increase, cfu or counts/100ml
$I_k(t)$	=	Input concentration as a function of time, cfu or counts/100ml
$V_{cell}\,.\,C_k$	=	Total number of coliform forming units in the cell
$Q_p\,.\,I_k(t)$	=	Total number of coliform forming units in the inputs

The point input flow rate is a combination of a base-flow and the direct runoff due to rainfall on the catchment.

4.2.3 Surface Advection Current

It is assumed that the pollution is transported from one cell to another by an advection current. The forcing mechanism of this advection current is assumed to be the local winds. The pollution from the point inputs comes in as a freshwater plume, which sits in the upper levels of the water column. The local winds generate wind driven currents in these upper layers of the water column.

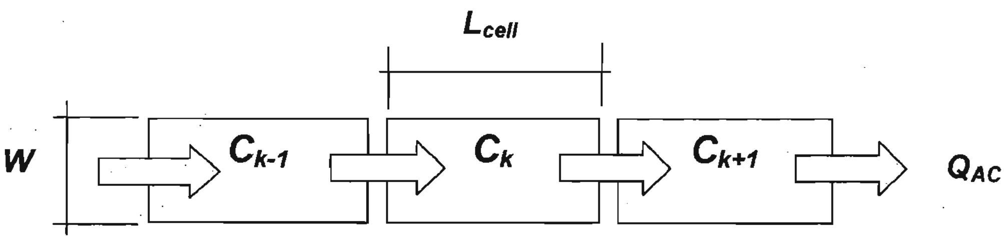

Figure 4-2: Formulation of the surface advection current

The conservation of species is used to model the effect of the advection current (Figure 4-2), using a timescale (T_{ADV}), surface current flow rate (Q_{AC}), surface current advection velocity (V_{AC}), cell length (L_{cell}), cell depth (D), cell width (W), and cell volume (V_{cell}).

$$\begin{aligned} Q_{AC} &= V_{AC}\cdot(D\cdot W) \\ &= V_{AC}\cdot Area \\ &= \frac{L_{cell}}{T_{AC}}\cdot Area \end{aligned}$$

Therefore:

$V_{cell} \cdot C_k =$ Number of coliform forming units in cell C_k

$Q_{AC}\, C_k$ = Number of coliform forming units removed from cell C_k

$Q_{AC}\, C_{k-1}$ = Number of coliform forming units added to cell C_k

From the species conservation equation:

$$\therefore \frac{\partial}{\partial t}\left(V_{cell} \cdot C_k\right) = -Q_{AC} \cdot \left(C_k - C_{k-1}\right)$$

$$\therefore \left(L_{cell} \cdot Area\right) \cdot \frac{\partial}{\partial t}\left(C_k\right) = -\left(\frac{L_{cell} \cdot Area}{T_{ADV}}\right) \cdot \left(C_k - C_{k-1}\right) \qquad (4\text{-}5)$$

$$\therefore \frac{\partial C_k}{\partial t} = -\frac{\left(C_k - C_{k-1}\right)}{T_{ADV}}$$

The advection timescale is the time that it would take for an indicator microorganism to cross the length of the cell if it were being advected in this current.

$$T_{ADV} = \frac{L_{Cell}}{S_{AC}} \qquad (4\text{-}6)$$

Where:

L_{Cell} = Cell length, in metres

S_{AC} = Speed of the advection current, in m/hr

The speed of the advection current is related to the wind speed and scaling coefficient, C_{AC}, as described in Section 2.5.1.

Using the individual cell directions an average coastline direction can be determined. The wind direction is compared against the coastline direction to determine if it is blowing in a positive direction (left to right) or in a negative direction (right to left), further clarification of the positive or negative direction is discussed in Section 4.6.2.1.

In Section 2.5.1 the wind driven advection currents were reported to propagate within a 45-degree sector of the wind direction. Therefore the absolute speed of the wind is used to determine the speed of the advection current.

$$S_{AC} = C_{AC} * S_{wind} * 3600$$

Where:

S_{AC} = Speed of the advection current, in m/hr

S_{Wind} = Absolute wind speed, in m/s

C_{AC} = Wind / Current advection coefficient

The coefficient of advection C_{AC} is generally dependant on the wind fetch length, increasing as the fetch length of the wind increases and approaches a constant value. In Section 2.5.1

maximum value of 3.5% for long fetches is suggested. The fetch length of the model is assumed to be short thus the value of C_{AC} is expected to be significantly less than 3.5%.

4.2.4 Cross-shore Mixing Exchange Flow

Cross-shore mixing and exchange flow is the mixing between the cell volume and the volume of water seaward of the cell boundary. The cells are not conceived as a fixed body of water but as a control volume, therefore the actual water defined by the volume can be exchanged with water from outside the cells.

The cross-shore mixing is parameterized using a timescale, T_{CM}, where the species conservation equation applied to cross-shore mixing yields:

$$\frac{\partial C_k}{\partial t} = -\frac{(C_k - C_{outside})}{T_{CM}} \tag{4-7}$$

where:

C_k	=	Concentration of the cell to be calculated
$C_{outside}$	=	Concentration of the waters seaward of the cell boundary
T_{CM}	=	Cross-shore mixing timescale, in hours

The concentration of the coastal waters outside the boundary is assumed to be zero ($C_{outside} = 0$). Thus the effect on the cell concentration by cross-shore mixing is:

$$\frac{\partial C_k}{\partial t} = -\frac{C_k}{T_{CM}} \tag{4-8}$$

The cross-shore mixing timescale represents the time taken to exchange the cell volume by the cross-shore exchange flow. The exchange flow is dependant on natural conditions such as:

1. Wave climate
2. The effect that tidal variations has on the replacement of the cell volumes.
3. Physical bathymetrical features such as reefs and sand bars that may restrict the exchange flow between the cells and deeper waters.

4.2.5 The Lumped Advection Diffusion Mathematical Description

All processes of the model are formulated as linear processes. They may therefore be superimposed to yield a lumped advection diffusion model. Combining all advective-diffusive and input processes from sections 4.2.1, 4.2.2 and 4.2.3 yields

$$\frac{\partial C_k}{\partial t} = -\frac{C_k}{T_d} - \frac{(C_k - C_{k-1})}{T_{ADV}} - \frac{C_k}{T_{CM}} + \frac{I_k}{T_P} \tag{4-9}$$

Combining similar parameters:

$$\frac{\partial C_k}{\partial t} = -C_k\left(\frac{1}{T_d} + \frac{1}{T_{ADV}} + \frac{1}{T_{CM}}\right) + \frac{C_{k-1}}{T_{ADV}} + \frac{I_k}{T_P}$$

A timescale T is found as a combination of the individual timescales affecting the target cell, namely

$$\frac{1}{T}=\left(\frac{1}{T_d}+\frac{1}{T_{ADV}}+\frac{1}{T_{CM}}\right) \tag{4-10}$$

Thus the lumped advection-diffusion model is described by the first order differential equation:

$$\underbrace{\frac{\partial C_k}{\partial t}}_{\dot{x}}=\underbrace{\frac{-C_k}{T}+\frac{C_{k-1}}{T_{ADV}}}_{A\cdot x}+\underbrace{\frac{I_k}{T_p}}_{B\cdot u} \tag{4-11}$$

Which can be written in the form of a linear dynamic system:

$$\dot{x}_t = A_t \cdot x_t + B_t \cdot u_t \tag{4-12}$$

The A-matrix looks as follows:

$$A_t=\begin{bmatrix} -\frac{1}{T_1} & 0 & 0 & \ldots & 0 \\ \frac{1}{T_{ADV_1}} & -\frac{1}{T_2} & 0 & \ldots & 0 \\ 0 & \frac{1}{T_{ADV_2}} & -\frac{1}{T_3} & \ldots & 0 \\ \ldots & \ldots & \ldots & \ldots & \ldots \\ 0 & 0 & 0 & \ldots & -\frac{1}{T_n} \end{bmatrix} \tag{4-13}$$

The diagonal elements of the matrix relate to the disappearance of the coliforms from the respective cells. The off-diagonal terms relate to the advection of the coliforms between adjacent cells. In the A-matrix shown above the advection is in the positive direction, from cell i to i+1.

$$B_t=\begin{bmatrix} \frac{1}{T_{P_1}} & 0 & \ldots & 0 \\ 0 & \frac{1}{T_{P_2}} & \ldots & 0 \\ \ldots & \ldots & \ldots & \ldots \\ 0 & 0 & 0 & \frac{1}{T_{P_n}} \end{bmatrix} \tag{4-14}$$

The B-matrix is a diagonal matrix. If there is no input into that cell during the time interval then the relative T_P is infinite and the diagonal element at that cell position becomes zero.

4.3.1 Defining the Parameters of the CWQM

4.3.1.1 The Disappearance Parameter

The decay and cross-shore mixing parameters (T_d and T_{CM}) perform the same function within the model and it is therefore impossible to decouple them for parameter fitting purposes. A new parameter T_D is defined as the dissipation parameter (the combined effect of both T_d and T_{CM}).

$$\frac{1}{T_D}=\left(\frac{1}{T_d}+\frac{1}{T_{CM}}\right) \tag{4-15}$$

The T- timescale for cell i is therefore redefined as:

$$\frac{1}{T_i}=\left(\frac{1}{T_D}+\frac{1}{T_{ADV_i}}\right) \tag{4-16}$$

4.3.1.2 The Advection Coefficient

The advection timescale (T_{ADV}) cannot be defined directly; rather it is dependent on the average wind speed during the timestep and the individual cell length. Recall Section 4.2.3, where

$$T_{ADV}=\frac{L_{Cell}}{C_{AC}*S_{wind}*3600} \tag{4-17}$$

The wind-current advection coefficient (C_{AC}) is the independent variable and therefore parameterized within the CWQM.

The CWQM is essentially a two-parameter model, defined using a dissipation parameter and an advection coefficient.

4.4 The State Space Equation Formulation

The dynamics of the system shown above in Figure 4-1 can be mathematically described using a set of system equations that may be formulated as a linear, first order, vector differential equation, as shown by Equation (4-12). This is called the *state equation* is given by (Jazwinski, 1970):

$$\dot{x}(t) = A(t) \cdot x(t) + B(t) \cdot u(t) \tag{4-18}$$

Where:

$x(t) = [C_1 \quad C_2 \quad C_3 \quad .... \quad C_n]^T$ is a (n x 1) dimensional column vector containing the concentrations of pollution in each cell, where n is the number of cells describing the coastline. This is called the state vector since it is a vector containing the state variables of the system, namely the concentration C_i.

$u(t) = [I_1 \quad I_2 \quad I_3 \quad .... \quad I_n]^T$ is a (n x 1) dimensional column vector containing the point input concentrations to each cell

A(t) is a (n x n) time varying coefficient matrix containing the parameters that specify the advection and diffusion of pollution. (See (4-13))

B(t) is a (n x n) time varying coefficient matrix that scales the inputs appropriately. (See (4-14))

The states of the system, ie. the cell concentrations, are "observed" by the use of an *output equation* given by :

$$y(t) = D \cdot x(t) \tag{4-19}$$

where:

y(t) is a (m x 1) column vector containing the observed concentrations at the m-sampled bathing beaches.

D is a (m x n) transformation matrix that transforms the state vector, *x(t)*, into the sampled vector, *y(t)*

Therefore the system is specified by a combination of the state equation and output equation to define the *dynamic equations of the system*:

$$\begin{aligned} \dot{x}(t) &= A(t) \cdot x(t) + B(t) \cdot u(t) \\ y(t) &= D \cdot x(t) \end{aligned} \tag{4-20}$$

4.3.1 The Solution of the Dynamic Equations

If we consider the deterministic system of dynamic equations given by (4-20) namely:

$$\dot{x}(t) = A(t) \cdot x(t) + B(t) \cdot u(t)$$
$$y(t) = D \cdot x(t)$$

The solution of the dynamic equations can be written as: (eg. Brown et al, 1992)

$$x(t) = \Phi(t, t_0) \cdot x(t_0) + \int_{t_0}^{t} \Phi(t, \tau) \cdot B(\tau) \cdot u(\tau) \cdot dt$$
$$y(t) = D \cdot x(t) \tag{4-21}$$

where:

$x(t_0)$ is the deterministic initial state of the system.

$\Phi(t, \tau)$ is the state transition matrix of the homogeneous equation $\dot{x} = A \cdot x(t)$ whose solution for a constant coefficient matrix A in the interval (t_0, t) is given by (Brown et al, 1992; Chen, 1970):

$$\Phi(t_0, t) = e^{A(t - t_0)} \tag{4-22}$$

4.3.2 The Coastal Water Quality Model as a Stochastic System

The dynamic equations of the system given by the equations (4-20) are implicitly deterministic. The CWQM is however attempting to model a real system in which assumptions have been made in order to describe it mathematically. There is therefore a need to include a degree of uncertainty about the system. The state variables $u(t)$ and $y(t)$ cannot be measured exactly: rather they are determined by the method discussed in Section 2.3.1, as a count per 100ml which is subject to measurement uncertainty. There is also a degree of uncertainty in the parameterization of the advection and mixing processes.

The uncertainty of the system is incorporated by adding stochastic 'noise' to the expression. The noise is assumed to be Gaussian with zero mean and a zero correlation function (Jazwinski, 1970). The resulting stochastic system is defined by the *linear stochastic system equations*:

$$\dot{x}(t) = A(t) \cdot x(t) + B(t) \cdot u(t) + \omega(t)$$
$$y(t) = D \cdot x(t) + \varepsilon(t) \tag{4-23}$$

where $\omega(t)$ is defined as the (n x 1) zero mean Gaussian white noise process incorporating the uncertainty in the inputs and $\varepsilon(t)$ is the zero mean Gaussian white noise process describing the measurement uncertainties. That is:

$$P\{\omega\} = N\{0 \quad Q\}$$
$$P\{\varepsilon\} = N\{0 \quad R\}$$

Where Q and R are n x n and m x m (diagonal) variance or co-variance matrices for ω and ε respectively.

The two white noise processes are assumed to be independent of each other. Therefore:

$$E\{\varepsilon(t) \quad \omega^T(t)\} = 0$$

Another source of uncertainty in the real system comes from the initial estimates of the states. The initial conditions of the states, $x(t_0)$, are assumed to be Gaussian random variables of known mean, $\hat{x}(t_0)$, and covariance $P(t_0)$.

$$\begin{aligned} &E\{x(t_0)\} = \hat{x}(t_0) \\ &E\{[x(t_0)-\hat{x}(t_0)]\cdot[x(t_0)-\hat{x}(t_0)]\} = P(t_0) \end{aligned} \tag{4-24}$$

4.4 The Discrete Time Coastal Water Quality Model

Since we are interested in estimating the system states at regular time intervals, we require a *discrete time dynamic system* that corresponds to the continuous dynamic system. This comprises a sequence $\{x(k)$, k=0,1,2,.......} at discrete instants of time {k, k+1, k+2,...} which are separated by the interval Δt. The system inputs and parameters are required for the discrete intervals of time, and are assumed to be invariant during these time intervals.

4.4.1 Discretizing the Inputs and Parameters

The inputs to the system are determined by two factors: the point input flow rates and the point input pollution concentration. For the purpose of discretizing the input two assumptions are made about the characteristics of the input:

$I(t,t+\Delta t)$	is assumed to be a constant value in the interval (t,t+Δt), in CFU/100ml.
$q(t,t+\Delta t)$	is assumed to be a constant flow rate from the point input source over the time interval Δt, in units of $m^3/\Delta t$

The continuous input is therefore modelled as a step input function where the inputs are averaged over the time interval.

The parameters used in the coefficient matrix, $A(t)$, are expected to vary continuously. For example the diffusion may vary daily or even hourly. The advection is determined by local wind conditions, which also varies continuously. As with the input parameters the assumption is made that these processes are invariant during the interval (t;t+Δt) and are parameterized by constant, average values over the time interval.

4.4.2 The Discrete Dynamic Equations

Using the above assumptions, the continuous time linear system equations described by (4-20)

$$\dot{x}(t) = A(t)\cdot x(t) + B(t)\cdot u(t)$$
$$y(t) = D\cdot x(t)$$

has a corresponding discretely co-incident discrete system given by (Jazwinski, 1970)

$$\begin{aligned} x(k+1) &= \Phi(k+1,k)\cdot x(k) + H\cdot \bar{u}(k) \\ y(k) &= D\cdot x(k) \end{aligned} \tag{4-25}$$

where:

$\bar{u}$ is a vector of average input concentrations for the interval (t,t+Δt).

$$\Phi(k+1,k) = \Phi(t+\Delta t, t) = e^{\bar{A}\cdot\Delta t}$$

where $\bar{A}$ is the coefficient matrix using averaged parameters for the interval (t,t+Δt).

$$H = \int_t^{t+\Delta t} \Phi(t+\Delta t,\tau)\cdot B(\tau)\cdot d\tau = \frac{1}{\bar{A}}\left[\Phi(t+\Delta t,t) - I\right]\cdot\bar{B} \tag{4-26}$$

where $\bar{B}$ is an average coefficient matrix for the interval (t, t+Δt). I is an (n x n) identity matrix.

As occurred in Section 4.3.2, discrete time system and measurement noise processes are added to account for uncertainties. Thus a discrete time representation of the CWQM is given by

$$\begin{aligned} x(k+1) &= \Phi(k+1,k)\cdot x(k) + H\cdot \bar{u}(k) + \omega(k) \\ y(k) &= D\cdot x(k) + \varepsilon(k) \end{aligned} \tag{4-27}$$

4.5 Using Filtering Theory to Estimate the CWQM

Introduction of the State Estimation Problem

The CWQM models pathogenic pollution, indicated by an indicator organism (E.coli), along stretch of coastline that is divided up into a number of cells. The pathogenic pollution inputs to the system are unknown, but estimated from historical information and daily rainfall runoff. The coastal system is simplified and characterized by two parameters. Observations of the water quality at specific beaches (Cells) are made fortnightly, and have levels of uncertainty associated. The problem is how best to estimate the states of the system given the limited observations available and the large uncertainties involved.

Filtering Theory

The system is not fully deterministic but assumed to be governed by the linear stochastic equations (4-27). The application of filtering theory is particularly useful in this context since it offers inherent flexibility in the treatment of the time variation and in the specification of the model itself.

Firstly, the discrete linear Kalman filter (KF) is introduced as a method of estimating the states of the linear stochastic system. Secondly, the Extended Kalman filter (EKF) is discussed as a method for estimating both the states and parameters of the linear dynamic system.

4.5.1 The Discrete Linear Kalman Filter

Kalman (1960) first published a paper describing a recursive solution to the discrete-time linear filtering problem. With the advances in digital computing the Kalman Filter (KF) has been the subject of extensive research and has been applied to a wide variety of problems. A detailed review of the Kalman Filter can be found in Jazwinski (1970). The following provides a brief derivation of the KF as shown in Brown & Hwang (1992).

4.5.1.1 Defining the linear state estimation problem

The objective of the Kalman Filter is to obtain optimal estimates of the states for a process that is governed by a set of linear stochastic equations.

The system is assumed to be described by:

$$x_{k+1} = \Phi_k \cdot x_k + S \cdot u_{k+1} + \omega_k \tag{4-28}$$

With an observation or measurement of the system assumed to occur at discrete intervals of time according to the equation:

$$y_k = D_k x_k + \varepsilon_k \tag{4-29}$$

The definition of the notation in equations (4-28) and (4-29) are:

x_k is the (n x 1) process state vector at time t_k.

Φ_k is the (n x n) state transition matrix relating x_k to x_{k+1}.

ω_k is the (n x 1) process or state noise, assumed to be Gaussian white noise with known covariance.

y_k is the (m x 1) measurement vector at time t_k.

D_k is the (m x n) matrix that gives the ideal, noiseless, connection between the measurement and state vectors at time t_k.

ε_k is the (m x 1) measurement error assumed to be Gaussian white noise with known covariance.

The process and measurement noises are assumed to be independent with covariance matrices given by:

$$
\begin{aligned}
&E\left[\omega_k \omega_k^{\,T}\right] = \begin{cases} Q_k & ,i=k \\ 0 & ,i \neq k \end{cases} \\
&E\left[\varepsilon_k \varepsilon_k^{\,T}\right] = \begin{cases} R_k & ,i=k \\ 0 & ,i \neq k \end{cases} \\
&E\left[\omega_k \varepsilon_k^{\,T}\right] = 0
\end{aligned}
\tag{4-30}
$$

4.5.1.2 Description of the Kalman filter algorithm

It is assumed that an initial estimate of the states at time t_k is found, and that this estimate is based on observations or measurements prior to the time t_k. This estimate is defined as the *a priori* estimate and is denoted by, $\hat{x}_k^-$, where the "hat" denotes an estimate and the "super minus" denotes that this is the best estimate prior to assimilating the observations at time t_k. If x_k is the "true" value of the state vector, then the estimation error is defined as

$$e_k^- = x_k - \hat{x}_k^- \tag{4-31}$$

with an associated *a priori* error covariance matrix

$$P_k^- = E\left[e_k^- e_k^{-T}\right] = E\left[\left(x_k - \hat{x}_k^-\right)\left(x_k - \hat{x}_k^-\right)^T\right] \tag{4-32}$$

With the assumption of an a priori estimate $\hat{x}_k^-$, and a new measurement y_k the *a priori* estimate is improved to an *a posteriori* estimate $\hat{x}_k$ in accordance with the equation

$$\hat{x}_k = \hat{x}_k^- + K_k\left(y_k - D_k \hat{x}_k^-\right) \tag{4-33}$$

where:

$\hat{x}_k$ is the *a posteriori* estimate of the states

K_k is a blending or gain factor

The difference ($y_k - D_k\hat{x}_k^-$) in (4-33) is referred to as the measurement innovation, or residual. The residual reflects the discrepancy between the predicted measurement and the actual measurement, therefore a zero residual means that the two are in complete agreement.

The errors in the *a posteriori* estimate can therefore be defined as:

$$e_k = x_k - \hat{x}_k \tag{4-34}$$

With an associated *a posteriori* error covariance matrix

$$P_k = E\left[e_k e_k^T\right] = E\left[\left(x_k - \hat{x}_k\right)\left(x_k - \hat{x}_k\right)^T\right] \tag{4-35}$$

The (n x m) matrix $\boldsymbol{K_k}$ is the Kalman gain matrix that is chosen to minimise the *a posteriori* error covariance (4-35) therefore yielding the minimum mean-squares error as the selection criterion. Using (4-33), (4-34) and (4-35), the *a posteriori* error covariance matrix may be derived as:

$$P_k = \left(I - K_k D_k\right) P_k^- \left(I - K_k D_k\right)^T + K_k R_k K_k^T \tag{4-36}$$

Taking the derivative of the trace of (4-36) with respect to $\boldsymbol{K}$ and setting that result equal to zero and then solving for $\boldsymbol{K}$, the optimal $\boldsymbol{K}$ can be found. The resulting K that minimises the *a posteriori* estimate error covariance is given by:

$$K_k = P_k^- D_k^T \left(D_k P_k^- D_k^T + R_k\right)^{-1} \tag{4-37}$$

Note that as the measurement error covariance $\boldsymbol{R_k}$ approach zero, the gain $\boldsymbol{K_k}$ weights the residuals more heavily. However if the *a priori* estimate error covariance (4-32) approaches zero, the gain $\boldsymbol{K_k}$ weights the residuals less heavily. Therefore the more the actual measurements are trusted the greater their weighting by the gain. Alternatively, the more the predicted measurements are trusted the less weights given to new measurements.

Substitution of the optimum Kalman gain (4-37) into the *a posteriori* error covariance matrix given by equation (4-36) leads to:

$$P_k = \left(I - K_k D_k\right) P_k^- \tag{4-38}$$

The error covariance matrix associated with the $\hat{x}_{k+1}^-$ is derived by considering the *a priori* expression for the estimate error.

$$\begin{aligned} e_{k+1}^- &= x_{k+1} - \hat{x}_{k+1}^- \\ e_{k+1}^- &= \left(\Phi_k x_k + \omega_k\right) - \Phi_k \hat{x}_k \\ e_{k+1}^- &= \Phi_k e_k + \omega_k \end{aligned} \tag{4-39}$$

It is noted that e_k and ω_k are defined as having zero cross-correlation, because ω_k is the process noise for the step ahead of t_k. An expression for the *a priori* error covariance P_{k+1}^- as:

$$
\begin{aligned}
P_{k+1}^{-} &= E\left[e_{k+1}^{-}e_{k+1}^{-\,T}\right] \\
P_{k+1}^{-} &= E\left[\left(\Phi_k e_k + \omega_k\right)\left(\Phi_k e_k + \omega_k\right)^{T}\right] \\
P_{k+1}^{-} &= \Phi_k e_k \Phi_k^{T} + Q_k
\end{aligned}
\tag{4-40}
$$

In implementations of the Kalman filter, the measurement covariance $\boldsymbol{R}$ is usually known and reflects what is known about the measurement process. The determination of the process noise covariance Q is generally more difficult due to it being intrinsically linked to the actual process that is modelled. Relatively simple models can give good results if enough uncertainty is added to the system. However, it is necessary that the process noise be accurately specified for the Kalman filter to retain it's optimality.

The Kalman filter thus estimates a process by using a form of feedback control. The filter estimates the process state at some given time and then obtains feedback in the form of measurements. The equations for the Kalman filter therefore fall into two groups: the *time update equations* (predictor) and the *measurement equations* (corrector) as shown in Figure 4-1.

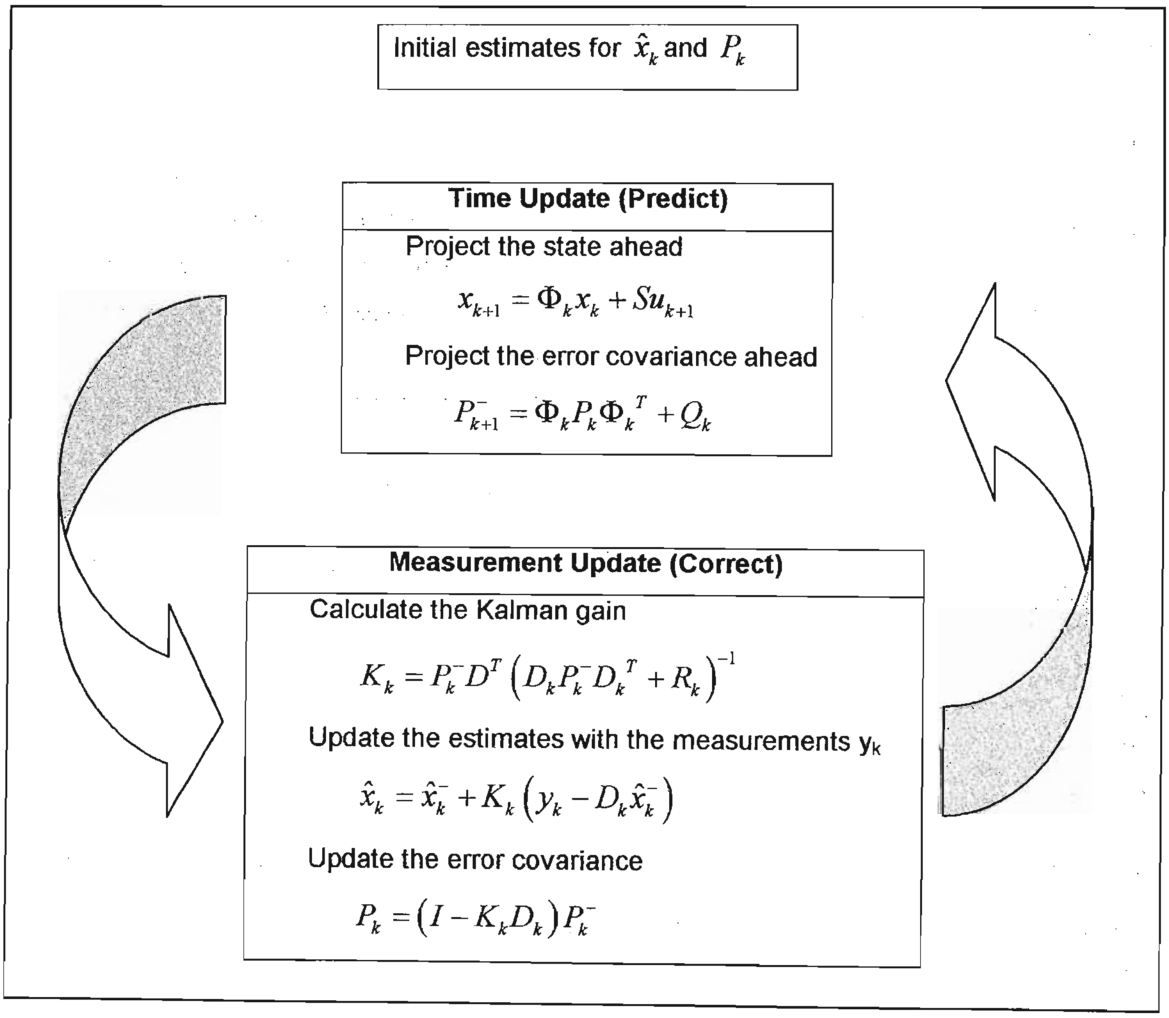

Figure 4-3: The complete Kalman filter operation cycle (Brown & Hwang, 1992).

4.5.2 The Extended Kalman Filter

Introduction of the State and Parameter Estimation Problem

Recall the state estimation problem of the CWQM as introduced previously. Consider now that the exact values of the states and parameters are unknown. Given the low frequency and number of observations and large uncertainties with respect to the inputs, how can the best estimates of both the states and parameters be achieved?

Extended Kalman Filtering Theory

The linear Kalman filter discussed in Section 4.5.1 is suitable for the state estimation of linear systems. However, the case where both the states and the parameters of a stochastic system need to be estimated leads to a non-linear estimation problem which is not solvable with the linear Kalman filter. One solution is to "extend" the Kalman filter by applying statistical linearization techniques.

A Kalman filter that linearizes about the current mean and covariance of the system is referred to as an extended Kalman filter or EKF.

4.5.2.1 Reviewing the non-linear system estimation problem

Recall the linear stochastic dynamic system defined by

$$\begin{aligned} \dot{x}_t &= A_{\theta,t}x_t + B_t u_t + \omega_t \\ y_{t_k} &= D_{t_k}x_{t_k} + v_{t_k} \end{aligned} \tag{4-41}$$

where $\boldsymbol{A}$, $\boldsymbol{B}$ and $\boldsymbol{D}$ are coefficient matrices depend on a finite parameter set θ. The vectors $\boldsymbol{x}$, $\boldsymbol{u}$, $\boldsymbol{y}$ and θ have dimensions (n_x x 1), (n_u x 1), (n_y x 1), and (n_θ x 1) respectfully. The characteristics of the noise are the same as given previously.

Definition of the parameter evolution

Suppose that the evolution, in time, of the parameter set θ is described by a random walk type stochastic differential equation (Jazwinski, 1970):

$$\dot{\theta}(t) = \xi_t \tag{4-42}$$

where:

$\theta(t) = \begin{bmatrix} \theta_1 & \theta_2 & \ldots.. & \theta_{n_\theta} \end{bmatrix}^T$ and has initial condition $\theta(t_0)$ assumed to be a Gaussian random vector, with properties as given by :

$$\begin{aligned} E\left[\theta_{t_0}\right] &= \hat{\theta}_{t_0} \\ E\left[\theta_{t_0} \cdot \theta_{t_0}^{\ T}\right] &= P_{\theta_{t_0}} \end{aligned} \tag{4-43}$$

ξ_t is a (n_θ x 1) zero mean Gaussian white noise process, with the usual characteristics (specific to each parameter):

$$E\left[\xi_{t_0}\right]=0$$

$$E\left[\xi_{t_0}\cdot\xi_{t_0}^{\ T}\right]=\begin{cases}Q_{\xi_{t0}} & i=k\\ 0 & i\neq k\end{cases}$$

This model is widely used to model slowly varying parameters that evolve in accordance with the characteristics of the noise process $\xi_{.}$ (see e.g. Stretch, 1980). The magnitude of Q reflects the degree of variability of the parameters.

If the parameters were expected to be constant throughout the process, then the random walk model can be modified to:

$$\dot{\theta}(t)=0 \tag{4-44}$$

i.e. all or some of the parameter elements of Q could be specified as zero, forcing them to remain constant.

Definition of an augmented system

The parameters and states are to be estimated simultaneously. They are combined into an (n_x+n_θ x 1) augmented state vector z_t

$$z_t=\begin{bmatrix}x_t^{\ T}\\ \theta_t^{\ T}\end{bmatrix} \tag{4-45}$$

The dynamics of the augmented system can therefore be described by the non-linear stochastic differential equation defined by:

$$\dot{z}_t=f\left(z_t,u_t,t\right)+\eta_t \tag{4-46}$$

where:

$f\left(z,u,t\right)$ is a (n_x+n_θ x 1) vector function $\begin{bmatrix}f_1 & f_2 & \ldots\ldots & f_{n_x+n_\theta}\end{bmatrix}^T$ such that:

$$f\left(z,u,t\right)=\begin{bmatrix}A_{\theta,t}x_t+B_{\theta,t}u_t\\ 0\end{bmatrix}$$

η_t is an (n_x+n_θ by 1) vector of the Gaussian white noise process such that $\eta_t=\left[\omega_t \quad \xi_t\right]^T$ with noise properties given as:

$$E\left[\eta_t\right]=0$$

$$E\left[\eta_t\cdot\eta_t^{\ T}\right]=\begin{cases}Q_t & i=k\\ 0 & i\neq k\end{cases}$$

The process noise covariance matrix Q_t can then be defined by a (n_x+n_θ)-square partitioned matrix

$$Q_t = \begin{bmatrix} Q_{\omega_t} & 0 \\ 0 & Q_{\xi_t} \end{bmatrix}$$

Initial estimates of the augmented system are assumed to be Gaussian with a mean of $\hat{z}_{t_0}$ and a covariance of P_{t_0}.

$$z_{t_0} = N\left[\hat{z}_{t_0}; P_{t_0}\right]$$

The $\hat{z}_{t_0}$ is partitioned as the augmented vector

$$\hat{z}_{t_0} = \begin{bmatrix} \hat{x}_{t_0} \\ \hat{\theta}_{t_0} \end{bmatrix}$$

where:

$$E\left[x_{t_0}\right] = \hat{x}_{t_0}$$
$$E\left[\theta_{t_0}\right] = \hat{\theta}_{t_0}$$

The error covariance matrix P_{t_0} is a (n_x+n_θ)-square partitioned matrix

$$P_{t_0} = \begin{bmatrix} P_{x_{t_0}} & P_{x_{t_0}\theta_{t_0}} \\ P_{x_{t_0}\theta_{t_0}} & P_{\theta_{t_0}} \end{bmatrix}$$

where:

$$P_{x_{t_0}} = E\left[x_{t_0} \cdot x_{t_0}^{\ T}\right]$$
$$P_{\theta_{t_0}} = E\left[\theta_{t_0} \cdot \theta_{t_0}^{\ T}\right]$$
$$P_{x_{t_0}\theta_{t_0}} = E\left[x_{t_0} \cdot \theta_{t_0}^{\ T}\right]$$

The non-linear measurement equation is given by:

$$y_{t_k} = h\left(z, t_k\right) + v_{t_k} \tag{4-47}$$

where:

$h\left(z,t\right)$ is an (n_y x 1) dimensional vector function (n_y = m + n_θ) such that:

$$h\left(z,t\right) = \begin{bmatrix} h_1 & h_2 & \ldots\ldots & h_{n_y} \end{bmatrix}$$
$$h\left(z,t\right) = D_{\theta,t} \cdot x_t$$

v_{t_k} is the (n_y x1) measurement noise assumed to be Gaussian white noise with known covariance.

The simultaneous state and parameter estimation concerns estimation of the augmented state vector z_{tk}. The dynamic equations of the system are non-linear due to the functions $f(.)$ and $h(.)$, where the non-linearities arise from the products between x_t and θ_t elements.

The normal Kalman filter cannot be applied directly due to the non-linear augmented system. The Kalman filter can however be applied to the non-linear system if a linearization procedure is employed.

4.5.2.2 Linearization of the non-linear system equations

Taylor series expansion is used to linearize the state equation about a "nominal" or "reference" trajectory, denoted by $\bar{z}_t$ (see Jazwinski, 1970). The trajectory has an initial condition of $\bar{z}_{t_0}$, and is assumed to satisfy the differential equation

$$\frac{d}{dt}[\bar{z}_t] = f(z,u,t) \qquad t \geq t_0 \tag{4-48}$$

Using first order Taylor series expansion and ignoring second and higher order terms yields a linearized augmented state equation

$$\frac{d}{dt}[\delta z_t] = F(\bar{z},u,t)\cdot \delta z_t + \eta_t \tag{4-49}$$

where $F(\bar{z},u,t)$ is a matrix of partial derivative evaluated along the reference trajectory.

$$F(\bar{z},u,t) \triangleq \left. \left\{ \frac{\partial f_i(z,u,t)}{\partial f_j} \right\} \right|_{z=\bar{z}} \tag{4-50}$$

The F-matrix is a (n_x+n_θ)-square partitioned matrix comprising the $\boldsymbol{A}$ and $\boldsymbol{B}$ coefficient matrices and a matrix M of partial derivatives of $f(\bullet)$ with respect to the parameters $\{\theta_t\}$:

$$F(\bar{z},u,t) = \begin{bmatrix} A_{\theta,t}x_t + B_{\theta,t}u_t & M_{x,\theta,t} \\ 0 & 0 \end{bmatrix} \tag{4-51}$$

The M-matrix is a (n_x x n_θ) dimensional matrix given by,

$$M_{x,\theta,t} = \frac{\partial}{\partial \theta}\left[A_{\theta,t}x_t + B_{\theta,t}u_t\right] \tag{4-52}$$

Linearization of the measurement equation

Linearization of the measurement equation is similar to that of the state equation (see Jazwinski, 1970). A reference trajectory of the measurements is defined as:

$$\bar{y}_{t_k} \triangleq h(\bar{z},t_k)$$

Using first order Taylor series expansion and ignoring second and higher order terms a linearized measurement equation can be obtained as:

$$\delta y_{t_k} \approx H(\bar{z},t_k)\cdot \delta z_{t_k} + v_{t_k} \tag{4-53}$$

where the linearized coefficient matrix $\boldsymbol{H}$, is given by:

$$H\left(\bar{z},t_k\right)=\left\{\frac{\partial h_i\left(z,t_k\right)}{\partial z_j}\right\}\Bigg|_{z=\bar{z}} \tag{4-54}$$

$H(.)$ is a (n_y x (n_x+n_θ))-dimensional matrix given by

$$H\left(z,t\right)=\left[D_{\theta,t} \quad L_{x,\theta,t}\right]$$

where L is a (n_y by n_θ) dimensional matrix of partial derivatives.

$$L_{x,\theta,t}=\frac{\partial}{\partial\theta}\left[D_{\theta,t}\cdot x_t\right]$$

4.5.2.3 The EKF algorithm applied to the augmented system

The linear Kalman filters can be applied to the linearized system given by (4-49) and (4-53). Therefore, given reference trajectory $\bar{z}_t$ and measurements $\bar{y}_{t_k}$, the measurement deviations δy_{t_k} may be processed to give estimates of the state deviations δz_t. The continuous-discrete extended Kalman filter algorithm is summarized as follows (Jazwinski, 1980, theorem 8.1).

Time update / Prediction step

$$\hat{z}_{t_{k+1}|t_k}=\hat{z}_{t_k|t_k}+\int_{t_k}^{t_{k+1}} f\left(z_{t|t_k},u,t\right)\cdot dt \tag{4-55}$$

$$P_{t_{k+1}|t_k}=\Phi\left(t_{k+1},t_k;\hat{z}_{t_k|t_k}\right)\cdot P_{t_k|t_k}\cdot\Phi^T\left(t_{k+1},t_k;\hat{z}_{t_k|t_k}\right)+Q_{t_{k+1}} \tag{4-56}$$

where:

$\Phi\left(t_{k+1},t_k;\hat{z}_{t_k|t_k}\right)$ is the state transition matrix of the linearized augmented system

$$\delta\dot{z}_t=F\left(\bar{z},u,t\right)\cdot\delta z_t$$

and

$$Q_{t_{k+1}}=\int_{t_k}^{t_{k+1}}\Phi\left(t_{k+1},\tau;\hat{z}_{t_k|t_k}\right)\cdot Q_\tau\cdot\Phi^T\left(t_{k+1},\tau;\hat{z}_{t_k|t_k}\right)\cdot d\tau$$

Measurement update / correction step

$$K\left(t_{k+1};\hat{z}_{t_{k+1}|t_k}\right)=P_{t_{k+1}|t_k}\cdot H\left(t_{k+1};\hat{z}_{t_{k+1}|t_k}\right)\cdot\left[H\left(t_{k+1};\hat{z}_{t_{k+1}|t_k}\right)\cdot P_{t_{k+1}|t_k}\cdot H^T\left(t_{k+1};\hat{z}_{t_{k+1}|t_k}\right)+R_{t_{k+1}}\right]^{-1} \tag{4-57}$$

$$\hat{z}_{t_{k+1}|t_{k+1}}=\hat{z}_{t_{k+1}|t_k}+K\left(t_{k+1};\hat{z}_{t_{k+1}|t_k}\right)\cdot\left[y_{t_{k+1}}-h\left(\hat{z}_{t_{k+1}|t_k};t_{k+1}\right)\right] \tag{4-58}$$

$$\begin{aligned}P_{t_{k+1}|t_{k+1}}=&\left[I-K\left(t_{k+1};\hat{z}_{t_{k+1}|t_k}\right)\cdot H\left(t_{k+1};\hat{z}_{t_{k+1}|t_k}\right)\right]\cdot P_{t_{k+1}|t_k}\cdot\left[I-K\left(t_{k+1};\hat{z}_{t_{k+1}|t_k}\right)\cdot H\left(t_{k+1};\hat{z}_{t_{k+1}|t_k}\right)\right]^T\\&+K\left(t_{k+1};\hat{z}_{t_{k+1}|t_k}\right)\cdot R_{t_{k+1}}\cdot K^T\left(t_{k+1};\hat{z}_{t_{k+1}|t_k}\right)\end{aligned} \tag{4-59}$$

4.5.2.4 Concluding remarks on the EKF algorithm

The extended Kalman filter is a filter in which the linearization of the non-linear system takes place about a predicted reference trajectory based on past observations. The partial derivatives are evaluated along this reference. The estimates depend on the measurements, so the filter gain sequence will depend on the sampled measurements sequence. The gain sequence is therefore not predetermined by the model assumptions, as is the case for the linear Kalman filter.

The use of updated estimates of the trajectories in the linearization process makes sense qualitatively since that is the best available information. A problem associated with the EKF is that the updated trajectories are only better from a statistical viewpoint. In practice the updated trajectory could be poorer than the predicted trajectory. This can lead to poor estimation results that may in turn compound into further errors, causing divergence of the filter. (Brown *et al*, 1992)

The EKF can therefore perform poorly in situations where the initial uncertainties and measurement errors are large. Therefore, special care may need to be taken to identify situations where divergence is likely to occur, and to restrain such divergence.

4.6 Adaption of the EKF for Estimating the CWQM

The Extended Kalman filter was utilised for the coastal water quality model, because of its ability to provide both parameter and state estimation. Note that the EKF reduces to the linear Kalman filter if the covariance matrix of the parameters is set to zero, ie. if the parameters are assumed to be known!

The EKF was applied to the CWQM, after incorporating a number of modifications to the version presented in section 4.5.2.

4.6.1 Prediction Phase of the EKF

The predictions of the augmented state vector between observations were calculated using equation (4-55).

$$\hat{z}_{t_{k+1}|t_k} = \hat{z}_{t_k|t_k} + \int_{t_k}^{t_{k+1}} f\left(z_{t|t_k}, u, t\right) \cdot dt$$

The predictions of the states and parameters are incorporated into the augmented state vector. There was however a difference in the propagation of the states and parameters. To clarify this the propagation of the state vector, x, and parameter vector, θ, are considered separately.

The parameter evolution was modelled by a random walk type model, whence:

$$\hat{\theta}_{t_{k+1}|t_k} = \hat{\theta}_{t_k|t_k} \tag{4-60}$$

The propagation of the state vector between observations in the continuous / discrete form is given by:

$$\hat{x}_{t_{k+1}|t_k} = \phi\left(t_{k+1}, t_k\right) \cdot \hat{x}_{t_k|t_k} + \int_{t_k}^{t_{k+1}} \phi\left(t_{k+1}, \tau\right) \cdot B_\tau \cdot u_\tau \cdot d\tau \tag{4-61}$$

where:

$\phi\left(t_{k+1}, t_k\right)$ is the state transition matrix of the system $\dot{x} = A \cdot x$, such that the solution is given as: $\phi\left(t_{k+1}, t_k\right) = e^{A \cdot (t_{k+1} - t_k)}$

Both the coefficient matrix A and input vectors B and u are assumed to be known and constant over the time interval t_k, to t_{k+1} the result of this assumption is further discussed below in section 4.6.1.1.

The prediction of the system covariance matrix between observations was given using equation (4-56).

$$P_{t_{k+1}|t_k} = \Phi\left(t_{k+1}, t_k; \hat{z}_{t_k|t_k}\right) \cdot P_{t_k|t_k} \cdot \Phi^T\left(t_{k+1}, t_k; \hat{z}_{t_k|t_k}\right) + Q_{t_{k+1}} \tag{4-62}$$

where:

$\Phi\left(t_{k+1},t_k;\hat{z}_{t_k|t_k}\right)$ is the augmented state transition matrix of the linearized solution of the system $\delta\dot{z}=F\cdot\delta z$. The matrix F is assumed to remain constant between observations thereby giving the solution:

$$\Phi\left(t_{k+1},t_k\right)=e^{F\cdot(t_{k+1}-t_k)}$$

$Q_{t_{k+1}}$ is the noise covariance matrix of the state noise process η_t which is given in the continuous/discrete form by:

$$Q_{t_{k+1}}=\int_{t_k}^{t_{k+1}}\Phi\left(t_{k+1},\tau;\hat{z}_{t_k|t_k}\right)\cdot Q_\tau\cdot\Phi^T\left(t_{k+1},\tau;\hat{z}_{t_k|t_k}\right)\cdot d\tau \tag{4-63}$$

The covariance matrix $Q_{t_{k+1}}$ may be specified directly if the properties of the discrete noise process n_{t+1} are known. Knowing the properties the formal definition may be given as:

$$n_{t+1}=\int_{t_k}^{t_{k+1}}\Phi\left(t_{k+1},\tau\right)\cdot n_\tau\cdot d\tau \tag{4-64}$$

The CWQM was designed to be a discrete filter making predictions of the water quality conditions at regular time intervals. A modification to the above mentioned continuous / discrete formulas, was needed for formulating the discrete EKF.

4.6.1.1 Multi-Step Predictions

The observations used by the CWQM (as discussed previously) are samples of specific bathing beaches taken on a fortnightly basis. During these 2-week sampling intervals large changes in the system occurred. The input concentrations and input flows fluctuate hourly as well as daily. The wind driven surface advection current, due to its dependence on the wind direction also fluctuates on a timescale much shorter than the 2-week sampling interval. These fluctuations would seriously invalidate the assumption that the F-matrix used to calculate the linearized state transition matrix remained constant between observations. This issue was addressed by making predictions at smaller time steps between observations.

The formulation of the predictions in this manner also satisfied a prerequisite of the CWQM, namely to provide daily predictions of the water quality conditions along the coastline. A basic timestep, Δt, of twenty-four hours was therefore used for inter-sample prediction steps and the states were propagated using:

$$x_{t+\Delta t}=\phi\left(t+\Delta t,t\right)\cdot x_t+\int_t^{t+\Delta t}\phi\left(t+\Delta t,\tau\right)\cdot B_\tau\cdot u_\tau\cdot d\tau \qquad \text{for}\quad t_k\le t\le\left(t_{k+\Delta t}\right) \tag{4-65}$$

The input matrices B and u are assumed to be constant over the 24-hr timestep Δt. The A-matrix used in the calculation of the state transition matrix was also assumed constant over the timestep Δt. The discrete state propagation equation (4-65) therefore simplifies to:

$$x_{t+\Delta t} = \phi(t+\Delta t,t)\cdot x_t + S(t+\Delta t,t)\cdot u_{t+\Delta t} \tag{4-66}$$

where

S(...) follows from the integration of the state transition matrix over the timestep Δt, ie:

$$S(t+\Delta t,t) = \frac{1}{A}\cdot\left[\phi(t+\Delta t,t) - I\right]\cdot B_{t+\Delta t}$$

x_t has the initial conditions of $x_t = \hat{x}_{t_k|t_k}$

The system covariance prediction is calculated using the state transition matrix linearized about the conditional mean. Using equation (4-62) the discrete formulation follows as

$$P_{t+\Delta t} = \Phi(t+\Delta t,t)\cdot P_t \cdot \Phi^T(t+\Delta t,t) + Q_{t+\Delta t} \tag{4-67}$$

with the initial condition of P_t given as $P_{t_k} = P_{t_k|t_k}$

4.6.2 Correction Phase of the EKF

When measurements are available, corrections to the state estimates are made using the update procedure reviewed in section 4.5.2.3. However, certain assumptions need clarification as a result of the implementation of the discrete-step predictions between sampling times.

The correction phase requires the prediction of the augmented state estimates, z, and the predicted system covariance matrix, P at the sampling time t_{k+1} from the previous sampling time t_k. Using the discrete multi-step predictions estimates of x and P were made until the sampling time t_{k+1} using incremental steps Δt. These estimates of the states were then used for the correction phase, augmented with previous parameter estimates.

$$\hat{z}_{t_{k+1}|t_k} = \left[\hat{x}_{t+\alpha\cdot\Delta t} \quad \hat{\theta}_{t_k|t_k}\right]^T$$
$$P_{t_{k+1}|t_k} = P_{t+\alpha\cdot\Delta t}$$

where:

$$(t+\alpha\cdot\Delta t) = (t_{k+1} - t_k)$$
$$\hat{\theta}_{t_{k+1}|t_k} = \hat{\theta}_{t_k|t_k}$$

Using these assumptions the correction phase of the EKF proceeded as follows:

Step 1: Calculate Kalman gain matrix

$$K(t_{k+1};\hat{z}_{t_{k+1}|t_k}) = P_{t_{k+1}|t_k}\cdot H(t_{k+1};\hat{z}_{t_{k+1}|t_k})\cdot\left[H(t_{k+1};\hat{z}_{t_{k+1}|t_k})\cdot P_{t_{k+1}|t_k}\cdot H^T(t_{k+1};\hat{z}_{t_{k+1}|t_k}) + R_{t_{k+1}}\right]^{-1}$$

Step 2: Make corrections to state estimates

$$\hat{z}_{t_{k+1}|t_{k+1}} = \hat{z}_{t_{k+1}|t_k} + K\left(t_{k+1};\hat{z}_{t_{k+1}|t_k}\right)\cdot\left[y_{t_{k+1}} - h\left(\hat{z}_{t_{k+1}|t_k};t_{k+1}\right)\right]$$

Step 3: Update covariance matrix

$$P_{t_{k+1}|t_{k+1}} = \left[I - K\left(t_{k+1};\hat{z}_{t_{k+1}|t_k}\right)\cdot H\left(t_{k+1};\hat{z}_{t_{k+1}|t_k}\right)\right]\cdot P_{t_{k+1}|t_k}\cdot\left[I - K\left(t_{k+1};\hat{z}_{t_{k+1}|t_k}\right)\cdot H\left(t_{k+1};\hat{z}_{t_{k+1}|t_k}\right)\right]^T + K\left(t_{k+1};\hat{z}_{t_{k+1}|t_k}\right)\cdot R_{t_{k+1}}\cdot K^T\left(t_{k+1};\hat{z}_{t_{k+1}|t_k}\right)$$

Modifications were made to the procedure described above in order for the model to remain robust and to assist in efficiency. The first involves a projection facility that alters the formulation of the state correction equation from step two above. The second involved a change to the entire update / correction procedure.

4.6.2.1 Projection facility

During the correction phase of the Kalman filter certain restrictions were placed on the magnitudes of the states and parameters. Two types of restrictions were used.

State restrictions

It was found that the correction phase of the Kalman filter could generate negative state estimates. This is unphysical since the state estimates are estimates of the average indicator concentrations within each cell, which must be non-negative

A constraint was thus specified that during any correction of the state estimates, all the states must remain positive.

$$x_i \geq 0 \qquad \text{for } i = 1,2,3,\ldots..n_x$$

Parameter restrictions

As mentioned previously the EKF can be divergent where initial uncertainties and measurement errors are large, as is the case with the system being modelled by the CWQM. The consequence of this is that constraints are also required on the parameter estimates.

A constraint was applied to ensure that all parameters used to describe the system were positive and non-zero. Thus:

$$\theta_j > 0 \qquad \text{for j} = 1,2,3,\ldots..n_\theta$$

The parameters of the model are associated with actual physical processes, so it was possible to make assumptions for a feasible range for each parameter. Each parameter was thus assigned a maximum and minimum value between which it was constrained.

$$\theta_{j_{MIN}} \leq \theta_j \leq \theta_{j_{MAX}} \qquad \text{for j} = 1,2,3,\ldots..n_\theta$$

Projection Facility (state and parameter estimates)

To force the state and parameter estimates to obey the above constraints, the state correction was modified to:

$$\hat{z}_{t_{k+1}|t_{k+1}} = \hat{z}_{t_{k+1}|t_k} + FACTOR \cdot K\left(t_{k+1};\hat{z}_{t_{k+1}|t_k}\right)\cdot\left[y_{t_{k+1}} - h\left(\hat{z}_{t_{k+1}|t_k};t_{k+1}\right)\right] \qquad (4\text{-}68)$$

where:

$$0 \le FACTOR \le 1.0$$

The $FACTOR$ was initially set equal to 1.0 and the correction to the state vector was calculated. The states and parameters were checked to see whether they violated any of their constraints. If a state or parameter was found to violate its constraint then the magnitude of $FACTOR$ was reduced by 20 percent and the correction repeated. The correction phase was therefore iterated until all constraints were satisfied.

4.6.2.2 Iterative Measurement Processing

The model formulation is based on the assumption that a coastline can be divided into a series of cells that act as homogenous units. Each of these cells is represented by an individual state in the state vector. Not every cell is a sampling site therefore only a certain number of the states are observed while others remain unobserved.

The $H(.)$ matrix is therefore a (n_x+n_θ)-square zero matrix with ones along the diagonal at positions which the states are measured, ie. the cells that are sampling sites.

$$H_{i,j}\left(t_{k+1};\hat{z}_{t_{k+1}|t_k}\right)\begin{cases}1 & i=j=Sampling\_Site \\ 0 & i\neq j\neq Sampling\_Site\end{cases}$$

Recall Equation (4-57), where the processing of observations requires the inversion of a n_y-square matrix in calculating the Kalman Gain.

$$K\left(t_{k+1};\hat{z}_{t_{k+1}|t_k}\right) = P_{t_{k+1}|t_k}\cdot H\left(t_{k+1};\hat{z}_{t_{k+1}|t_k}\right)\cdot\left[H\left(t_{k+1};\hat{z}_{t_{k+1}|t_k}\right)\cdot P_{t_{k+1}|t_k}\cdot H^T\left(t_{k+1};\hat{z}_{t_{k+1}|t_k}\right)+R_{t_{k+1}}\right]^{-1}$$

The solution of the inverse of a n_y-square matrix takes exponentially longer the greater the number of observation measurements available. It is of course far simpler to calculate the inverse of a single scalar quantity. The inversion of a n_y-square matrix may be avoided by processing the observations y_k one at a time and supposing there is no change in $\hat{x}$ or P due to the dynamics in the interim. (Jazwinski, 1970, Section 7.2). Therefore, the iterative measurement processing is accomplished by iterating the computational procedure [(4-55) to (4-59)] n_y times, setting $\Phi \equiv I$ and $Q \equiv S \equiv 0$ (4-28) after initial iteration.

Advantages of Using Iterative Measurement Processing

With the computational power available from most desktop computers, the advantage of using the iterative measurement processing procedure due its avoidance of inverting a n_y-square matrix is negligible. However the use of this procedure has certain merits when combined with the projection facility.

Using the projection facility the states and parameters of the augmented state vector are restrained from violating their given constraints.

Under the normal correction procedure, state or parameter constraints could be violated due to one observation from the set of observations, thereby requiring the use of the projection *FACTOR*. All the state corrections are therefore affected by the use of the projection *FACTOR*, resulting in poor updates for all the state and parameter estimates. With the iterative measurement processing procedure, only the observations that generate unrealistic state or parameter corrections would require the projection *FACTOR* applied to them. All the other corrections would update the augmented state vector in the normal unconstrained way. This resulted in superior corrections of the state and parameter estimates.

4.7 Summary of the Estimation procedure for the CWQM

The filtering approach to the estimation of the Coastal Water Quality Model has been introduced. It was decided to apply the EKF algorithm in the estimation of the CWQM due to its ability to provide recursive state estimates using a regular Kalman filter as well as parameter estimates using the Extended Kalman filter as required.

A summary of the assumptions and specification of the CWQM is given in the following section. A simple example is used to demonstrate the specification of the coefficient matrices and linearization techniques.

4.7.1 Model Specification

Prior to the application of the Kalman filter state and parameter estimation algorithm, the specification of the model needs to be provided. The CWQM is defined by the following equations (4-41).

$$\dot{x}_t = A_{\theta,t}x_t + B_t u_t + \omega_t$$
$$y_{t_k} = D_{t_k}x_{t_k} + v_{t_k}$$

The model therefore requires the definition of the parameters θ, and hence the specification of the system coefficient matrices $\boldsymbol{A}$ and $\boldsymbol{D}$ and the input matrix $\boldsymbol{B}$.

4.7.2 The CWQM States, Parameters and Inputs

The characteristics and initial conditions of the states and system inputs needed to be clarified before the EKF algorithm could be applied to the CWQM.

4.7.2.1 Details of the States

The states of the system are the indicator concentrations of the individual cells along the length of the coastline.

Their arrangement in the state vector x, was in the order of their sequence along the coastline as can be seen in the example shown in Figure 4-4. The positive direction is chosen in the following manner: If an observer was positioned in the cell and looked at the coastline (land) then the positive direction would be from left to right.

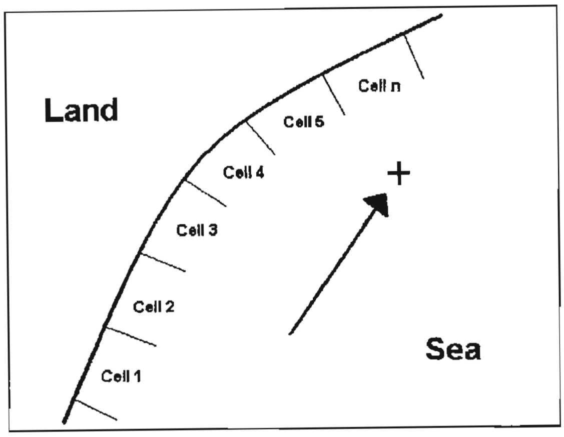

Figure 4-4: Specification of the positive direction

The initial conditions of the state vector were specified as

$$x_{t_0} = N\left[\hat{x}_{t_0} ; P_{x_{t_0}}\right]$$

The vector of the initial condition of the states, $\hat{x}_{t_0}$, was based on the historical average indicator concentrations of the cells

$$\hat{x}_{t_0} = \left[\bar{C}_1 \quad \bar{C}_2 \quad \bar{C}_3 \quad \cdots \quad \bar{C}_n\right]^T$$

The initial covariance of the system, $P_{x_{t_0}}$, specified as a diagonal matrix

$$P_{x_{t_0}} = \begin{bmatrix} p_{C_1} & & & & 0 \\ & p_{C_2} & & & \\ & & p_{C_3} & & \\ & & & \cdots & \\ 0 & & & & p_{C_n} \end{bmatrix}$$

where the individual variance estimates along the diagonal were specified using a percentage error estimate based on the standard deviation of all the historical indicator data.

$$p_{C_i} = \sigma_C{}^2$$

where:

p_{C_i} is the individual covariance estimate for that cell

4.7.2.2 Details of the Parameters

The parameter vector θ was made up of set of 2 parameters.

$$\theta_t = \begin{bmatrix} T_D & C_{AC} \end{bmatrix}^T$$

where

T_D is the indicator disappearance timescale, in hours

C_{AC} is a non-dimensional coefficient that scales wind speed to surface current speed

The evolution of the parameters were modelled using a random walk model, namely

$$\dot{\theta}_t = \xi_t$$

where ξ_t is a 5-dimensional vector of zero mean Gaussian white noise process

$$\xi_t = \begin{bmatrix} \xi_{T_D} & \xi_{C_{AC}} \end{bmatrix}$$

with

$$E\left[\xi_t \cdot \xi_t^T\right] = \begin{cases} Q_{\xi_i} & i = k \\ 0 & i \neq k \end{cases}$$

The matrix Q_ξ is a 2 x 2 covariance matrix that was assumed to be time invariant. The independence of the individual parameter noise processes is indicated by the assumption that Q_ξ is to remain diagonal at all times.

$$Q_\xi = \begin{bmatrix} q_{\xi_{T_D}} & 0 \\ 0 & q_{\xi_{C_{AC}}} \end{bmatrix}$$

The magnitudes of the individual noise processes $q_{\xi j}$ was chosen in an ad hoc manner. The magnitudes reflected the variability of the parameters concerned. Certain parameters were expected to vary seasonally, such as the decay timescale, while the other parameters were expected to remain fairly consistent throughout.

Initial parameter uncertainties were estimated by specifying the parameter covariance matrix $P_{\theta_{t0}}$ as:

$$P_{\theta_{t0}} = \begin{bmatrix} p_{T_{D_{t0}}} & 0 \\ 0 & p_{C_{AC_{t0}}} \end{bmatrix}$$

The individual variance estimates of the parameters along the diagonal were made in an ad hoc manner by specifying the percentage uncertainties in the parameters by:

$$p_{\theta_{i_{t0}}} = \left(\beta \cdot \theta_{i_{t0}}\right)^2$$

where:

θ_{i_0} was the initial estimate of the parameter

β was a global estimate of the parameter uncertainty, for example say 20%

4.7.2.3 Details of the Inputs

The Inputs to the system are defined by the input vector I_t and the input matrix B_t. The most important assumption made for the CWQM with regard to these inputs was that they remain constant over the time interval Δt. Each cell has the option of having a point input pollution source associated with it, however not every cell had a point input source.

The input vector I_t was a (n_x x 1)-dimensional vector with historical average indicator concentration levels of the point input sources to each cell over the time interval Δt. The cells that did not have point inputs pollution sources simply had the respective elements in the input vector set to zero.

$$I_t = \begin{bmatrix} \overline{I}_1 & \overline{I}_2 & \overline{I}_3 & \dots & \overline{I}_n \end{bmatrix}^T$$

The input matrix B_t was a n_x-square matrix which in practice scales the volume of the input to the storage volume of the cell. This is done using the timescale T_P derived previously in Section 4.2.2, as:

$$T_P = \frac{V_{cell}}{Q_P}$$

where:

V_{cell}	=	Cell volume, in m^3
Q_P	=	Point input flow rate, in m^3/hr
T_P	=	Point input timescale, hours

The estimate of the point input flow rate, Q_P, to each cell was calculated as an average flow rate from each point source over the time interval. The estimate was a combination of the runoff from the each cell's catchment and the average base flow estimated for each point input. The rainfall runoff was estimated using the rainfall experienced by the catchment over the time interval, factored by a runoff coefficient, C_{RC}, specific for each catchment.

The n_x-square matrix was formed with the diagonal elements representing the respective T_p for each cell and all off-diagonal elements set to zero. For cells that did not contain point input pollution sources, their respective elements along the diagonal were set to zero. Whence

$$B_t = \begin{bmatrix} \frac{1}{T_{P1}} & & & 0 \\ & \frac{1}{T_{P2}} & & \\ & & \cdots & \\ 0 & & & \frac{1}{T_{Pn}} \end{bmatrix}$$

Uncertainty with respect to these inputs was also added to the system. The uncertainties were due to two factors. The first being that the input concentration was set to a constant averaged value over the timestep while it is known that variations do occur over shorter timescales (Brahmin, 2002). The second factor concerns uncertainties in the estimates of cell storage volumes, and point input flow rates. Both uncertainties were incorporated by adding a zero mean Gaussian white noise processes to the inputs. The individual noise processes were specified in an ad hoc manner using a percentage-scaling factor indicating the confidence of the estimates.

$$Q_{I_t} = \begin{bmatrix} q_{u_1} & & & 0 \\ & q_{u_2} & & \\ & & \cdots & \\ 0 & & & q_{u_n} \end{bmatrix}$$

Where:

q_{u_i} is the noise process due to the input concentration.

$$q_{u_i} = \left(\gamma_I \cdot \overline{I}_i\right)^2$$

γ_I is a constant percentage-scaling factor of the uncertainty with respect to the input concentrations.

4.7.2.4 The Augmented System

The Extended Kalman Filter solves the augmented states of the non-linear system defined by the equations (4 – 29) and (4 – 30).

$$\dot{z}_t = f\left(z_t, u_t, t\right) + \eta_t$$
$$y_{t_k} = h\left(z, t_k\right) + v_{t_k}$$

The augmented state vector z_t is the combination of the state vector, x, and parameter vector, θ.

$$z_t = \begin{bmatrix} x_t \\ \theta_t \end{bmatrix}$$

The P and Q noise covariance matrices of the states and parameters are then augmented with each other to be utilized by the EKF algorithm.

$$P_{t_0} = \begin{bmatrix} P_{x_{t_0}} & 0 \\ 0 & P_{\theta_{t_0}} \end{bmatrix} \qquad Q_t = \begin{bmatrix} Q_{I_t} & 0 \\ 0 & Q_{\theta_t} \end{bmatrix}$$

4.7.3 Setup of the Coefficient Matrices Using a Simple Example

The setup of the coefficient matrices is dependant on the directions of assumed advection processes. An example of a simplified system is used to demonstrate how these matrices were set up.

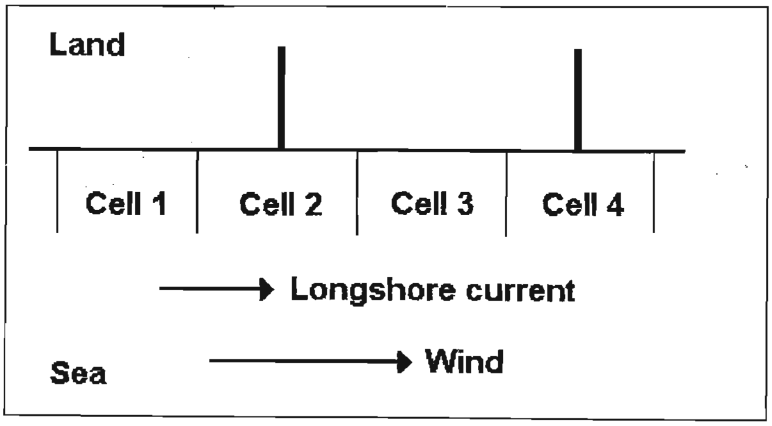

Figure 4-5: Drawing of the simplified system

The example system comprises 4 cells each defined using the cell properties. At any given increment of time the augmented state vector is defined as:

$$x_t = \begin{bmatrix} C_1 & C_2 & C_3 & C_4 \end{bmatrix}^T$$
$$\theta_t = \begin{bmatrix} T_D & C_{AC} \end{bmatrix}^T$$
$$z_t = \begin{bmatrix} C_1 & C_2 & C_3 & C_4 & T_D & C_{AC} \end{bmatrix}^T$$

Assumptions made of the system are:

1. The wind is assumed to be blowing parallel to the coastline
2. Cells two and four are assumed to have point input sources.
3. The system is observed by sampling cells one and three

4.7.3.1 Setup of Matrices A and D

Setup of coefficient matrix A

The continuity at the beginning and end of the modelled length of coastline allows the matrix A to be parameterised as follows

$$A = \begin{bmatrix} a_0 & a_2 & 0 & 0 \\ a_1 & a_0 & a_2 & 0 \\ 0 & a_1 & a_0 & a_2 \\ 0 & 0 & a_1 & a_0 \end{bmatrix}$$

Specification of element a_0

The element a_0 refers to the diffusion and mixing of the respective cell due to all the processes that are modelled. The combined timescale T is used, such that

$$a_{0_i} = -\frac{1}{T_i}$$

where

$$\frac{1}{T_i} = \left(\frac{1}{T_D} + \frac{1}{T_{ADV_i}} \right)$$

Specification of elements a_1 and a_2

The elements a_1 and a_2 refer to the advection and exchange of pollution from one cell to adjacent cells.

The elements a_1 or a_2 depend on the assumed direction of the advection process. Propagation in a positive direction are assigned to the a_1 element, propagation in the negative direction are assigned to the a_2 element.

For simplicity the coastline is assumed to be straight so that all elements a_1 and a_2 are constant for all cells.

If advection is propagating in the positive direction, the element a_1 is given by

$$a_{1_i} = \frac{1}{T_{ADV_i}}$$

While the element a_2 is given by

$$a_{2_i} = 0$$

Setup of coefficient matrix D

The CWQM models the indicator concentrations in a series of cells along a modelled coastline. The sampled observations are measurements of the actual states at given times. The coefficient matrix D transforms the state vector into the same dimension as the observation vector y_t.

The simplified example has a (2 x 1)-dimensional output vector y_t. The coefficient matrix D, with cells 1 and 3 sampled, is thus

$$D = \begin{bmatrix} 1 & 0 & 0 & 0 \\ 0 & 0 & 1 & 0 \end{bmatrix}$$

When iterative measurement processing is used, only one observation is processed at a time. In such a case the coefficient matrix $\boldsymbol{D}$ becomes a set of coefficient vectors, one for each state correction.

$$D^1 = \begin{bmatrix} 1 & 0 & 0 & 0 \end{bmatrix}$$
$$D^2 = \begin{bmatrix} 0 & 0 & 1 & 0 \end{bmatrix}$$

4.6.3.2 Setup of Augmented System Matrices F and H

The augmented system is described by the non-linear stochastic differential equation.

$$\dot{z}_t = f\left(z_t, u_t, t\right) + \eta_t$$
$$y_{t_k} = h\left(z, t_k\right) + v_{t_k}$$

The approximate linearized, augmented system is given by the equations

$$\delta z_t = F\left(\bar{z}, u, t\right) \cdot \delta z + \eta_t$$
$$\delta y_{t_k} \simeq H\left(\bar{z}, t_k\right) \cdot \delta z_{t_k} + v_{t_k}$$

Setup of matrix F

The linearized matrix $F\left(\bar{z}, u, t\right)$ was defined as a matrix of partial derivative evaluated along the nominal trajectory. The solution of which is given by

$$F\left(\bar{z}, u, t\right) = \begin{bmatrix} A_{\theta,t} & M_{x,\theta,t} \\ 0 & G_t \end{bmatrix}$$

where:

G_t is a n_θ-square zero matrix arising from the random walk type model used for parameters.

$A_{\theta,t}$ is the partial differential matrix of $f\left(z_t, u_t, t\right)$ with respect to the states and is therefore the coefficient matrix A specified previously in section 4.7.3.1

$M_{x,\theta,t}$ is the partial differential matrix of $f\left(z_t, u_t, t\right)$ with respect to the parameters.

For the present example the matrix M is given by

$$M_{x,\theta,t} = \begin{bmatrix} \frac{\partial f_1}{\partial T_D} & \frac{\partial f_1}{\partial C_{AC}} \\ \frac{\partial f_2}{\partial T_D} & \frac{\partial f_2}{\partial C_{AC}} \\ \frac{\partial f_3}{\partial T_D} & \frac{\partial f_3}{\partial C_{AC}} \\ \frac{\partial f_4}{\partial T_D} & \frac{\partial f_4}{\partial C_{AC}} \end{bmatrix}$$

where:

$$\frac{\partial f_j}{\partial \theta_i} = \sum_{k=1}^{4} \frac{\partial}{\partial \theta_i}\left[A_{j,k} \cdot x_j\right]$$

Setup of vector H

The linearized matrix $H\left(\overline{z}, t_k\right)$ is given by

$$H\left(z,t\right) = \left[D_{\theta,t} \quad L_{x,\theta,t}\right]$$

where:

$\boldsymbol{D}_{\theta,t}$ is the coefficient vector defined previously in section 4.7.3.1

$\boldsymbol{L}_{x,\theta,t}$ is the partial derivative vector of $h\left(z,t_k\right)$ with respect to the parameters in the coefficient matrix $\boldsymbol{D}$.

$$L_{x,\theta,t} = \frac{\partial}{\partial \theta}\left[D_{\theta,t} \cdot x_t\right] = 0$$

The coefficient matrix $\boldsymbol{D}$ does not contain any parameters. Therefore, vector $\boldsymbol{L}$ is a zero vector of length n_θ. The iterative measurement-processing algorithm may thus be employed using the H matrix when using the EKF algorithm.

CHAPTER 5:
COASTAL WATER QUALITY MODEL ESTIMATION

5.1 Introduction

The Coastal Water Quality Model (CWQM) was designed such that, given a set of physical and environmental information, the pathogenic pollution along any stretch of coastline may be predicted. A method of estimating optimal values for the model parameters is required. In this chapter an investigation of the applicability of the Extended Kalman Filter (EKF) for parameter estimation is reported. Since the EKF did not prove effective for this application, an alternative statistical estimation procedure is also described, and was used to obtain optimal parameter estimates for the case study site.

5.2 Problem Definition

Along the modelled Durban Bight region, pollution enters the nearshore zone from six stormwater drains and the Umgeni River. The volume of outflow may be predicted using simple rainfall runoff calculations. However, pathogen concentrations associated with particular outflows remain unknown. Measurements of concentrations have been made, but only at monthly intervals. The statistical distribution of the stormwater and river concentrations is known.

The pathogenic water quality conditions of the nearshore zone are measure fortnightly at ten locations. However, it is required that the CWQM make daily predictions of the pathogenic water quality conditions along the Durban Bight.

The following needed to be investigated:

1. Can the EKF be used as a parameter estimator for the CWQM?
2. What are the optimal parameter values for application of the CWQM to the case study site?
3. How well does the CWQM perform as a real-time daily predictor of pathogenic pollution levels at beaches along the coastline, given the currently available information?

5.3 Factors Influencing Model Estimation and Application

The quality of the parameter estimates and pollution predictions will be determined by the quality of the observations, and the physical and environmental information available.

5.3.1 Observations

The observations are based on fortnightly water sampling along the coastline. These observations of individual cell indicator concentrations are crucial to the estimation of the model parameters. The process by which these measurements are made is discussed in Section 2.3.1.

5.3.1.1 Accuracy of Observations

The sampling and testing procedures determine the degree of accuracy of the observations. Firstly, contamination of the samples could arise due to lack of adherence to correct sampling procedures (Section 2.3.1.1). It was assumed that the sampling was done professionally and therefore the analysis of the effect of such behaviour on the model was not deemed necessary.

The testing procedure is a major factor influencing the model estimation efficiency. The degree of accuracy of the results of the microbiological indictor levels is discussed in section 2.3.1.2. A key source of uncertainty is associated with the rounding off of the results when they are factored up to the standard units of CFU per 100ml.

For example significance levels of the observations may differ as follows:

1. Six significant figures (100m^3 cultured): 254.167894 CFU / 100ml
2. Integer values (100ml cultured): 254 CFU / 100ml
3. Unit of twenties (5ml cultured): 260 CFU / 100ml
4. Units of hundreds (1ml cultured): 300 CFU / 100ml

Although six-figure significance for indicator counts per 100ml is not physically possible, it represents model estimation using "perfect" observations ie. with no associated errors in the observations due to measurement noise.

The effect that the rounded up of observations has on the model estimation process is analysed by varying the significance levels of the observations.

5.3.1.2 Frequency of Observations

The frequency that the states are observed may influence the model estimation. The sampling of the beach sites by the EMWSS is done on a fortnightly basis as discussed in section 2.3.1.1. Since the model was to be implemented on the test coastline of Durban's golden mile, this was the only sampling frequency used for assessing the parameter estimation.

5.3.1.3 Number of Observations

The number of cells (states) of the CWQM that are observed may influence the efficiency of the state and parameter estimation. Only a percentage of the cells are actually observed, therefore some states remain completely unobserved. The smaller the number of observed states, the greater the number of unobserved states, which may lead to inefficiency in the state and parameter estimation. The ideal situation would be if sampling were done at all cell positions, thereby observing all states of the model. However, this would be unrealistic.

The ten positions along the case study coastline sampled by the EMWSS (see Section 3.1) are used for testing the CWQM.

5.3.2 Parameters

The efficiency of the CWQM to correctly estimate the parameter values may be influenced by the model formulation itself.

1. The greater the number of parameters that significantly affect the advection and diffusion of the pollution the less the CWQM may be able to correctly estimate the individual parameters.
2. The estimation of certain parameters may be more efficient than others

5.3.3 Point Input

The CWQM considers the point inputs as the source of all pollution to the modelled coastline; therefore, approximations made with regard to determining the inputs can have significant effects on the estimation of the CWQM and its predictive performance.

5.3.3.1 Input Concentrations

The pathogenic pollution concentrations at point input sources such as an urban stormwater drain or a river, is often difficult to estimate. As discussed in Section 2.4.1, the pathogenic pollution levels within urban runoff vary according to a wide range of factors such as: storm duration, duration of previous dry-days, time of year, sewage infiltration, etc. The concentration of the pathogenic pollution indicator E. coli was shown in Section 3.4.2 to follow a lognormal distribution in most stormwater drain and river inputs.

The uncertainty surrounding the input concentrations has the strongest influence on the estimation and application of the CWQM. The actual concentration of the point inputs remain unknown, rather the input concentration distributions (lognormal), fitted using sampled SWD and river concentrations, are used to set the discrete step input concentrations.

5.3.3.2 Input Flow Rates

The point input flow rates are an important issue to consider in both the prediction and estimation process. The volume of input introduced to the cells will directly influence the predicted pathogenic pollution of the system. The flow from point inputs may be classified into two categories.

1. The direct runoff volume due to rainfall on the catchment.
2. The base-flow from the catchment. Urban stormwater drains may have sources other than direct rainfall. The river flows may be estimated using a standard monthly or seasonally dependant base-flow combined with rainfall runoff from local catchments.

Rivers would normally have far greater outflow volumes than normal urban stormwater drains. The continuity of the coastal system assumed in the formulation of the CWQM means that the magnitude of the polluting potential of the rivers might adversely affect the state and parameter estimates along regions only affected by stormwater drains.

5.4 Synthetic Observation Data

In order to test the various aspects of the CWQM a set of state observations was needed. It was decided to generate synthetic observations; where the "true" parameter values, inputs and noise levels of the inputs and observations were known. Thus the model could be tested by varying the amount or quality of the input and observation data provided to the CWQM.

Synthetic observation sequences were generated using the following conditions:

1. The modelled coastline included Durban's "Golden-mile" beaches: from the harbour in the south stretching 10km northwards, including the Umgeni River.
2. The coastline was described by a series of fifty cells, each 200m in length.
3. Ten cell locations were "observed", corresponding to the normal EMWSS beach sampling positions.
4. Observations were "made" fortnightly - using a 14-day sampling average frequency, with a minimum and maximum sampling frequency of 12 and 16 days respectively.
5. Three observation significance levels were used, as discussed in Section 5.3.1.1.
6. The indicator disappearance timescale (T_D) and Wind-current advection coefficient (C_{AC}) were considered for testing parameter estimation (using the EKF).
7. Parameter values were fixed at constant values. (T_D = 12hrs and C_{AC} = 0.003)
8. All point input sources along the stretch of coastline were used.
9. Point input flow volumes were based on rainfall runoff (specified later), Generalised base-flow for stormwater drains (Table 5-1) and the calculated averaged monthly base-flow for the Umgeni River (Figure 3.10) was used.
10. The uncertainty surrounding the point input indicator concentrations were modelled using three different assumptions, discussed further in Sections 5.4.1, 5.4.2and 5.4.3.

Stormwater drain	Generalised Baseflow (m^3/s)
Hospital	0
Rutherford	0
West	0
Somtseu	0.005
Argyle	0.015
Walter Gilbert	0.005

Table 5-1: Generalised stormwater baseflow used for synthetic testing

5.4.1 Deterministic Input Concentrations

The deterministic input concentration simulation represented the case where all loading of pathogenic pollution to the system is known precisely. The point input concentrations of the stormwater drains and Umgeni River were set to constant values equal to the median of each respective lognormal E.coli distributions. (Sections 3.4.2 and 3.5.2.)

5.4.2 Gaussian Input Concentrations

The point input concentrations of the stormwater drains and Umgeni River were randomly generated at each step using a Gaussian distribution about the median values of the lognormal distribution fitted to each of the point inputs (Section 3.4.2 and 3.5.2). The standard deviation used was set at 20 percent of the median.

5.4.3 Lognormal Input Concentrations

The point input concentrations were randomly generated from a lognormal distribution fitted to each of the point inputs (Section 3.4.2 and 3.5.2). This is more representative of the current situation than the previous case.

5.5 Parameter Estimation Using the EKF

The CWQM was formulated with the intention of using the EKF for refining initial parameter estimates according to a least squares fitting criterion. The efficiency of the EKF to produce stable and optimal parameter estimates, given observation and input uncertainty required testing. This was done using synthetic data sequences generated with the model (Section 5.4).

The environmental information used for testing of the EKF algorithm was from 1998/01/01 to 2002/08/31 and as follows:

1. Daily rainfall totals taken from Durban Botanical Gardens.
2. Daily wind averages from weather station DB01 (Port of Durban)

The synthetic observations were generated using the parameter values shown in Table 5-2. Also shown are the maximum and minimum parameter restrictions used by the projection facility (Section 4.5.2.1) during parameter estimation.

Parameter	Original Value	Minimum Value	Maximum Value
T_D (hrs)	12	3	96
C_{AC}	0.003	0.00003	0.03

Table 5-2: Original, Maximum and Minimum parameter values

To simulate the effects that errors in the observations may have on the efficiency of parameter estimation, three measurement error levels were analysed, as shown in Table 5-3. The synthetic observations were rounded off using three different significance levels. The measurement error was known and used for parameter estimation.

Description	Significance level	Actual Measurement Error	Measurement Error Used
Perfect sampling	10^{-6}	± 5.0E-7	± 1
5ml sampling	Twenties	± 10	± 10
1ml sampling	Hundreds	± 50	± 50

Table 5-3: Measurement error used for parameter estimation

The input noise was predetermined by the assumptions made about the input concentrations used for generating of the synthetic observation sequence. (Sections 5.4.1 and 5.4.3)

5.5.1 Parameter Estimation Scenarios

Three parameter estimation scenarios were analysed. Table 5-4 describes the system error covariance (P_n), process noise (Q_n) and process noise decay ($Q_{n\text{-}decay}$) estimates of the parameters, used in each scenario.

Scenario	P_n	Q_n	$Q_{n\text{-}decay}$
1	100%	0%	0%
2	100%	50%	0%
3	100%	50%	80%

Table 5-4: Parameter estimation methods

In Scenario #1 the initial parameter error covariance allows the parameter value to be refined at each state correction step. The parameter covariance is reduced at each step until the covariance of the parameter estimate has reduced to a level where no further parameter variation occurs.

In Scenario #2 the parameter error covariance is continually supplemented by the process noise associated with the parameter. This maintains the parameter error covariance, which in turn implies that the EKF algorithm continues to change the parameter estimate at each correction step. This method may not be practical under real conditions, if the parameter was assumed to be constant. However it does give insight on how the model would estimate the parameter at each step, if given enough covariance. It has the effect of limiting the "memory" of the recursive estimation process. (Jazwinski, 1970)

Scenario #3 is a combination of the two previous methods. At each correction step the process noise variance is reduced by 20 percent, until a minimum of one percent of the original noise remains. This effectively allows the EKF more estimation phases before the parameter variance becomes small enough to limit variations. The EKF is therefore allowed to make large changes to the parameter estimates at the beginning, but for each successive parameter estimation step the allowed variation of the parameter estimate is increasingly limited. Under real conditions, by not reducing the process noise to zero, small seasonal or yearly variations in the parameter are allowed.

5.5.2 Deterministic Input Concentration

The deterministic input concentration simulation represents the case where the pollution loading of the system is known exactly for the purpose of state and parameter estimation. The convergence of each parameter to its true value, given observation uncertainties, was tested.

5.5.2.1 Estimation of the T_D Parameter

In Figure 5-1 the estimation of T_D with no measurement noise is demonstrated. In Scenario #1 the EKF algorithm refines the initial estimates, however after approximately the 30th correction the estimation effectively ceases and the parameter estimates remain stable at values different from the true value of 12 hours. This occurs due to the parameter error covariance having decayed to small enough values so as not to allow any further refinement. Using Scenario #3, the parameter estimates converge after approximately 30 corrections and then remain stable about the true parameter value of 12 hours.

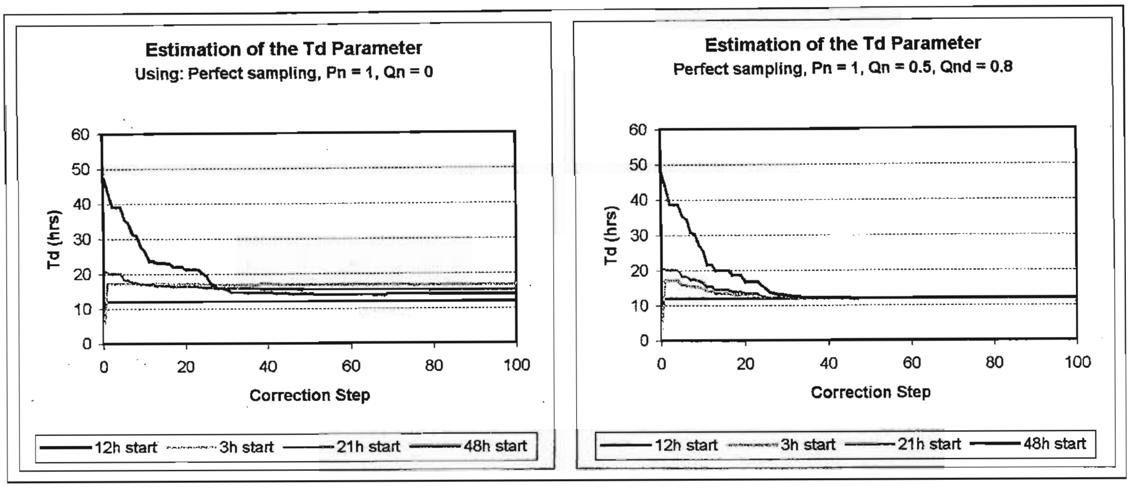

Figure 5-1: Graphs of Scenario #1 and Scenario #3 estimation of T_D using perfect sampling and deterministic input concentrations

The effect of measurement noise, due to 1ml sampling, is demonstrated by Figure 5-2. Scenario #2 illustrates what happens if the parameter error covariance is sustained throughout the estimation. The EKF refines the parameter estimates in accordance with the observations provided, but after approximately the 42nd correction, actually moves the parameter estimates away from the true value. Subsequently the parameter estimates correct the temporary divergence attempting to return to their true value. The reason for the temporary divergence in Scenario #2 is a combination of an over-estimated error covariance and the measurement noise.

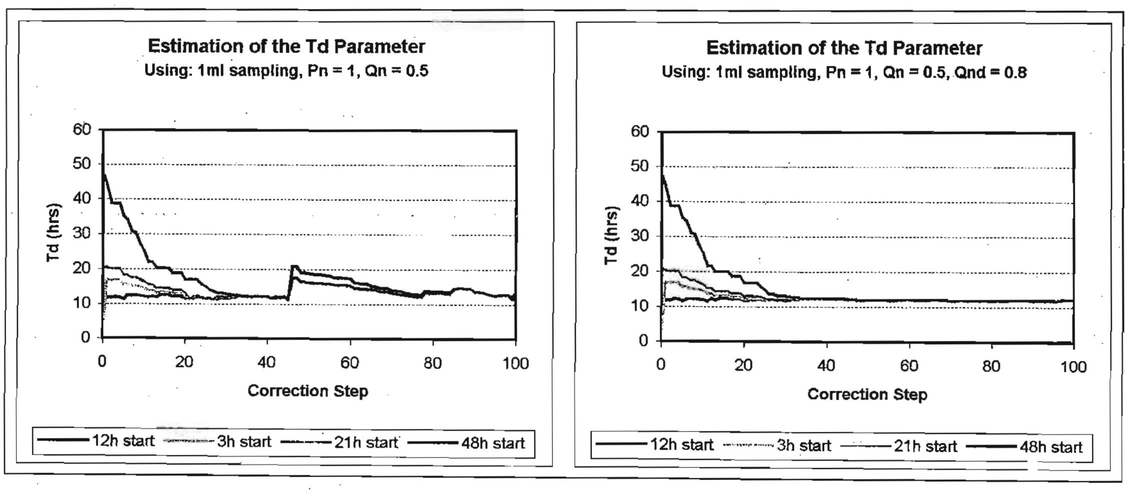

Figure 5-2: Graphs of Scenario #2 and Scenario #3 estimation of T_D using 1ml sampling and deterministic input concentrations

In Scenario #3 of Figure 5-2, the advantages of sustaining the parameter error covariance for a longer period is demonstrated. The parameter converges to its true value (of 12 hours) after approximately 30 corrections but then stays stable and does not show the divergent behaviour of Scenario #2. The small fluctuations in the parameter estimates are due to the parameter process noise not being allowed to decay further than 0.5%.

What was noticed in all estimates of the T_D parameter was that initial estimates, smaller than the true parameter value, converged quicker than initial estimates that were larger than the true value.

5.5.2.2 Estimation of the C_{AC} Parameter

The estimation efficiency of the EKF algorithm with respect to the advection coefficient parameter, in the absence of measurement noise is shown in Figure 5-3. As with the T_D parameter the use of Scenario #1 led to estimates of C_{AC} not converging quick enough before the decay of the error covariance. However by sustaining the parameter error covariance for longer, most of the parameter estimates converged to the correct value (of 0.003), as shown in Scenario #3.

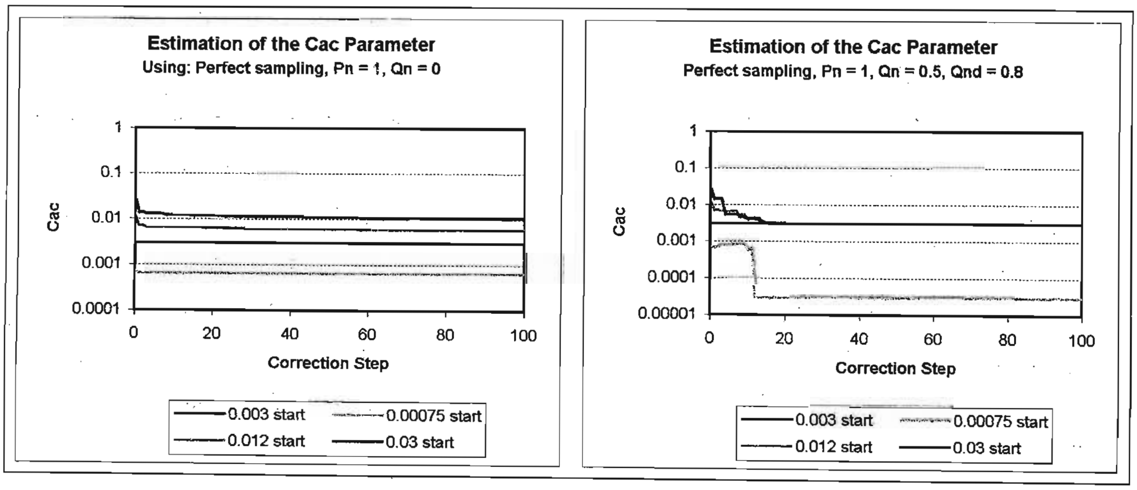

Figure 5-3: Graphs of Scenario #1 and Scenario #3 estimation of C_{AC} using perfect sampling and deterministic input concentrations

The effect of measurement noise on the estimation of C_{AC} (using known inputs) is shown in Figure 5-4. Most parameter estimates converge to the true values if allowed the required freedom by the parameter error covariance.

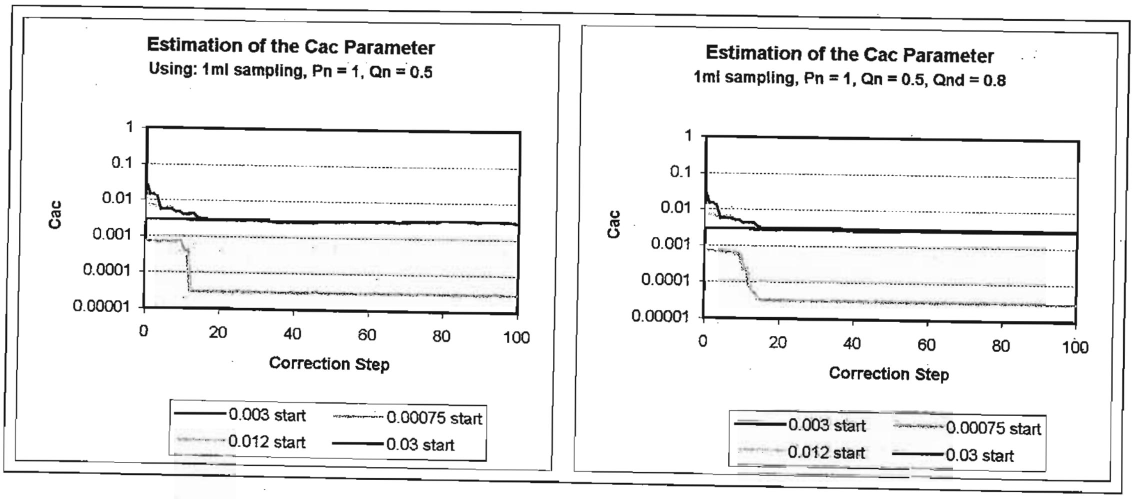

Figure 5-4: Graphs of Scenario #2 and Scenario #3 estimation of C_{AC} using 1ml sampling and deterministic input concentrations

A problem became evident in the estimation of C_{AC} if initial estimates were specified as less than the true parameter value, illustrated in both Figure 5-3 and Figure 5-4. The parameter estimate diverged and remained fixed at the minimum value allowed by the projection facility. The reason for this may be the following:

1. Most of the states (cells) of the system are unobserved with, on average, approximately three unobserved cells between observed cells.
2. The short timescale of the decay parameter means that only a small portion of pollution remains after each step.
3. The small advection coefficient means that the movement of pollution between cells is slow.

The above three factors combine to create a situation where there is a lack of "communication" between successive observed cells. When the initial estimates of C_{AC} are set larger than their true value the increased "communication" allows correct parameter estimation to occur. Both Figure 5-3 and Figure 5-4 show that the parameter estimates remain stable once they reach the true value. When initial estimates of the C_{AC} are set below their true value the decreased "communication" causes the EKF to diverge.

5.5.2.3 Conclusions of the Estimation Using Deterministic Inputs

It was concluded that parameter estimation for the CWQM using the EKF is possible given deterministic inputs even under large measurement noise conditions, similar to those expected in practice. The following specific conclusions were made:

Scenario #3 appears to be the best method to use for parameter estimation.

1. When estimating the decay timescale, it is best to under-predict the initial estimate.
2. When estimating the advection coefficient, it is best to over-predict the initial estimate.

5.5.3 Gaussian Input Concentrations

In this case the ability of the EKF to correctly estimate the model parameters given unknown Gaussian distributed input concentrations but of **known mean** and **standard deviation**, was tested. Mean input concentrations were used for each point input, with the process noise set at 20 percent of the mean values.

5.5.3.1 Results of T_D Parameter Estimation

The EKF was able to correctly estimate the T_D parameter, given only the statistical properties of the inputs. Parameter estimation using the largest measurement error (1ml samples) is shown in Figure 5-5. As with the deterministic input case, using Scenario #1 the initial parameter estimate begins to converge to the correct parameter value, however the decay of the parameter covariance restrains the parameter estimation before it has converged completely. Using Scenario #3 all parameter estimates eventually converge to the same value after about 40 corrections. The parameter estimates actually all stabilize at a parameter value of 16 hours but finally, after 100 corrections, are relatively stable and converged at 13.5 hours. This is close to the true value of 12 hours.

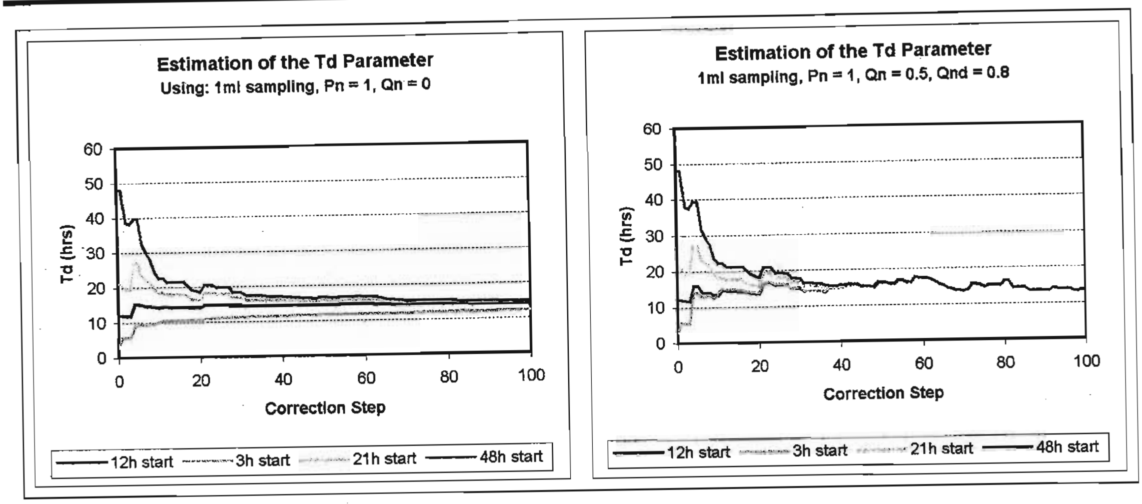

Figure 5-5: Graphs of Scenario #1 and Scenario #3 estimation of T_D using 1ml sampling and Gaussian distributed input concentrations

Under-predictions of the T_D parameter converged quicker (5 corrections using Scenario #2), and therefore initial estimates of T_D should be under predicted for best convergence properties.

5.5.3.2 Results of C_{AC} Parameter Estimation

The estimation of the C_{AC} parameter with no measurement noise is shown in Figure 5-6.

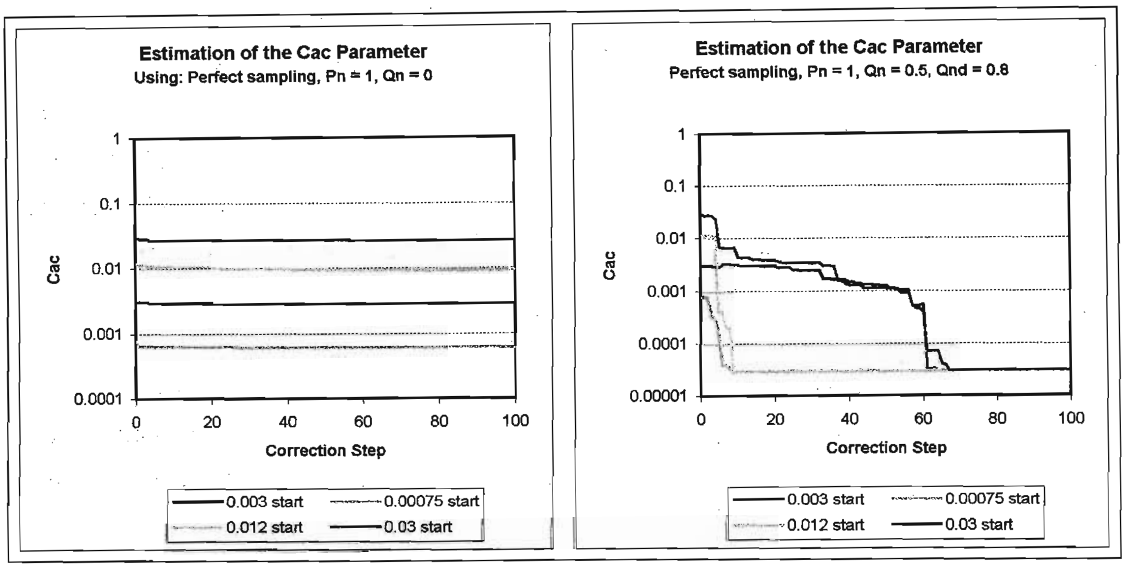

Figure 5-6: Graphs of Scenario #1 and Scenario #3 estimation of C_{AC} using perfect sampling and Gaussian distributed input concentrations

Using Scenario #1 almost no parameter estimation was achieved before the parameter error covariance restricted refinement. The initial estimate using the true parameter value remained constant, suggesting that the parameter may remain stable given normally distributed unknown inputs and associated noise. However, Scenario #3 shows that the C_{AC} is unstable under these conditions and therefore cannot be reliably estimated by the EKF.

5.5.3.3 Conclusions of the Estimation Using Gaussian Inputs

In summary it was concluded that limited parameter estimation using the EKF is possible if the inputs are normally distributed and the distribution known. Convergence of T_D is reliable under these conditions. Prediction of the C_{AC} parameter can be unstable under these conditions and cannot therefore be reliably done with the proposed EKF scheme.

5.5.4 Lognormal Input Concentrations

The lognormally distributed input concentration case is a more realistic representation of actual conditions under which the parameter estimation was to be applied. The median value of each point input was used as the input concentration and the input noise variance was set at 200 times the median value.

5.5.4.1 Results of T_D Parameter Estimation

Using perfect observations the parameter estimation of the T_D parameter is shown in Figure 5-7.

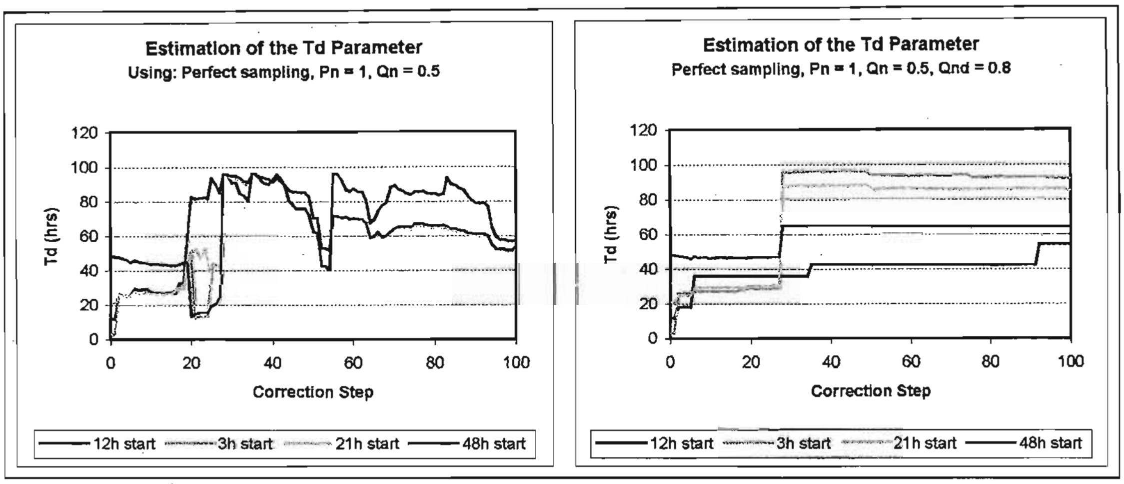

Figure 5-7: Graphs of Scenario #1 and Scenario #3 estimation of T_D using perfect sampling and lognormally distributed input concentrations

In Scenario #1 the error covariance was maintained and the parameter estimates varied over a large range and did not converge to their true values. Using Scenario #3 the estimates all stabilize at significantly larger values, indicating that the parameter estimation had failed. This is perhaps not surprising since the median value is used and is often too small, the EKF compensates by increasing the T_D and thus reducing the decay at each step.

5.5.4.2 Results of C_{AC} Parameter Estimation

The results of trying to estimate the C_{AC} parameter under these conditions are shown in Figure 5-8. Parameter estimates decrease until insignificant and are stable at the minimum value allowed by the projection facility.

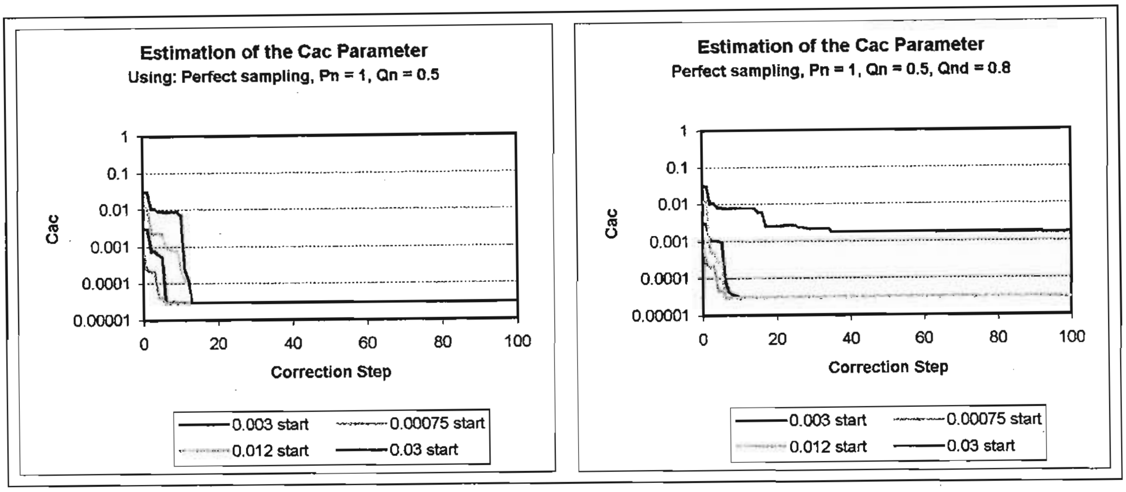

Figure 5-8: Graphs of Scenario #1 and Scenario #3 estimation of C_{AC} using perfect sampling and lognormally distributed input concentrations

5.5.4.3 Conclusions of the Estimation Using Lognormal Inputs

It can be concluded that parameter estimation under realistic conditions with lognormally distributed inputs of unknown concentrations and large measurement error is not possible using the EKF approach.

5.5.5 Conclusions of Parameter Estimation Using the CWQM

The EKF performed adequately under certain conditions, and is able to handle large measurement errors and limited Gaussian distributed but unknown input concentrations. Parameter estimation of the T_D parameter under these conditions was promising. However, it was impossible to estimate accurate and stable estimation of the C_{AC} parameter, unless the input concentrations were known exactly (deterministic). This was because of the insensitivity of the C_{AC} parameter.

Therefore, the EKF cannot be expected to perform parameter estimation under realistic conditions where the input concentrations are unknown and have lognormal distributions.

Conditions may be significantly improved by using more frequent observations and good predictions (or measurements) of the actual input concentrations.

5.6 Estimation of Coastal Water Quality Model

It has been shown in Section 5.5 that recursive estimates with the Extended Kalman Filter algorithm is not effective for unknown inputs in the present context. Therefore, an alternative strategy for determining the parameters is proposed by fitting the statistics of CWQM output to actual sampled statistics of the case study region (Durban Bight).

The parameter estimates, from the statistical estimation, combined with a Kalman Filter may be used for recursive state estimation.

5.7 Statistical Estimation of the Coastal Water Quality Model

An intended use of the CWQM is to provide decision makers with a 'what-if' tool, which may be used to predict the effects that changes, due to new developments etc., might have on the pathogenic pollution levels at beaches along a coastline. In order for the model to provide these predictions, it was first necessary to determine the choice of parameters (T_D and C_{AC}) that best described the current and historical pathogenic indicator levels.

5.7.1 Parameter Fitting Method

The environmental information used for parameter fitting was from 1995/01/01 to 2002/08/31 and as follows:

1. Daily rainfall totals taken from Durban Botanical Gardens.
2. Daily wind averages from weather station DB01 (Port of Durban). Where gaps existed in the data Durban Louis Botha Airport was used.

A unique set of parameter values, T_D and C_{AC}, were selected for each model run.

The CWQM model was run, using the chosen parameter values and environmental information. The point input concentrations were generated as lognormal random E.coli input concentrations appropriate to each point input. Both Annual and seasonal distributions were analysed. The model simulations produced 2800 daily indicator concentrations for each of the coastline cells.

Using the 2800 daily simulated E.coli concentrations of the cells; two data sets were extracted:

1. All daily simulated concentrations for the EMWSS sampled cells
2. Five sets of 14-day synthetic observations for the EMWSS sampled cells

From the two extracted data sets and the real measured EMWSS E.coli concentrations (at the sampling beaches) for the modelled period (1995/01/01 to 2002/08/31) the following statistical and exceedance information was extracted:

1. The exceedance percentages for the following indicator concentrations were calculated for each of the beaches: 2000, 1000, 200, 100 and 10 CFU per 100ml.
2. The average, standard deviation and geometric mean (GM) for each of the beaches.
3. The geometric mean exceedance (GME) for each of the beaches.

The geometric mean exceedance was the percentage of times the calculated running geometric mean exceeded the US EPA E.coli WQ standard of 126 CFU per 100ml. The running geometric mean was calculated differently for the various data sets.

1. For the daily-simulated counts, the running GM was calculated from 30 days of consecutive predictions.
2. For the measured and synthetic observations the running GM was calculated from 3 consecutive observed predictions.

Two different beach groupings were considered:

1. All the EMWSS sampling beaches
2. EMWSS sampled bathing beaches (i.e. All excluding Umgeni South Beach)

Using each of the beach groupings, the sum of the absolute differences between the simulated and measured statistical results was calculated. The statistical analysis results compared were as follows:

1. Percentage exceedance of 2000 CFU/100ml for each of the beaches.
2. Percentage exceedance of 100 CFU/100ml for each of the beaches.
3. Percentage exceedance for all indicator concentrations levels for each of the beaches.
4. Arithmetic mean concentrations for each of the beaches.
5. Standard deviation of the beach concentrations.
6. Geometric mean concentrations for each of the beaches.
7. Geometric mean exceedance for each of the beaches.

For each of the statistical analyses the absolute errors were normalised in the usual manner. Three different combinations of the normalised statistical analyses were considered and absolute errors were summed for each selected parameter combination. The three combination were:

1. All statistical analyses
2. All exceedance analyses
3. All exceedance analyses and geometric mean exceedance

The "best" parameter pairing was selected as the parameter combination that gave the least combined error. The "Best" annual and seasonal parameter pairs were also selected using annual and seasonal input concentration distributions.

5.7.2 Parameter Fitting Results

To determine roughly the appropriate parameter values the following "course" resolved set of parameter values was used for simulations:

T_D - [3,6,9,12,18,24,36,48]

C_{AC} - [0.03, 0.01, 0.006, 0.003, 0.001, 0.0006, 0.0003, 0.0001]

Parameter values were calculated as the average of the best-fit parameters found from analysis of four different sampling scheme analyses:

1. Daily simulated concentrations for all beaches
2. Daily simulated concentrations for bathing beaches
3. Average of the 5, 14-day, synthetic observations for all beaches
4. Average of the 5, 14-day, synthetic observations for bathing beaches

The averaged results of the course parameter set are presented in Table 5-5. Using the general parameter set it was found that the "best" parameter combination was a T_D value of 8.75 hours and C_{AC} value of 0.0033.

	Annual input distribution		**Seasonal input distribution**	
	Average T_D	**Average C_{AC}**	**Average T_D**	**Average C_{AC}**
All statistics	9.00	0.0030	7.50	0.0045
Only exceedance	9.00	0.0030	9.00	0.0030
Exceedance and GME	8.25	0.0038	9.00	0.0030
Average "best" parameter value	***8.75***	***0.0033***	***8.50***	***0.0035***

Table 5-5: Parameter fitting results using the rough set of parameter values

Considering the results obtained from the course parameter set, a finer resolved parameter set was used to refine the search for an optimal set:

T_D - [8.0, 8.5, 9.0, 9.5, 10.0, 10.5, 11.0]

C_{AC} - [0.0020, 0.0025, 0.0030, 0.0035, 0.0040]

	Annual input distribution		**Seasonal input distribution**	
	Average T_D	**Average C_{AC}**	**Average T_D**	**Average C_{AC}**
All statistics	9.25	0.0033	9.25	0.0031
Only exceedance	10.25	0.0025	8.13	0.0034
Exceedance and GME	10.25	0.0025	8.75	0.0031
Average "best" parameter value	***9.92***	***0.0028***	***8.71***	***0.0032***

Table 5-6: Parameter fitting results using the finer set of parameter values

The results for the finer parameter set are presented in Table 5-6. The "best" parameter combinations for annual and seasonal input concentration distributions are indicated. If the C_{AC} parameter was approximated as 0.003 and annual input concentration distributions are considered, the normalised error curves for each of the statistical analyses were as shown in Figure 5-9.

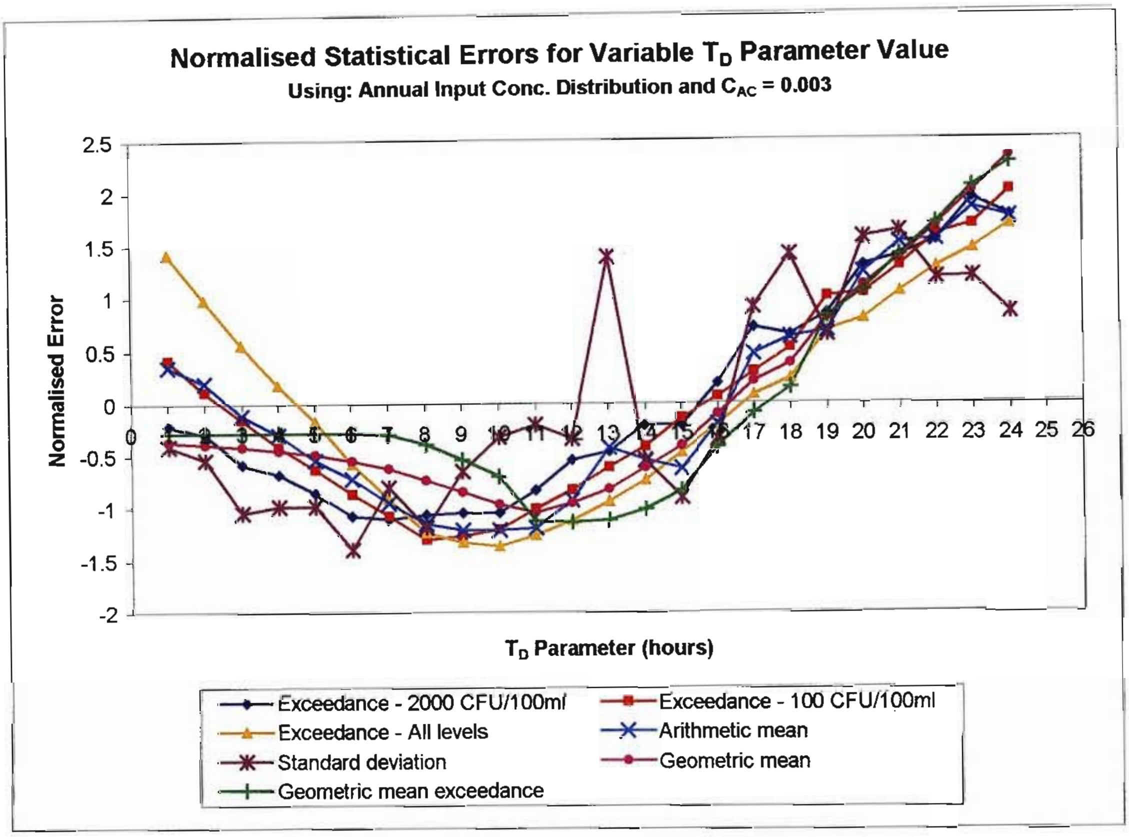

Figure 5-9: Determination of optimum T_D parameter value using C_{AC} = 0.003

The optimum timescales therefore appear to be about 9 to 10 hours with a visually estimated standard deviation of 2 hours. The optimal parameter set is slightly dependent on the input concentration choices as shown in Table 5-7.

Parameter	Annual input concentration distribution	Seasonal input concentration distribution
T_D (hrs)	10	9
C_{AC}	0.003	0.003

Table 5-7: Durban's proposed CWQM parameter sets dependent on input distributions

The estimates of the T_D parameter using statistical fitting compares favourably with the E.coli disappearance timescale of 9.5 hours calculated in Section 3.10.

5.7.3 Examination of the CWQM Results

The CWQM was proposed to simulate the dynamics of the natural system to analyse the effects of possible changes. The CWQM simulated beach concentrations were fitted against the known behaviour of Durban's beaches presented in Chapter 3.

A further comparison using the cross-correlations of the simulated beach E.coli concentrations is presented in Table 5-8.

	Vetches	Addington	South	Wedge	North	Bay of Plenty	Battery	Country Club	Laguna	Umgeni South
Vetches	1.00	0.71	---	0.21	0.65	0.35	0.23	---	---	---
Addington	0.71	1.00	---	---	0.47	0.33	0.21	---	---	---
South	---	---	1.00	0.87	---	---	---	0.21	---	---
Wedge	0.21	---	0.87	1.00	0.23	---	---	---	---	---
North	0.65	0.47	---	0.23	1.00	0.79	0.48	---	---	---
Bay of Plenty	0.35	0.33	---	---	0.79	1.00	0.53	---	---	---
Battery	0.23	0.21	---	---	0.48	0.53	1.00	0.46	0.19	---
Country Club	---	---	0.21	---	---	---	0.46	1.00	0.43	---
Laguna	---	---	---	---	---	---	0.19	0.43	1.00	0.44
Umgeni South	---	---	---	---	---	---	---	---	0.44	1.00

Table 5-8: Cross-correlation of CWQM simulated beach E.coli concentrations

The measured beach cross-correlations are presented in Table 3-27 (Section 3.8.1) but those cross-correlations were improved using thresholding techniques. Therefore, the non-threshold measured beach cross-correlations are shown in Table 5-9.

	Vetches	Addington	South	Wedge	North	Bay of Plenty	Battery	Country Club	Laguna	Umgeni South
Vetches	1.00	---	0.47	---	0.32	0.29	---	0.39	---	---
Addington	---	1.00	---	---	---	---	---	---	---	---
South	0.47	---	1.00	0.80	0.55	0.24	0.31	0.42	---	---
Wedge	---	---	0.80	1.00	0.51	---	---	0.46	---	---
North	0.32	---	0.55	0.51	1.00	0.29	---	0.41	---	---
Bay of Plenty	0.29	---	0.24	---	0.29	1.00	---	0.44	---	---
Battery	---	---	0.31	---	---	---	1.00	0.19	---	---
Country Club	0.39	---	0.42	0.46	0.41	0.44	0.19	1.00	0.34	0.34
Laguna	---	---	---	---	---	---	---	0.34	1.00	0.24
Umgeni South	---	---	---	---	---	---	---	0.34	0.24	1.00

Table 5-9: Cross-correlation of non-threshold true beach E.coli concentrations

There are similarities between the correlations calculated using simulated and measured E.coli concentration values. It was judged that the CWQM adequately models the processes and interrelations between beaches along Durban nearshore zone.

5.8 Real-Time Application of the Coastal Water Quality Model

The other application of the CWQM was to provide decision makers with a real-time beach management tool. The Real-Time CWQM beach management tool may provide for example, daily predictions of the pathogenic pollution levels at selected beaches along a coastline. The CWQM has been shown to be unable to perform automated parameter estimation given the uncertainty of the inputs under normal "realistic" conditions (Section 1.1). The question was therefore:

> "Given that the states of the CWQM are observed on a fortnightly basis and are corrected accordingly; that the point input concentrations are lognormally distributed but predictions are made using fixed monthly, seasonally or yearly values; and that the parameters are fixed. What would be the *best strategy* for making daily predictions of the states during the unobserved period?"

A significant percentage of the errors associated with the predictions are due to errors in estimating the pollutant loading of the system. These are mainly associated with the uncertainty associated in the pollution concentrations of the point inputs. The best strategy would involve a combination of the following:

1. Modifying the input concentrations
2. Modifying the input noise characteristics

Daily predictions were made using a statistical average input concentration value for each of the point inputs representative of the annual or seasonal indicator concentration distributions of the inputs. Modification of the input concentrations involved determining which statistical average input concentration value would give the "best" predictions of pathogenic pollution levels during the unobserved period.

Modification of the input noise characteristics required determining what associated noise level would give the best-corrected predictions after processing the observations.

5.8.1 Best Strategy Analysis Method

The "best" predictive strategy for daily predictions was determined using synthetic observation sequences and fixed model parameter values.

The model parameters used for 'Best Strategy' analysis were those determined in Section 5.7 They were:

T_D = 10 hours

C_{AC} = 0.003

The environmental information used for best strategy analysis was from 1998/01/01 to 2002/08/31 and as follows:

1. Daily rainfall totals taken from Durban Botanical Gardens.
2. Daily wind averages from weather station DB01 (Port of Durban)

This provided 1461 daily indicator concentration predictions.

The synthetic observation sequences were generated using the method described in Section 5.4.3. Input concentrations of the point input were randomly selected from the relevant lognormal input distributions and the CWQM was run three times, producing three different synthetic sequences. Using these synthetic sequences, the "true" daily values, and 14-day observation sequences and exceedance percentages were created.

1. The "true" daily predictions were extracted as daily observations of the pathogenic indicator levels for the ten EMWSS sampling beaches. The daily predictions were considered as perfect and thus no measurement error was added.
2. The synthetic observation sequences were created with observations every fourteen days, on average, for the ten EMWSS sampling beaches. Three measurement errors were considered: Six-figure significance (representing 'perfect' observations); as well as those associated with standard EMWSS testing – twenties (5ml sample) and hundreds (1ml sample).
3. The "true" exceedance percentages for a range of selected pathogenic indicator concentrations were calculated for the ten EMWSS sampling beaches from the "true" daily predictions.

The CWQM was run using standard input concentrations for each of the point inputs, input noise percentage estimate and appropriate synthetic observations and model parameters. The choice of the standard input concentration for each of the inputs was made using the lognormal cumulative distributions functions (CDF) specific to each point input. Using, a certain probability value (for example P = 60%) and appropriate scale and shape parameter (μ' and σ') for each point input, the input concentration value was calculated as the inverse of the cumulative distributions function.

$$Value = F\left(x \middle| \mu', \sigma'\right) = \frac{1}{\sigma'\sqrt{2\pi}} \int_0^x \frac{e^{-\frac{(\ln(t)-\mu')^2}{2\sigma'^2}}}{t} \cdot dt \tag{5-1}$$

The appropriate point input distribution probability value to use was determined using the following method, performed on each model run using a range of probability values.

1. Using the daily predictions and the true daily predictions, the sums of the squares of the errors, for each of the prediction at the observed beaches, was calculated.

2. Using the daily predictions, the exceedance percentages for the range of indicator concentrations were calculated. The sum of the absolute differences between the calculated exceedance percentages and true exceedance percentages was calculated.

The input noise percentage estimate was scrutinized by the following method:

1. Using the corrected step predictions and the "perfect" synthetic observations (10^{-6} significance level) the error between the prediction and the "true" concentration is calculated. The error is squared and summed both for all observed beaches and each beach individually.
2. Using the state covariance and absolute difference between the predicted and observed indicator concentration, at the observed beaches, it is checked that there exists sufficient state covariance to satisfy the difference. The formulation of the KF and EKF assumes noise process and therefore the state covariance of the errors to be Gaussian. One standard deviation of the system covariance should satisfy 67% of the differences.

The best predictive strategy was determined as: the cumulative input concentration distribution probability and input noise percentage estimate that best satisfied all constraints.

5.8.2 Best Strategy Analysis Results

5.8.2.1 Determination of Appropriate CDF Probability Value

The exceedance distribution errors using varying probability values are shown in Figure 5-9. The minimum exceedance distribution error for all observation accuracy levels was found using a probability value of 0.63 (63%).

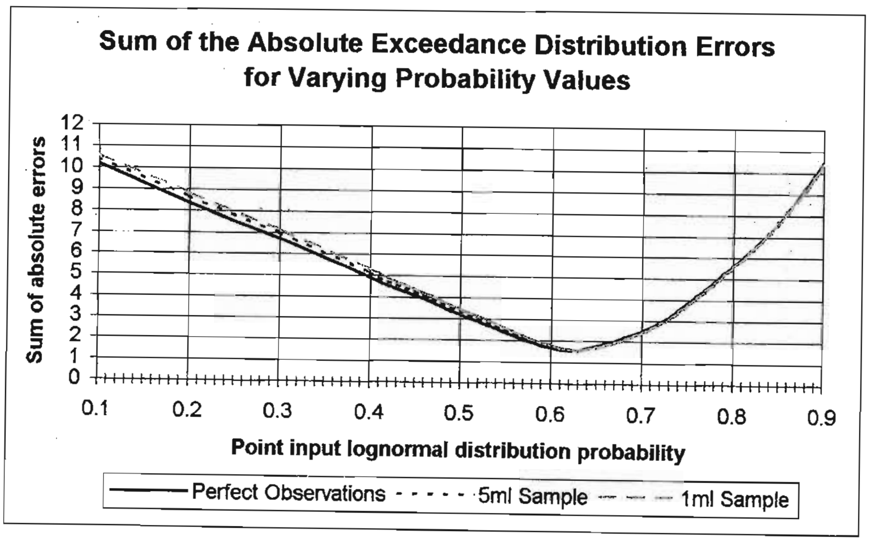

Figure 5-10: Exceedance distribution errors

However, for real-time predictions the accuracy of the actual daily beach prediction is of more concern. Figure 5-11 shows the sum of the squares of the daily prediction errors using varying probability values.

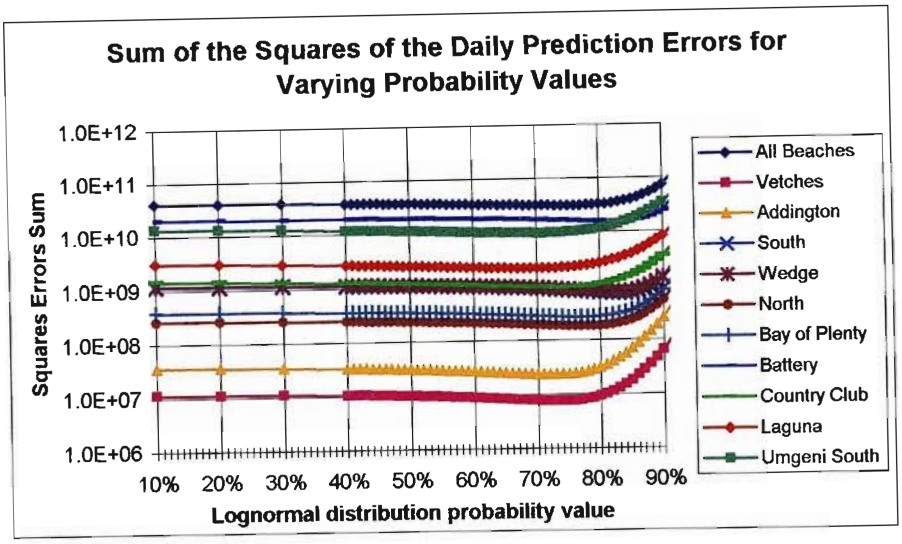

Figure 5-11: Sum of the squares of the daily prediction errors

There were three orders of magnitude in the range of prediction errors between beaches, with Battery Beach and Umgeni South Beach having larger errors. The prediction error curves shown in Figure 5-11 were normalised and shown in Figure 5-12, so that they could be compared. The curves were normalised using the mean and standard deviations of each of the prediction errors as follows:

$$P_{Err}{}^{N} = \frac{P_{Err} - \overline{P_{Err}}}{\sigma_{P_{Err}}} \tag{5-2}$$

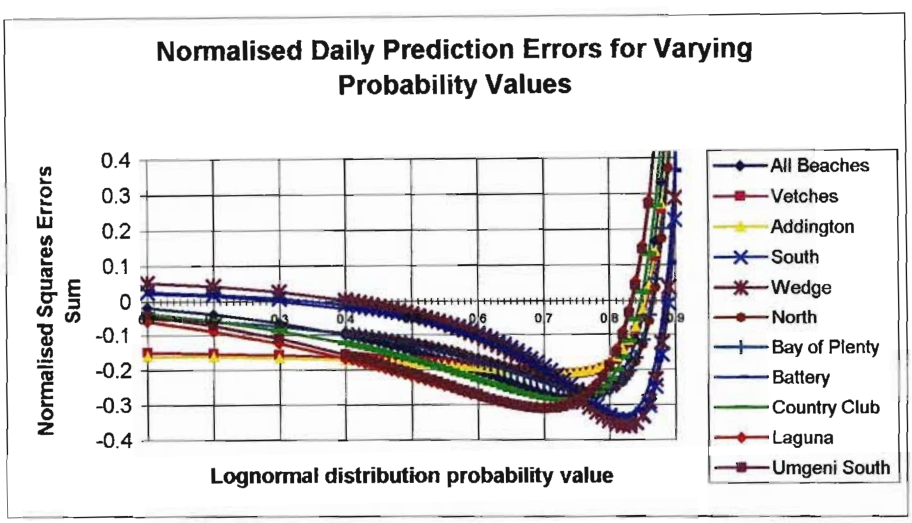

Figure 5-12: Normalised sum of the squares of the daily prediction errors

Figure 5-12 shows that Battery, Wedge and South Beaches are more sensitive to the probability value used and require a larger probability value to minimise the prediction errors. The input distribution errors that gave the minimum sum of square prediction error for each of the sampling beaches are presented in Table 5-2.

Sampling Site	Min Error Probability
All Beaches	0.75
Vetches Beach	0.74
Addington Beach	0.73
South Beach	0.83
Wedge Beach	0.82
North Beach	0.78
Bay of Plenty Beach	0.77
Battery Beach	0.82
Country Club Beach	0.73
Laguna Beach	0.70
Umgeni South Beach	0.70

Table 5-10: Optimum input distribution probability value for minimum prediction errors

It appears that beaches that are more affected by stormwater drains, with sporadic input from rainfall runoff and whose input concentrations have higher variability, require higher single value concentrations, determined by the input distribution probability, to minimise the prediction errors. The 0.75 or 75% input concentration distribution percentage was selected to best satisfy all beaches.

5.8.2.2 Determination of Appropriate Input Noise Percentage

The aim is to provide a satisfactory amount of noise to the system to allow corrections to be made to predicted beach concentrations when observations of the states become available. However, providing too much noise to the system might adversely affect the corrections.

The errors in the prediction of pathogenic pollution indicator concentrations are associated with the essentially unknown magnitudes of the point input concentrations. To get a rough estimate of the appropriate input noise percentage the CV(75%) value was used. The CV(75%) is a non-dimensional value similar to the standard coefficient of variation, Equation (5-3)(a), except that instead of the arithmetic mean the 75% probability value is used and instead of the standard deviation about the arithmetic mean the standard deviation about the 75% probability value is used, Equation (5-3)(b)

$$CV = \frac{\sigma_x}{\bar{x}} \quad \text{(a)}; \qquad CV(75\%) = \frac{\sigma_{x_{P75}}}{x_{P75}} \quad \text{(b)} \qquad (5\text{-}3)$$

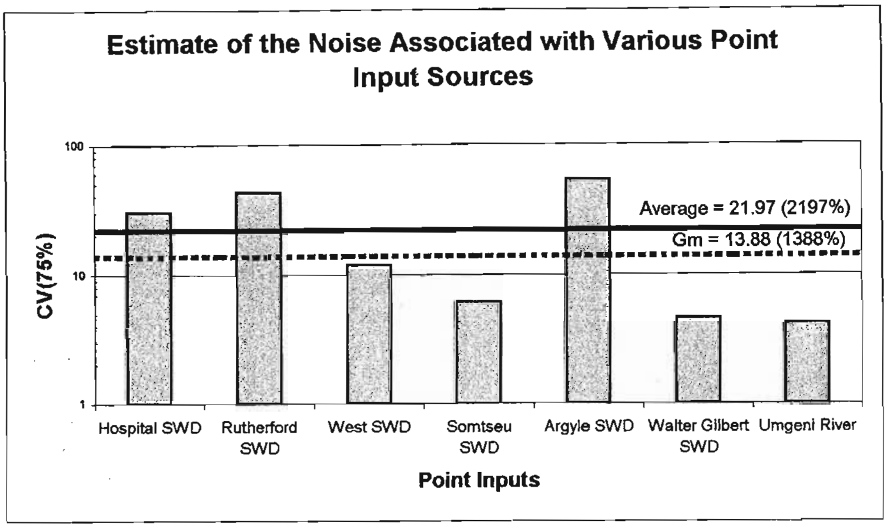

Figure 5-13: Preliminary estimation of required point input noise

The CV(75%) value was calculated for each of the point input sources and is presented in Figure 5-13. The averaged CV(75%) value for the point input sources was calculated as 22. This suggests that if each of the inputs contributed equally to the system the input noise percentage should be around 2200%. However, the point inputs have different catchment runoff areas and baseflow volumes and don't contribute equally to the system. Therefore, the actual input noise percentage required might be higher or lower depending on which input influences the system the most.

The Kalman Filter assumes that the noise process (system error covariance) is Gaussian. The percentage of the corrections that were within the estimated variance, for varying input noise percentages, are shown in Figure 5-14. This suggests that the input noise percentage needs to be approximately around 500% or greater.

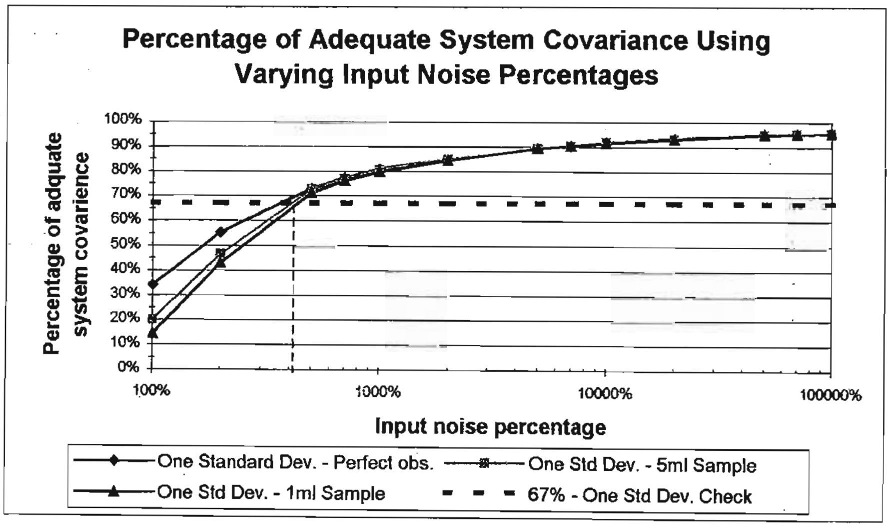

Figure 5-14: Testing the percentage of prediction errors that are satisfactorily bounded by the system covariance

The input noise percentage that gave the minimum sum of the square corrected prediction errors for varying observation noise are plotted in Figure 5-15.

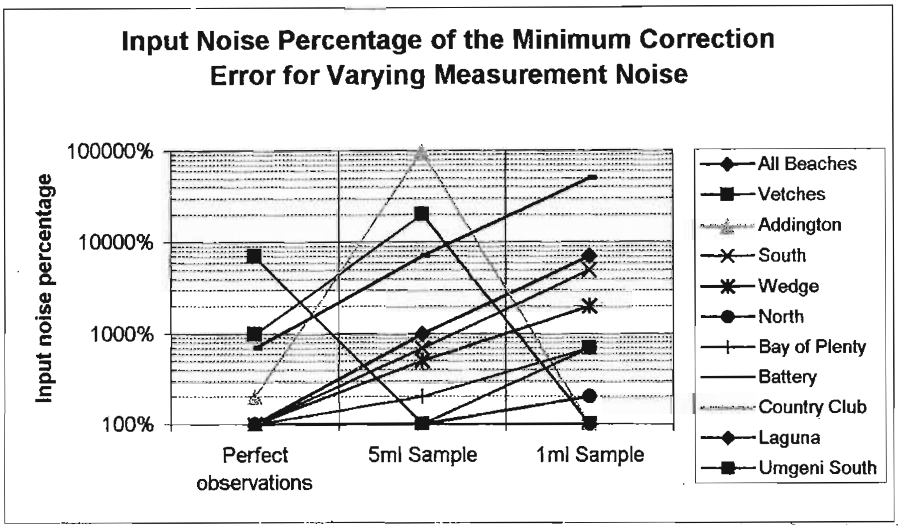

Figure 5-15: Input noise percentage for the minimum correction error

If perfect observations of the indicator concentration levels at sampled beach were available then an input noise of 100% may be sufficient. However, the observations are effected by measurement noise and thus more input noise is required. Considering the system as a whole the 5ml and 1ml measurements require 1000% and 7000% input noise, respectfully. Certain other beaches require the specification of significantly more input noise; therefore an input noise percentage of 5000% is suggested.

5.8.3 The 'Best' Strategy

To provide daily pathogenic pollution predictions of Durban's bathing beaches using the Real-Time CWQM, the 'best' strategy was as follows:

1. Use fixed E.coli concentration values calculated for each point input from their associated lognormal cumulative E.coli distribution function using a distribution probability of 75%.
2. Use an input noise percentage of 5000%

5.8.4 Reliability of Daily Predictions

The CWQM makes daily predictions of the E.coli concentrations for selected beaches using fixed input concentration values. The beaches are observed every 14^{th} day and the beach concentrations and system are corrected to incorporate these observations. However, the question remains:

> *"How much confidence may one have in the predicted pathogenic indicator concentration for each of the beaches (given that the actual input concentrations are unknown) for successive days after an observation?"*

5.8.4.1 Analysis Method

The daily predictions for each of the beaches were sorted into separate groups. Each prediction was sorted by the number of days that the prediction was subsequent to an observation/ correction. The sorting was as follows:

Day 0: The corrected predictions.
Day 1: One day after an observation / correction step was made.
Day 2: Two days after an observation / correction step was made.
...
Day 13: Thirteen days after and observation / correction step was made.

The prediction errors were calculated by subtracting the "true" indicator concentrations from the predicted concentrations. Positive prediction errors mean that the system was over-predicted and negative prediction errors mean that the system was under-predicted. The prediction errors for each of the day groups and beaches were then analysis by determining the following statistical information:

1. The 90% prediction error (ie. the value that is greater than 90% of the prediction errors)
2. The 84% prediction error
3. The median prediction error (50% distribution value)
4. The 16% prediction error
5. The 10% prediction error

The error ranges were then calculated using the percentage prediction errors. Using the 90% and 10% prediction errors the 80% prediction error range about the median error was calculated. This means that 80% of the prediction errors fell within the range about the median error. The 68% prediction error range about the median error was calculated using the 84% and 16% prediction errors.

The various prediction errors should be compared with a water quality guideline values. However, the only guideline that could be used was the US EPA Single Sample Limit (SSL) values for freshwater E.coli samples, Table 5-11.

Beach Use	E.coli SSL (cfu/100ml)
Designated bathing beach	235
Moderated use for bathing	298
Light use for bathing	410
Infrequent use for bathing	576

Table 5-11: US EPA Single sample limit for freshwater E.coli

5.8.4.2 Discussion of Results

Except for Umgeni South Beach, all other beaches are designated as bathing beaches and should conform to the US EPA designated bathing beach use. However, certain beaches are of critical concern due to their location and use. These beaches are those that directly serve the tourism and local community, from Addington Beach to Bay of Plenty Beach. Battery Beach should be included in this group, but based on historical records, its classification as a designated bathing beach should be reviewed. The same factors that have historically caused this beach to regularly fail WQ standards should influence the prediction errors.

Beach Sampling Site	Geometric Mean Conc. (CFU/100ml)
Vetches	0
Addington	0
South	2
Wedge	2
North	7
Bay of Plenty	13
Battery	114
Country Club	83
Laguna	119
Umgeni South	246

Table 5-12: Geometric mean E.coli concentrations for sampling beaches

The geometric mean (GM) E.coli concentrations for the sampling beaches are shown in Table 5-12. The various prediction errors and error ranges should be evaluated against the GM for each of the beaches to determine the significance of the prediction errors.

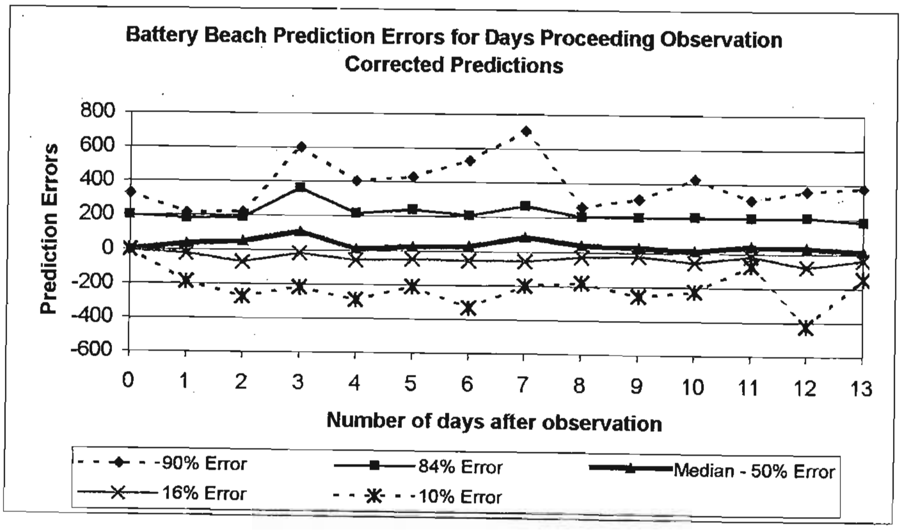

Figure 5-16: Battery Beach percentage prediction error values

The various prediction errors for each successive day for Battery beach are shown in Figure 5-16. The median prediction error is small and generally significantly less than the GM E.coli prediction for Battery beach. Note that the model should over-predict more than under-predict due to the non-negativity constraint placed on the model (The model cannot make negative concentration predictions).

The median prediction errors of each successive day for the various beaches are shown in Figure 5-17.

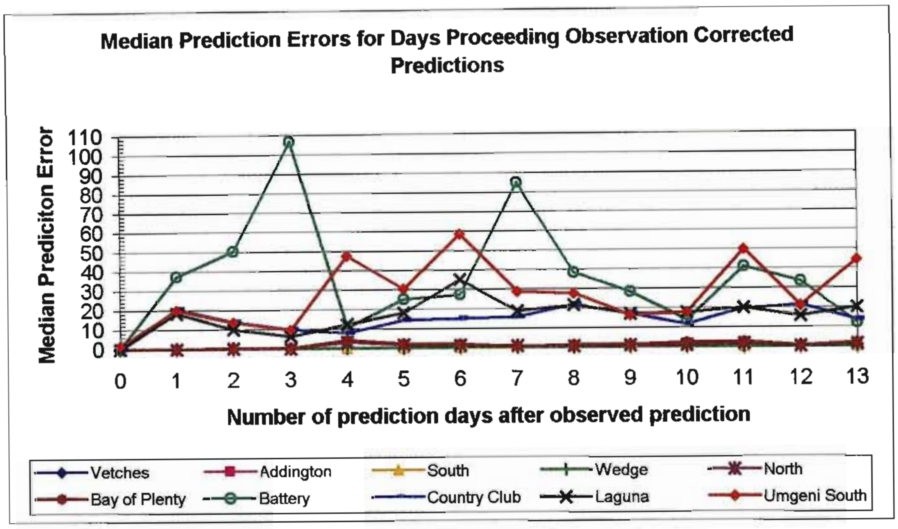

Figure 5-17: Median Prediction Errors for number of days proceeding observations

The first observation is that the median prediction error is never negative. This is a primary concern since it is better that the model on average over-predicts the pathogenic pollution rather than under-predict (and not detect possible poor WQ conditions). The median prediction errors for all unobserved days of the critical beaches are effectively zero, which means that the predictions should be reliable. The median prediction errors for the Beaches from Battery to Umgeni South are positively biased and non-zero. However, when compared against the US EPA single value E.coli limits (Table 5-11) and geometric mean E.coli concentrations of the beaches (Table 5-12) these errors are generally small and therefore insignificant.

However, of greater significance than the median error is the range of the prediction errors. The 80 percent and 68 percent prediction error ranges are presented inFigure 5-18 and Figure 5-19. The error prediction ranges for all the beaches don't significantly increase the further the prediction is from an observation, this may be influenced by the disappearance timescale being relatively short (T_D = 10 hrs). As expected, due to its close proximity to the Umgeni River the Umgeni South Beach has the largest prediction error range.

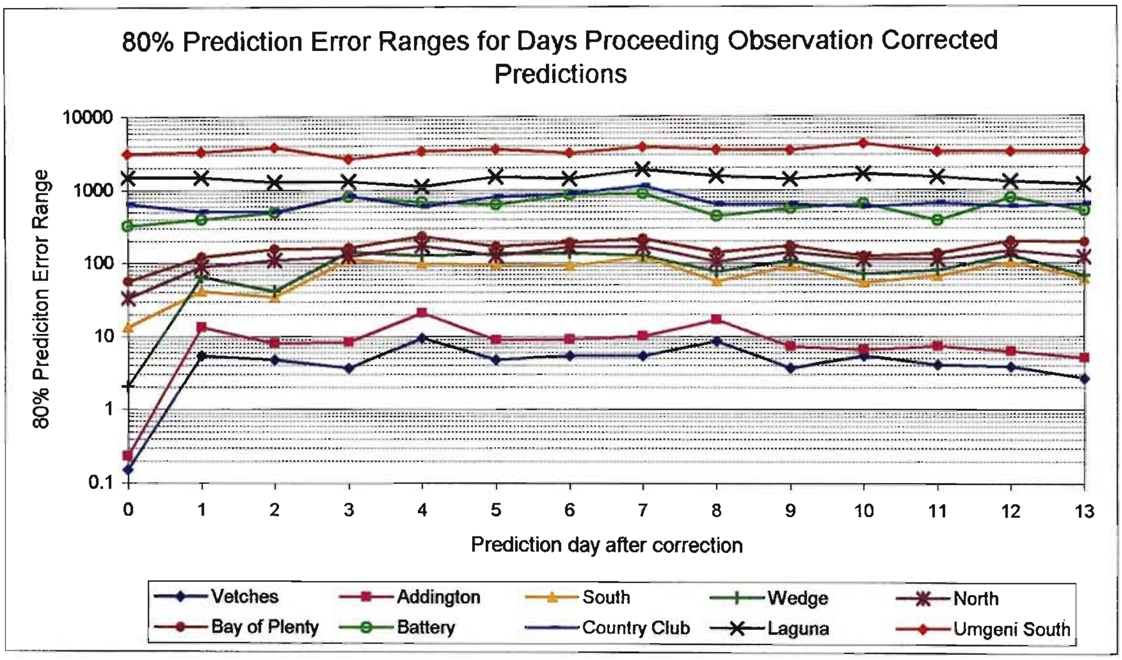

Figure 5-18: 80% Prediction Error Ranges

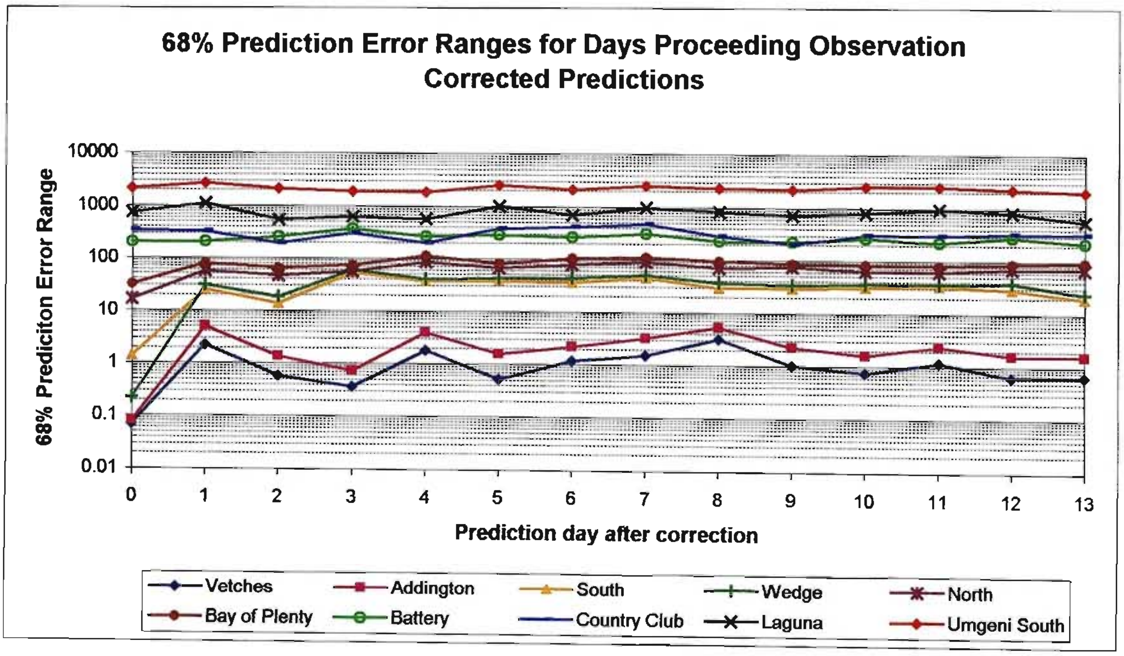

Figure 5-19: 68% Prediction Error Ranges

Of the critical beaches, Bay of Plenty Beach has the largest prediction error range. The average prediction error range for Bay of Plenty for the two ranges are as follows:

1. 80% - Prediction Error range of ±200 CFU/100ml
2. 68% - Prediction Error range of ±90 CFU/100ml

Compared against the US EPA-SSL of 235 CFU/100ml both these ranges are satisfactory. Considering that most of the other sensitive beaches have significantly smaller ranges the CWQM appears to operate adequately.

The remaining bathing beaches (Battery to Laguna Beach) have larger prediction error ranges. However, if these beaches are classified for light or infrequent bathing use the US EPA-SSL values compare favourably. Therefore, the CWQM again appears to function adequately.

It should be remembered that the US EPA-SSL for E.coli is defined for freshwater and may not be fully applicable. Another consideration is that US EPA-SSL for E.coli was calculated using the freshwater log-standard deviation value of 0.4 set for E.coli and Enterococcus. Although for marine recreational waters only Enterococcus is specified, a log-standard deviation value of 0.7 is used. If 0.7 were used for the marine application of E.coli the SSL values would be significantly larger, as shown in Table 5-13. This would further support the applicability of the CWQM for producing realistic predictions.

Table 5-13: US EPA SSL for Applied Marine E.coli (log-standard deviation value of 0.7)

Beach Use	Single sample E.coli count limit (cfu/100ml)
Designated bathing beach	374
Moderated use for bathing	569
Light use for bathing	992
Infrequent use for bathing	1800

5.9 Conclusions

It was shown that it might be possible to estimate or refine the model parameters using the EKF algorithm. However, accurate knowledge of the loading to the nearshore system is required. In the case of the present case study site where the input concentrations are not accurately known it was found that the EKF was unable to perform parameter estimation.

The CWQM was fitted to the case study region (Durban Bight) using a statistical fitting procedure based on the measured statistics of the region. The Durban Bight was found to be best modelled using an E.coli disappearance value (T_D) of 10 hours and an advection coefficient (C_{AC}) of 0.003. The average daily wind speed is 5.1 m/s (Section 3.6.2) implying an average daily current speed of 0.0153 m.s^{-1} (15.3 cm.s^{-1}) and an average advection timescale of 3.63 hours, for a cell length of 200m.

Using the CWQM to make real-time predictions of beach E.coli concentration levels required the input indicator (E.coli) concentrations to be set at values corresponding to probability values (75%) of the lognormal distributions specific for each input. The ability of the CWQM to produce realistic real-time predictions of possible pathogenic pollution levels was investigated. The CWQM was shown to produce viable real-time predictions with acceptable errors associated.

CHAPTER 6:
COASTAL WATER QUALITY MODEL APPLICATION: BATTERY BEACH CASE STUDY

6.1 Introduction

On the basis of historical data, full contact bathing at Battery Beach has been a health risk for a number of years. As shown in Section 3.2, Battery Beach fails South African and International guidelines for safe recreational water quality. The beach is by far the most pathogenically polluted designated bathing beach along Durban's coastline. On occasions the *Natal Mercury* Newspaper has features articles relating to poor water quality at Battery Beach (Carnie, 2003) and public concerns over the urban stormwater outlets on the Durban beachfront (Carnie, 2002).

Battery Beach has for many years been the northern-most beach of the Durban beachfront. The beach was not seen as supporting any of the main hotels near North and South Beaches, and thus the historically poor water quality conditions may not have been perceived as influencing Durban's tourism industry. With the development of the Suncoast Casino this situation has now changed. The Suncoast Casino is envisaged as one of Durban's main tourism draw cards. The casino is to offer gambling and accommodation facilities as well as conference facilities and other related activities. Unlike other hotels along Durban's beachfront where a road and markets or other activities separate the hotels from the beach, the Suncoast Casino is situated with direct access to the beach. The developers view the beach as a key attraction to the entire development with and aim of renaming the beach, in front of the development, as Suncoast Beach (see Plate 6-1(a)). It can therefore be argued that the water quality of the Battery Beach region needs immediate attention and improvement. It would also be highly advantageous for Battery Beach to be awarded "Blue Flag" status. However given the present water quality conditions that would be impossible.

The purpose of this chapter is to analyse more specifically the causes of the poor water quality experienced at Battery Beach and to propose possible schemes to improve the water quality of the Battery Beach region. Then to use the CWQM to analyse the proposed solution schemes and the specific improvements levels needed to satisfy SA and International WQ guidelines.

6.2 The Problem - The Argyle Stormwater Drain

The most dominant source of pollution to the Battery Beach nearshore region is the Argyle Road stormwater drain.

The location of the Suncoast Casino complex and its proximity to the Argyle SWD is shown in Plate 6-1(a). The access to the beach from the casino and most likely site of the Suncoast Beach bathing area is only 400 metres from the Argyle SWD discharge position.

Plate 6-1: (a) Proximity of Suncoast Casino Beach to Argyle Road SWD (b) Approximate catchment of Argyle SWD

The Argyle Road SWD catchment is shown in Plate 6-1(b). Only a small percentage of the catchment area appears to be used for residential activities. The railway station complex utilises a large percentage of the catchment area, as shown in Table 6-1, and may be the dominant source of pathogenic pollution.

Land Use	Percentage of the Catchment Area
Residential	4.2%
Open Spaces	4.7%
Streets and Roads	14.7%
Commercial and Business	37.3%
Industrial (Railway)	39.1%

Table 6-1: Argyle SWD catchment land use (Wesson, 2001)

Wesson (2001) discussed problems associated with an extensive informal settlement located at the Durban Railway Station (see Plate 6-1(b)). The informal settlement consisted of approximately 430 people; with daily fluctuations of up to 200 people per day. Approximately 61 percent of inhabitants use the station floor for sleeping while the remaining 39 percent sleep in makeshift structures or in the open air on the street. It was reported that a large percentage of waste and faecal pollution was discharged directly into the stormwater drain system. Furthermore, the poor quality of life of the informal residents suggests a greater likelihood that the faecal pollution would contain disease-causing pathogens.

6.3 Proposed Solutions to Argyle SWD Pollution levels

A number of different approaches are available to improve the Argyle stormwater discharges and consequently the pathogenic pollution of Battery Beach.

6.3.1 Cleaning up of the Catchment

Cleaning up of the catchment would involve finding the dominant sources of pollution and creating measures whereby they were either removed or minimised. This solution would seem to be the most intuitive - rather solve the problem at its source than try and solve the effects of the problem. This may not prove effective, as the removal of pollution sources may be costly or impossible.

For example: The pollution emanating from the informal settlements may be improved by short and long term planning. A short-term solution could include provision of sanitation and health-care facilities to improve the quality of life for the informal dwellers. A long-term solution would involve the eventual relocation and housing of the inhabitants.

6.3.2 Rerouting of Stormwater

The water quality of the discharged stormwater may be improved by removing the portions that emanate from the most polluted areas. These may then be rerouted to the sewage system, stormwater drains or separate treatment facility.

For example: The stormwater from Durban Station could be rerouted to the Somtseu stormwater drain, which discharges its stormwater further out to sea than Argyle SWD.

The disadvantages of these schemes are:

1. If the most polluted areas were dispersed over the catchment, stormwater separation and rerouting may be difficult and prove costly.
2. The rerouting of stormwater to the sewage system may place additional strain on the existing sewage system. The sewage system may not be designed to deal with the increases in volume especially during high rainfall events. These events may actually lead to breakages in the sewage lines and contamination of the stormwater system, which would be counterproductive.
3. Separate stormwater treatment facilities may prove costly.
4. Diversion to other stormwater drains may cause new pollution problems at other beaches, which could be even more of a problem.

6.3.3 Lengthening of the Outfall Pipe

Another possible solution to improving the beach water quality may be to extend the outfall pipe further out to sea. Most of the other stormwater drains along Durban's beachfront discharge further out to sea, whereas Argyle discharges into the nearshore region.

The advantages of this solution are:

1. It is a fairly simple solution to implement.
2. It may be the cheapest scheme to implement
3. No additional stormwater quality improvement may be necessary.

The disadvantages of this solution are:

1. Any solid structure built within the nearshore zone may restrict littoral drift, and possibly lead to beach erosion.
2. Large stormwater pipes are unsightly and detract from the visual attributes of the coastline.
3. Detailed analysis is required to determine the required length of outfall in order to prevent the pollution from returning to the inshore region and thus limiting the improvements to the water quality.

6.3.4 Constructed Stormwater Wetland

Constructed stormwater wetlands are artificial wetlands designed to treat wastewater and stormwater using natural processes. A brief discussion on constructed wetlands is presented in Appendix E.

The advantages of a wetland scheme are:

1. Wetlands offer effective treatment in a passive manner, minimising mechanical equipment, energy and skilled operator requirements.
2. Wetlands may be less expensive to construct and are less costly to operate and maintain than conventional treatment systems.
3. Wetland systems provide a valuable addition to the 'green space' in a community.
4. Wetland systems produce no residual biosolids or sludges requiring subsequent treatment and disposal.
5. Removal efficiencies are nearly always greater than 90% for coliforms and greater then 80% for faecal streptococcus (Kadlec and Knight, 1996)

The disadvantages of a wetland scheme are:

1. A large area may be required which may prove unfeasible in urban areas, where land is often scare and prime.
2. Mosquitoes and other insect vectors can be a problem.

6.4 Analysis Using The CWQM

The CWQM was used to analyse two solutions for improving the Argyle stormwater drain effluent and the resultant water quality conditions of Battery Beach. In both schemes the improvement of the water quality conditions was measured using E.coli as the indicator organism. The two proposed improvement schemes were:

1. General improvement of the stormwater discharge
2. Improvement of the stormwater discharge using a constructed wetland

The improvements yielded by each of the schemes were analysed using the South African marine water quality (SA WQ) guidelines and US EPA guidelines set for E.coli. It should be remembered that SA WQ Guidelines are used by FEE in considering South African beaches for "Blue Flag" status. The SA WQ guidelines are as follows:

1. Only 20 percent of individual samples may exceed 100 CFU/100ml.
2. Only 5 percent of individual samples may exceed 2000 CFU/100ml

The US EPA single sample limits (SSL) and the geometric mean exceedance (GME) were also used. Since the EPA guidelines for marine-use do not use E.coli as an indicator, the freshwater guidelines were used for analysis purposes. The GME guideline is that the geometric mean of at least five equally spaced samples over a 30-day window should not exceed 126 CFU/100ml. The SSL guideline for a designated bathing beach is 235 CFU/100ml

The environmental information used for model simulations was from 1995/01/01 to 2002/08/31 and comprised:

1. Daily rainfall totals taken from Durban Botanical Gardens.
2. Daily wind averages from weather station DB01 (Port of Durban).

Where gaps existed in the data, information from the weather station at Durban International Airport was used.

6.4.1 CWQM Predictions of Present Conditions

Model predictions of the current water quality conditions at Battery Beach are given in Table 6-2. It is also of interest to know how the water quality of surrounding beaches.

Season	SA WQ Guidelines		US EPA Guidelines	
	2000 CFU/100ml	100 CFU/100ml	Full Bathing SSL	30-day GME
Annual	3.5%	26.7%	16.6%	9.0%
Summer	4.5%	32.6%	21.3%	14.1%
Autumn	2.9%	25.3%	15.3%	4.9%
Winter	2.0%	18.2%	11.1%	1.4%
Spring	5.0%	31.9%	19.6%	11.9%

Table 6-2: CWQM prediction of current WQ at Battery Beach: Exceedance percentages using SA WQ and US EPA Guidelines

The water quality of surrounding beaches may be improved if the quality of the discharge from Argyle SWD was to improve. The surrounding beaches considered were Bay of Plenty Beach and North Beach to the south and Country Club Beach to the north. The model predictions of the current water quality conditions experienced at these beaches are given in Table 6-3, Table 6-4, Table 6-5 and Table 6-6 respectively.

Season	SA WQ Guidelines		US EPA Guidelines	
	2000 CFU/100ml	100 CFU/100ml	SSL - Full Bathing	30-day GME
Annual	0.3%	11.6%	4.5%	3.6%
Summer	0.8%	18.0%	8.1%	7.0%
Autumn	0.1%	8.3%	2.7%	2.0%
Winter	0.0%	6.3%	1.4%	1.1%
Spring	0.5%	14.5%	6.1%	4.6%

Table 6-3: CWQM prediction of current North Beach WQ conditions (Exceedance percentages using SA WQ and US EPA Guidelines)

Season	SA WQ Guidelines		US EPA Guidelines	
	2000 CFU/100ml	100 CFU/100ml	SSL - Full Bathing	30-day GME
Annual	0.5%	16.9%	6.8%	5.0%
Summer	1.3%	22.4%	11.3%	8.5%
Autumn	0.3%	14.1%	4.6%	3.4%
Winter	0.0%	12.4%	3.4%	1.9%
Spring	0.5%	19.2%	8.4%	6.5%

Table 6-4: CWQM prediction of current Bay of Plenty Beach WQ conditions (Exceedance percentages using SA WQ and US EPA Guidelines)

Season	SA WQ Guidelines		US EPA Guidelines	
	2000 CFU/100ml	100 CFU/100ml	SSL - Full Bathing	30-day GME
Annual	0.9%	20.7%	11.0%	8.8%
Summer	1.2%	31.3%	17.0%	13.3%
Autumn	0.6%	15.0%	7.6%	6.0%
Winter	0.4%	8.7%	4.2%	3.5%
Spring	1.5%	29.8%	16.3%	13.3%

Table 6-5: CWQM prediction of current Country Club Beach WQ conditions (Exceedance percentages using SA WQ and US EPA Guidelines)

The model predictions compare favourably with exceedance statistics calculated from sampled water quality conditions as presented in Section 3.2. However, it should be noted that direct comparisons are not possible. The model predictions are averaged from multiple model runs (for this analysis the average of three model runs was used) and the 30-day GME was calculated using five equally spaced samples (from a 30-day window). The GME from the measurements was not directly comparable since the samples were taken fortnightly, which meant that the GME had to be calculated from only three samples that covered between 36 and 42-days.

6.4.2 The General Improvement Scheme

The general improvement approach involved improvement of the pathogenic content of the stormwater discharge using measures such as cleaning up of the catchment or treatment of the stormwater.

6.4.2.1 General Improvement Scheme Method

The CWQM analysis used random input concentrations from lognormal distributions, specific to each stormwater drain (see section 3.4.2). Water quality improvements were specified as percentage improvements relative to current conditions.

The improvements were assumed to affect only the lognormal mean values whilst keeping the lognormal standard deviation constant. The change in the lognormal mean value was calculated as follows:

$$\mu'_{New} = \ln\left[(1-P)*e^{\mu'}\right] \tag{6-1}$$

where: μ' is the lognormal mean of the SWD lognormal distribution
P is the percentage improvement in water quality
μ'_{New} is the lognormal mean of the improved SWD distribution

No restriction was placed on the rainfall runoff process that determines the flow-rates of the stormwater outflows.

6.4.2.2 Results of the General Improvement Scheme

The 2000 CFU/100ml exceedance percentage is shown in Figure 6-1, for both annual and seasonal data. The model predicts that Battery beach currently exceeds the SA WQ Guideline maximum exceedance (5%) during the spring and (marginally) the summer seasons. Any improvement in pathogenic content of Argyle SWD leads to Battery beach passing this guideline for all seasons.

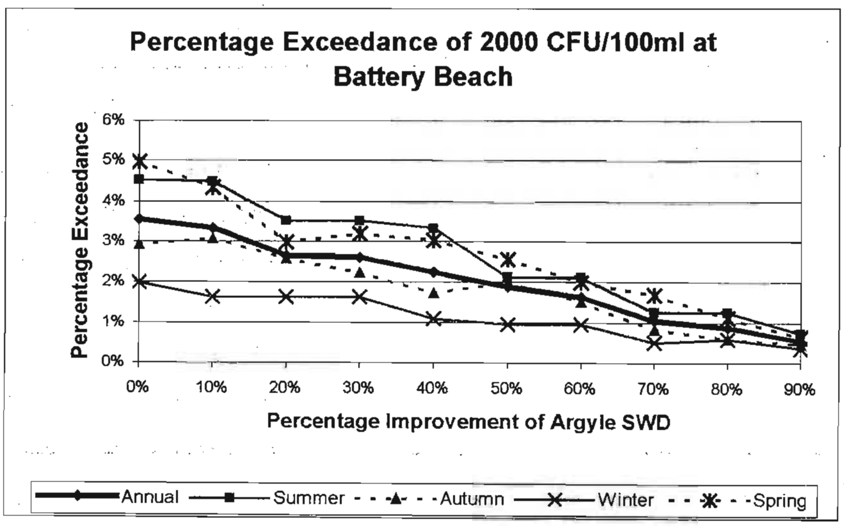

Figure 6-1: Model results for the general improvements scheme at Battery Beach (Percentage Exceedance of 2000 CFU/100ml)

The 100 CFU/100ml exceedance percentages are shown in Figure 6-2. The model predicts that currently Battery beach fails the SA WQ guideline maximum exceedance of 20% annually and for all seasons, except winter.

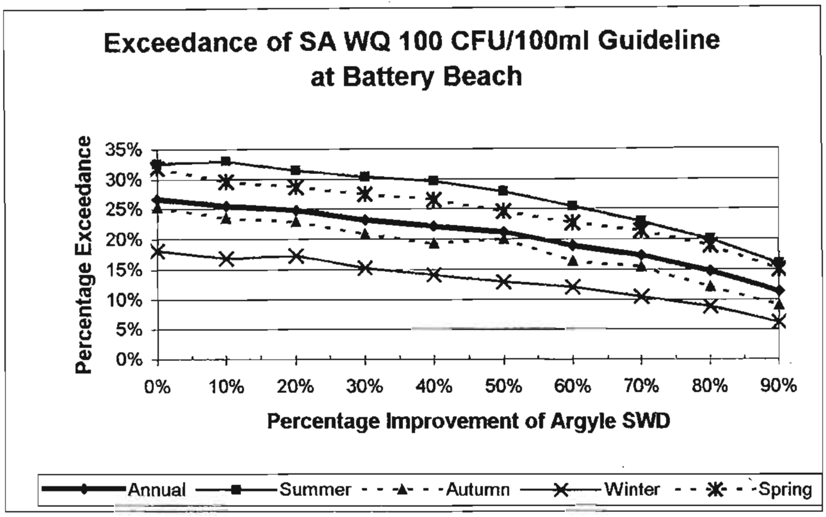

Figure 6-2: Model results for the general improvements scheme at Battery Beach (Percentage Exceedance of 100 CFU/100ml)

The pathogenic content of Argyle SWD needs an improvement of 55% for Battery Beach to pass the SA WQ Guidelines. However, the seasonal adherence of the guidelines is of more concern. The summer season is the major bathing season and an improvement of approximately 80% is required. An improvement of 80% would satisfy both SA WQ Guidelines, for all other seasons.

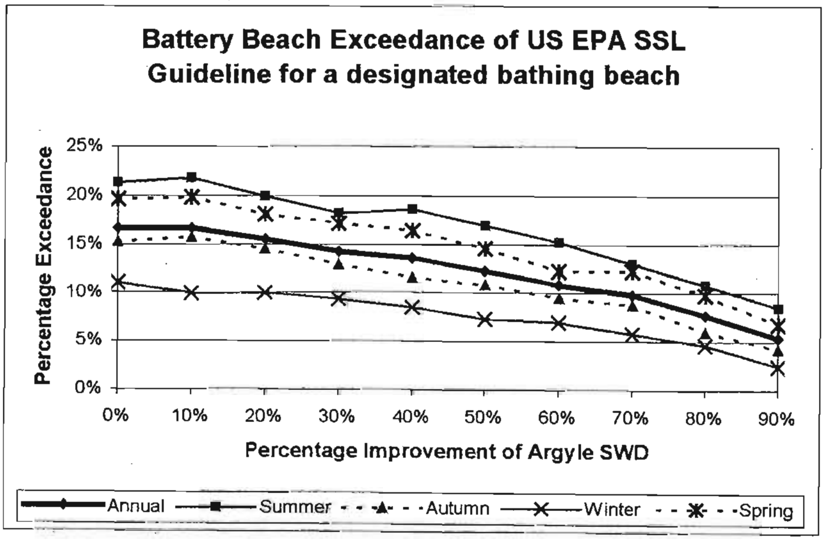

Figure 6-3: General scheme percentage exceedance of the US EPA SSL for a designated bathing beach

If the pathogenic content of Argyle SWD were improved by 80% then Battery beach may be used as a designated full-contact bathing beach for 89% of the summer season, as indicated in

Figure 6-3, and for more than 90% of the other seasons. Battery beach would satisfy the US EPA single sample limit for a designated bathing beach.

An 80% improvement would improve the US EPA 30-day geometric mean guideline as indicated in Figure 6-4. For summer, there is only 2% likelihood that the geometric mean would exceed the US EPA limit and less than 1% for other seasons.

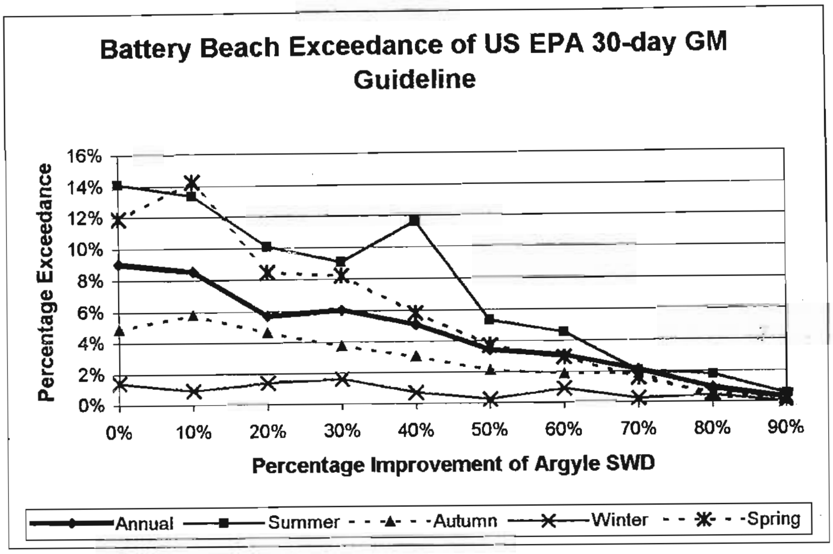

Figure 6-4: General scheme percentage exceedance of the US EPA 30-day GM guideline

6.4.2.3 Discussion of the General Improvement Scheme Results

The CWQM predicts that an 80% improvement of the pathogenic content (as indicated by E.coli) of Argyle stormwater drain is required for Battery Beach to satisfy water quality guidelines. The impact of this scheme on other beaches (for example if the pollution is redirected to other stormwater drains) was not analysed.

6.4.3 The Constructed Wetland Scheme

The constructed wetland scheme involved the improvement of the Argyle stormwater drain pollution using a constructed wetland.

6.4.3.1 Constructed Wetland Scheme Method

The treatment and physical processes of a constructed wetland are discussed in Appendix G. A hydraulic residence time (HRT) of 5 days was used for analysis.

The pollution content of the outflow from the wetland is by and large the pollution content of the wetland and not greatly effected by the individual pollution content of the inflow into the wetland. Simulations using the CWQM were therefore done using the mean concentration determined from the lognormal E.coli distribution of specific stormwater drains. The new mean for each of the percentage improvements was calculated using equation (6-2) and are given in Table 6-6:

$$\mu_{New} = e^{\mu'_{New} + \frac{1}{2}\sigma'^2} \qquad (6\text{-}2)$$

where: σ' is the lognormal standard deviation of the true SWD distribution

μ'_{New} is the lognormal mean of the improved SWD distribution, Equation (6-2).

Percentage Improvement	Mean Output Conc. (CFU/100ml)
0%	108009
10%	44802
20%	18584
30%	7709
40%	3198
50%	1326
60%	550
70%	228
80%	95
90%	39
95%	25

Table 6-6: Percentage improvement and mean Argyle wetland output concentrations used for CWQM analysis

6.4.3.2 Results of the Constructed Wetland Scheme

The results of the SA WQ guideline with respect to 2000 CFU/100ml exceedance is shown in Figure 6-5. A percentage improvement in the mean E.coli concentration from the wetland of 15 percent may adequately satisfy the guideline for all seasons.

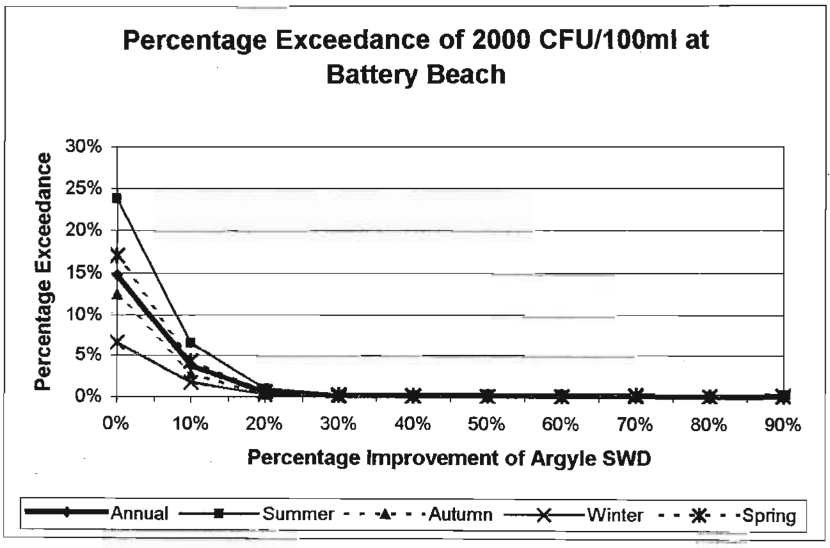

Figure 6-5: Model results for wetland scheme at Battery Beach (Percentage exceedance of 2000 CFU/100ml)

To satisfy the SA WQ guideline with respect to 100 CFU/100ml exceedance a percentage improvement of approximately 45 percent may be adequate for the summer season. This improvement should be more than adequate for the other seasons as shown in Figure 6-6.

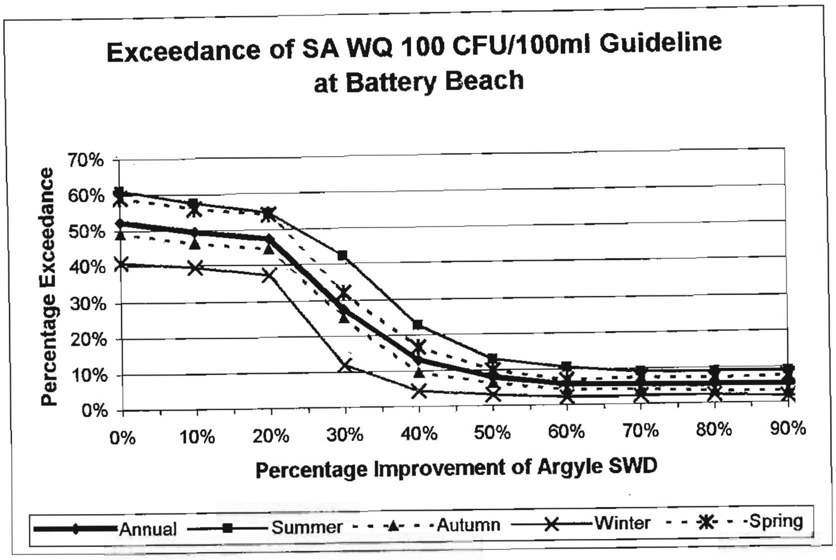

Figure 6-6: Model results for wetland scheme at Battery Beach (Percentage exceedance of 100 CFU/100ml)

If the wetland was effective in improving the stormwater by 45 percent or more the CWQM suggests that the exceedance of the US EPA SSL for a designated beach should only be approximately 5 percent, as shown in Figure 6-7.

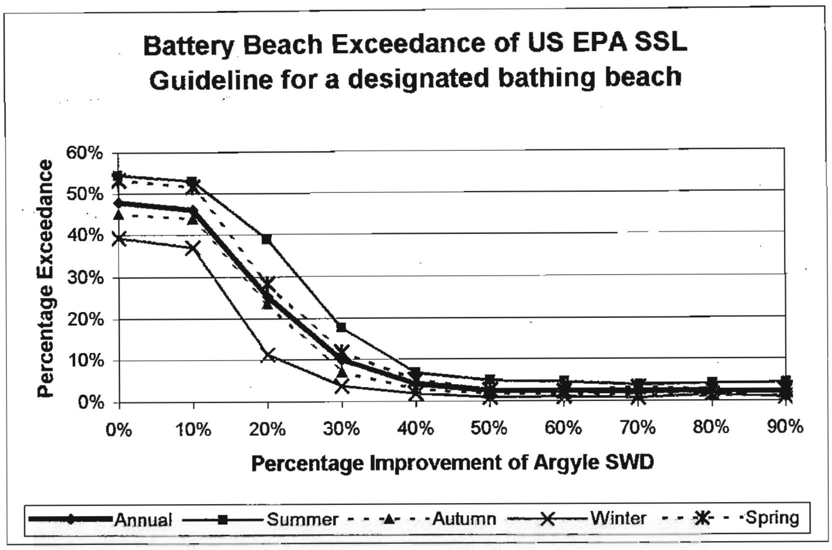

Figure 6-7: Model results for wetland scheme percentage exceedance of the US EPA SSL for a designated bathing beach

The reason for the US EPA SSL exceedance at Battery Beach never being less than approximately 5 percent is most likely caused by pathogenic pollution from other sources, such as the Walter Gilbert and Somtseu stormwater drains or even the Umgeni River.

The exceedance of the US EPA 30-day geometric mean limit at Battery Beach for each of the percentage improvement for the Argyle stormwater drain is shown in Figure 6-8. The CWQM indicated that an improvement of 45 percent would mean that the geometric mean of 126 CFU/100ml is never exceeded.

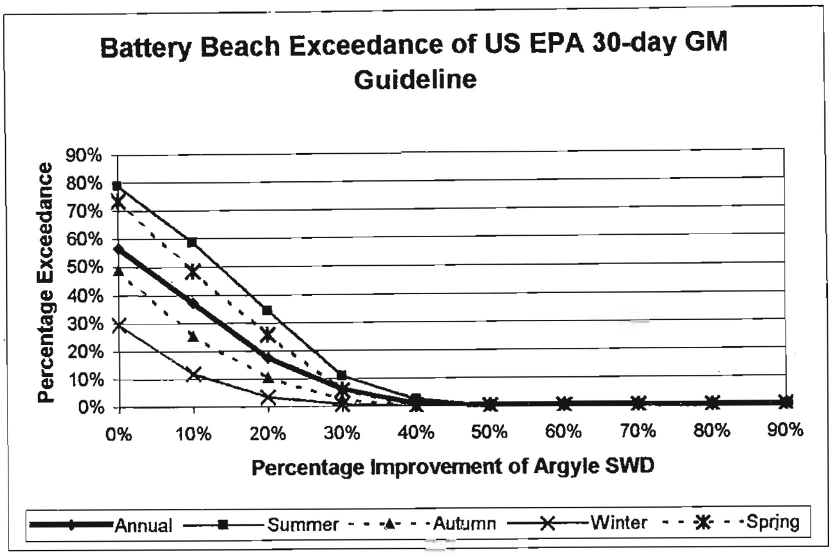

Figure 6-8: Model results for wetland scheme percentage exceedance of the US EPA 30-day GM guideline

6.4.3.3 Discussion of the Constructed Wetland Scheme Results

Constructed wetlands should be able to improve the pathogenic indicator concentrations by more than 90 percent for E.coli (Appendix E). However, the background concentration levels influence the effectiveness of the wetlands. The wetland will not be able to improve the stormwater lower than the background level of the wetland.

Typical wetland background levels for faecal coliforms are given as around 50 to 500 CFU/100ml (Appendix E) Comparing this against Table 6-6, the treatment efficiency should then range from approximately 60 to 85 percent. This is greater than the minimum percentage improvement of 45 percent required.

Another concern is that the CWQM used mean levels for the outflow from the wetland, when large inputs could conceivably increase the output concentrations temporarily. However flows of greater than the 1 or 2 year designed storm would usually be designed to bypass the wetland (Melbourne Water, 2002). Therefore, the volume of the wetland should be designed so that any flow of lesser volume with significant pathogenic pollution content should not significantly affect the outflow concentration. The fact that the wetland need only be approximately 45 percent efficient should provide a significant buffer if the outflow concentration was influenced.

6.4.4 Improvements of Surrounding Beaches due to Argyle Wetland

If the Argyle effluent was improved by only 50 percent using a constructed wetland, the improvement in water quality of the surrounding beaches, projected by the CWQM, are given in Table 6-7, Table 6-8 and Table 6-9. These may be compared against the present conditions predicted by the CWQM in Section 6.4.1.

Season	SA WQ Guidelines		US EPA Guidelines	
	2000 CFU/100ml	100 CFU/100ml	SSL - Full Bathing	30-day GME
Annual	0.06%	5.73%	2.36%	0.12%
Summer	0.05%	9.79%	3.96%	0.00%
Autumn	0.05%	5.03%	2.31%	0.00%
Winter	0.00%	2.85%	1.09%	0.00%
Spring	0.16%	5.44%	2.15%	0.00%

Table 6-7: CWQM predicted WQ improvements at North Beach (Exceedance percentages using SA WQ and US EPA Guidelines)

Season	SA WQ Guidelines		US EPA Guidelines	
	2000 CFU/100ml	100 CFU/100ml	SSL - Full Bathing	30-day GME
Annual	0.10%	7.65%	2.60%	0.18%
Summer	0.19%	11.34%	4.58%	0.00%
Autumn	0.05%	7.25%	2.17%	0.00%
Winter	0.00%	5.16%	1.22%	0.00%
Spring	0.16%	7.01%	2.51%	0.00%

Table 6-8: CWQM predicted WQ improvements at Plenty Beach (Exceedance percentages using SA WQ and US EPA Guidelines)

Season	SA WQ Guidelines		US EPA Guidelines	
	2000 CFU/100ml	100 CFU/100ml	SSL - Full Bathing	30-day GME
Annual	0.67%	16.67%	8.32%	1.19%
Summer	1.06%	25.33%	12.54%	3.03%
Autumn	0.36%	11.96%	5.53%	0.46%
Winter	0.50%	6.75%	3.22%	0.00%
Spring	0.78%	24.18%	12.87%	1.32%

Table 6-9: CWQM predicted WQ improvements at Laguna Beach (Exceedance percentages using SA WQ and US EPA Guidelines)

There are improvements in all the beaches to varying degrees. At North Beach the 30-day GME is improved in addition to the 100 CFU/100ml exceedance percentages. Bay of Plenty Beach now does not fail the 100 CFU/100ml guideline during summer months. At Laguna Beach, the CWQM predicts failure of SA WQ 100 CFU/100ml guideline during the summer and spring seasons, however the source of this pollution is most likely a combination of the Walter Gilbert SWD and Umgeni River.

6.5 Conclusions

The ability of the CWQM to be used as a "what-if" tool by developers and water quality managers was tested on the problem associated with Argyle Stormwater Drain and Battery Beach pollution. The improvements that might be expected by using a constructed stormwater wetland or an alternative general improvements scheme were investigated. The CWQM simulations showed that the constructed wetland scheme could produce a viable solution to the poor water quality experienced at Battery Beach. It also showed that the water quality of surrounding beaches would be improved as well.

CHAPTER 7:
SUMMARY AND CONCLUSIONS

A review of international trends in marine water quality characterization suggests that the SA water quality guidelines for marine recreational water, with respect to pathogenic pollution, should be revised. The use of Escherichia coli (E.coli) as an indicator is questionable since international research has shown that Enterococcus is a better indicator in the marine environment. New guidelines should be developed similar to those developed by the US Environmental Protection Agency, defining methods by which long-term and short-term analysis of beach water quality samples may be made.

Most of Durban's bathing beaches were found to have suitable water quality for full-contact recreation (bathing). However, beaches that are situated close to problematic stormwater drains or the Umgeni River regularly fail water quality guidelines for bathing beaches. The beach of most concern is Battery Beach, which although a designated bathing beach, is the second most polluted beach after Umgeni South Beach. Given the new tourism developments that will utilise Battery Beach, there is an urgent need to improve the water quality of this beach.

The inter-relationships that exist between beach water quality, pollution sources and environmental factors such as rainfall were quantified. The correlation coefficient was used to quantify the relationships. Accumulated rainfall and pollution indicator levels at the beaches were found to be only weakly correlated, and for most beaches statistically significant correlations were only found by accumulation of three or more days of rainfall. These weak correlations demonstrated the underlying relationship between the input of pollution from the stormwater drains and Umgeni River and the pollution that is found on the beaches. A possible reason for the low correlations was the lack of sufficient data around rainfall events. No correlation was found between successive fortnightly beach samples indicating that the timescales of the coastal processes are significantly shorter than the beach sampling interval.

The main pollution sources of the nearshore zone were identified as the six stormwater drains and the Umgeni River. The pathogenic content of these sources was analysed. Unfortunately of the two indicators only E.coli was regularly measured. It was found that the stormwater drain E.coli concentrations were approximately lognormally distributed.

A detailed analysis of Argyle stormwater and Battery Beach E.coli concentrations (Brahmin, 2001) showed that if the concentrations of the input into the nearshore zone were known then reasonable predictions of the nearshore zone can be made.

The CWQM was formulated as a state space dynamic system suitable for estimation using Kalman Filtering. Parameter estimation using the extended Kalman filter was tested using synthetic data. It was shown that the EKF was only effective for parameter estimation if the inputs to the system were accurately known.

The CWQM was fitted to the Durban Bight using a statistical estimation approach and optimal parameters were found. A dissipation timescale of 10 hours and an advection coefficient of 0.003 were obtained. The ability of the CWQM to produce realistic real-time predictions of pathogenic pollution levels was investigated. The CWQM was shown to produce accurate predictions with an acceptable error range.

The ability of the CWQM to be used as a "what-if" tool by developers and water quality managers was tested on the problem associated with Argyle Stormwater Drain and Battery Beach pollution. The improvements that might be expected by using a constructed stormwater wetland or an alternative general improvements scheme were investigated. The CWQM simulations showed that the constructed wetland scheme could produce a viable solution to the poor water quality experienced at Battery Beach. It also showed that the water quality of surrounding beaches would be improved as well.

In summary the CWQM is a viable tool that may be used to make informed decisions concerning the environment or public health.

APPENDICES

TABLE OF CONTENTS

LIST OF FIGURES

LIST OF TABLES

APPENDIX A:
NEWSPAPER ARTICLES

Water test results still not known

TONY CARNIE

DURBAN surfers have been asked to report cases of illness and sea pollution following recent reports of stomach bugs among local surfers.

The call has been made by Dr Alan Smith, director of the Surfers' Environmental Alliance. Smith said he was concerned about recent reports of stomach sickness and ear infections which he suspected were linked to pollution from stormwater outlets on the Durban beachfront.

Earlier this week, the city's wastewater management department said it would collect water samples off Durban, ahead of the world surfing championships which start in the city today.

However, the department has not released test results, despite repeated requests by Independent Newspapers.

Smith said his association was urging surfers to e-mail information on polluted sea water to begin a national database from popular surfing beaches. His address is: allan@ionet.co.za

The association is particularly concerned about stormwater discharges next to the Ocean Sport Centre at New Pier, immediately adjacent to North Beach. Smith said three concrete piers on the beachfront were fitted with stormwater outfall drains, which appeared to run continually whether it was raining or not.

"Where is this extra water coming from?" he asked.

Officials have been unable to find traces of a deadly cholera-like bacteria in Durban harbour.

The tests were conducted after the recent death of Durban angler Eric Erasmus, 55, who died in hospital after wading for sand prawns near the Bluff Yacht Club. Blood tests showed he was poisoned by Vibrio vulnificus, a bacteria closely related to cholera.

All test results were negative, Smith said, suggesting that the bacteria might have been discharged from the bilge waters of a foreign ship.

However, the angler's death had highlighted the dangers of wading barefoot in the harbour. Erasmus is believed to have contracted the fatal infection from an open leg wound.

Anglers and other bay users often toss bottles and cans into the harbour creating health risks for people who cut their feet while wading barefoot.

WARY WAVE RIDER: Surfers have been asked to be on the lookout for pollution and to report cases of illness.

Figure A-1: "Water test results still not known" (Carnie, 2002)

Beachgoers asked to help find source of beach pollution

TONY CARNIE

SURFERS and bathers at Battery Beach in Durban have been asked to help officials track down the source of recent sea pollution from stormwater drains.

Metro wastewater director Frank Stevens was reacting yesterday to a formal complaint by a regular bodyboarder at Battery Beach, Christo Haupt.

Haupt said a sign was erected several months ago warning surfers and bathers that the water could be contaminated at certain times, indicating that the city had been aware of the problem for a considerable time.

Haupt also saw large volumes of yellowish effluent with a solvent-type smell coming out of a drain last Monday and suspected that a local chemical company was dumping effluent into stormwater.

He reported this to pollution officials the following day.

Stevens said his staff had investigated Haupt's complaint but could not find the pollution source.

"Bacteriological results of the Battery Beach outfall show an improvement in quality over time, especially since August last year.

"However, the catchment area has been plagued by polluted runoff especially from informal trading areas, which resulted in the request to the city medical officer of health to erect the sign on the beach in November 2001."

Visitors could help by phoning 0800 323235 as soon as they noticed anything out of the ordinary.

Figure A-2: "Beachgoers asked to help find source of beach pollution" (Carnie, 2003)

APPENDIX B:
ANALYSIS OF DURBAN BEACHES

B.1 Vetches Beach

B.1.1 Escherichia coli Analysis Results

	Annual	Summer	Autumn	Winter	Spring
Average	28.7	31.5	27.1	33.9	22.0
Standard Deviation	57.8	46.8	47.0	84.7	38.6
95% Confidence	8.6	18.6	16.5	16.5	17.5

Table B-1: General Statistics of E. coli at Vetches Pier Beach (1995 - 2002)

	>10	>100	>200	>1000	>2000
Annual	42.77%	6.94%	1.73%	0.00%	0.00%
Summer	48.65%	8.11%	0.00%	0.00%	0.00%
Autumn	44.68%	6.38%	2.13%	0.00%	0.00%
Winter	42.55%	8.51%	4.26%	0.00%	0.00%
Spring	35.71%	4.76%	0.00%	0.00%	0.00%

Table B-2: Percentage Exceedance of E. coli at Vetches Pier Beach (1995 - 2002)

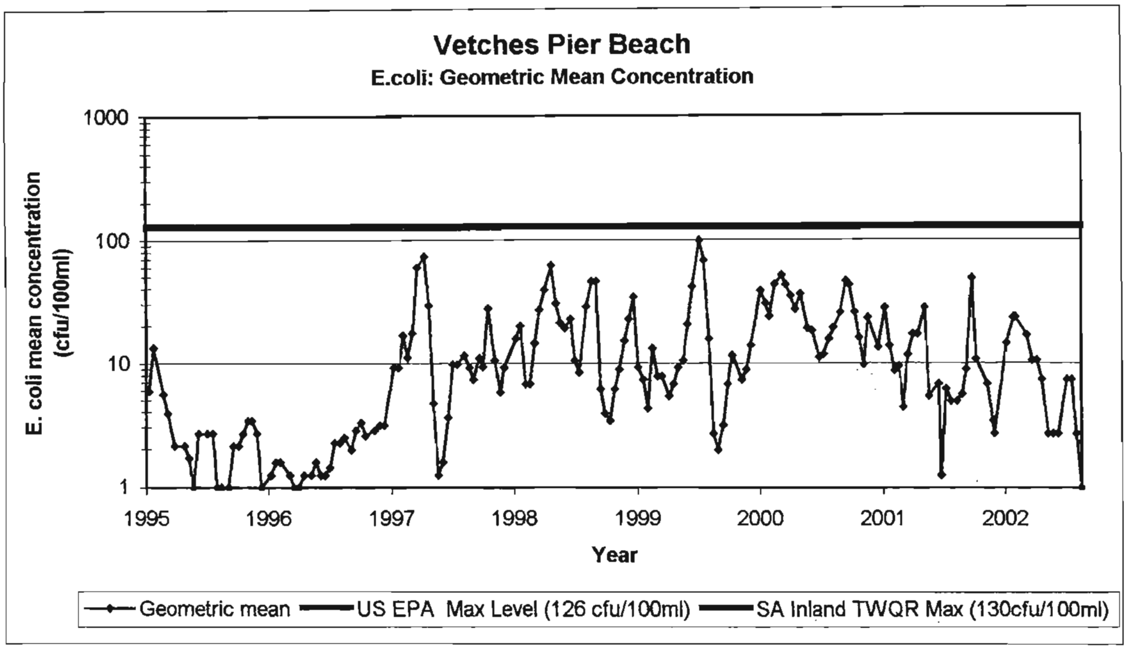

Figure B-1: Geometric means of E.coli concentrations at Vetches Pier Beach

Beach Status	Jan	Feb	Mar	Apr	May	Jun	Jul	Aug	Sep	Oct	Nov	Dec
Beach Open	94%	100%	100%	93%	100%	100%	88%	80%	94%	100%	100%	100%
Beach Closure	6%	0%	0%	7%	0%	0%	12%	20%	6%	0%	0%	0%

Table B-3: Beach status according to US EPA max mean conc. at Vetches Pier Beach

Beach Use	Jan	Feb	Mar	Apr	May	Jun	Jul	Aug	Sep	Oct	Nov	Dec
Full Bathing	100%	100%	94%	100%	100%	100%	94%	93%	100%	100%	100%	100%
Moderated use	0%	0%	6%	0%	0%	0%	0%	0%	0%	0%	0%	0%
Light use	0%	0%	0%	0%	0%	0%	6%	7%	0%	0%	0%	0%
Infrequent use	0%	0%	0%	0%	0%	0%	0%	0%	0%	0%	0%	0%
Beach Closure	0%	0%	0%	0%	0%	0%	0%	0%	0%	0%	0%	0%

Table B-4: Beach use according to US EPA single sample limits at Vetches Pier Beach

Indicator	Escherichia coli		Enterococcus
Start Date	Jan-1995	Mar-1999	Mar-1999
End Date	Aug-2002	Aug-2002	Aug-2002
Failure w.r.t. US EPA Criteria	0.0%	0.0%	6.4%
Failure w.r.t. SA Inland Criteria	0.0%	0.0%	11.5%

Table B-5: Results of the Geometric Mean Analysis at Vetches Pier Beach

B.1.2 Enterococcus Analysis Results

	Annual	Summer	Autumn	Winter	Spring
Average	41.4	62.9	24.2	20.8	79.4
Standard Deviation	107.9	90.8	50.4	73.8	193.0
95% Confidence	23.9	56.5	43.2	43.2	52.9

Table B-6: General Statistics of Enterococcus at Vetches Pier Beach (1999 – 2002)

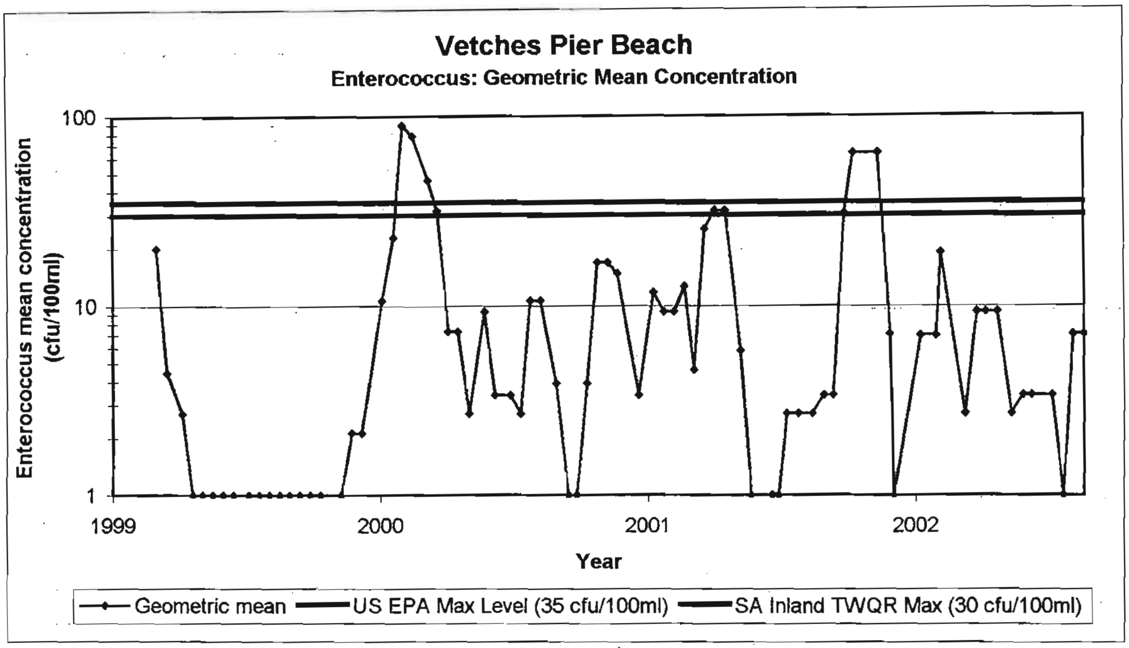

Figure B-2: Geometric means of Enterococcus concentrations at Vetches Pier Beach

Beach Status	Jan	Feb	Mar	Apr	May	Jun	Jul	Aug	Sep	Oct	Nov	Dec
Beach Open	100%	60%	88%	100%	100%	100%	100%	100%	100%	75%	83%	100%
Beach Closure	0%	40%	13%	0%	0%	0%	0%	0%	0%	25%	17%	0%

Table B-7: Beach status according to US EPA max mean conc. at Vetches Pier Beach

Beach Use	Jan	Feb	Mar	Apr	May	Jun	Jul	Aug	Sep	Oct	Nov	Dec
Full Bathing	83%	100%	100%	100%	100%	100%	100%	89%	83%	75%	100%	100%
Moderated use	0%	0%	0%	0%	0%	0%	0%	0%	0%	0%	0%	0%
Light use	17%	0%	0%	0%	0%	0%	0%	11%	0%	25%	0%	0%
Infrequent use	0%	0%	0%	0%	0%	0%	0%	0%	0%	0%	0%	0%
Beach Closure	0%	0%	0%	0%	0%	0%	0%	0%	17%	0%	0%	0%

Table B-8: Beach use according to US EPA single sample limits at Vetches Pier Beach

B.2 Addington Beach

B.2.1 Escherichia coli Analysis Results

	Annual	Summer	Autumn	Winter	Spring
Average	46.7	29.9	22.9	101.4	27.4
Standard Deviation	286.8	46.6	39.3	547.0	40.9
95% Confidence	42.3	93.7	80.3	81.1	84.8

Table B-9: General Statistics of E. coli at Addington Beach (1995 - 2002)

	>10	>100	>200	>1000	>2000
Annual	42.37%	6.21%	1.69%	0.56%	0.56%
Summer	47.22%	11.11%	0.00%	0.00%	0.00%
Autumn	42.86%	2.04%	2.04%	0.00%	0.00%
Winter	35.42%	6.25%	4.17%	2.08%	2.08%
Spring	45.45%	6.82%	0.00%	0.00%	0.00%

Table B-10: Percentage Exceedance of E. coli at Addington Beach (1995 - 2002)

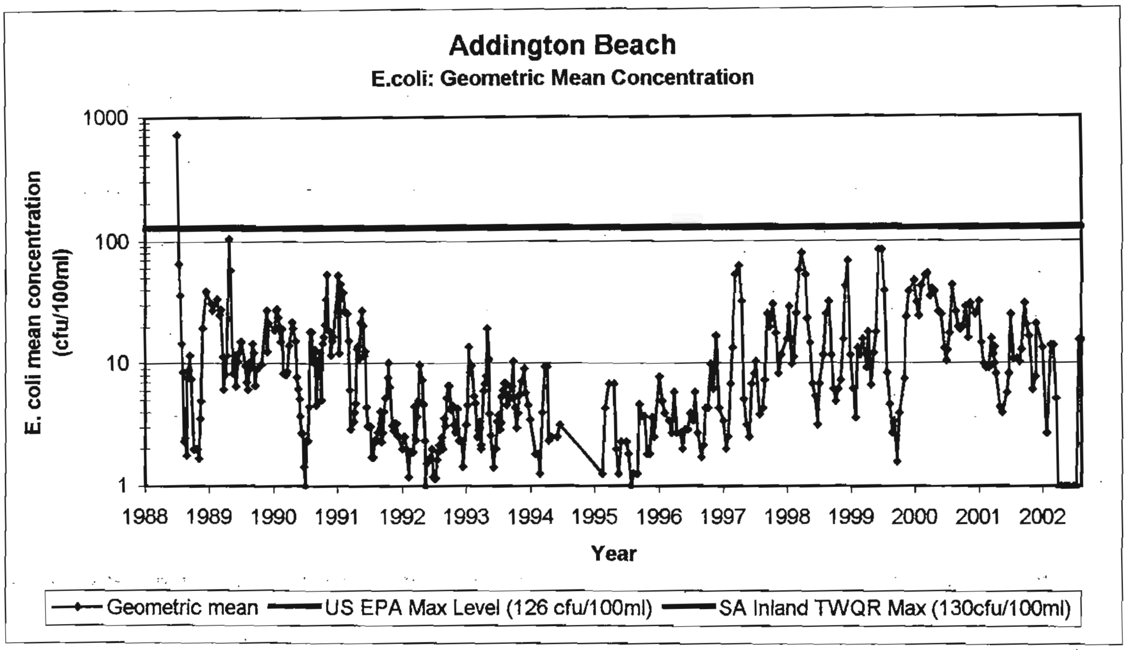

Figure B-3: Geometric means of E.coli concentrations at Addington Beach

Beach Status	Jan	Feb	Mar	Apr	May	Jun	Jul	Aug	Sep	Oct	Nov	Dec
Beach Open	100%	100%	100%	100%	100%	100%	100%	100%	100%	100%	100%	100%
Beach Closure	0%	0%	0%	0%	0%	0%	0%	0%	0%	0%	0%	0%

Table B-11: Beach status according to US EPA max mean conc. at Addington Beach

Beach Use	Jan	Feb	Mar	Apr	May	Jun	Jul	Aug	Sep	Oct	Nov	Dec
Full Bathing	100%	100%	94%	100%	100%	100%	100%	93%	100%	100%	100%	100%
Moderated use	0%	0%	6%	0%	0%	0%	0%	0%	0%	0%	0%	0%
Light use	0%	0%	0%	0%	0%	0%	0%	0%	0%	0%	0%	0%
Infrequent use	0%	0%	0%	0%	0%	0%	0%	0%	0%	0%	0%	0%
Beach Closure	0%	0%	0%	0%	0%	0%	0%	7%	0%	0%	0%	0%

Table B-12: Beach use according to US EPA single sample limits at Addington Beach

Indicator	Escherichia coli		Enterococcus
Start Date	Jan-1995	Mar-1999	Mar-1999
End Date	Aug-2002	Aug-2002	Aug-2002
Failure w.r.t. US EPA Criteria	0.2%	0.0%	4.9%
Failure w.r.t. SA Inland Criteria	0.2%	0.0%	4.9%

Table B-13: Results of the Geometric Mean Analysis at Addington Beach

B.2.2 Enterococcus Analysis Results

	Annual	Summer	Autumn	Winter	Spring
Average	29.5	40.0	16.2	20.9	52.9
Standard Deviation	86.9	68.0	28.3	49.5	168.4
95% Confidence	18.8	44.0	33.4	34.8	41.3

Table B-14: General Statistics of Enterococcus at Addington Beach (1999 – 2002)

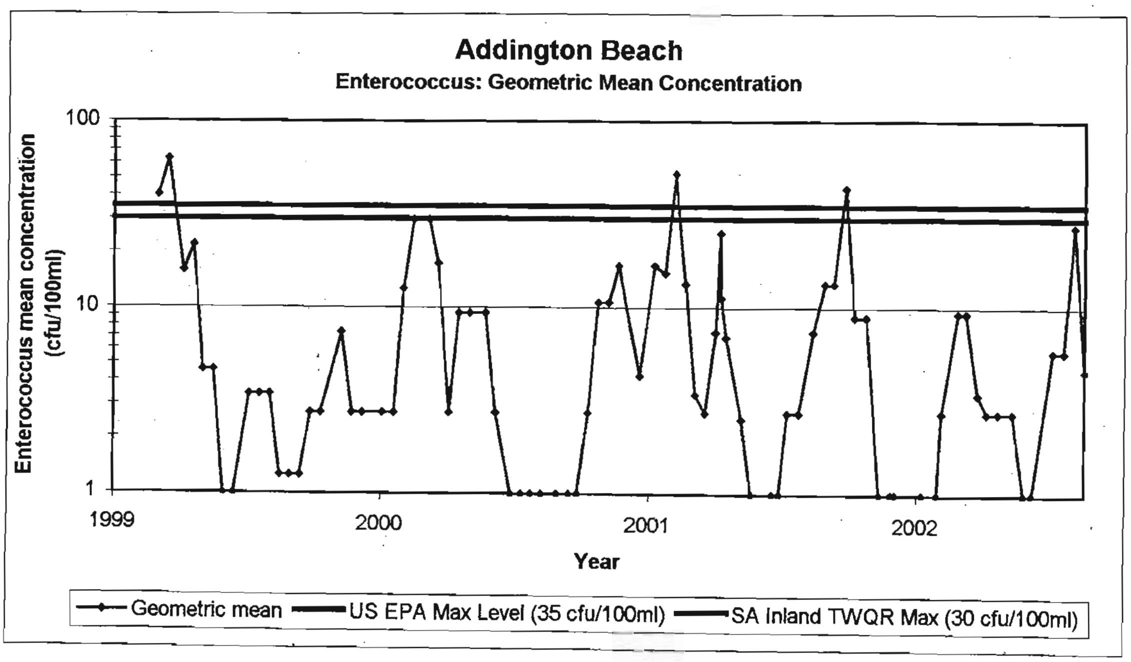

Figure B-4: Geometric means of Enterococcus concentrations at Addington Beach

Beach Status	Jan	Feb	Mar	Apr	May	Jun	Jul	Aug	Sep	Oct	Nov	Dec
Beach Open	100%	83%	75%	100%	100%	100%	100%	100%	83%	100%	100%	100%
Beach Closure	0%	17%	25%	0%	0%	0%	0%	0%	17%	0%	0%	0%

Table B-15: Beach status according to US EPA max mean conc. at Addington Beach

Beach Use	Jan	Feb	Mar	Apr	May	Jun	Jul	Aug	Sep	Oct	Nov	Dec
Full Bathing	100%	83%	100%	100%	100%	100%	100%	100%	83%	100%	100%	100%
Moderated use	0%	17%	0%	0%	0%	0%	0%	0%	0%	0%	0%	0%
Light use	0%	0%	0%	0%	0%	0%	0%	0%	0%	0%	0%	0%
Infrequent use	0%	0%	0%	0%	0%	0%	0%	0%	0%	0%	0%	0%
Beach Closure	0%	0%	0%	0%	0%	0%	0%	0%	17%	0%	0%	0%

Table B-16: Beach use according to US EPA single sample limits at Addington Beach

B.3 South Beach

B.3.1 Escherichia coli Analysis Results

	Annual	Summer	Autumn	Winter	Spring
Average	27.6	34.7	26.3	27.1	23.1
Standard Deviation	42.2	43.9	38.4	51.1	33.8
95% Confidence	6.2	13.2	11.8	11.9	12.5

Table B-17: General Statistics of E. coli at South Beach (1995 - 2002)

	>10	>100	>200	>1000	>2000
Annual	48.89%	5.56%	0.56%	0.00%	0.00%
Summer	58.97%	7.69%	0.00%	0.00%	0.00%
Autumn	48.98%	4.08%	0.00%	0.00%	0.00%
Winter	39.58%	8.33%	2.08%	0.00%	0.00%
Spring	50.00%	2.27%	0.00%	0.00%	0.00%

Table B-18: Percentage Exceedance of E. coli at South Beach (1995 - 2002)

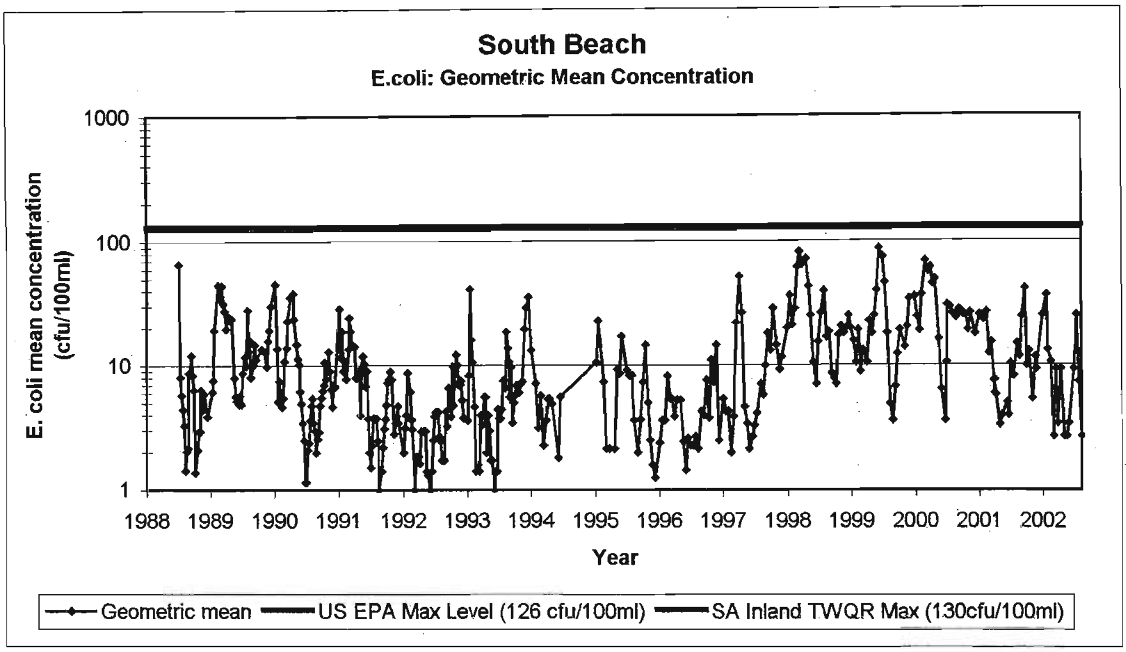

Figure B-5: Geometric means of E.coli concentrations at South Beach

Beach Status	Jan	Feb	Mar	Apr	May	Jun	Jul	Aug	Sep	Oct	Nov	Dec
Beach Open	100%	100%	100%	100%	100%	100%	100%	100%	100%	100%	100%	100%
Beach Closure	0%	0%	0%	0%	0%	0%	0%	0%	0%	0%	0%	0%

Table B-19: Beach status according to US EPA max mean conc. at South Beach

Beach Use	Jan	Feb	Mar	Apr	May	Jun	Jul	Aug	Sep	Oct	Nov	Dec
Full Bathing	100%	100%	100%	100%	100%	100%	94%	100%	100%	100%	100%	100%
Moderated use	0%	0%	0%	0%	0%	0%	6%	0%	0%	0%	0%	0%
Light use	0%	0%	0%	0%	0%	0%	0%	0%	0%	0%	0%	0%
Infrequent use	0%	0%	0%	0%	0%	0%	0%	0%	0%	0%	0%	0%
Beach Closure	0%	0%	0%	0%	0%	0%	0%	0%	0%	0%	0%	0%

Table B-20: Beach use according to US EPA single sample limits at South Beach

Indicator	Escherichia coli		Enterococcus
Start Date	Jan-1995	Mar-1999	Mar-1999
End Date	Aug-2002	Aug-2002	Aug-2002
Failure w.r.t. US EPA Criteria	0.0%	0.0%	6.1%
Failure w.r.t. SA Inland Criteria	0.0%	0.0%	6.1%

Table B-21: Results of the Geometric Mean Analysis at South Beach

B.3.2 Enterococcus Analysis Results

	Annual	Summer	Autumn	Winter	Spring
Average	27.4	41.3	24.7	24.2	23.6
Standard Deviation	50.8	46.3	61.3	44.9	47.0
95% Confidence	11.0	25.7	19.5	20.3	24.1

Table B-22: General Statistics of Enterococcus at South Beach (1999 – 2002)

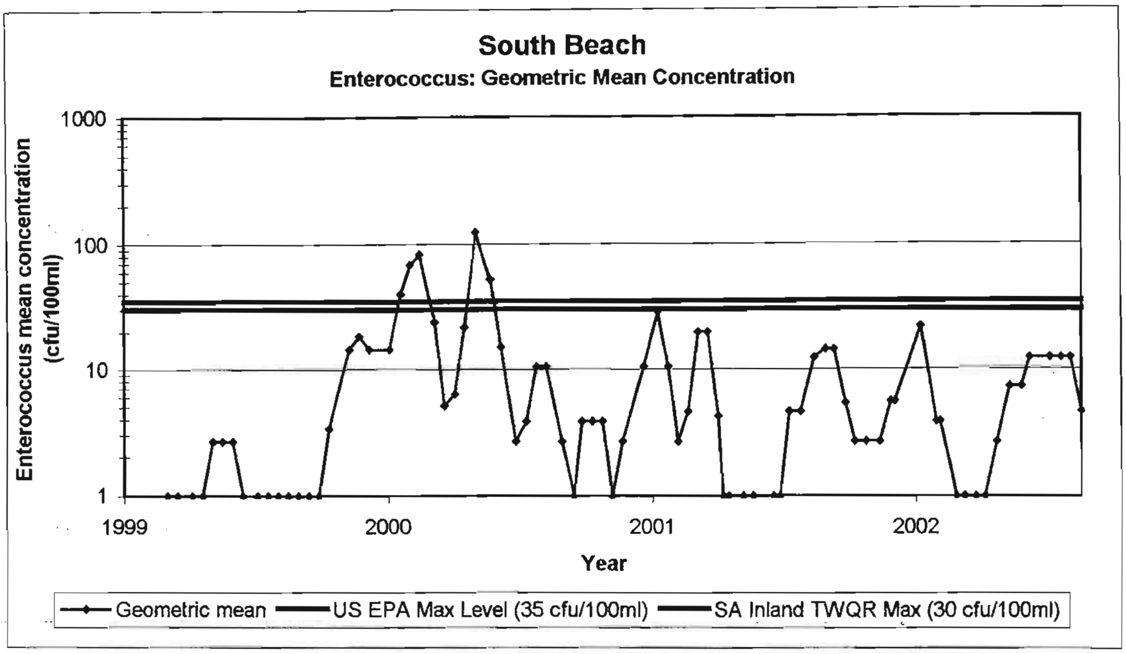

Figure B-6: Geometric means of Enterococcus concentrations at South Beach

Beach Status	Jan	Feb	Mar	Apr	May	Jun	Jul	Aug	Sep	Oct	Nov	Dec
Beach Open	83%	67%	100%	100%	75%	100%	100%	100%	100%	100%	100%	100%
Beach Closure	17%	33%	0%	0%	25%	0%	0%	0%	0%	0%	0%	0%

Table B-23: Beach status according to US EPA max mean conc. at South Beach

Beach Use	Jan	Feb	Mar	Apr	May	Jun	Jul	Aug	Sep	Oct	Nov	Dec
Full Bathing	100%	100%	100%	90%	100%	100%	100%	100%	100%	100%	100%	100%
Moderated use	0%	0%	0%	10%	0%	0%	0%	0%	0%	0%	0%	0%
Light use	0%	0%	0%	0%	0%	0%	0%	0%	0%	0%	0%	0%
Infrequent use	0%	0%	0%	0%	0%	0%	0%	0%	0%	0%	0%	0%
Beach Closure	0%	0%	0%	0%	0%	0%	0%	0%	0%	0%	0%	0%

Table B-24: Beach use according to US EPA single sample limits at South Beach

B.4 Wedge Beach

B.4.1 Escherichia coli Analysis Results

	Annual	Summer	Autumn	Winter	Spring
Average	34.2	22.4	12.6	59.5	37.4
Standard Deviation	76.8	17.5	26.5	129.5	55.1
95% Confidence	20.9	47.6	40.2	38.9	41.8

Table B-25: General Statistics of E. coli at Wedge Beach (2000 - 2002)

	>10	>100	>200	>1000	>2000
Annual	44.23%	7.69%	3.85%	0.00%	0.00%
Summer	70.00%	0.00%	0.00%	0.00%	0.00%
Autumn	21.43%	0.00%	0.00%	0.00%	0.00%
Winter	40.00%	13.33%	13.33%	0.00%	0.00%
Spring	53.85%	15.38%	0.00%	0.00%	0.00%

Table B-26: Percentage Exceedance of E. coli at Wedge Beach (2000 - 2002)

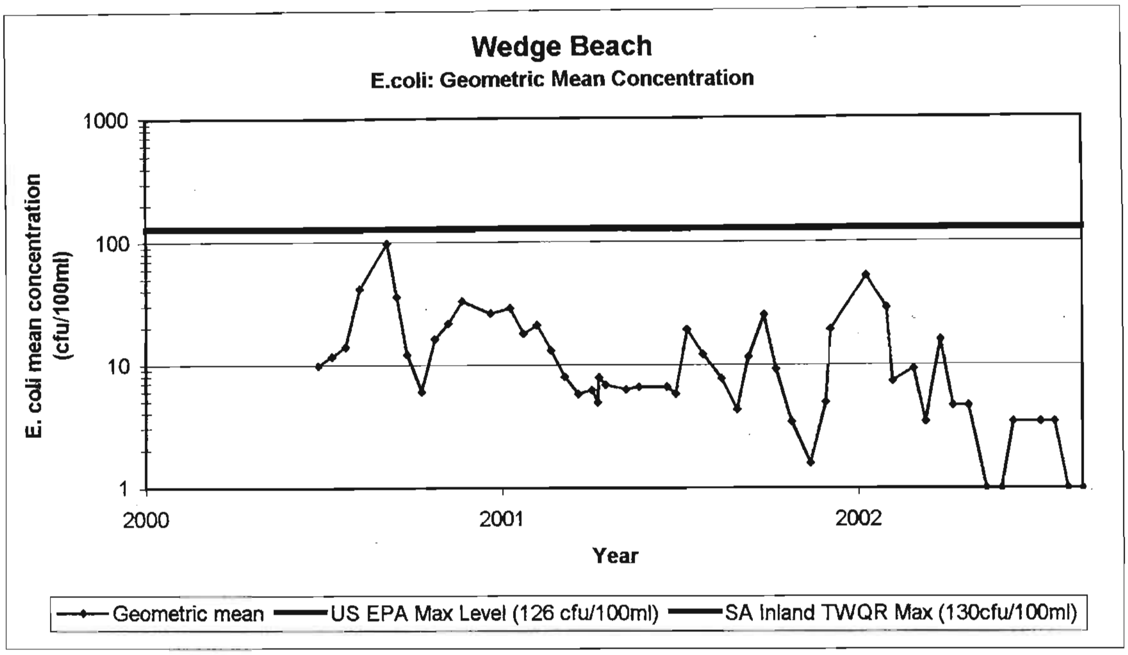

Figure B-7: Geometric means of E.coli concentrations at Wedge Beach

Beach Status	Jan	Feb	Mar	Apr	May	Jun	Jul	Aug	Sep	Oct	Nov	Dec
Beach Open	100%	100%	100%	100%	100%	100%	100%	100%	100%	100%	100%	100%
Beach Closure	0%	0%	0%	0%	0%	0%	0%	0%	0%	0%	0%	0%

Table B-27: Beach status according to US EPA max mean conc. at Wedge Beach

Beach Use	Jan	Feb	Mar	Apr	May	Jun	Jul	Aug	Sep	Oct	Nov	Dec
Full Bathing	100%	100%	100%	100%	100%	100%	83%	80%	100%	100%	100%	100%
Moderated use	0%	0%	0%	0%	0%	0%	0%	20%	0%	0%	0%	0%
Light use	0%	0%	0%	0%	0%	0%	0%	0%	0%	0%	0%	0%
Infrequent use	0%	0%	0%	0%	0%	0%	17%	0%	0%	0%	0%	0%
Beach Closure	0%	0%	0%	0%	0%	0%	0%	0%	0%	0%	0%	0%

Table B-28: Beach use according to US EPA single sample limits at Wedge Beach

Indicator	Escherichia coli		Enterococcus
Start Date	Jan-1995	Mar-1999	Mar-1999
End Date	Aug-2002	Aug-2002	Aug-2002
Failure w.r.t. US EPA Criteria	0.0%	0.0%	9.6%
Failure w.r.t. SA Inland Criteria	0.0%	0.0%	11.5%

Table B-29: Results of the Geometric Mean Analysis at Wedge Beach

B.4.2 Enterococcus Analysis Results

	Annual	Summer	Autumn	Winter	Spring
Average	27.3	14.0	24.3	34.7	32.3
Standard Deviation	35.0	25.0	26.2	42.4	40.4
95% Confidence	9.5	21.7	18.3	17.7	19.0

Table B-30: General Statistics of Enterococcus at Wedge Beach (1999 – 2002)

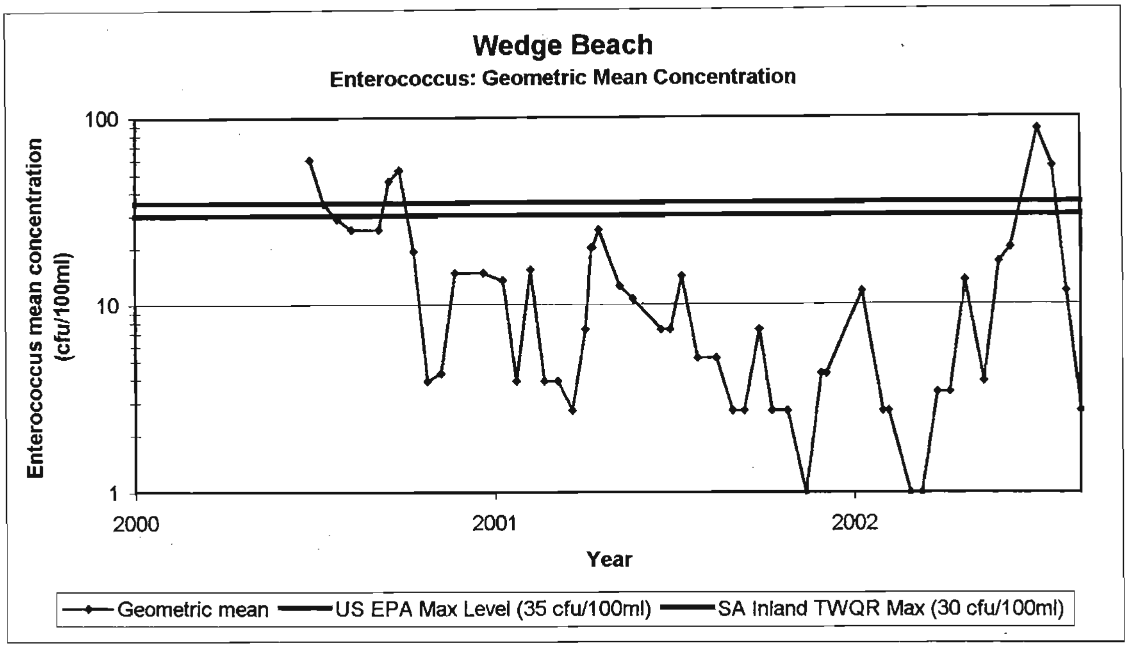

Figure B-8: Geometric means of Enterococcus concentrations at Wedge Beach

Beach Status	Jan	Feb	Mar	Apr	May	Jun	Jul	Aug	Sep	Oct	Nov	Dec
Beach Open	100%	100%	100%	100%	100%	75%	67%	100%	60%	100%	100%	100%
Beach Closure	0%	0%	0%	0%	0%	25%	33%	0%	40%	0%	0%	0%

Table B-31: Beach status according to US EPA max mean conc. at Wedge Beach

Beach Use	Jan	Feb	Mar	Apr	May	Jun	Jul	Aug	Sep	Oct	Nov	Dec
Full Bathing	100%	100%	100%	100%	100%	100%	100%	100%	100%	100%	100%	100%
Moderated use	0%	0%	0%	0%	0%	0%	0%	0%	0%	0%	0%	0%
Light use	0%	0%	0%	0%	0%	0%	0%	0%	0%	0%	0%	0%
Infrequent use	0%	0%	0%	0%	0%	0%	0%	0%	0%	0%	0%	0%
Beach Closure	0%	0%	0%	0%	0%	0%	0%	0%	0%	0%	0%	0%

Table B-32: Beach use according to US EPA single sample limits at Wedge Beach

B.5 North Beach

B.5.1 Escherichia coli Analysis Results

	Annual	Summer	Autumn	Winter	Spring
Average	32.4	58.6	26.5	26.3	22.5
Standard Deviation	67.0	117.0	45.2	49.1	31.2
95% Confidence	9.7	21.0	18.4	18.9	19.8

Table B-33: General Statistics of E. coli at North Beach (1995 - 2002)

	>10	>100	>200	>1000	>2000
Annual	42.86%	7.69%	2.20%	0.00%	0.00%
Summer	53.85%	17.95%	7.69%	0.00%	0.00%
Autumn	43.14%	3.92%	1.96%	0.00%	0.00%
Winter	35.42%	8.33%	0.00%	0.00%	0.00%
Spring	40.91%	2.27%	0.00%	0.00%	0.00%

Table B-34: Percentage Exceedance of E. coli at North Beach (1995 - 2002)

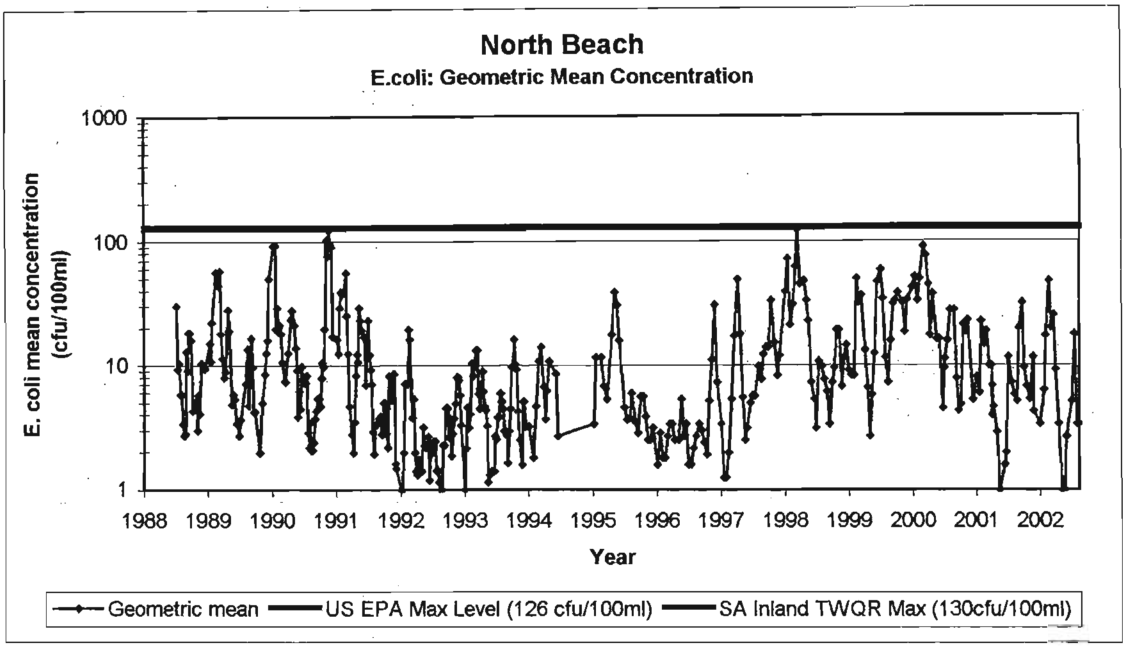

Figure B-9: Geometric means of E.coli concentrations at North Beach

Beach Status	Jan	Feb	Mar	Apr	May	Jun	Jul	Aug	Sep	Oct	Nov	Dec
Beach Open	100%	100%	100%	100%	100%	100%	100%	100%	100%	100%	100%	100%
Beach Closure	0%	0%	0%	0%	0%	0%	0%	0%	0%	0%	0%	0%

Table B-35: Beach status according to US EPA max mean conc. at North Beach

Beach Use	Jan	Feb	Mar	Apr	May	Jun	Jul	Aug	Sep	Oct	Nov	Dec
Full Bathing	94%	93%	100%	100%	94%	100%	100%	100%	100%	100%	100%	88%
Moderated use	6%	0%	0%	0%	6%	0%	0%	0%	0%	0%	0%	0%
Light use	0%	0%	0%	0%	0%	0%	0%	0%	0%	0%	0%	13%
Infrequent use	0%	0%	0%	0%	0%	0%	0%	0%	0%	0%	0%	0%
Beach Closure	0%	7%	0%	0%	0%	0%	0%	0%	0%	0%	0%	0%

Table B-36: Beach use according to US EPA single sample limits at North Beach

Indicator	Escherichia coli		Enterococcus
Start Date	Jan-1995	Mar-1999	Mar-1999
End Date	Aug-2002	Aug-2002	Aug-2002
Failure w.r.t. US EPA Criteria	0.0%	0.0%	3.6%
Failure w.r.t. SA Inland Criteria	0.0%	0.0%	3.6%

Table B-37: Results of the Geometric Mean Analysis at North Beach

B.5.2 Enterococcus Analysis Results

	Annual	Summer	Autumn	Winter	Spring
Average	20.7	61.3	12.9	12.5	9.4
Standard Deviation	39.1	70.7	21.9	19.4	17.5
95% Confidence	8.4	19.8	14.5	15.6	18.6

Table B-38: General Statistics of Enterococcus at North Beach (1999 – 2002)

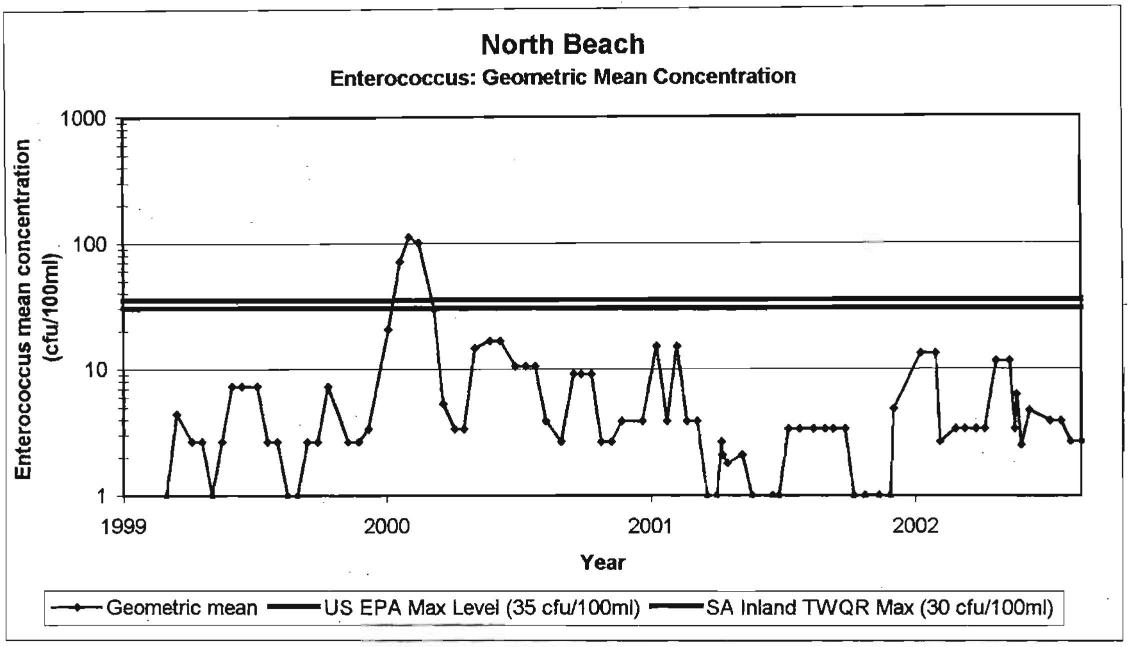

Figure B-10: Geometric means of Enterococcus concentrations at North Beach

Beach Status	Jan	Feb	Mar	Apr	May	Jun	Jul	Aug	Sep	Oct	Nov	Dec
Beach Open	83%	67%	100%	100%	100%	100%	100%	100%	100%	100%	100%	100%
Beach Closure	17%	33%	0%	0%	0%	0%	0%	0%	0%	0%	0%	0%

Table B-39: Beach status according to US EPA max mean conc. at North Beach

Beach Use	Jan	Feb	Mar	Apr	May	Jun	Jul	Aug	Sep	Oct	Nov	Dec
Full Bathing	100%	100%	100%	100%	100%	100%	100%	100%	100%	100%	100%	100%
Moderated use	0%	0%	0%	0%	0%	0%	0%	0%	0%	0%	0%	0%
Light use	0%	0%	0%	0%	0%	0%	0%	0%	0%	0%	0%	0%
Infrequent use	0%	0%	0%	0%	0%	0%	0%	0%	0%	0%	0%	0%
Beach Closure	0%	0%	0%	0%	0%	0%	0%	0%	0%	0%	0%	0%

Table B-40: Beach use according to US EPA single sample limits at North Beach

B.6 Bay of Plenty Beach

B.6.1 Escherichia coli Analysis Results

	Annual	Summer	Autumn	Winter	Spring
Average	62.9	86.4	52.3	69.1	47.7
Standard Deviation	157.1	174.0	111.8	178.4	164.9
95% Confidence	22.8	49.3	42.7	44.4	46.4

Table B-41: General Statistics of E. coli at Bay of Plenty Beach (1995 - 2002)

	>10	>100	>200	>1000	>2000
Annual	42.62%	12.57%	6.56%	0.55%	0.00%
Summer	61.54%	15.38%	10.26%	0.00%	0.00%
Autumn	34.62%	15.38%	9.62%	0.00%	0.00%
Winter	35.42%	16.67%	4.17%	0.00%	0.00%
Spring	43.18%	2.27%	2.27%	2.27%	0.00%

Table B-42: Percentage Exceedance of E. coli at Bay of Plenty Beach (1995 - 2002)

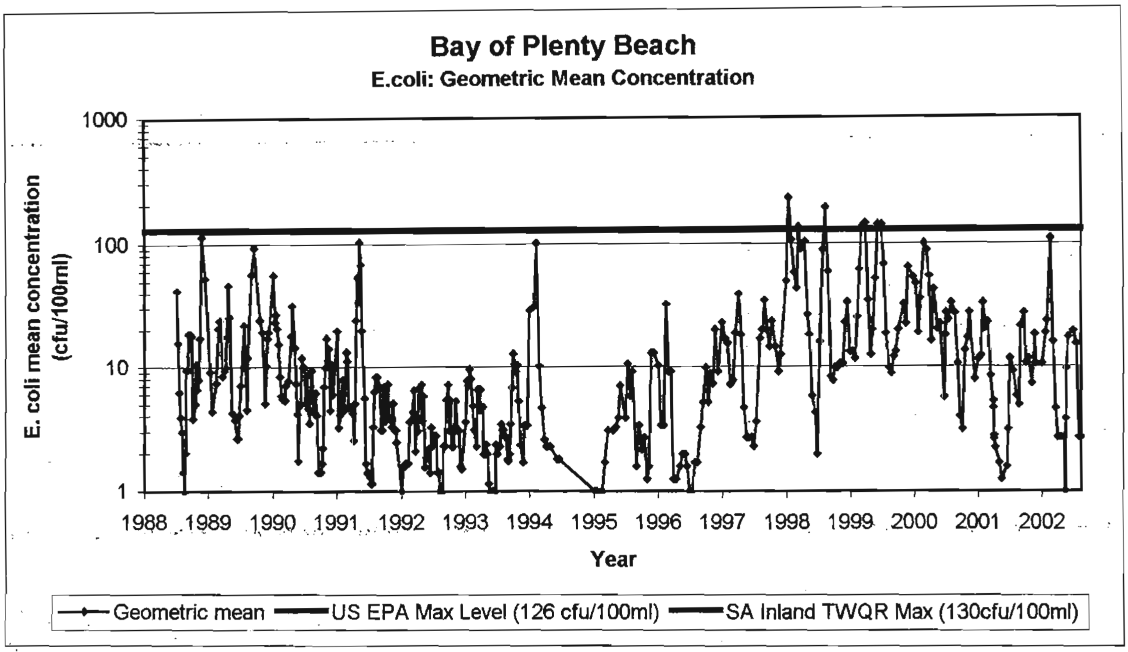

Figure B-11: Geometric means of E.coli concentrations at Bay of Plenty Beach

Beach Status	Jan	Feb	Mar	Apr	May	Jun	Jul	Aug	Sep	Oct	Nov	Dec
Beach Open	94%	100%	88%	94%	100%	93%	94%	93%	100%	100%	100%	100%
Beach Closure	6%	0%	12%	6%	0%	7%	6%	7%	0%	0%	0%	0%

Table B-43: Beach status according to US EPA max mean conc. at Bay of Plenty Beach

Beach Use	Jan	Feb	Mar	Apr	May	Jun	Jul	Aug	Sep	Oct	Nov	Dec
Full Bathing	88%	93%	88%	100%	94%	100%	94%	93%	100%	100%	93%	88%
Moderated use	0%	0%	0%	0%	0%	0%	0%	0%	0%	0%	0%	0%
Light use	6%	0%	6%	0%	6%	0%	0%	0%	0%	0%	0%	0%
Infrequent use	0%	0%	0%	0%	0%	0%	0%	0%	0%	0%	0%	13%
Beach Closure	6%	7%	6%	0%	0%	0%	6%	7%	0%	0%	7%	0%

Table B-44: Beach use according to US EPA single sample limits at Bay of Plenty Beach

Indicator	Escherichia coli		Enterococcus
Start Date	Jan-1995	Mar-1999	Mar-1999
End Date	Aug-2002	Aug-2002	Aug-2002
Failure w.r.t. US EPA Criteria	3.8%	4.7%	5.9%
Failure w.r.t. SA Inland Criteria	3.8%	4.7%	7.1%

Table B-45: Results of the Geometric Mean Analysis at Bay of Plenty Beach

B.6.2 Enterococcus Analysis Results

	Annual	Summer	Autumn	Winter	Spring
Average	22.4	44.0	17.3	18.3	17.6
Standard Deviation	42.2	72.2	37.3	24.3	31.5
95% Confidence	9.0	21.4	15.4	16.9	20.1

Table B-46: General Statistics of Enterococcus at Bay of Plenty Beach (1999 – 2002)

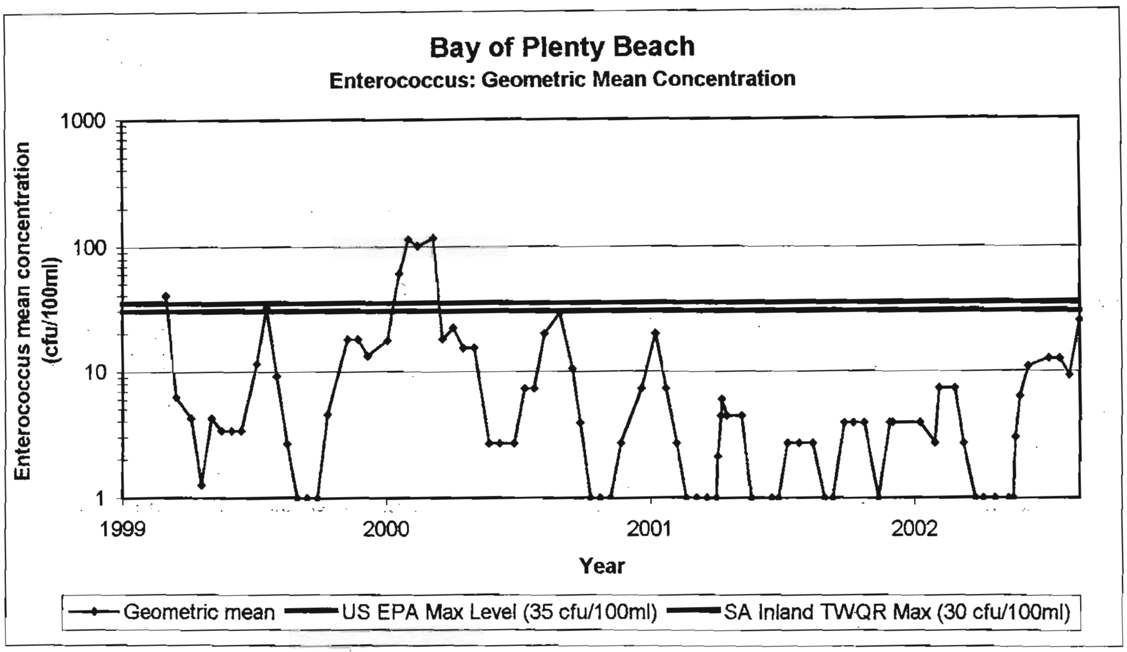

Figure B-12: Geometric means of Enterococcus concentrations at Bay of Plenty Beach

Beach Status	Jan	Feb	Mar	Apr	May	Jun	Jul	Aug	Sep	Oct	Nov	Dec
Beach Open	83%	67%	75%	100%	100%	100%	100%	100%	100%	100%	100%	100%
Beach Closure	17%	33%	25%	0%	0%	0%	0%	0%	0%	0%	0%	0%

Table B-47: Beach status according to US EPA max mean conc. at Bay of Plenty Beach

Beach Use	Jan	Feb	Mar	Apr	May	Jun	Jul	Aug	Sep	Oct	Nov	Dec
Full Bathing	100%	83%	100%	100%	100%	100%	100%	100%	100%	100%	100%	100%
Moderated use	0%	17%	0%	0%	0%	0%	0%	0%	0%	0%	0%	0%
Light use	0%	0%	0%	0%	0%	0%	0%	0%	0%	0%	0%	0%
Infrequent use	0%	0%	0%	0%	0%	0%	0%	0%	0%	0%	0%	0%
Beach Closure	0%	0%	0%	0%	0%	0%	0%	0%	0%	0%	0%	0%

Table B-48: Beach use according to US EPA single sample limits at Bay of Plenty Beach

B.7 Battery beach

B.7.1 Escherichia coli Analysis Results

	Annual	Summer	Autumn	Winter	Spring
Average	378.6	385.5	757.0	189.9	144.8
Standard Deviation	1681.9	1206.4	2972.6	293.5	222.3
95% Confidence	243.7	527.9	461.6	475.8	491.4

Table B-49: General Statistics of E. coli at Battery Beach (1995 - 2002)

	>10	>100	>200	>1000	>2000
Annual	78.69%	34.43%	24.04%	4.92%	3.28%
Summer	79.49%	28.21%	23.08%	7.69%	5.13%
Autumn	84.31%	41.18%	27.45%	9.80%	7.84%
Winter	77.08%	39.58%	22.92%	2.08%	0.00%
Spring	73.33%	26.67%	22.22%	0.00%	0.00%

Table B-50: Percentage Exceedance of E. coli at Battery Beach (1995 - 2002)

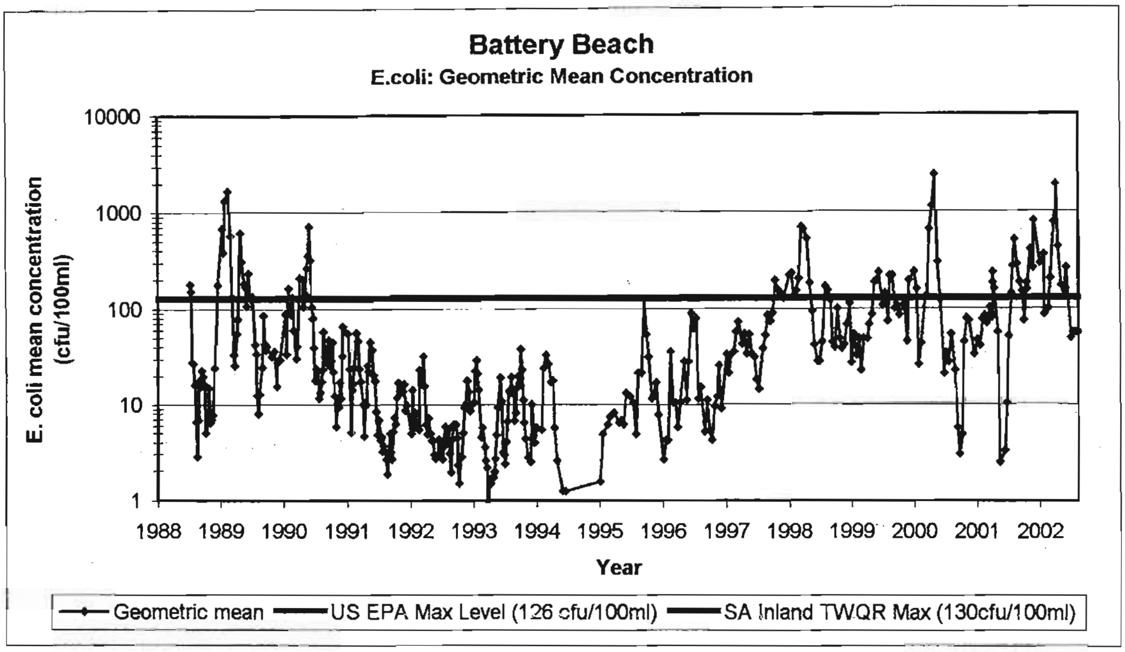

Figure B-13: Geometric means of E.coli concentrations at Battery Beach

Beach Status	Jan	Feb	Mar	Apr	May	Jun	Jul	Aug	Sep	Oct	Nov	Dec
Beach Open	63%	87%	61%	53%	63%	80%	88%	56%	88%	79%	73%	63%
Beach Closure	38%	13%	39%	47%	38%	20%	12%	44%	13%	21%	27%	38%

Table B-51: Beach status according to US EPA max mean conc. at Battery Beach

Beach Use	Jan	Feb	Mar	Apr	May	Jun	Jul	Aug	Sep	Oct	Nov	Dec
Full Bathing	81%	80%	67%	71%	81%	80%	88%	63%	88%	71%	87%	63%
Moderated use	0%	0%	0%	0%	0%	0%	0%	0%	0%	0%	0%	0%
Light use	13%	0%	6%	0%	19%	7%	0%	13%	0%	14%	7%	13%
Infrequent use	6%	7%	0%	0%	0%	0%	6%	13%	6%	0%	0%	0%
Beach Closure	0%	13%	28%	29%	0%	13%	6%	13%	6%	14%	7%	25%

Table B-52: Beach use according to US EPA single sample limits at Battery Beach

Indicator	Escherichia coli		Enterococcus
Start Date	Jan-1995	Mar-1999	Mar-1999
End Date	Aug-2002	Aug-2002	Aug-2002
Failure w.r.t. US EPA Criteria	29.0%	44.2%	33.7%
Failure w.r.t. SA Inland Criteria	27.9%	43.0%	38.4%

Table B-53: Results of the Geometric Mean Analysis at Battery Beach

B.7.2 Enterococcus Analysis Results

	Annual	Summer	Autumn	Winter	Spring
Average	358.5	178.7	856.4	60.0	148.3
Standard Deviation	2267.7	394.5	3951.0	94.0	404.7
95% Confidence	479.3	1147.6	840.0	888.9	1047.6

Table B-54: General Statistics of Enterococcus readings at Battery Beach (1999 – 2002)

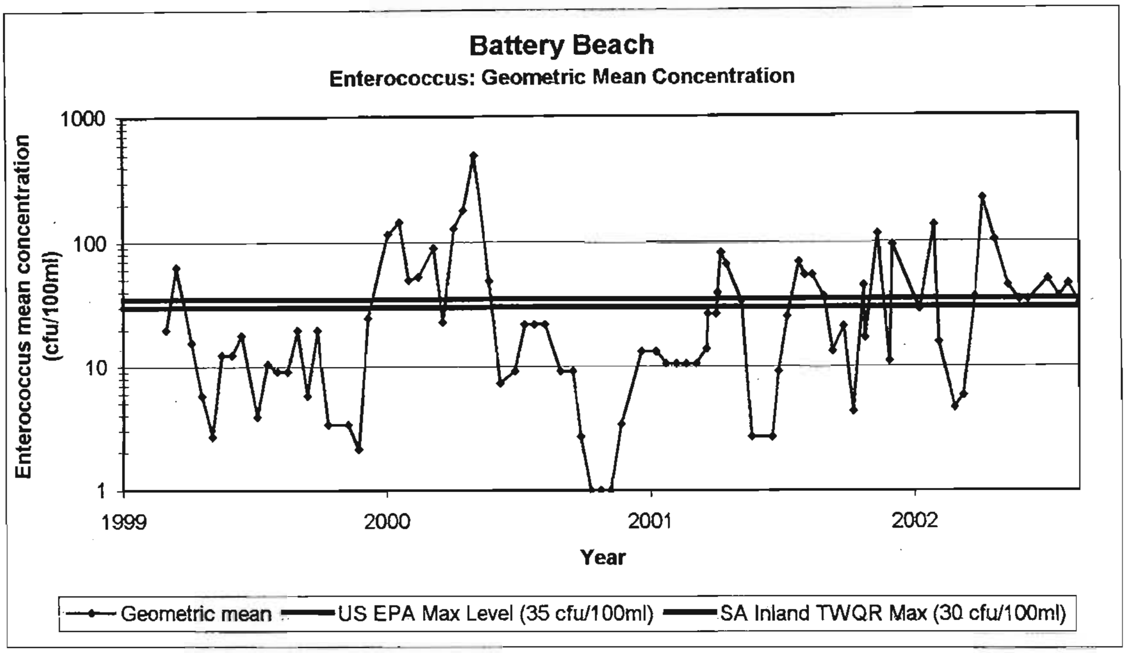

Figure B-14: Geometric means of Enterococcus concentrations at Battery Beach

Beach Status	Jan	Feb	Mar	Apr	May	Jun	Jul	Aug	Sep	Oct	Nov	Dec
Beach Open	67%	100%	100%	73%	88%	100%	100%	100%	100%	100%	100%	100%
Beach Closure	33%	0%	0%	27%	13%	0%	0%	0%	0%	0%	0%	0%

Table B-55: Beach status according to US EPA max mean conc. at Battery Beach

Beach Use	Jan	Feb	Mar	Apr	May	Jun	Jul	Aug	Sep	Oct	Nov	Dec
Full Bathing	100%	100%	89%	73%	100%	100%	75%	100%	100%	83%	83%	33%
Moderated use	0%	0%	11%	9%	0%	0%	13%	0%	0%	0%	0%	0%
Light use	0%	0%	0%	0%	0%	0%	13%	0%	0%	0%	0%	0%
Infrequent use	0%	0%	0%	0%	0%	0%	0%	0%	0%	0%	0%	0%
Beach Closure	0%	0%	0%	18%	0%	0%	0%	0%	0%	17%	17%	67%

Table B-56: Beach use according to US EPA single sample limits at Battery Beach

B.8 Country Club beach

B.8.1 Escherichia coli Analysis Results

	Annual	Summer	Autumn	Winter	Spring
Average	125.3	180.2	136.4	122.1	66.1
Standard Deviation	253.1	318.0	272.3	267.1	93.7
95% Confidence	37.1	79.4	70.2	72.4	75.6

Table B-57: General Statistics of E. coli at Country Club Beach (1995 - 2002)

	>10	>100	>200	>1000	>2000
Annual	71.51%	20.11%	12.29%	1.68%	0.00%
Summer	74.36%	25.64%	23.08%	2.56%	0.00%
Autumn	74.00%	22.00%	10.00%	2.00%	0.00%
Winter	70.21%	17.02%	10.64%	2.13%	0.00%
Spring	67.44%	16.28%	6.98%	0.00%	0.00%

Table B-58: Percentage Exceedance of E. coli at County Club Beach (1995 - 2002)

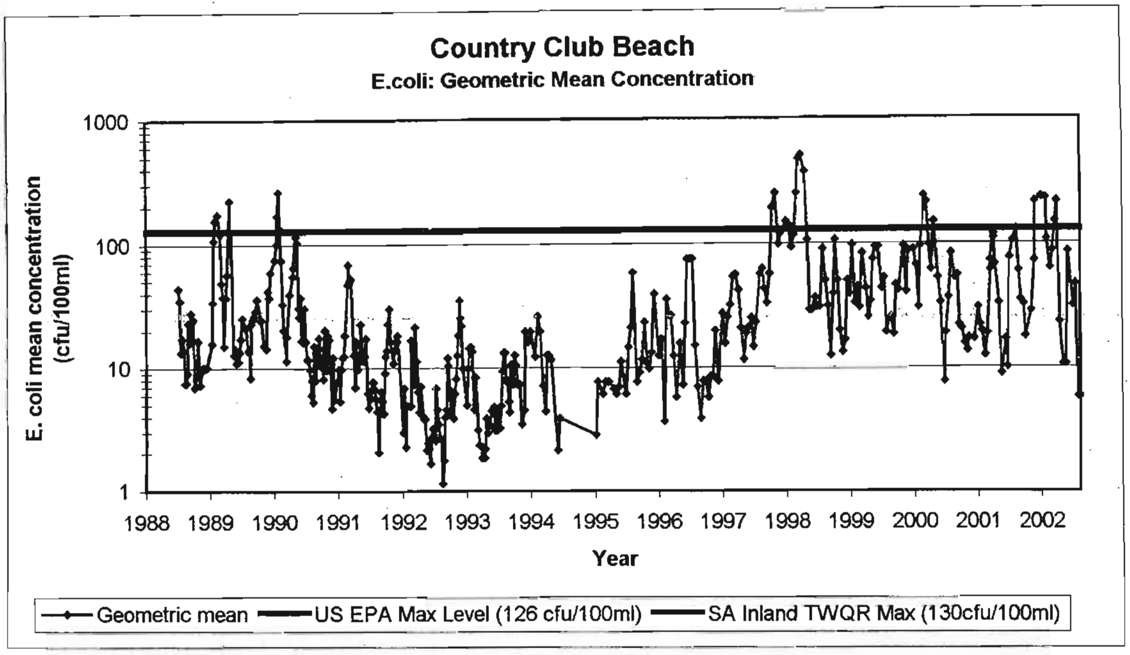

Figure B-15: Geometric means of E.coli concentrations at Country Club Beach

Beach Status	Jan	Feb	Mar	Apr	May	Jun	Jul	Aug	Sep	Oct	Nov	Dec
Beach Open	75%	100%	67%	88%	94%	100%	100%	93%	100%	92%	93%	88%
Beach Closure	25%	0%	33%	13%	6%	0%	0%	7%	0%	8%	7%	13%

Table B-59: Beach status according to US EPA max mean conc. at Country Club Beach

Beach Use	Jan	Feb	Mar	Apr	May	Jun	Jul	Aug	Sep	Oct	Nov	Dec
Full Bathing	81%	80%	78%	100%	94%	87%	88%	93%	94%	92%	93%	63%
Moderated use	0%	0%	0%	0%	0%	0%	0%	0%	0%	0%	0%	0%
Light use	19%	0%	0%	0%	0%	0%	6%	0%	6%	8%	7%	13%
Infrequent use	0%	0%	0%	0%	0%	7%	0%	0%	0%	0%	0%	0%
Beach Closure	0%	20%	22%	0%	6%	7%	6%	7%	0%	0%	0%	25%

Table B-60: Beach use according to US EPA single sample limits at Country Club Beach

Indicator	Escherichia coli		Enterococcus
Start Date	Jan-1995	Mar-1999	Mar-1999
End Date	Aug-2002	Aug-2002	Aug-2002
Failure w.r.t. US EPA Criteria	9.5%	11.0%	19.5%
Failure w.r.t. SA Inland Criteria	8.9%	9.8%	23.2%

Table B-61: Results of the Geometric Mean Analysis at Country Club Beach

B.8.2 Enterococcus Analysis Results

	Annual	Summer	Autumn	Winter	Spring
Average	64.9	120.0	57.0	60.9	32.5
Standard Deviation	136.9	230.7	97.1	135.8	51.6
95% Confidence	29.6	69.3	51.6	54.8	67.1

Table B-62: General Statistics of Enterococcus at Country Club Beach (1999 – 2002)

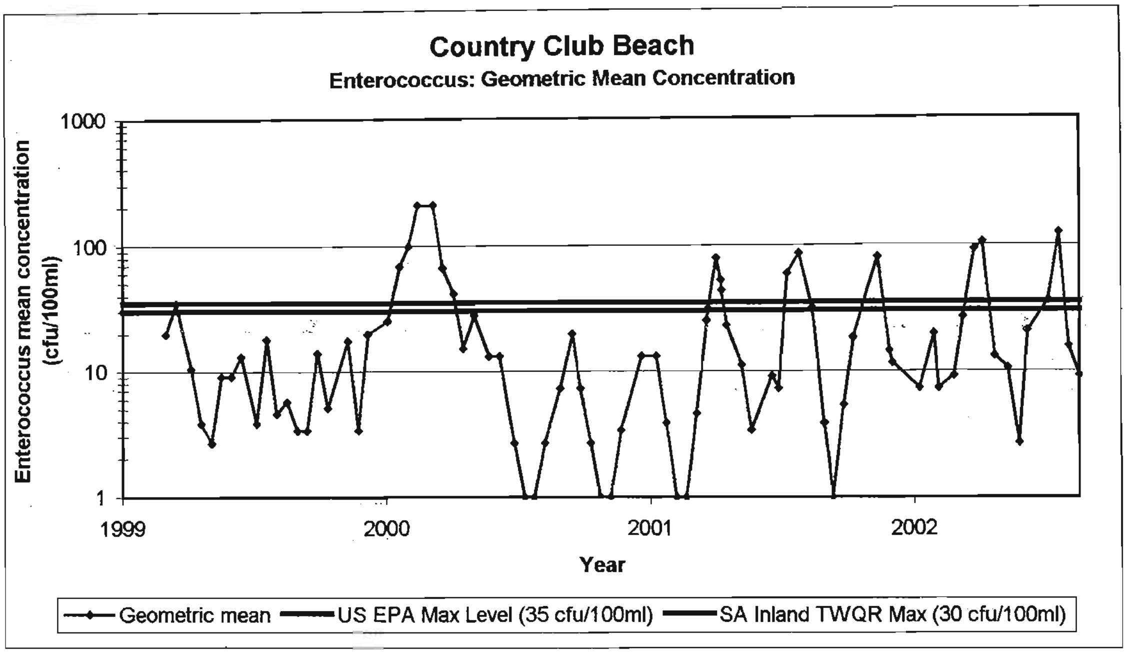

Figure B-16: Geometric means of Enterococcus concentrations at Country Club Beach

Beach Status	Jan	Feb	Mar	Apr	May	Jun	Jul	Aug	Sep	Oct	Nov	Dec
Beach Open	83%	67%	67%	50%	100%	100%	50%	100%	100%	100%	83%	100%
Beach Closure	17%	33%	33%	50%	0%	0%	50%	0%	0%	0%	17%	0%

Table B-63: Beach status according to US EPA max mean conc. at Country Club Beach

Beach Use	Jan	Feb	Mar	Apr	May	Jun	Jul	Aug	Sep	Oct	Nov	Dec
Full Bathing	100%	67%	89%	100%	100%	86%	88%	100%	100%	100%	100%	100%
Moderated use	0%	0%	0%	0%	0%	0%	0%	0%	0%	0%	0%	0%
Light use	0%	0%	0%	0%	0%	0%	0%	0%	0%	0%	0%	0%
Infrequent use	0%	0%	11%	0%	0%	14%	13%	0%	0%	0%	0%	0%
Beach Closure	0%	33%	0%	0%	0%	0%	0%	0%	0%	0%	0%	0%

Table B-64: Beach use according to US EPA single sample limits at Country Club Beach

B.9 Laguna Beach

B.9.1 Escherichia coli Analysis Results

	Annual	Summer	Autumn	Winter	Spring
Average	205.1	319.5	117.7	286.2	105.2
Standard Deviation	583.5	442.9	212.0	1026.8	182.3
95% Confidence	85.7	185.5	163.4	168.6	172.4

Table B-65: General Statistics of E. coli at Laguna Beach (1995 - 2002)

	>10	>100	>200	>1000	>2000
Annual	66.29%	27.53%	22.47%	3.93%	0.56%
Summer	78.95%	47.37%	42.11%	10.53%	0.00%
Autumn	73.47%	24.49%	16.33%	2.04%	0.00%
Winter	54.35%	21.74%	17.39%	4.35%	2.17%
Spring	59.09%	18.18%	15.91%	0.00%	0.00%

Table B-66: Percentage Exceedance of E. coli at Laguna Beach (1995 - 2002)

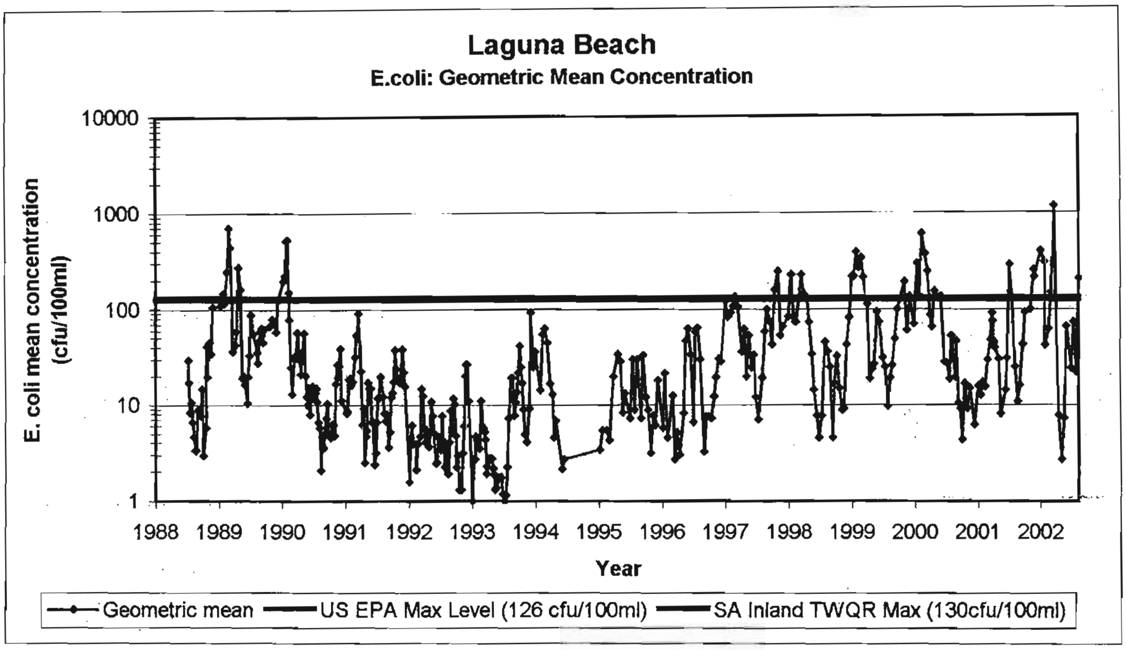

Figure B-17: Geometric means of E.coli concentrations at Laguna Beach

Beach Status	Jan	Feb	Mar	Apr	May	Jun	Jul	Aug	Sep	Oct	Nov	Dec
Beach Open	63%	71%	47%	94%	88%	93%	88%	93%	100%	92%	80%	75%
Beach Closure	38%	29%	53%	6%	13%	7%	12%	7%	0%	8%	20%	25%

Table B-67: Beach status according to US EPA max mean conc. at Laguna Beach

Beach Use	Jan	Feb	Mar	Apr	May	Jun	Jul	Aug	Sep	Oct	Nov	Dec
Full Bathing	63%	50%	71%	100%	81%	87%	76%	80%	88%	75%	87%	63%
Moderated use	6%	7%	6%	0%	0%	0%	0%	0%	0%	8%	0%	0%
Light use	13%	14%	12%	0%	6%	7%	0%	0%	0%	0%	7%	13%
Infrequent use	0%	14%	6%	0%	6%	0%	6%	7%	6%	8%	0%	0%
Beach Closure	19%	14%	6%	0%	6%	7%	18%	13%	6%	8%	7%	25%

Table B-68: Beach use according to US EPA single sample limits at Laguna Beach

Indicator	Escherichia coli		Enterococcus
Start Date	Jan-1995	Mar-1999	Mar-1999
End Date	Aug-2002	Aug-2002	Aug-2002
Failure w.r.t. US EPA Criteria	17.9%	25.3%	20.5%
Failure w.r.t. SA Inland Criteria	17.3%	24.1%	25.3%

Table B-69: Results of the Geometric Mean Analysis at Laguna Beach

B.9.2 Enterococcus Analysis Results

	Annual	Summer	Autumn	Winter	Spring
Average	104.1	306.7	65.4	71.8	32.5
Standard Deviation	348.3	757.5	157.3	144.8	36.7
95% Confidence	74.9	176.3	131.4	139.3	165.6

Table B-70: General Statistics of Enterococcus at Laguna Beach (1999 – 2002)

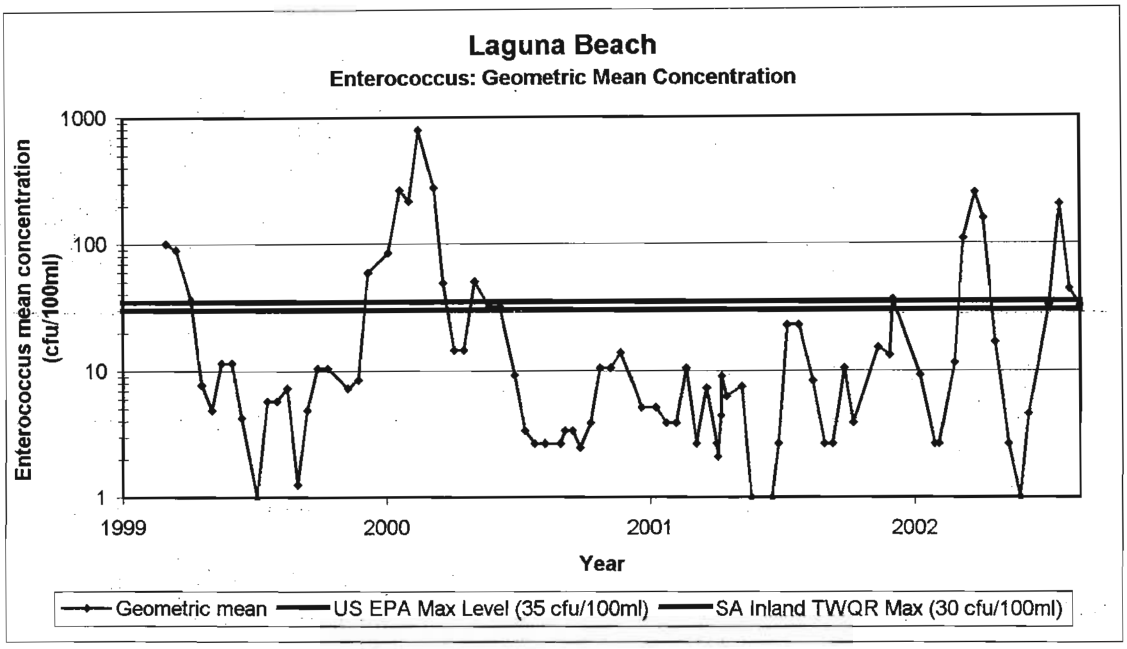

Figure B-18: Geometric means of Enterococcus concentrations at Laguna Beach

Beach Status	Jan	Feb	Mar	Apr	May	Jun	Jul	Aug	Sep	Oct	Nov	Dec
Beach Open	67%	67%	25%	82%	88%	100%	88%	89%	100%	100%	100%	33%
Beach Closure	33%	33%	75%	18%	13%	0%	13%	11%	0%	0%	0%	67%

Table B-71: Beach status according to US EPA max mean conc. at Laguna Beach

Beach Use	Jan	Feb	Mar	Apr	May	Jun	Jul	Aug	Sep	Oct	Nov	Dec
Full Bathing	83%	83%	75%	100%	100%	100%	63%	100%	100%	100%	100%	67%
Moderated use	0%	0%	13%	0%	0%	0%	13%	0%	0%	0%	0%	0%
Light use	0%	0%	0%	0%	0%	0%	13%	0%	0%	0%	0%	33%
Infrequent use	0%	0%	0%	0%	0%	0%	0%	0%	0%	0%	0%	0%
Beach Closure	17%	17%	13%	0%	0%	0%	13%	0%	0%	0%	0%	0%

Table B-72: Beach use according to US EPA single sample limits at Laguna Beach

B.10 Umgeni South Beach

B.10.1 Escherichia coli Analysis Results

	Annual	Summer	Autumn	Winter	Spring
Average	988.9	1635.1	994.5	1028.8	463.2
Standard Deviation	2385.4	2729.8	2277.0	2828.4	1510.9
95% Confidence	351.4	748.7	661.2	697.0	713.0

Table B-73: General Statistics of E. coli at Umgeni South Beach (1995 - 2002)

	>10	>100	>200	>1000	>2000
Annual	81.36%	48.02%	39.55%	18.08%	11.86%
Summer	89.74%	71.79%	58.97%	28.21%	20.51%
Autumn	89.58%	45.83%	37.50%	16.67%	12.50%
Winter	77.78%	37.78%	31.11%	17.78%	11.11%
Spring	67.44%	39.53%	32.56%	9.30%	2.33%

Table B-74: Percentage Exceedance of E. coli at Umgeni South Beach (1995 - 2002)

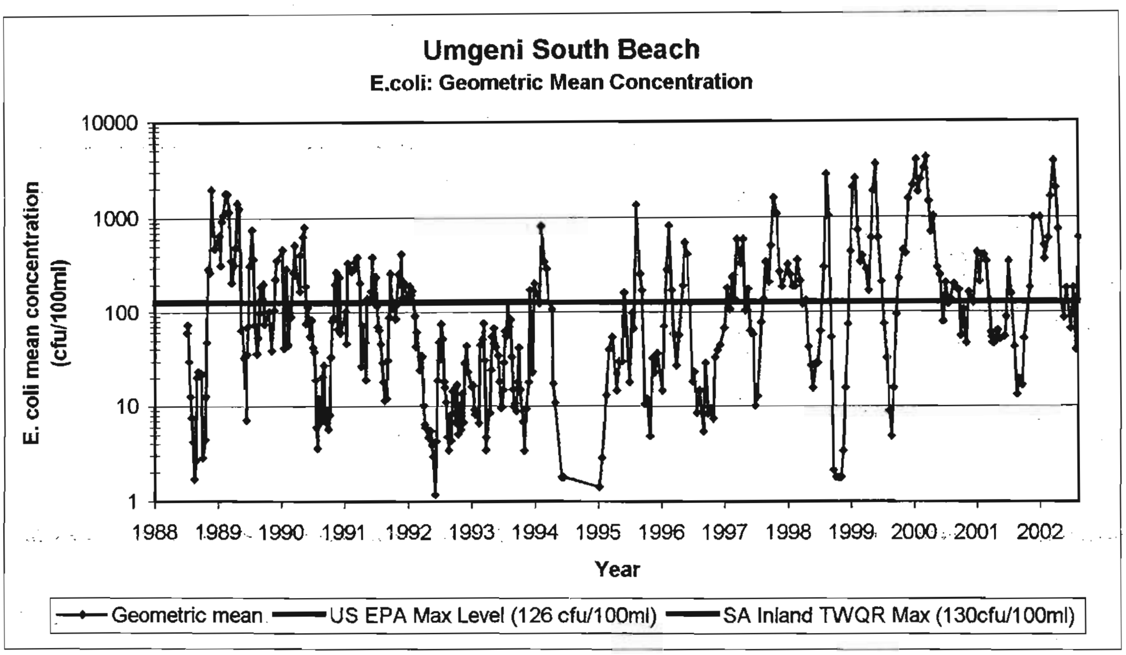

Figure B-19: Geometric means of E.coli concentrations at Umgeni South Beach

Beach Status	Jan	Feb	Mar	Apr	May	Jun	Jul	Aug	Sep	Oct	Nov	Dec
Beach Open	31%	13%	24%	47%	56%	60%	71%	53%	50%	83%	53%	63%
Beach Closure	69%	87%	76%	53%	44%	40%	29%	47%	50%	17%	47%	38%

Table B-75: Beach status according to US EPA max mean conc. at Umgeni South Beach

Beach Use	Jan	Feb	Mar	Apr	May	Jun	Jul	Aug	Sep	Oct	Nov	Dec
Full Bathing	44%	27%	53%	76%	56%	67%	82%	53%	75%	75%	60%	63%
Moderated use	0%	0%	0%	0%	0%	0%	0%	7%	0%	8%	0%	0%
Light use	6%	7%	12%	6%	0%	13%	0%	0%	19%	0%	7%	0%
Infrequent use	6%	13%	0%	12%	0%	0%	0%	7%	0%	0%	0%	0%
Beach Closure	44%	53%	35%	6%	44%	20%	18%	33%	6%	17%	33%	38%

Table B-76: Beach use according to US EPA single sample limits at Umgeni South Beach

Indicator	Escherichia coli		Enterococcus
Start Date	Jan-1995	Mar-1999	Mar-1999
End Date	Aug-2002	Aug-2002	Aug-2002
Failure w.r.t. US EPA Criteria	50.8%	63.4%	63.4%
Failure w.r.t. SA Inland Criteria	50.8%	63.4%	67.1%

Table B-77: Results of the Geometric Mean Analysis at Umgeni South Beach

B.10.2 Enterococcus Analysis Results

	Annual	Summer	Autumn	Winter	Spring
Average	383.2	908.0	348.3	211.7	207.6
Standard Deviation	629.9	1196.6	366.0	319.8	244.7
95% Confidence	136.3	318.8	237.6	252.0	308.7

Table B-78: General Statistics of Enterococcus at Umgeni South Beach (1999 – 2002)

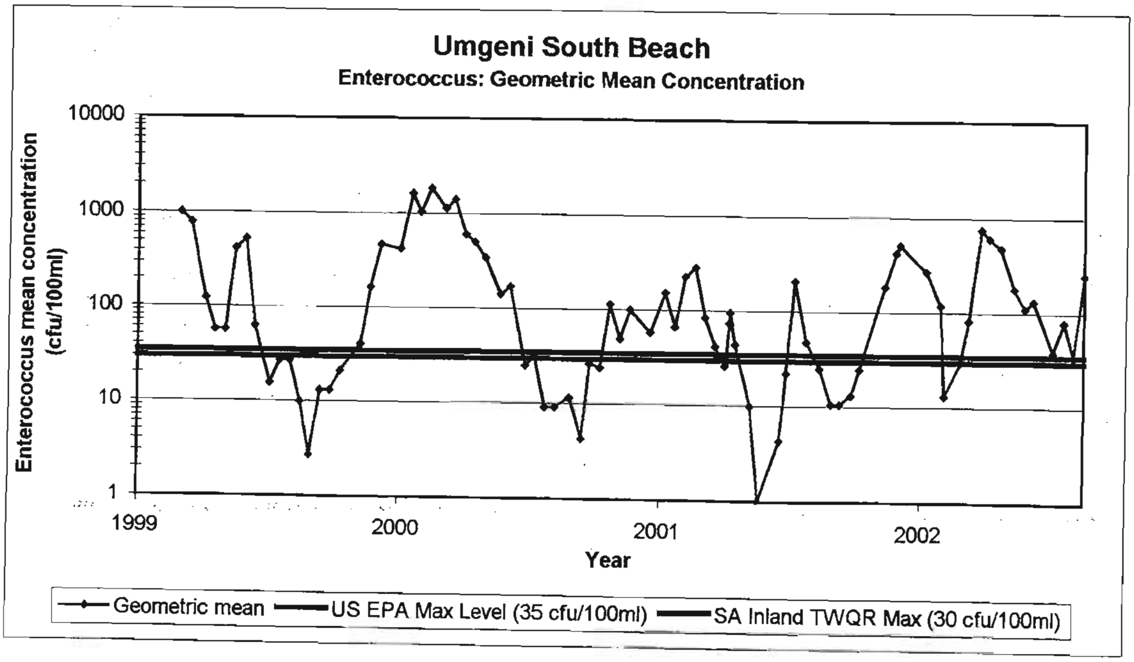

Figure B-20: Geometric means of Enterococcus concentrations at Umgeni South Beach

Beach Status	Jan	Feb	Mar	Apr	May	Jun	Jul	Aug	Sep	Oct	Nov	Dec
Beach Open	0%	33%	0%	18%	25%	43%	50%	89%	100%	75%	0%	0%
Beach Closure	100%	67%	100%	82%	75%	57%	50%	11%	0%	25%	100%	100%

Table B-79: Beach status according to US EPA max mean conc. at Umgeni South Beach

Beach Use	Jan	Feb	Mar	Apr	May	Jun	Jul	Aug	Sep	Oct	Nov	Dec
Full Bathing	50%	17%	25%	55%	63%	71%	63%	89%	83%	75%	33%	33%
Moderated use	0%	0%	0%	9%	0%	0%	0%	0%	17%	0%	0%	0%
Light use	17%	0%	0%	27%	13%	0%	0%	11%	0%	25%	17%	0%
Infrequent use	0%	17%	0%	9%	0%	0%	0%	0%	0%	0%	33%	0%
Beach Closure	33%	67%	75%	0%	25%	29%	38%	0%	0%	0%	17%	67%

Table B-80: Beach use according to US EPA single sample limits at Umgeni South Beach

APPENDIX C:
ANALYSIS OF URBAN STORMWATER DRAINS AND UMGENI RIVER

C.1 Hospital Stormwater Drain

	Geometric Mean	Average	Standard Deviation	Coeff. of Variation	Kurtosis	Skewness
Annual Data	801	124004	441737	356%	19.50	4.43
Summer	235	19743	59427	301%	20.68	4.39
Autumn	322	107245	477628	445%	29.23	5.30
Winter	3365	227442	555425	244%	8.06	2.99
Spring	1548	120215	441887	368%	24.06	4.84

Table C-C-1: Hospital SWD Annual and Seasonal E. coli statistics

	Geometric Mean	Average	Standard Deviation	Coeff. of Variation	Kurtosis	Skewness
Jan	357	2452	3775	154%	4.85	2.20
Feb	1086	47732	93493	196%	7.32	2.63
Mar	298	82657	264478	320%	10.99	3.32
Apr	295	217247	764047	352%	13.00	3.60
May	380	10617	18610	175%	6.13	2.44
Jun	3010	97123	136377	140%	-0.15	1.13
Jul	550	215683	655762	304%	10.82	3.28
Aug	28524	409790	752932	184%	2.27	1.86
Sep	9052	82500	133917	162%	3.70	2.00
Oct	5878	269111	743700	276%	8.94	2.99
Nov	85	4843	8993	186%	5.44	2.28
Dec	15	4458	9695	217%	6.08	2.45

Table C-C-2: Hospital SWD Monthly E. coli statistics

	Annual	Summer	Autumn	Winter	Spring
Number of Samples	123	27	36	34	26
Zero Count	33	9	12	6	6
Percentage Zero	26.8%	33.3%	33.3%	17.6%	23.1%

Table C-3: Characteristics of Hospital SWD E.coli Data Set

	Annual	Summer	Autumn	Winter	Spring
Jarque-Bera Test	Pass	Pass	Pass	Pass	Pass
Lilliefors Test	Fail	Pass	Pass	Pass	Pass
Mean	233999	56437	133952	881500	148126
Standard Deviation	5887008	882893	3106014	40516219	1557763
Scale Parameter - μ'	9.1371	8.1888	8.6607	9.8613	9.5484
μ' - lower 95% C.L.	8.6051	7.0221	7.6017	8.7884	8.5321
μ' - upper 95% C.L.	9.6691	9.3554	9.7196	10.9342	10.5646
Shape parameter - σ'	2.5401	2.3461	2.5078	2.767	2.1714
σ' - lower 95% C.L.	2.2155	1.7605	1.9491	2.1876	1.6513
σ' - upper 95% C.L.	2.977	3.5172	3.5179	3.7662	3.1715

Table C-4: Lognormal Distribution results for Hospital SWD

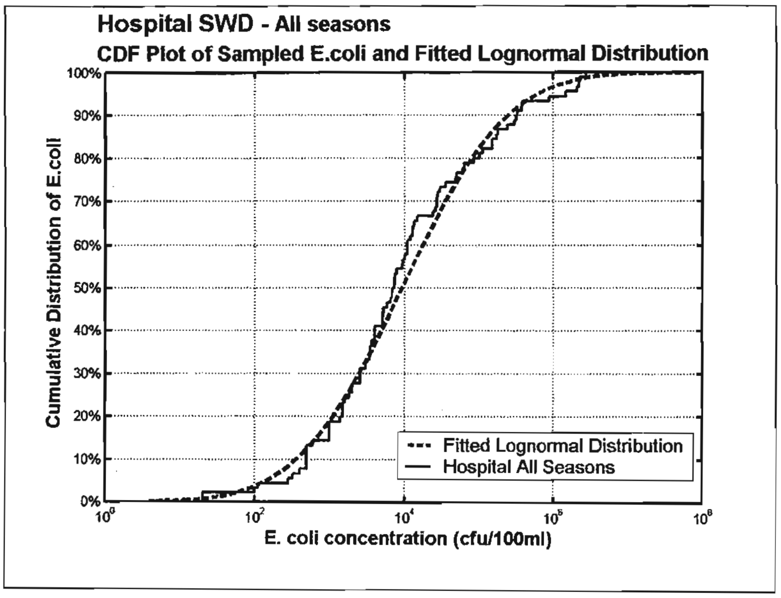

Figure C-1: Hospital SWD E.coli distribution and fitted lognormal distribution

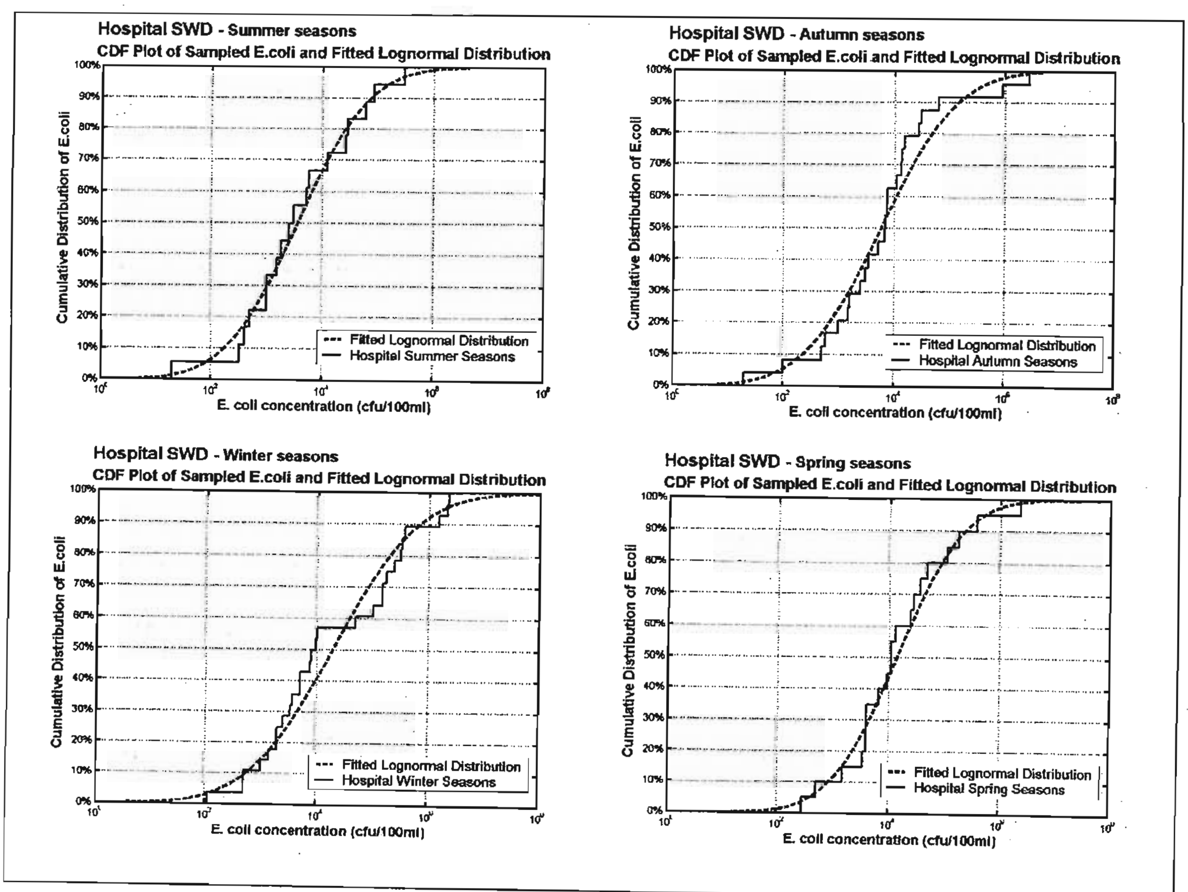

Figure C-2: Hospital SWD Seasonal E.coli distributions and fitted lognormal distributions

C.2 Rutherford Road Stormwater Drain

	Geometric Mean	Average	Standard Deviation	Coeff. of Variation	Kurtosis	Skewness
Annual Data	1032	43481	113105	260%	23.92	4.38
Summer	3567	46631	100547	216%	8.61	3.03
Autumn	2651	31722	85276	269%	15.93	4.02
Winter	70	47055	168254	358%	23.58	4.76
Spring	1023	57710	96325	167%	2.14	1.77

Table 2-C-5: Rutherford SWD Annual and Seasonal E. coli statistics

	Geometric Mean	Average	Standard Deviation	Coeff. of Variation	Kurtosis	Skewness
Jan	4602	89464	153670	172%	1.24	1.67
Feb	3059	22275	32495	146%	3.36	1.96
Mar	1611	45786	103099	225%	11.60	3.32
Apr	6070	38853	100996	260%	14.21	3.74
May	1811	7265	13860	191%	8.66	2.87
Jun	711	105857	258215	244%	9.50	3.03
Jul	30	9488	24487	258%	7.93	2.81
Aug	7	3771	10598	281%	8.00	2.83
Sep	2107	64125	84587	132%	1.99	1.46
Oct	3864	68332	102110	149%	2.11	1.59
Nov	155	42002	112371	268%	7.98	2.82
Dec	3014	15834	12156	77%	-1.50	-0.32

Table 2-C-6: Rutherford SWD Monthly E. coli statistics

	Annual	Summer	Autumn	Winter	Spring
Number of Samples	117	25	42	27	23
Zero Count	27	3	4	14	6
Percentage Zero	23.1%	12.0%	9.5%	51.9%	26.1%

Table C-7: Characteristics of Rutherford SWD E.coli Data Set

	Annual	Summer	Autumn	Winter	Spring
Jarque-Bera Test	Pass	Pass	Pass	Pass	Pass
Lilliefors Test	Pass	Pass	Pass	Pass	Pass
Mean	103297	78449	35977	518110	626889
Standard Deviation	1468124	696406	240339	39367918	33261269
Scale Parameter - μ'	8.8888	9.0804	8.5804	8.8273	9.377
μ' - lower 95% C.L.	8.406	8.1525	7.9379	7.0489	7.9279
μ' - upper 95% C.L.	9.3715	10.0083	9.2229	10.6058	10.826
Shape parameter - σ'	2.305	2.0927	1.9546	2.943	2.8184
σ' - lower 95% C.L.	2.0105	1.6101	1.5935	2.1104	2.099
σ' - upper 95% C.L.	2.7015	2.9907	2.5288	4.8581	4.2893

Table C-8: Lognormal Distribution results for Rutherford SWD

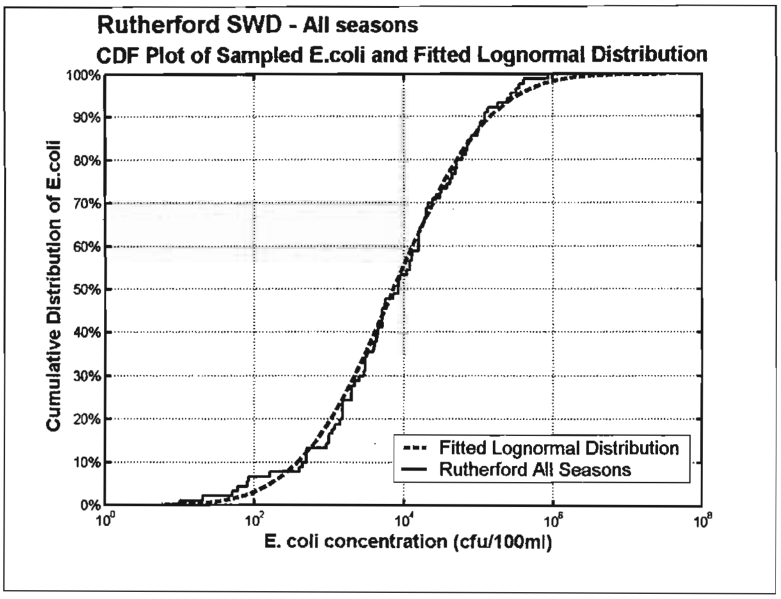

Figure C-3: Rutherford SWD E.coli distribution and fitted lognormal distribution

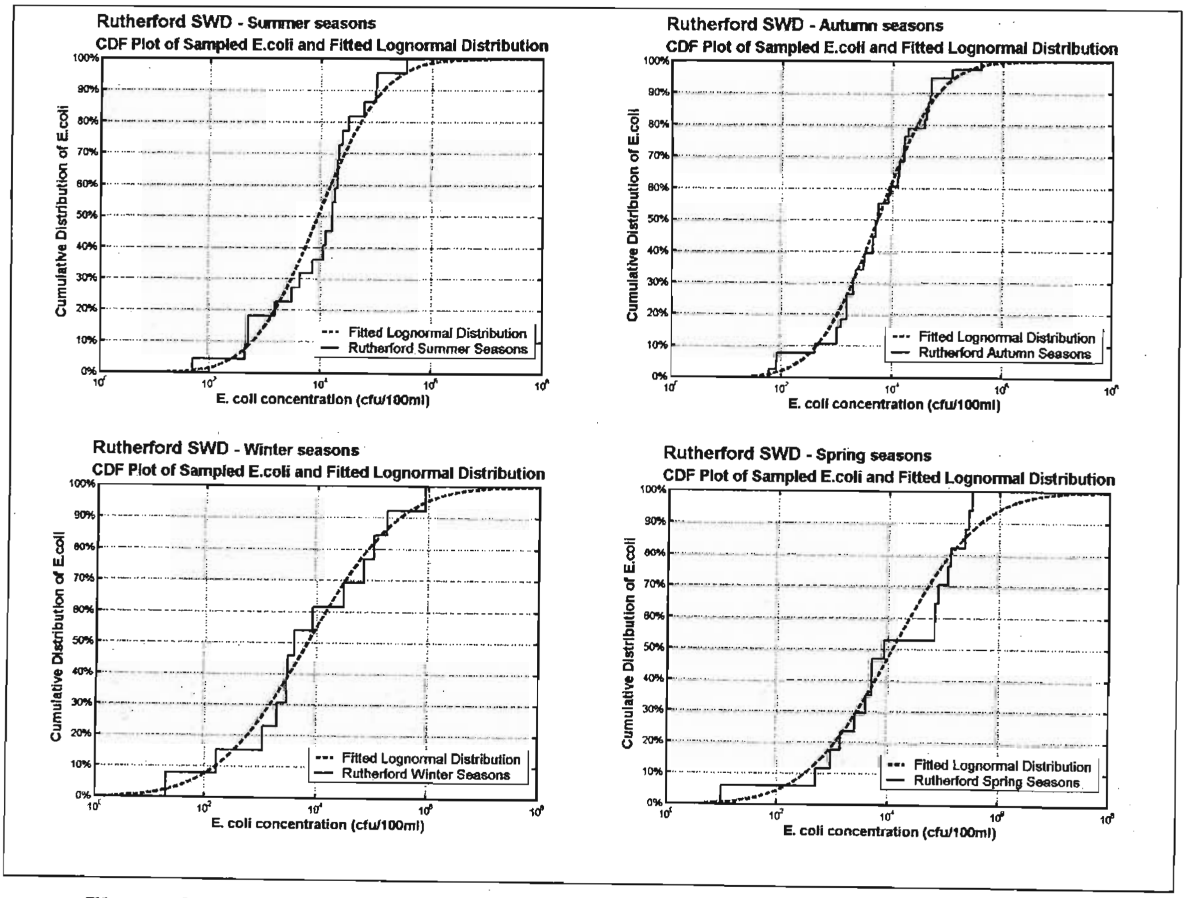

Figure C-4: Rutherford SWD Seasonal E.coli distributions and fitted lognormal distributions

C.3 West Street Stormwater Drain

	Geometric Mean	Average	Standard Deviation	Coeff. of Variation	Kurtosis	Skewness
Annual Data	178	8661	27253	315%	40.13	5.73
Summer	318	10071	24062	239%	8.35	2.99
Autumn	118	8002	23661	296%	27.91	4.98
Winter	172	10597	37977	358%	36.10	5.80
Spring	199	5708	16999	298%	29.96	5.32

Table 2-C-9: West SWD Annual and Seasonal E. coli statistics

	Geometric Mean	Average	Standard Deviation	Coeff. of Variation	Kurtosis	Skewness
Jan	412	12735	25854	203%	7.45	2.68
Feb	295	11558	28261	245%	7.47	2.79
Mar	116	3796	7471	197%	8.50	2.79
Apr	119	11062	34257	310%	17.77	4.15
May	118	8101	18470	228%	8.68	2.97
Jun	127	5221	15890	304%	16.69	4.04
Jul	359	20759	63661	307%	14.72	3.82
Aug	115	6620	15249	230%	11.97	3.38
Sep	218	3412	5245	154%	2.44	1.73
Oct	566	12309	29284	238%	10.60	3.24
Nov	76	2065	4690	227%	10.31	3.15
Dec	238	2316	2345	101%	-1.21	0.40

Table 2-C-10: West SWD Monthly E. coli statistics

	Annual	Summer	Autumn	Winter	Spring
Number of Samples	170	34	54	47	35
Zero Count	58	9	21	17	11
Percentage Zero	34.1%	26.5%	38.9%	36.2%	31.4%

Table C-11: Characteristics of West SWD E.coli Data Set

	Annual	Summer	Autumn	Winter	Spring
Jarque-Bera Test	Pass	Pass	Pass	Pass	Pass
Lilliefors Test	Pass	Pass	Pass	Pass	Pass
Mean	17388	24781	25614	15853	9707
Standard Deviation	115174	241579	266921	77550	40756
Scale Parameter - μ'	7.8616	7.8355	7.8025	8.0631	7.7182
μ' - lower 95% C.L.	7.4964	6.9536	7.034	7.3935	6.9961
μ' - upper 95% C.L.	8.2268	8.7174	8.5709	8.7328	8.4404
Shape parameter - σ'	1.9503	2.1365	2.1672	1.7933	1.7102
σ' - lower 95% C.L.	1.7241	1.6683	1.7428	1.4282	1.3292
σ' - upper 95% C.L.	2.2455	2.9722	2.8666	2.4108	2.399

Table C-12: Lognormal Distribution results for West SWD

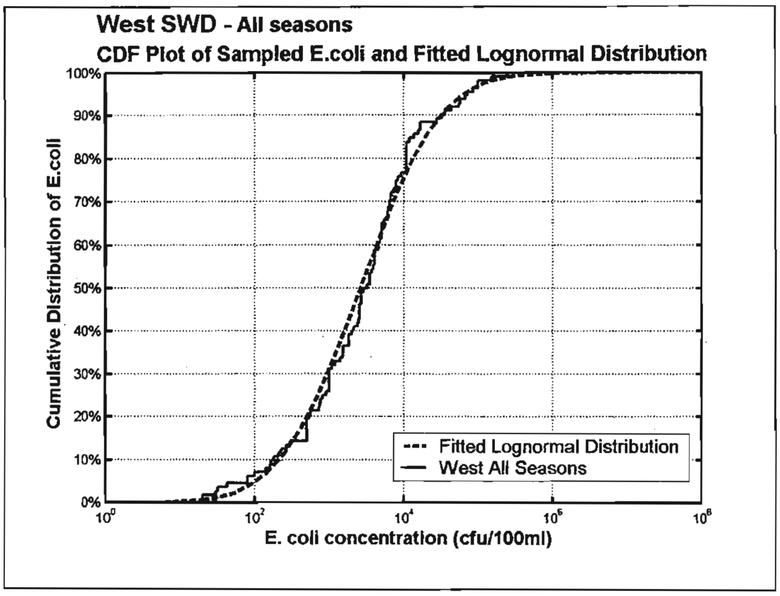

Figure C-5: West SWD E.coli distribution and fitted lognormal distribution

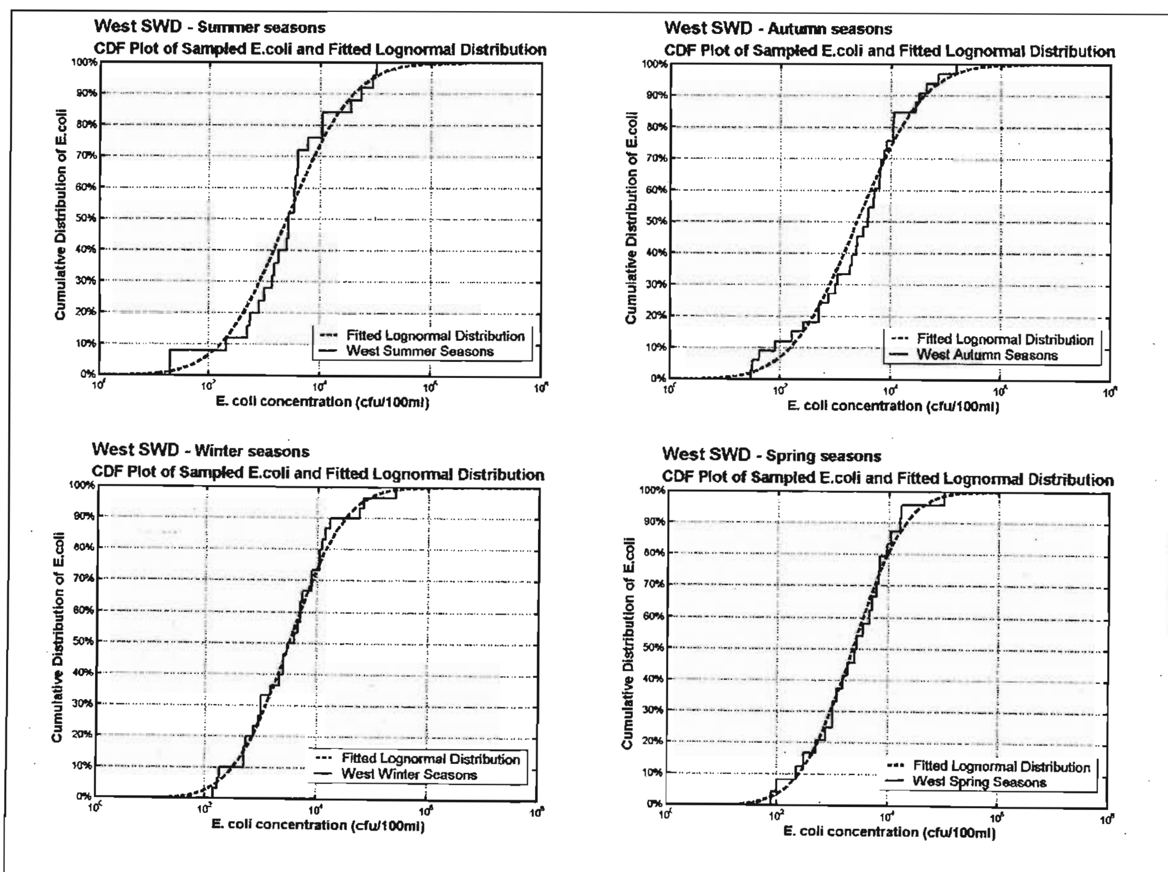

Figure C-6: West SWD Seasonal E.coli distributions and fitted lognormal distributions

C.4 Somtseu Road Stormwater Drain

	Geometric Mean	Average	Standard Deviation	Coeff. of Variation	Kurtosis	Skewness
Annual Data	2031	14352	37631	262%	29.11	4.72
Summer	8993	27484	62940	229%	20.72	4.32
Autumn	1472	9630	27812	289%	38.82	6.03
Winter	702	9601	18276	190%	5.89	2.49
Spring	2216	12574	26010	207%	5.99	2.60

Table 2-C-13: Somtseu SWD Annual and Seasonal E. coli statistics

	Geometric Mean	Average	Standard Deviation	Coeff. of Variation	Kurtosis	Skewness
Jan	10943	14825	11789	80%	-1.07	0.82
Feb	4980	10008	16845	168%	10.67	3.19
Mar	1409	16877	44590	264%	15.66	3.90
Apr	2458	7707	9249	120%	0.58	1.44
May	896	2890	4063	141%	6.09	2.35
Jun	71	1077	2147	199%	5.00	2.39
Jul	2127	17070	25022	147%	3.37	1.87
Aug	4042	13858	20543	148%	3.48	1.90
Sep	4829	20178	35436	176%	2.87	1.93
Oct	1221	2292	3140	137%	4.85	2.20
Nov	1805	15588	27370	176%	5.75	2.35
Dec	19247	81643	123454	151%	3.83	1.93

Table 2-C-14: Somtseu SWD Monthly E. coli statistics

	Annual	Summer	Autumn	Winter	Spring
Number of Samples	137	32	46	33	26
Zero Count	10	0	4	5	1
Percentage Zero	7.3%	0.0%	8.7%	15.2%	3.8%

Table C-15: Characteristics of Somtseu SWD E.coli Data Set

	Annual	Summer	Autumn	Winter	Spring
Jarque-Bera Test	Pass	Pass	Pass	Pass	Pass
Lilliefors Test	Fail	Pass	Pass	Pass	Pass
Mean	16672	23319	10093	20459	11749
Standard Deviation	73244	55794	33039	183788	44230
Scale Parameter - μ'	8.2162	9.1041	7.9891	7.7246	8.0118
μ' - lower 95% C.L.	7.9115	8.6064	7.5002	6.911	7.3311
μ' - upper 95% C.L.	8.5209	9.6019	8.4779	8.5383	8.6925
Shape parameter - σ'	1.7351	1.3805	1.5688	2.0983	1.6491
σ' - lower 95% C.L.	1.5448	1.1067	1.2908	1.659	1.2876
σ' - upper 95% C.L.	1.9794	1.8353	2.0004	2.8561	2.2941

Table C-16: Lognormal Distribution results for Somtseu SWD

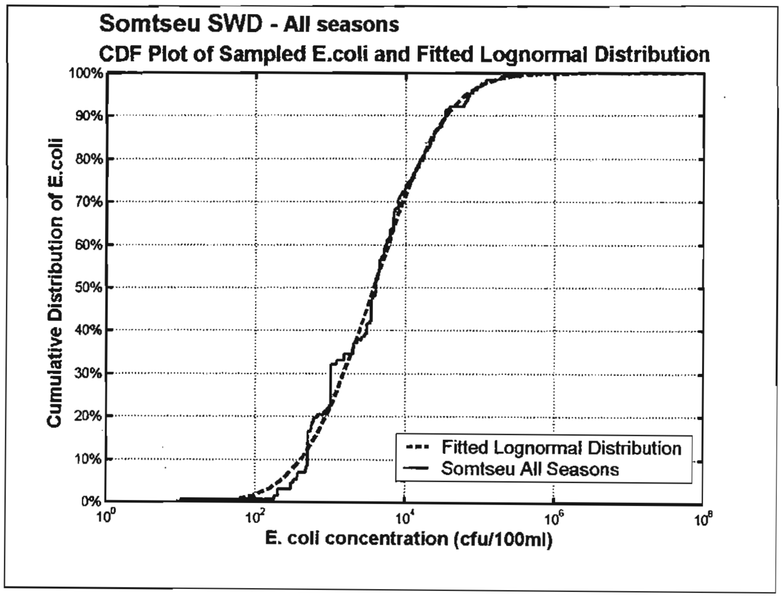

Figure C-7: Somtseu SWD E.coli distribution and fitted lognormal distribution

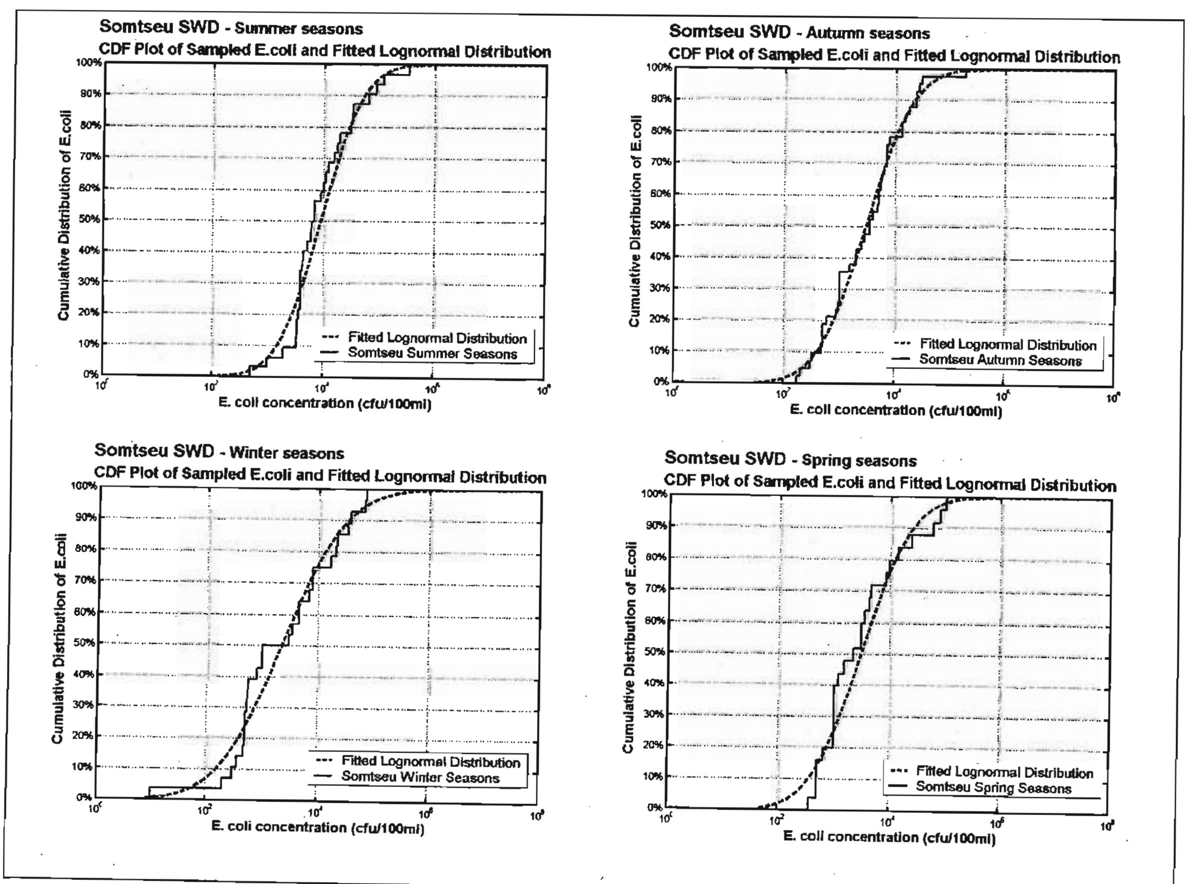

Figure C-8: Somtseu SWD Seasonal E.coli distributions and fitted lognormal distributions

C.5 Argyle Road Stormwater Drain

	Geometric Mean	Average	Standard Deviation	Coeff. of Variation	Kurtosis	Skewness
Annual Data	6581	83846	241009	287%	13.08	3.57
Summer	9621	114017	377190	331%	29.20	5.14
Autumn	6303	53855	105436	196%	5.74	2.58
Winter	4180	35053	79564	227%	11.79	3.32
Spring	7921	143391	289123	202%	2.85	2.05

Table 2-C-17: Argyle SWD Annual and Seasonal E. coli statistics

	Geometric Mean	Average	Standard Deviation	Coeff. of Variation	Kurtosis	Skewness
Jan	7739	94185	269805	286%	13.15	3.57
Feb	8389	60955	173522	285%	19.95	4.42
Mar	2171	30274	87556	289%	17.99	4.15
Apr	10198	67926	117810	173%	4.34	2.26
May	10542	61653	108312	176%	5.28	2.40
Jun	3239	25158	49914	198%	8.22	2.81
Jul	7521	32930	57910	176%	2.50	1.97
Aug	3009	46074	114091	248%	7.07	2.84
Sep	7467	127010	264213	208%	3.61	2.16
Oct	7033	164925	320715	194%	2.01	1.82
Nov	9433	140234	297425	212%	5.32	2.48
Dec	16128	221943	648509	292%	13.53	3.66

Table 2-C-18: Argyle SWD Monthly E. coli statistics

	Annual	Summer	Autumn	Winter	Spring
Number of Samples	235	55	63	62	55
Zero Count	3	0	2	1	0
Percentage Zero	1.3%	0.0%	3.2%	1.6%	0.0%

Table C-19: Characteristics of Argyle SWD E.coli Data Set

	Annual	Summer	Autumn	Winter	Spring
Jarque-Bera Test	Pass	Pass	Pass	Pass	Pass
Lilliefors Test	Pass	Pass	Pass	Pass	Pass
Mean	108015	139071	84806	37286	355154
Standard Deviation	1756287	2005384	1046981	310397	18361683
Scale Parameter - μ'	8.7995	9.1717	8.8315	8.4	8.8346
μ' - lower 95% C.L.	8.4939	8.5469	8.257	7.8718	8.0752
μ' - upper 95% C.L.	9.105	9.7966	9.4061	8.9281	9.5941
Shape parameter - σ'	2.3624	2.3113	2.2435	2.0622	2.8091
σ' - lower 95% C.L.	2.1653	1.9458	1.9041	1.7502	2.3649
σ' - upper 95% C.L.	2.5995	2.8471	2.7313	2.5106	3.4604

Table C-20: Lognormal Distribution results for Argyle SWD

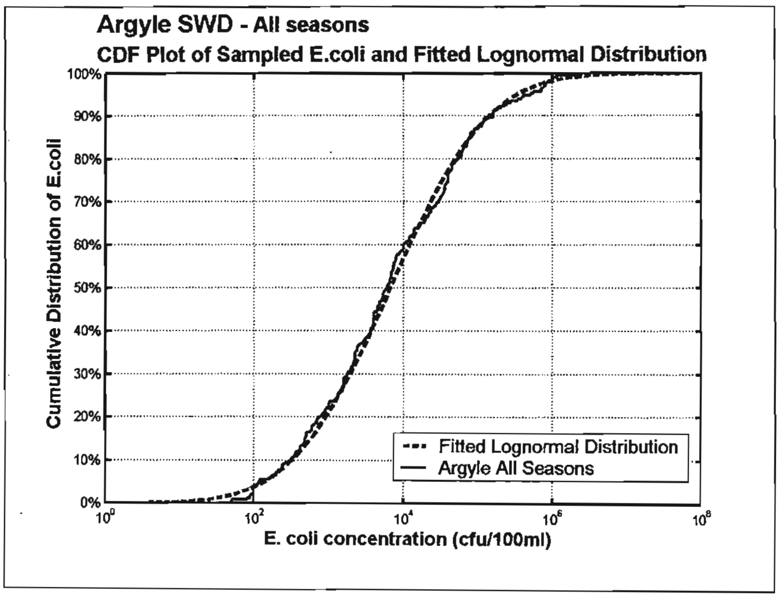

Figure C-9: Argyle SWD E.coli distribution and fitted lognormal distribution

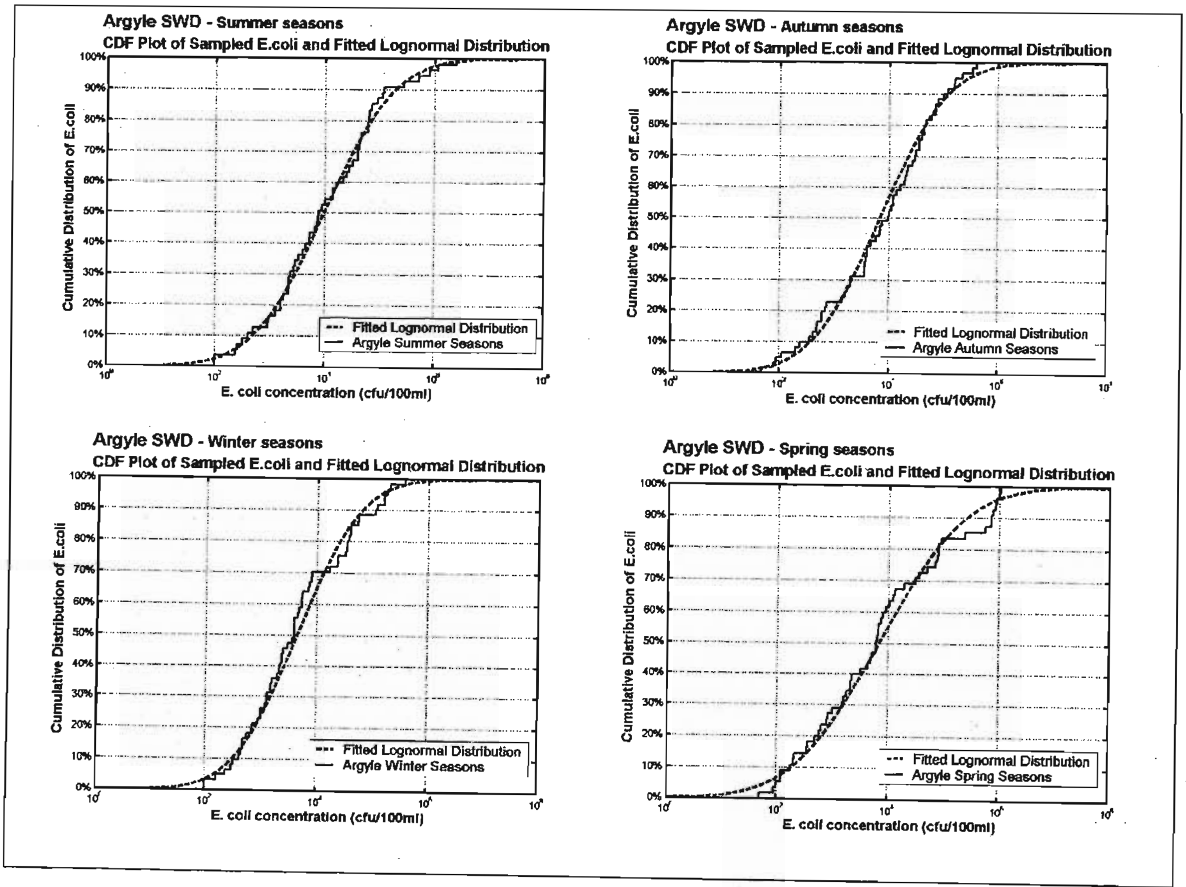

Figure C-10: Argyle SWD Seasonal E.coli distributions and fitted lognormal distributions

C.6 Walter Gilbert Road Stormwater Drain

	Geometric Mean	Average	Standard Deviation	Coeff. of Variation	Kurtosis	Skewness
Annual Data	3305	16160	43152	267%	59.33	7.14
Summer	6992	19023	20007	105%	2.33	1.47
Autumn	4093	12260	20866	170%	11.89	3.24
Winter	1023	4065	4352	107%	3.26	1.60
Spring	3780	31388	84928	271%	17.87	4.12

Table C-21: Walter Gilbert SWD Annual and Seasonal E. coli statistics

	Geometric Mean	Average	Standard Deviation	Coeff. of Variation	Kurtosis	Skewness
Jan	1575	9644	15865	165%	5.78	2.36
Feb	16648	26500	23960	90%	1.79	1.33
Mar	8128	14314	13885	97%	5.21	1.97
Apr	4165	17473	32707	187%	5.20	2.35
May	2274	5771	7707	134%	5.29	2.16
Jun	812	4552	6524	143%	3.32	1.87
Jul	966	3643	3091	85%	-2.17	0.02
Aug	1252	4020	3652	91%	-0.19	0.78
Sep	1132	8043	12389	154%	3.11	1.88
Oct	7856	81296	148231	182%	4.74	2.18
Nov	6658	11063	9789	88%	0.85	1.11
Dec	12022	19067	14250	75%	-1.07	0.31

Table C-22: Walter Gilbert SWD Monthly E. coli statistics

	Annual	Summer	Autumn	Winter	Spring
Number of Samples	104	24	33	24	23
Zero Count	5	1	0	3	1
Percentage Zero	4.8%	4.2%	0.0%	12.5%	4.3%

Table C-23: Characteristics of Walter Gilbert SWD E.coli Data Set

	Annual	Summer	Autumn	Winter	Spring
Jarque-Bera Test	Pass	Pass	Pass	Pass	Pass
Lilliefors Test	Pass	Pass	Pass	Pass	Pass
Mean	18867	25843	16365	5641	39051
Standard Deviation	69011	59638	63361	10088	274637
Scale Parameter - μ'	8.5123	9.2375	8.317	7.9206	8.612
μ' - lower 95% C.L.	8.1867	8.6502	7.7266	7.3754	7.7341
μ' - upper 95% C.L.	8.838	9.8248	8.9073	8.4658	9.49
Shape parameter - σ'	1.6327	1.3582	1.6649	1.1977	1.9802
σ' - lower 95% C.L.	1.4326	1.0504	1.3389	0.91632	1.5235
σ' - upper 95% C.L.	1.8982	1.9223	2.2022	1.7296	2.8298

Table C-24: Lognormal Distribution results for Walter Gilbert SWD

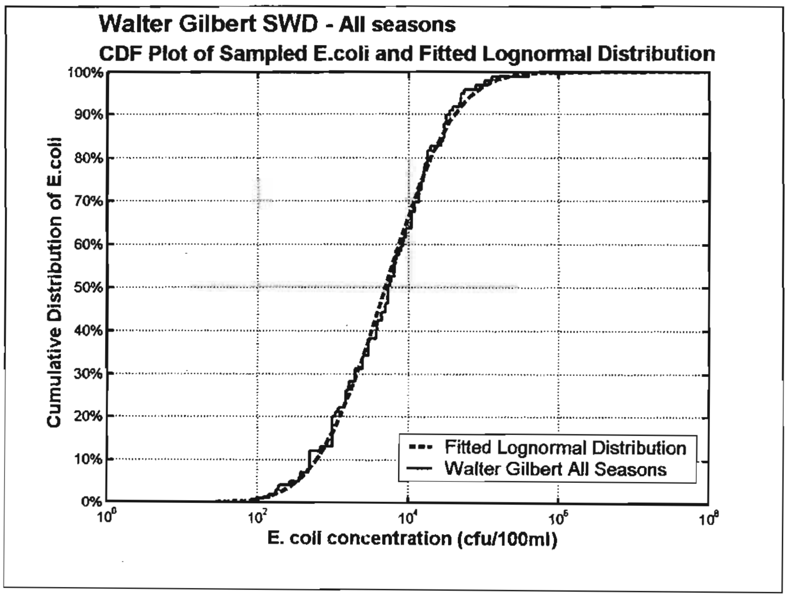

Figure C-11: Walter Gilbert SWD E.coli distribution and fitted lognormal distribution

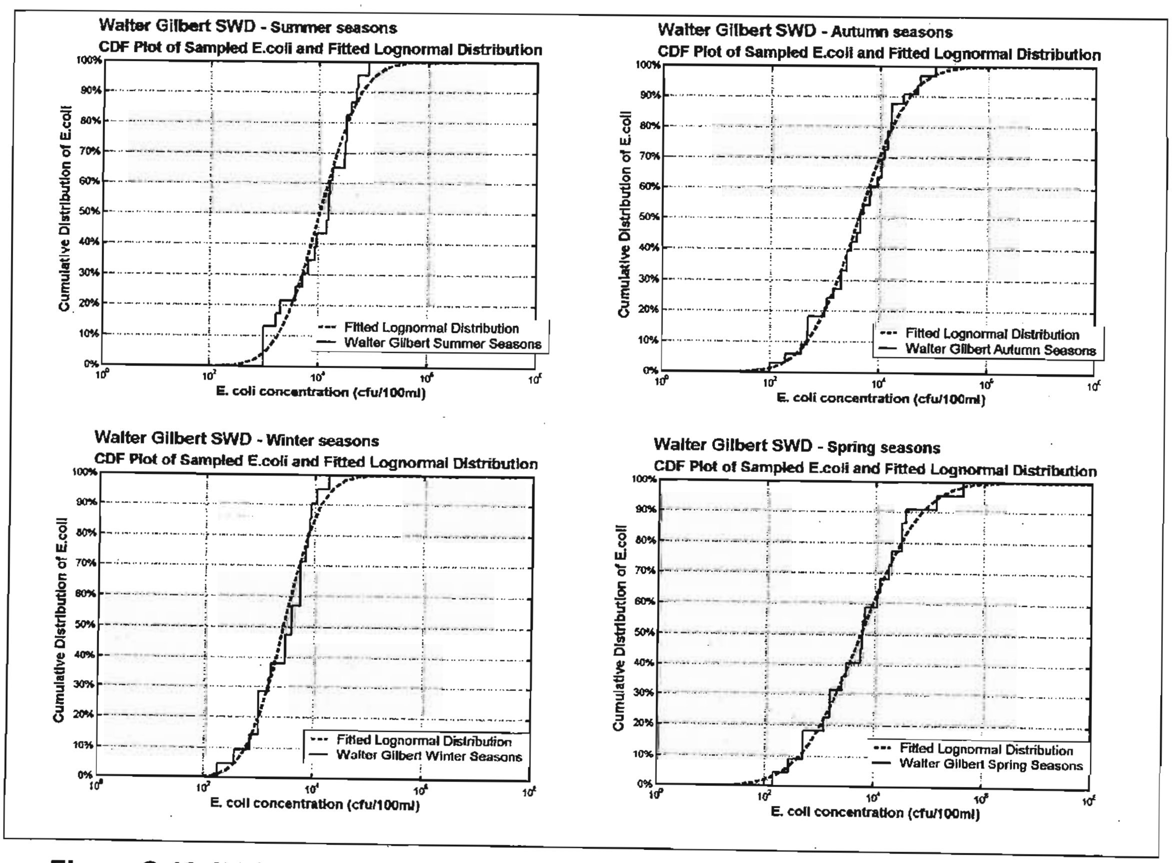

Figure C-12: Walter Gilbert SWD Seasonal E.coli distributions and fitted lognormal distributions

C.7 Umgeni River (Sampling Position 13)

	Geometric Mean	Average (cfu/100ml)	Standard Deviation	Coeff. of Variation
1987	1153	1269	751	59.2%
1988	2643	6107	9464	155.0%
1989	3543	4873	3956	81.2%
1990	703	943	872	92.5%
1991	696	1856	2557	137.8%
1992	679	9944	50603	508.9%
1993	502	807	824	102.1%
1994	4078	15938	24681	154.9%
1995	2763	8060	17024	211.2%
1996	1560	2043	2026	99.1%
1997	1650	4409	6177	140.1%
1998	2025	21896	60677	277.1%
1999	1842	9200	20164	219.2%
2000	6460	12340	16526	133.9%
2001	3893	23972	59512	248.3%

Table C-25: Yearly Statistics of E.coli at postion 13

	Geometric Mean	Average (cfu/100ml)	Standard Deviation	Coeff. of Variation
Jan	2325	20256	57718	285%
Feb	1359	3092	3208	104%
Mar	1791	7705	24455	317%
April	3045	19009	52389	276%
May	1881	7201	17142	238%
Jun	2170	4224	5335	126%
Jul	1869	16428	46252	282%
Aug	1630	2045	1218	60%
Sep	986	3115	6004	193%
Oct	2306	17227	53761	312%
Nov	1101	3008	4578	152%
Dec	3465	8448	11409	135%

Table C-26: Monthly Statistics of E.coli at postion 13 (Annual Data: 1987 – 2001)

	Geometric Mean	Average (cfu/100ml)	Standard Deviation	Coeff. of Variation
Annual	1765	9477	32867	300%
Summer	2023	12413	41492	334%
Autumn	2081	10349	31835	308%
Winter	1896	8985	30954	344%
Spring	1273	6601	27402	415%

Table C-27: Seasonal Statistics of E.coli at postion 13 (Annual Data: 1987 – 2001)

	Geometric Mean	Average (cfu/100ml)	Standard Deviation	Coeff. of Variation
Jan	1960	10195	19692	193%
Feb	2257	3671	3494	95%
Mar	2088	11707	34180	292%
April	3827	22067	62444	283%
May	4443	11879	22560	190%
Jun	2967	5069	5831	115%
Jul	5642	28354	59723	211%
Aug	1694	2211	1390	63%
Sep	1341	4915	8063	164%
Oct	3445	21936	60597	276%
Nov	910	3115	5316	171%
Dec	5516	10550	12628	120%

Table C-28: Monthly Statistics of E.coli at postion 13 (1995 – 2001)

	Geometric Mean	Average (CFU/100ml)	Standard Deviation	Coeff. of Variation
Annual	2535	11497	33889	295%
Summer	2431	7847	14645	187%
Autumn	3262	14875	41008	276%
Winter	3261	12983	37634	290%
Spring	1645	10288	36444	354%

Table C-29: Seasonal Statistics of E.coli at postion 13 (1995 – 2001)

APPENDIX D:
ENVIRONMENTAL ANALYSIS OF CASE STUDY REGION

D.1 Rainfall Characteristics

	Jan	Feb	Mar	Apr	May	Jun	Jul	Aug	Sep	Oct	Nov	Dec
Average Rainfall per Day (mm)	3.9	4.0	3.6	2.5	1.1	0.8	1.6	1.0	1.8	4.2	3.4	4.5
Average No. of Rainy Days (per month)	9.0	9.4	9.2	6.7	5.8	3.3	4.3	4.8	6.8	12.9	11.1	12.3
Average Rainfall per Rainy Day (mm)	13.5	12.1	12.0	11.1	8.2	10.5	13.5	7.2	8.1	10.1	9.2	11.3
Maximum Rainfall (mm)	106.5	204.0	117.0	108.0	92.3	65.0	92.0	41.0	74.5	192.0	63.9	100.5
Median Rainfall (mm)	7.5	6.0	4.5	4.8	3.5	4.3	3.0	3.0	3.5	4.9	5.0	5.3
Minimum Rainfall (mm)	0.1	0.1	0.1	0.1	0.2	0.2	0.1	0.2	0.1	0.1	0.1	0.1

Table D-1: Monthly Analysis Result of Botanical Gardens Rain Gauge (1990 - 2002)

	Summer	Autumn	Winter	Spring
Average Rainfall per Day (mm)	4.1	2.4	1.1	3.2
Average No. of Rainy Days (per season)	29.8	19.8	10.2	30.8
Average Rainfall per Rainy Day (mm)	12.2	10.9	10.1	9.3
Maximum Rainfall (mm)	204.0	117.0	92.0	192.0
Median Rainfall (mm)	6.5	4.5	3.0	4.5
Minimum Rainfall (mm)	0.1	0.1	0.1	0.1

Table A-2: Seasonal Analysis Results of Botanical Gardens Rain Gauge (1990 - 2002)

D.2 Beaufort Scale used for Wind Characteristics

Beaufort Force	Description	Sea State	Speed			
			knots	mph	km/h	m/s
0	Calm	Sea like a mirror	< 1	< 1	< 1	< 0.5
1	Very Light	Ripples with appearance of scales, no form crests	1 - 3	1 - 3	1 - 5	0.5 - 1.5
2	Light breeze	Wavelets, small but pronounced. Crests with glassy appearance, but do not break.	4 - 6	4 - 7	6 - 11	1.6 - 3.1
3	Gentle breeze	Large wavelets, crests begin to break. Glassy looking foam, occasional white horses.	7 - 10	8 - 12	12 - 19	3.2 - 5.1
4	Moderate breeze	Small waves becoming longer, frequent white horses.	11 - 16	13 - 18	20 - 29	5.2 - 8.2
5	Fresh breeze	Moderate waves of pronounced long form. Many whit horses, some spray.	17 - 21	19 - 24	30 - 39	8.3 - 10.8
6	Strong breeze	Some large waves, extensive white foam crests, some spray.	22 - 27	25 - 31	40 - 50	10.9 - 13.9
7	Near gale	Sea heaped up, white foam from breaking waves blowing in streaks with the wind.	28 - 33	32 - 38	51 - 61	14.0 - 17.0
8	Gale	Moderately high and long waves. Crests break into spindrift, blowing foam in well-marked streaks.	34 - 40	39 - 46	62 - 74	17.1 - 20.6
9	Strong gale	High waves, dense foam streaks in wind, wave crests topple, tumble and roll over. Spray reduces visibility.	41 - 47	47 - 54	75 - 87	20.7 - 24.2
10	Storm	Very high waves with long overhanging crests. Dense blowing foam, sea surface appears white. Heavy tumbling of sea, shock-like, poor visibility.	48 - 55	55 - 63	88 - 101	24.3 - 28.3
11	Violent storm	Exceptionally high waves, sometimes concealing small and medium sized ships. Sea completely covered with long white patches of foam. Edges of wave crests blown into froth. Poor visibility.	56 - 63	64 - 73	102 - 117	28.4 - 32.4
12	Hurricane	Air filled with foam and spray, sea white with driving spray, visibility.	>64	>74	>119	> 32.5

Table A-3: Beaufort Wind Scale for Marine winds

D.3 Incident Solar Radiation Fitted E.coli Decay Parameter

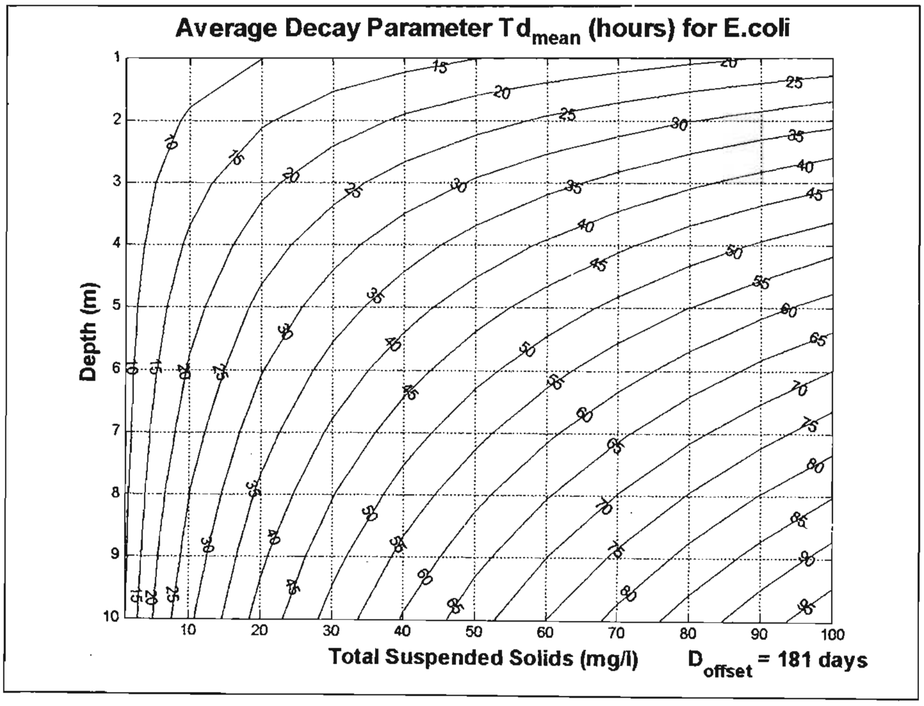

Figure A-1: Contour plot of the Td_{mean} parameter for average E.coli decay based on Durban's solar radiation characteristics

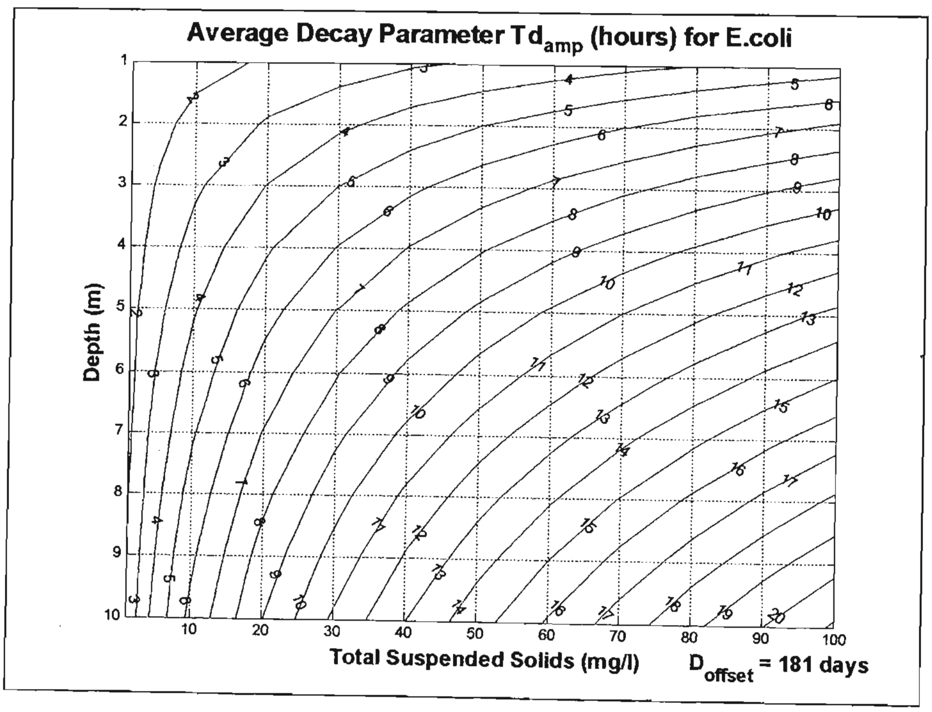

Figure A-2: Contour plot of the Td_{amp} parameter for average E.coli decay based on Durban's solar radiation characteristics

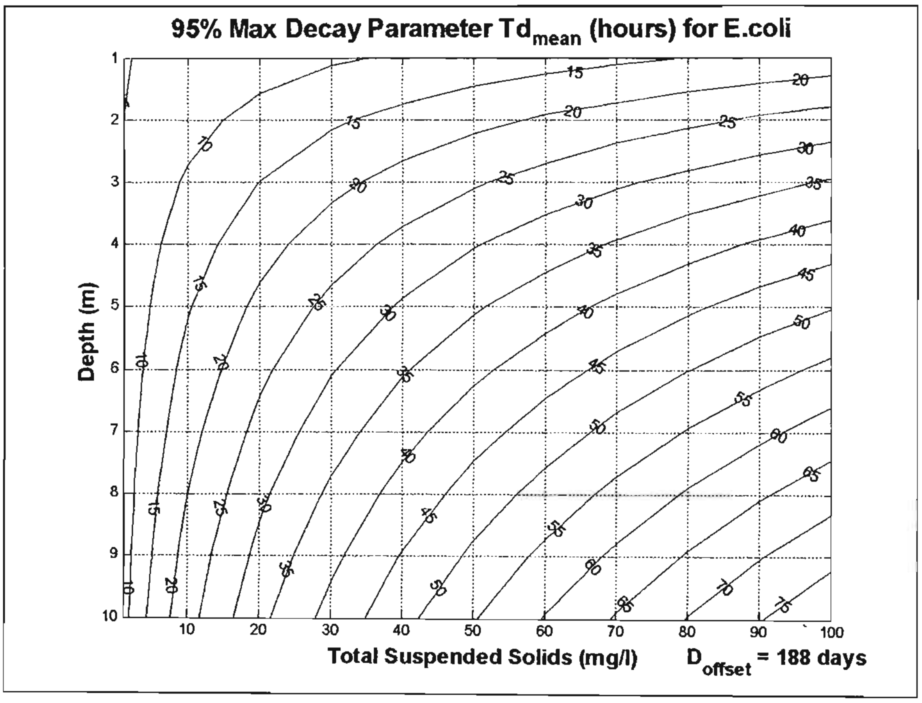

Figure A-3: Contour plot of the Td_{mean} parameter for 95% max E.coli decay based on Durban's solar radiation characteristics

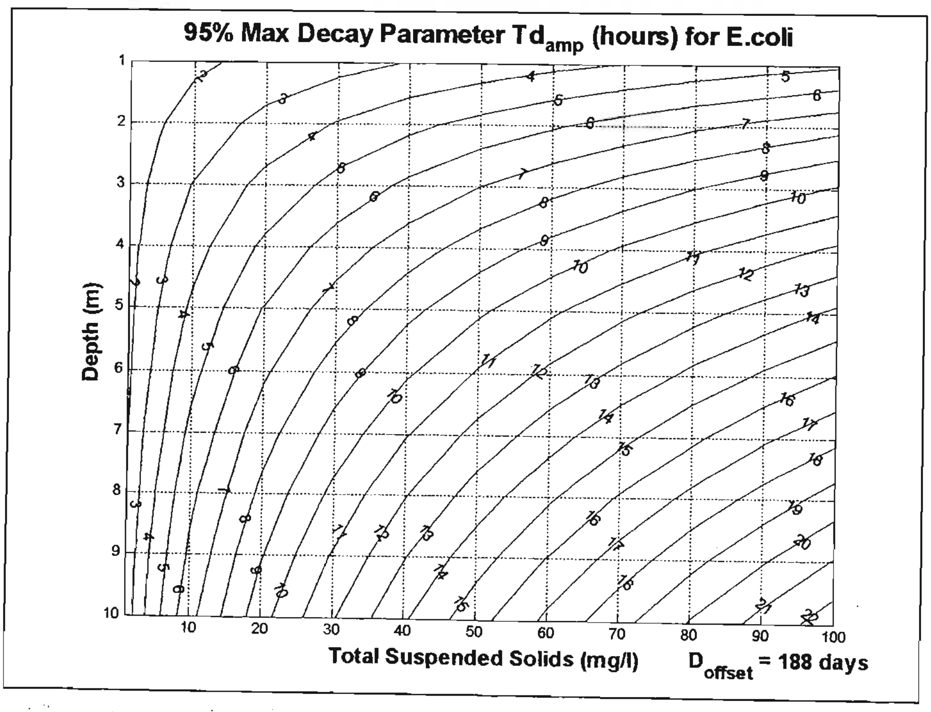

Figure A-4: Contour plot of the Td_{amp} parameter for 95% max E.coli decay based on Durban's solar radiation characteristics

D.4 Case Study Analysis Using Brahmin (2001) WQ Samples

DATE	Argyle Drain E.coli MPC (CFU/100ml)	Rainfall Runoff and Baseflow (m3/s)	SWD E.coli Loading (CFU)	Total E.coli Load (CFU)	Predicted Total E.coli (CFU)	Measured Average E.coli (CFU/100ml)	Predicted Average E.coli (CFU/100ml)
2002/08/26	45250	0.1603	6.269E+12	4.450E+11	4.897E+11	809	890
2002/08/27	34500	0.0300	8.942E+11	1.450E+11	1.081E+11	264	197
2002/08/28	8500	0.0300	2.203E+11	1.158E+11	2.565E+10	211	47
2002/08/29	14500	0.0300	3.758E+11	2.225E+11	3.136E+10	405	57
2002/08/30	27000	0.0300	6.998E+11	1.875E+11	5.711E+10	341	104
2002/08/31	28000	0.0300	7.258E+11	1.225E+11	6.115E+10	223	111
2002/09/01	300000	0.0300	7.776E+12	6.050E+11	6.122E+11	1100	1113
2002/09/02	34500	0.0300	8.942E+11	1.750E+10	1.177E+11	32	214
2002/09/03	19000	0.0300	4.925E+11	6.750E+10	4.766E+10	123	87
2002/09/04	80000	0.0767	5.305E+12	5.108E+11	4.181E+11	929	760
2002/09/05	37750	0.1720	5.611E+12	4.333E+11	4.709E+11	788	856
2002/09/06	3250	0.0300	8.424E+10	2.250E+10	4.337E+10	41	79
2002/09/07	10750	0.0660	6.126E+11	1.000E+10	5.124E+10	18	93
2002/09/08	19250	0.0300	4.990E+11	1.000E+10	4.298E+10	18	78

Table A-4: Measured vs. Predicted E.coli concentrations at Battery Beach (2002/08/26 – 2002/09/06)

APPENDIX E:
CONSTRUCTED WETLANDS

E.1 Introduction

Natural wetlands have been studied for their capacity to improve the water quality of polluted inputs (US EPA 1, 1999). Research has focussed on the water quality and habitat benefits of natural wetlands in a constructed ecosystem.

Constructed wetlands are land-based treatment systems designed to remove contaminants from wastewater. They typically consist of one or more shallow basins or channels and a submerged soil layer to support the roots of selected macrophyte vegetation (see Figure E-1). Systems may be installed in indigenous soils and discharge to surface and groundwater, or be lined with clay soils, bentonite or synthetic basal liners to prevent seepage to sensitive groundwater. Constructed wetlands differ from natural wetlands in that the operators have greater control over natural processes due to more control over the flows. The treatment in wetlands involves a combination of physical, chemical and biological mechanisms and relies upon vegetation, water depth, substrates and microbiological populations (US EPA 1, 1999; Kadlec & Knight, 1996).

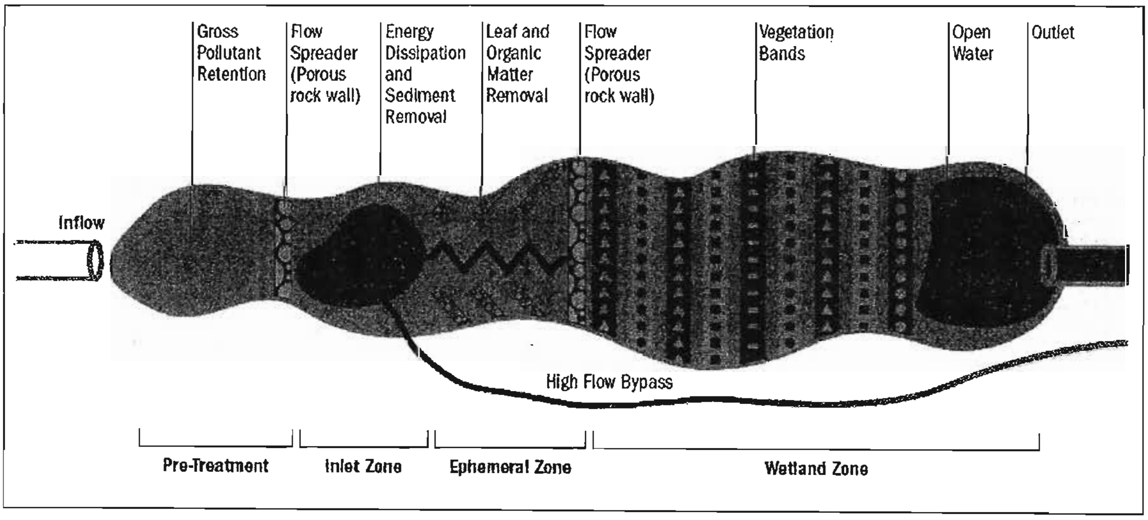

Figure E-1: Illustration of a constructed wetland (Melbourne Water, 2002)

E.1 Types of Constructed Wetlands

There are two basic types of constructed wetland treatment systems: The surface flow (SF) and subsurface flow (SSF) wetland. Most natural wetlands are FWS systems: examples include bogs, swamps and marshes. Surface flow wetlands are densely vegetated by a variety of plant species and typically have water depths less than 0.4m. Open water areas may be used to optimise hydraulics or provide wildlife habitat. Subsurface flow wetlands are different in that a bed of gravel or soil is used in which rooted wetland plants are grown. Wastewater is usually pre-treated and then allowed to flow either horizontally or vertically through the bed. The wastewater comes in contact with a mixture of facultative microbes living amongst the plant roots. The depth of the SSF bed is typically from 0.6 to 1.0 meters, with the bottom sloped to minimise flow (Haberl 2001).

The treatment of wastewaters is achieved by retaining the polluted inflow to the wetland for a specified residence time so that optimum water quality improvement efficiency may be achieved. The hydraulic residence time is defined as the mean storage divided by the mean outflow rate.

E.2 Treatment Ability for Urban Stormwater

Constructed wetlands can provide treatment or removal of various contaminants from wastewater, including:

1. Biochemical Oxygen Demand (effective after some sort of pre-treatment)
2. Total Suspended Solids
3. Nitrogen
4. Phosphorous
5. Pathogens
6. Metals and Organic Contaminants

The treatment or removal of pathogens is of special interest with respect to the problem associated with Argyle Road SWD. A wetland environment is generally very hostile to pathogens and their survival is reduced by natural factors such as temperature, ultraviolet radiation, sedimentation, predation, adsorption, unfavourable water chemistry and natural die-off (Kadlec and Knight, 1996). Studies have shown that constructed wetlands are effective in reducing pathogen pollution (e.g. Sauer and Kimber, 2001).

The removal of indicator organisms may be correlated with the hydraulic residence times (Gearheart et al., 1999). According to Kadlec and Knight (1996) removal efficiencies are nearly always greater than 90% for coliforms and greater then 80% for faecal streptococcus. In US EPA (2000a) it is reported that in a sample of 27 wetland systems, the mean influent of 73000 CFU/100ml was improved to a mean effluent of 1320 CFU/100ml. Ninety-nine percent total coliform removal was achieved at Santee, California using a hydraulic retention time (HRT) of 5.5 days. Ninety percent removal was achieved in Ontario, Canada using a HRT of 6 to 7 days (US EPA, 1988).

Wetland systems are living systems and therefore there will always be a residual background of BOD, TSS, nitrogen, phosphorous and faecal coliforms. Normal wetland background concentrations of 50 to 500 CFU/100ml may be expected for faecal coliforms.

E.3 Design Criteria for Constructed Wetlands

A constructed wetland needs to be designed for the site based on the specific geographic region, topography, hydrology, vegetation, influent pollution characteristics and effluent requirements. The following textbooks may be consulted for selection of the best design method: Reed, et at. (1995), Kadlec & Knight (1996) and Crites & Tchobanoglous (1998). A number of design manuals are also available such as: WEF (2000), US EPA (2000b) and Melbourne Water (2002).

E.4 Advantages and Disadvantages

The advantages and disadvantages of FWS wetlands are discussed in US EPA (2000a):

Advantages

1. Wetlands offer effective treatment in a passive manner, minimising mechanical equipment, energy and skilled operator requirements.
2. Wetlands may be less expensive to construct and are less costly to operate and maintain than conventional treatment systems.
3. Year-round operation for advanced or tertiary treatment is possible in warm to moderate temperature climates.
4. Wetland systems provide a valuable addition to the 'green space' in a community.
5. Wetland systems produce no residual biosolids or sludges requiring subsequent treatment and disposal.
6. The removal of BOD, TSS, COD, metals and persistent organics can be very effective with reasonable residence times. Removal of nitrogen and phosphorous can also be effective, but requires significantly longer residence times.

Disadvantages

1. The land areas required for wetlands may be large and possible unfeasible in urban area where land may be prime and therefore expensive.
2. The removal of BOD, COD and nitrogen are biological processes and essentially renewable. The phosphorous, metals and some persistent organics removed by the system are bound in the wetland sediments and accumulate over time.
3. Mosquitoes and other insect vectors can be a problem.
4. Constructed wetlands can remove faecal coliforms by at least one logarithm from typical municipal wastewaters. This may not be sufficient to meet discharge limits in all locations, requiring supplementary disinfection. It may however be sufficient for treating stormwater runoff.

REFERENCES

Adams, T. R. & Strong R. A. (1997). "Recurrence Interval/Rainfall Intensity: A Sensible Alternative to the 'First Flush' as a Design Parameter". *Vortechnics, Inc.* Portland, Maine.

AGU (1995). "U.S. National Report to International Union of Geodesy and Geophysics 1991-1994". *Reviews of Geophysics,* American Geophysical Union, Vol. 33, 1995.

Anderson, J. R., "Rip currents in the nearshore zone" (2002). Online Image. Georgia Perimeter College Geology. 30 August, 2002. (http://www.gpc.peachnet.edu/~janderso/images/ripcur.jpg)

Brahmin, A. (2001). "Urban Runoff Water Quality." B.Sc. Dissertation, School of Civil Engineering, Surveying and Construction, University of Natal, Durban

Brown, R. G. (1983). *Introduction to the Random Signal Analysis and Kalman Filtering.* John Wiley Sons, USA, 1983

Brown, R G & Hwang P (1992). *Introduction to the Random Signal Analysis and Applied Kalman Filtering.* John Wiley Sons, USA, 1983

Cabelli, V. J. (1981). *Epidemiology of Enteric Viral Infections.* Viruses and Wastewater Treatment. ed. M. Goddard, & M. Butler. Pergamon Press, New York. p.291.

Carnie, T. (2002). "Water test results still not known." *Natal Mercury,* Durban, July 5.

Carnie, T. (2003). "Beachgoers asked to help find source of beach pollution." *Natal Mercury,* Durban, Feb. 6

CEM (2002). *Coastal Engineering Manual.* USACE.

Chao, S. Y. (1988). "Wind-driven motion of estuarine plumes." J. Phys. Oceanogr., 18(8), 1144-1166.

Chen, C. T. (1970). *Introduction to Linear Systems Theory.* Holt, Reinhart & Winston, USA

Chow, V. T.; Maidment, D. R.; Mays, L. W. (1988). *Applied Hydrology.* McGraw-Hill Book Company.

Chamberlin, C. & Mitchell, R. (1978). "A Decay Model for Enteric Bacteria in Natural Waters." *Water Pollution Microbiology*, Vol. 2, John Wiley & Sons, New York, pp. 325-348

Cheng, Z. & Mitsuyasu, H. (1992), "Laboratory study on the surface drift current induced by wind and swell." *J. Fluid Mech.*, Vol. 243, p. 247-259.

Clesceri, L. S., Greenberg, A. E. & Strussell, R. R. (eds) (1992) *Standard Methods for the Examination of Water and Waste Waters.* American Public Health Association, 18th ed, 1992.

COM (2002). *Proposal for a Directive of the European Parliament and of the Council Concerning the Quality of Bathing Water.* Commission of the European Communities, 2002/0254 (COD), Brussels, Nov. 24.

Conover, W. J. (1980). *Practical Nonparametric Statistics.* New York, Wiley.

Crites, R. W. & Tchobanoglous, G (1998). *Small and Decentralized Wastewater Management Systems.* McGraw Hill Co., New York, NY.

CSIR (1989). "The Impact of the September 1987 Floods on the Estuaries of Natal/Kwazulu: A Hydro-Photographic Perspective." *CSIR Research Report: 640*, Stellenbosch, June.

De Mora, S. (2000) *The Effects of UV Radiation in the Marine Environment.* Ed. S. De Mora, S. Demmers, & M. Vernet. Cambridge Press, Cambridge, UK

Dufour, A. P. (1976). "E.coli: The Faecal Coliform." *Bacterial Indicators/Health Hazards Associated with Water.* Eds. A.W. Hoadley, and B.J. Dutka. ASTM, Philadelphia, PA. p. 48.

DWAF (1995), *South African Water Quality Guidelines for Coastal Marine Waters. Volume 2: Recreational Use.* Department of Water Affairs and Forestry, First edition, 1995

DWAF (1996). *South African Water Quality Guidelines. Volume 2: Recreational Use (second edition).* Department of Water Affairs and Forestry, Second edition, 1996

ECSD (1990). "The First Flush of Runoff and its Effects on Control Structure Design." Environmental and Conservation Services Department, Environmental Resources Management Division, City of Austin, Texas

EEC (1976). *European Union Bathing Water Directive*. Council of European Communities Directive (76/160/EEC)

EMWSS (2002a). "MM002: Analysis of Total coliform and E.coli on Chromocult Medium Using the Membrane Filter Procedure." eThekwini Water Services Waste Water Laboratory, Durban

EMWSS (2002b). "MM006: Analysis of Enterococcus Species on Enterococcus Selective Agar Using Membrane Filtration." eThekwini Water Services Waste Water Laboratory, Durban

FEE (2003). *Guidance Notes to the European Blue Flag Beach Criteria*. Foundation for Environmental Education, Copenhagen, Denmark, (www.fee-international.org)

Fattal, B.; Vasl R. J.; Katzenelson, E. & Shuval, H. I. (1983). "Survival of Bacterial Indicator Organism and Enteric Viruses in Mediterranean Coastal Waters Off Tel-Aviv." *Water Res.*17:397.

Frost, W. H. & Streeter, H. W. (1924). "Public Health Bulletin 143." U.S. Public Health Service, Washington, D.C.

Gabor, T. S. & Murkin, H. R. (2002). "Wetlands, Clean Water and Healthy Watersheds." *National Conference on Canadian Wetlands Stewardship*, December 2002.

Gameson, A. L. H. & Gould D. J. (1975). "Effects of solar radiation on the mortality of some terrestrial bacteria in sea water." *Discharge of Sewage from Sea Outfalls*. Pergamon Press, Oxford and New York, 209–19.

Gearheart, R. A. (1996). "Free Water Surface Wetlands for Wastewater Treatment: A Technology Assessment." U.S. Environmental Protection Agency, Office of Water Management, Washington.

Guillaud, J. F.; Derrien, A.; Gourmelon, M. & Pommepuy, M. (1997). "T90 As A Tool For Engineer: Interest and Limits." IFREMER, DEL, BP. 70, 29280 Plouzané, France

Haberl, R. (2001). "Constructed Wetland Technology and it's Worldwide Practice and Application." University of Agricultural Science, Institute for Water Provision, Vienna.

Hamerick, J. M. & Neilson, B. J. (1989). "Determination of Marina Buffer Zones Using Simple Mixing and Transport Models." Virginia Institute of Marine Science, College of William and Mary, Gloucester Point, Virginia.

Helsel, D. R. & Hirsh, R. M. (2002). "Statistical Methods in Water Resources" *Techniques of Water-Resources Investigations of the United States Geological Survey*, Book 4, Chapter A3, USGS, USA

Hoadley, A.W. & Dutka, B.J. (1976). *Bacterial Indicators / Health Hazards Associated with Water.* ASTM, Philadelphia,

Jazwinski, A. H. (1970). *Stochastic Processes and Filtering Theory.* Academic Press. New York

Judge, G. G.; Hill, R. C.; Griffiths, W. E.; Lutkepohl, H.; & Lee, T. C. (1988). *Introduction to the Theory and Practice of Econometrics.* New York, Wiley.

Kadelec, R. H. & Knight, R. L. (1996). *Treatment Wetlands*, Lewis Publishers, New York, New York.

Kapuscinski, R. B. & Mitchell R. (1983). "Sunlight-Induced Mortality of Viruses and Escherichia coli in Coastal Seawater." *Environ. Sci. Technol.*, Vol. 17, No. 1, 1983, PP. 1-6

Kienzle, S. W.; Lorentz, S. A.; & Schulze, R. E. (1997), "Hydrology and Water Quality of the Mgeni Catchment." Water Research Commission, Pretoria, Report TT 87/97

Kuntz, J. E. (1998). "Non-point sources of bacteria on beaches." City of Stamford Health Department, Stamford, Connecticut.

Lantrip, B. M. (1983). "The Decay of Enteric Bacteria in an Estuary." PhD thesis, School of Hygiene and Public Health, The Johns Hopkins University, Baltimore, Maryland.

Laubscher, W. I.; Swart, D. H.; Schoonees, J. S.; Pfaff, W. M.; & Davis, A. B. (1990). "The Durban Beach Restoration Scheme after 30 years." *Proceedings of Twenty-Second Coastal Engineering Conference*, July 1990, Delft, Netherlands.

Mancini, J. L. (1978). "Numerical Estimates of Coliform Mortality Rates Under Various Conditions." *JWPCF*, 50(11):2477-2484.

Manolis, R.; Zdragas, A.; Katsavouni, S.; Eskridge, K.; Takavakoglou, V. & Zalidis, G. (2001). "Municipal Wastewater Disinfection Using a Constructed Wetland." Wastewater treatment and plants as a 'green liver': The European approach, experience and trends, *4th Management Committee meeting of COST*, Larnaca, Cyprus

Mardon, D. W. (2000). "The Effects of Wind Speed, Direction and Duration on Cross-Currents at the Port of Durban Entrance." B.Sc. Dissertation, School of Civil Engineering, Surveying and Construction, University of Natal, Durban.

Masse, A. K. & Murthy C. R. (1990). "Observations of the Niagara River thermal plume." *J. Geophys. Res.*, *95*(C9), 16,097-16,110.

Melbourne Water (2002). *Constructed Wetland Systems: Design Guidelines for Developers*. Melbourne Water, Melbourne 3002, July 2002, (www.melbournewater.com.au)

Metcalf and Eddy (1991), *Wastewater engineering: Treatment, disposal and reuse*. McGraw-Hill, New York.

Mitchell, R. & Chamberlin, C. (1978). "Factors Affecting the Survival of Indicator Organisms in the Aquatic Environment.", Ed. G. Berg, *Indicators of Enteric Contamination in Natural Waters*, Ann Arbour Press, Ann Arbour, Michigan.

Munchow, A. & Garvine, R. W. (1993). "Buoyancy and wind forcing of a coastal current." *J. Marine Res.*, 51, 293-322.

Namsoo S. Suk, N. S.; Guo, Q. & Psuty, N. P. (1998). "Feasibility of Using a Turbidimeter to Quantify Suspended Solids Concentration in a Tidal Salt Marsh Creek." *Estuarine, Coastal, and Shelf Science*, Vol. 46, 1998, pp. 383-391

NTAC (1968). *Water Quality Criteria*. National Technical Advisory Committee, Federal Water Pollution Control Adm., Department of the Interior, Washington, DC.

Packman, J. J.; Comings, K. J.;& Booth, D. B. (1999). "Using Turbidity to Determine Total Suspended Solids in Urbanising Streams in the Puget Lowlands." College of Forest Resources, University of Washington, Seattle, Washington, USA

Phelps, E. B. (1944). *Stream Sanitation*. Whiley & Sons, New York, p. 209.

Prüss, A. (1998) "A review of epidemiological studies from exposure to recreational water." *Int. J. Epidemiol.*, 27: 1-9.

Reed, S. C.; Crites R. W. & Middlebrooks E. J. (1995). *Natural Systems for Waste Management and Treatment*, Second Edition, McGraw Hill Co., New York, NY.

Sauer, P. A. & Kimber, A. (2001). "Technical Assessment of Constructed Wetlands for Wastewater Treatment in Iowa." Iowa Association of Municipal Utilities, Ankeny, Iowa, 2001.

Schombert, J. (2002). "Albedo." Retrieved on 2 Aug, 2002, from Dept. of Physics, University of Oregon website: (http://zebu.uoregon.edu/~js/glossary/albedo.html)

Schueler, T. R. (1994). "First Flush of Stormwater Pollutants Investigated in Texas." *Watershed Protection Techniques*, Vol. 1, No. 2, p.88.

Sieracki, M. (1980). "The Effects of Short Exposure of Natural Sunlight on the Decay Rates of Enteric Bacteria and a Coliphage in a Simulated Sewage Outfall Microcosm." M.Sc. Thesis, University of Rhode Island, Kingston, Rhode Island.

Skinner, B. J.; Porter S. C. & Botkin, D. B. (1999). *The Blue Planet: An Introduction to Earth System Science*, 2nd Edition, John Wiley and Sons

"Storm Water Management Model" (2003). Retrieved 4 Feb, 2003, from U.S. Environmental Protection Agency website: (http://www.epa.gov/ednnrmrl/swmm)

Stretch, D. D. (1980). "Continuous Streamflow Modelling." M.Sc. Dissertation, Department of Civil Engineering, University of Natal, Durban.

Taylor, H. N., K. D. Choate, and G. A. Brodie. (1993). "Storm event effects on constructed wetland discharges." *Constructed Wetlands for Water Quality Improvement*, pp 139-145G. A. Moshiri (ed.). CRC Press, Boca Raton, FL.

"The effects of urbanization on water quality: Waterborne pathogens" (2003). Retrieved 10 July, 2003, from USGS: Water science for schools website: (http://ga.water.usgs.gov/edu/urbanpath.html)

Tsanis, I. K. (1987). "Simulation of Wind-Induced Water Currents." *J. Hydraul. Eng.*, Vol. 115, No. 8, August.

USACE (2001). *Water Qualtiy Studies in the Vicinity of the Washington Aqueduct*. US Army Corps of Engineers, Baltimore District, USA

US EPA (1976). *Quality Criteria for Water*, U.S. Environmental Protection Agency, Washington, DC.

US EPA (1985). *Rates, Constants and Kinetic Formulations in Surface Water Quality Modelling.* Second Edition, Environmental Research Laboratory, U.S. Environmental Protection Agency, Athens, Georgia.

US EPA (1986) *Ambient Water Quality Criteria for Bacteria*, U.S. Environmental Protection Agency, Washington, DC.

US EPA (1988). "Design Manual: Constructed Wetlands and Aquatic Plant Systems for Municipal Wastewater Treatment." *EPA/625/1-88/022*, U.S. Environmental Protection Agency, CERI, Cincinnati, OH.

US EPA (1999a). "Review of Potential Modelling Tools and Approaches to Support the BEACH Program." U.S. Environmental Protection Agency, Washington, DC.

US EPA (1999b). "Constructed Wetlands Treatment of Municipal Wastewaters." *EPA/625/R/010*, U.S. Environmental Protection Agency, Cincinnati, OH, Sept.

US EPA (2000a). "Wastewater Technology Fact Sheet: Free Water Surface Wetlands." *EPA 832-F-00-024*, U.S. Environmental Protection Agency, Office of Water, Washington, DC.

US EPA (2000b). "Design Manual Constructed Wetlands for Municipal Wastewater treatment." U.S. Environmental Protection Agency, CERI, Cincinnati, OH

US EPA (2002). "Implementation Guidance for Ambient Water Quality Criteria for Bacteria - May 2002 (Draft)." *EPA-823-B-02-003.* U.S. Environmental Protection Agency, Office of Water, Washington, DC

"Water Pollution in the Umgeni River" (2003). Retrieved 10 July, 2003, from Infomags website: <http://www.infomags.co.za/dbn/dbninfo/wp_umgeni.asp>

WEF (2000). "Natural Systems for Wastewater Treatment." *MOP FD-16*, Water Environmental Federation, Alexandria, VA.

Welch, G. & Bishop, G. (2001). *An Introduction to the Kalman Filter.* TR 95-041. Department of Computer Science, University of North Carolina at Chapel Hill, Chapel Hill, NC 27599-3175

Wesson, S. (2001). "The Effects of River and Stormwater Outflows on Beach Water Quality." B.Sc. Dissertation, School of Civil Engineering, Surveying and Construction, University of Natal, Durban.

Whitehead, R. F. De Mora, S. J. Demers, S. (2000). "Enhanced UV Radiation – A New Problem for the Marine Environment." *The Effects of UV Radiation in the Marine Environment*, Cambridge Press, Cambridge, UK, pg1

WHO (2001). "Bathing Water Quality and Human Health: Faecal Pollution." *Outcome of an Expert Consultation*, Vol.1 Chap.4, Farnham, UK, April 2001, *WHO/SDE/WSH/01.2*.

WU, J. (1974). "Wind-Induced Drift Currents." *J. Fluid Mech.*, Vol. 68, p. 49-70.

Zoppou, C. (2000). "Review of Urban Stormwater Models." *Environmental Modelling & Software*, Elsevier, 16(2001) 1995-231